Pyridoxine radiotracers for imaging metabolic alterations

Émile Pinault-Masson

Thesis submitted to the University of Ottawa
in partial Fulfillment of the requirements for the
Master's thesis in Chemistry

Department of Chemistry and Biomolecular Sciences
Faculty of Science
University of Ottawa

Acknowledgements

There are many people who have been instrumental to the completion of this thesis which deserve my gratitude. The first person I would like to acknowledge is Mojmir Suchy, who taught me and trained me on almost all of the chemistry I did. Mojmir also helped drew up the initial synthesis scheme for the compounds and was very insightful for all the steps of the project. Secondly, I would like to acknowledge Peter Scott and Allen Brooks from the University of Michigan. Peter Scott let me into his lab for my Michael Smith Foreign Study Supplement award and even after I was gone, he was still happy to discuss about the project and give insight on the next steps. Allen Brook trained me and did most of the manipulation related to the radio fluorinations attempts done at the University of Michigan. Similarly, to Peter, Allen was helpful after I was gone from Ann Arbor. Another person I would like to acknowledge is Andre Beauchemin. Andre was very insightful for this project as he gave advice on how to analyse the reactions in order to get a proper idea of what was happening and how to adapt in order to get positive results. Lastly, I would like to acknowledge Adam Shuhendler for helping me with this project and with the thesis.

Table of contents

List of Figure

List of schemes

List of Tables

List of Appendices

Abbreviations

Ac Acetyl (H_3CCO-)

ATP Adenosine Triphosphate

DAST Diethylaminosulfur trifluoride

DCM Dichloromethane

DMAP 4-dimethylaminopyridine

DMF Dimethylformamide

DMSO Dimethyl sulfoxide

DNA Deoxyribonucleic acid

dTMP deoxythymidylate monophosphate

dUMP deoxyuridylate monophosphate

FAD Flavin adenine dinucleotide

[^{18}F] FDG 2-[^{18}F]fluoro-2-deoxy-d-glucose

FDG 2-Fluoro-2-deoxy-d-glucose

[^{18}F] FETA ^{18}F-fluoroetani-dazole

[^{18}F] FES ^{18}F-Fluoroestradiol

[^{18}F] FLT 3′-deoxy-3′-[^{18}F]fluorothymidine

[^{18}F]6-FPN [^{18}F] 6-Fluoropyridoxine

6-FPN 6-Fluoropyridoxine

[^{18}F]2'-FPN [^{18}F] 2'-Fluoropyridoxine

2'-FPN 2'-Fluoropyridoxine

HPLC High performance liquid chromatography

LC-MS Liquid Chromatography-Mass spectrometry

NSCLC Non-Small Cell Lung Cancer

NMR Nuclear Magnetic Resonance

MTBE Methyl tert-butyl ether

PBSF Perfluorobutanesulfonyl fluoride

PDXK Pyridoxal kinase

PDXP Pyridoxal phosphatase

PET Positron emission tomography

PL Pyridoxal

PLP Pyridoxal-5'-phosphate

PM Pyridoxamine

PMP Pyridoxamine-5'-phosphate

PN Pyridoxine

PNP Pyridoxine-5'-phosphate

PNPO Pyridoxamine phosphate oxidase

ROS Reactive Oxygen Species

SAH S-adenosylhomocysteine

SAM S-adenosylmethionine

SHMT N-5-methyltetrahydrofolate serine hydroxylmethyltransferase

SPIAd spiroadamantyl-1,3-dioxane-4,6-dione

TBDMSCl Tert-butyldimethylsilyl chloride

[^{18}F]TEAF ^{18}F-Tetraethylammonium fluoride

TFA Trifluoroacetic acid

TFAA Trifluoroacetic anhydride

THF Tetrahydrofuran

TBAF Tetrabutylammonium fluoride

TBAF(Pin)$_2$ Tetrabutylammonium fluoride bis pinacol

Tf Trifluoromethanesulfonyl (F_3CSO_2)

TMAF Tetramethylammonium fluoride

Tosyl Toluenesulfonyl ($H_3CC_6H_4SO_3$)

Triflate Trifluoromethanesulfonyl (F_3CSO_2R)

Ts Toluenesulfonyl ($H_3CC_6H_4SO_3$)

TsCl Para-toluenesulfonyl chloride

Abstract

Vitamin B_6 was discovered almost 90 years ago, and since then it has received a lot of interest from the scientific community due to its role in human health and its impact on several biochemical processes. One of the most interesting aspect of vitamin B_6 studied in the past decade is its role in cancer. From the research on this subject so far, the following can be suggested: early-stage cancer cells have a higher vitamin B_6 content than normal cells due to its role in metabolic processes. As the cancer makes progress, there is a change in vitamin B_6 activation and trapping in the cell, decreasing the amount of active vitamin B_6 in the cell in order to resist cell death. From these conclusions, we can see that vitamin B_6 could potentially be an interesting radiotracer to use for diagnosis and staging of cancers. One of the most predominant form of imaging which is done nowadays to detect and diagnose cancers is Positron Emission Tomography (PET) imaging. Research on PET imaging is driven by the potential of new radiotracers which can be added to the current arsenal of tools for the fight against cancer. Therefore, this project focuses on the attempted synthesis of two potential radiotracers derived from vitamin B_6 based on the insertion of fluorine-18. None of the two proposed radiotracers were successfully synthesized but we successfully synthesized one cold standard and difluorinated pyridoxine with cold conditions similar to radiochemistry. The main issues which were faced were the degradation of the potential precursors when attempting fluorination, the lack of reactivity of intermediates for the formation of precursors and an acetyl migration leading to the wrong precursors. By using a milder fluorination strategy to avoid degradation (room temperature, no free fluoride source: AgF_2 as fluorinating agent), the 6-Fluoropyridoxine cold standard was synthesized. By changing the protection strategy (not using any acetyl groups), acetyl migration was avoided which led to the synthesis of a difluorinated pyridoxine using mild conditions (room temperature). The difluorination was also successful using harsher conditions (heat). There is still a lot of work to do to synthesize a radiotracer derived from vitamin B_6 but there are some signs that this may be possible with additional work.

Chapter 1. Introduction

Part 1. Preface: History of vitamin discovery and comprehension

Vitamins are pillars of a large scale of biochemical and cellular processes which make them some of the most important nutrients for human health. The importance of these nutrients is being unveiled more and more with our understanding of their functions in the body, which research have shown can span from simple metabolism to the relationship with complex diseases such as cancer. The crucial role of vitamins has only been truly understood in the last decades and the existence of vitamins has only been known since the 19th century. Researchers have come a long way since then, discovering the 13 vitamins and, with the evolution of biochemistry and cellular biology methods, understanding the roles of these compounds. Even nowadays, new roles are being discovered along with new applications.

Part 1.1. Discovery of vitamins

It is surprising to believe that with so much focus on nutrition and its impact on society nowadays, that only about 200 years ago it was believed that food contained fats, proteins carbohydrates and ash (the term used for minerals) as the only form of nutrients.[1] It wasn't until the 20th century that physicians and scientists understood that diets include many vital nutrients and that a lack of some of these nutrients may lead to disease.[1,2] The path towards our modern understanding of the relationship between health and our diets began to truly take form in the late 1800s in a relentless effort to understand the cause as well as a possible cure for the disease known as "beriberi",[2] which was later understood to be due to a deficiency in the vitamin known today as thiamin or vitamin B_1. Christiaan Eijkman (Nobel prize in Medicine, 1929),[3] a Dutch physician from the University of Amsterdam, was sent to the Dutch East indies to study the cause of beriberi amongst a commission sent by Dutch authorities during the end of the 19th century.[2,3] Certain that the disease was due to a microorganism, Eijkman tried unsuccessfully to transfer the disease from sick chickens to healthy ones at the laboratory for bacteriology and pathology, to which he was named director of at the time.[4] Surprisingly, the disorder in the sick chickens mysteriously cleared after a few weeks of experiment and Eijkman learned that the chicken were now fed brown unpolished rice[3] instead of polished white rice.[4] Excited by this unforeseen clue, Eijkman shared his observations with his colleague, who was the physician inspector of the prisons of the colony, and this led to the observation that prisoners fed

unpolished brown rice had a lower tendency to develop beriberi than prisoners who were fed white rice.[4] Eijkman later found that this "antiberiberi factor" could be extracted from rice hulls and concluded that this was an antidote to the microbe causing the disease. Gerrit Grinjs, Eijkman's successor, tried to understand what the process of polishing had to do with the curative effect[1,2,4] and discovered that mung beans could also be used to treat beriberi.[4] Based on these observations, Grinjs came to another conclusion and stated that there are substances that cannot be absent in the diet. This was the first recognition of "accessory factors"[4] in the diet and was followed by a world wide effort to understand the impact of nutrition on health. One of the more famous examples were the experiments by Frederick Gowland Hopkins[4] with which he concluded that there are various substances other than proteins, fats and carbohydrates in food and that there is a connection between these substance and disease.[4] Hopkins made this conclusion by extracting the factors necessary for growth in mice from milk and yeast. These were found to be necessary for mice to survive if placed on a synthetic diet of protein, fats and carbohydrates only.[4] Others followed in this field and tried to extract such "accessory factors" such as Polish biochemist Casimir Funk, who experimented with the extraction of the antiberiberi factor from rice husk. Funk observed that the conditions needed for the extraction of this factor pointed towards a nitrogenous base as its nature. Thus, he decided to name these substances "vital amines", which turned into the term "vitamine" and was use to describe all these "accessory factors" which could prevent disease if provided in the diet.[1,2,4] A lot of research was done following these crucial observations and this led to the isolation of the antiberiberi "vitamine" from rice and elucidation of the chemical formula in 1933, which is $C_{12}H_{16}N_4OS$-2(HCl).[2] This was followed by the discovery of the chemical structure and the first full synthesis of thiamin in 1936 by Robert R. Williams.[2]

Between Funk's historical paper "the vitamine theory" in 1912 to the elucidation of the structure and synthesis of thiamine in 1936,[4] multiple other "vitamines" were discovered in the meantime. Only 3 years after the publication of Funk's article, Elmer McCollum demonstrated that two factors different from the factors discovered by Hopkins were required for the growth of rats[4,5] and both could be extracted from eggs, although one was extractable with water and the other was not.[4,5] McCollum baptized these factor fat-soluble A and water-soluble B. After confirming that the water-soluble B factor had similar effect than the antiberiberi vitamine, it became known as vitamine B.[4] Because of this new knowledge, that the so-called "accessory factors" had the

same activity as vitamines, the definition of vitamines was changed to include compounds which are not of nitrogenous in character which led to the modern term for the antiberiberi factor, vitamin B.[4] Most of the vitamins were all discovered in the first three decades of the 1900s including vitamin C, which was discovered in 1932, vitamin D in 1923 and the discovery of the several different vitamin B in the 1920 and 1930s such as the first mention of vitamin B_6 in 1934, amongst others.[4]

Part 1.2. Modern definition of vitamin

Since the term vitamin was invented, the knowledge about the concept of a vitamin has evolved and thus the definition of a vitamin as evolved with it. Based on Combs and McClung,[1] a vitamin is an organic compound naturally present in food in minute amounts, which is distinct from fats, carbohydrates as well as proteins and is essential for normal physiological functions. It can prevent a specific deficiency syndrome linked to its absence and cannot be synthesized by the host in sufficient amounts for its needs. It is important to note that based on this definition, some compounds would be considered vitamins for some species and not for others, and that some compounds are only vitamins under specific dietary and environmental conditions.[1] Nowadays thirteen substances or groups of substances are recognized as vitamins: vitamin A, vitamin D, vitamin E, vitamin K, vitamin C, Niacin, Folic acid, Biotin, Pantothenic acid, vitamin B_1, B_2, B_6 and vitamin B_{12}.[1] Some of these vitamins are described with a familiar name which describes a family of related compound having similar activities, which is the case for vitamin B_6. Pyridoxal, pyridoxol and pyridoxamine are all considered to be vitamin B_6. In this case, members of the same vitamin family are called vitamers.[1]

Even though they are all considered vitamins, these substances are very different from each other, varying not only in their function and chemical structure but also in their solubility. Vitamin D, A, E and K are aromatic and/or aliphatic in character, making them fat soluble, whereas vitamin C, biotin, folate, pantothenic acid, vitamin B_1, B_2, B_6 and vitamin B_{12} have polar ionizable groups therefore favoring water.[4] These characteristics will determine their fate in the body including absorption, tissue distribution and function.[4]

Part 1.3. Modern comprehension of the functions of vitamins

As previously mentioned, the comprehension of the nature of vitamins has evolved since their discovery. Consequently, the relationship between vitamins and health has grown hand in hand with the increasing knowledge of the functions of vitamins.

The advances in our mechanistic knowledge of cellular and biochemical functions were crucial to the study of the functions of the vitamins. Marks made use of concepts of microbiology and biochemistry in a study on the depletion of Thiamin in human.[6] He demonstrated that after 5-10 days of a thiamin-free diet there was a decrease in the the saturation of erythrocyte transketolase with its coenzyme thiamine pyrophosphate. It took 200 days of this diet to observe weight loss, insomnia and other clinical signs attributed to thiamin deficiency.[6,7] With these results in hand, Marks proposed the four progressive stages of vitamin deficiency: depletion of vitamin stores followed by cellular metabolic changes, functional defects and finally morphological changes.[6,7] This discovery couldn't have happened if the concept of cofactors itself was not understood, which was recognized in 1906 by Harden and Youndin.[8] In such a way, the identification of the functions of vitamins was not always directly due to research on vitamins themselves but emerged from our grasp of cellular biochemistry.

The functions that a vitamin can have which are known today can be generalized into the following five categories: Coenzyme; Electron/Hydrogen donor or acceptor; Antioxidant; Hormone; Effector of gene transcription.[9]

Part 1.4. Modern knowledge of the relationship between vitamins and health: link to carcinogenesis

With the wide range of functions described above, it shouldn't come as a surprise that there is a strong relationship between diseases other than the ones due to hypovitaminosis (vitamin-deficiency) and vitamin levels.[10–13] Ranging from their role in cardiovascular diseases to cancer formation and progression,[10,13] the field of study on vitamins has truly shown more and more importance in the past decades as we decipher more of the secrets behind these substances.

The role of vitamins in cancer was first studied in Vitamin A[14] since vitamin A is essential for differentiation of epithelial tissue and cancer involves abnormal differentiation.[14] Moreno and colleagues showed that vitamin A deficiency enhanced the susceptibility to chemical

carcinogenesis in animal tumor models.[15] It is believed that this effect is due to immunosuppression, since animal studies have demonstrated that vitamin A increases immune response.[14] However, more research on the role of vitamin A and cancer led to conflicting results. A meta-analysis in 2015 of 15 prospective studies showed that there is a positive relationship between cancer risk and plasma vitamin A levels.[16] Contrary to this observation, a 2009 meta-analysis of retrospective case-control studies found that there was an inverse association with plasma level of vitamin A and cancer risk.[17]Therefore, there is not yet a clear interpretation of the role of vitamin A in carcinogenesis but there are some clues that this vitamin is involved in carcinogenesis in some way. Other diseases in which vitamin A is involved include diabetes/obesity[18,19] and myocardial infarction.[20]

Due to the interesting results on the relationship between vitamin A and cancer, researchers around the world have been studying the role of other vitamins in this complex disease.

Part 2. Establishment of Vitamin B_6 as an important factor in carcinogenesis

Even though vitamins were discovered 200 years ago and a huge amount of research has been done on the relationship between vitamins and diseases such as cancer, there is still some uncertainty about the specific mechanism they play and how to use vitamins for prevention of disease. Fortunately, a vitamin of particular interest for its role in cancer has emerged in the last decades: vitamin B_6. Similarly to other vitamins studied in carcinogenesis, vitamin B_6 was studied in cancer due to its function as a co-enzyme for >150 important metabolic enzymes,[21] which makes it interesting for cancer since metabolic changes are a familiar characteristic of cancerous cells.[22] From its discovery in 1934[4] to the recent theory about its role in carcinogenesis, vitamin B_6 has come a long way and could prove to be a crucial tool for cancer diagnosis.

Part 2.1. Discovery of vitamin B_6

The first vitamin to be discovered was thiamin or vitamin B_1, which was proposed in 1906.[4] The actual term vitamin B wasn't used until 1916 when McCollum and colleagues demonstrated that what they called water-soluble B factor (a factor extracted from egg yolks required for normal growth in rats) had the same antipolyneuritis effect as the vitamin proposed in 1906, therefore naming it vitamin B.[4,5] Very soon, it became obvious that vitamin B could not be a single

vitamin due to the finding that yeast could not only prevent beriberi, but also pellagra.[4,23] Since thiamin was discovered first, it was named vitamin B_1 and the antipellagra vitamin was called vitamin B_2.[4,24] Due to the different responses in various species to a preparation of vitamin B_2, it was determined that vitamin B_2 was in fact a complex of several factors.[4] Kuhn and colleagues elucidated the first factor in 1933, which was called riboflavin or vitamin B_2.[25] A decade and a half later, an animal model was established for pellagra by Goldberger in 1922,[4,23] the compounds that could cure the disease were isolated from liver extracts and separated from the other B_2 complex.[4,26] These two factors, nicotinamide and nicotinic acid are now called niacin or vitamin B_3.[4] In the 1930s, researchers were interested in a skin condition seen in rat which was different from the one that could be treated with vitamin B_1 or vitamin B_2.[24] Reader and colleagues observed that rats feed with a diet with added vitamin B_1 and B_2 developed this skin condition characterized by edema, redness and scaliness in extremities such as paws and ears.[24,27,28] The newly discovered factor was named vitamin B_4 by the research group since yeast concentrate could prevent this skin condition and yeast was known to contain the B_2 complex.[24,27,28] After more analysis, the same research group dismissed the existence of vitamin B_4 due to new observations[24,29] even if there was a new disease, rat acrodynia, which could not be explain by lack of vitamin B_1 and/or riboflavin and could be cured by yeast extracts.[24] It was Paul György who first mentioned this as vitamin B_6 activity in 1934[4,24] and 4 years later his group isolated vitamin B_6 in crystalline form at the same time as 4 other research groups.[4,30–33] This was followed by the elucidation of the structure which is 3-hydroxy-4,5-bis-(hydroxymethyl)-2-methylpyridine along with its synthesis in 1939.[34,35] György then proposed the name pyridoxine[36] for this compound which was accepted by the scientific community.

Part 2.2. Vitamin B_6: more than pyridoxine

Not long after the elucidation of the structure and full synthesis of pyridoxine, Esmond Snell developed an important microbiological growth assay[24,37] with which he observed that the addition of amino acids increased the activity of pyridoxine in bacteria.[24,38,39] It was discovered that this increased activity was due to the aminated version of pyridoxine, which was named pyridoxamine, and to the formyl derivative of pyridoxine, pyridoxal.[40]

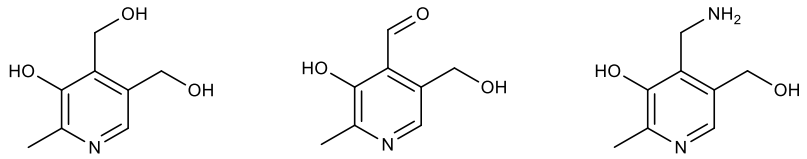

Pyridoxine Pyridoxal Pyridoxamine

Figure 1. Structures of pyridoxine, pyridoxal and pyridoxamine.

During the same time, Dexter Bellamy and Irwin Gunsalus at Cornell University tried to understand the function of tyrosine decarboxylase,[41] which was discovered in *Streptococcus faecalis* by Ernest Gale in 1940.[42] They observed that there was no tyrosine decarboxylase activity if the cell medium did not contain pyridoxine even though the cell had normal growth, and that pyridoxine did not rescue the activity if it was left in a refrigerator or autoclaved with cystine before its addition.[43,44] After they learned the discovery of Esmond Snell[40] and that pyridoxal was synthesized by Merk (synthesis by Folkers and colleagues, 1944)[45] they used pyridoxal in their experiment and observed that pyridoxal restored the activity of the enzyme.[46] They then succeeded in producing the apo-tyrosine decarboxylase (the enzyme without its coenzyme, vitamin B_6) by drying the cells over Drierite.[47] They quickly realised that pyridoxal did not activate the purified apo-decarboxylase without the presence of ATP,[47] and with the help of Wayne Umbreit discovered a method to synthetically phosphorylate pyridoxal and demonstrated that this was able to reactivate the apo-decarboxylase.[48,49] This was followed by the observation that all other vitamers of vitamin B_6 could also be used to activate the apo-decarboxylase if they were phosphorylated, therefore confirming the existence of pyridoxamine phosphate and pyridoxine phosphate and their roles as co-enzymes.[50] In the same year, they were able to characterize pyridoxine phosphate (PLP)[51] and confirmed a few years later that the phosphorylation site was at the 5' hydroxyl group position.[52,53]

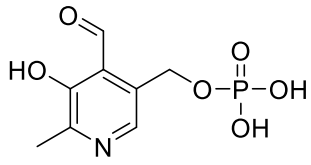

Figure 2. Structure of pyridoxal-5'-phosphate (PLP)

Part 2.3. Interconversion of the vitamers of vitamin B_6 and human metabolism

Interestingly, vitamin B_6 does not only exist in the form of pyridoxine (PN), pyridoxamine (PM) and pyridoxal (PL) as well as their phosphorylated forms (Pyridoxine-5'-phosphate, PNP; pyridoxamine-5'-phosphate, PMP; pyridoxal-5'-phosphate, PLP),[21] but each of the vitamers can also be converted to each other with the help of enzymes.

First and foremost, the free base vitamers of vitamin B_6 (PN, PM and PL) can be phosphorylated by pyridoxal kinase, which is an ATP-dependant enzyme found in mammals and some bacteria.[54] In mammals, which cannot synthesize vitamin B_6 *in vivo*,[55] the three vitamers in the free base form are available in the diet[56] and are absorbed in the intestine (mostly in the jejunum) by passive diffusion.[55,57] Somewhat similarly, the phosphorylated versions of the vitamers are also present in the diet[56]. They are transformed into the free base by non-specific intestinal alkaline phosphatase[55,57,58] which is followed by passive diffusion. There also exists a specific phosphatase enzyme, pyridoxal phosphatase, which can hydrolyse the 5'-phosphorylated vitamers back to their free base form[59] and is expressed in all organs.[60] Another important enzyme in what is called the "vitamin B_6 salvage pathway"[61] is pyridoxamine-5'-phosphate (PMP) oxidase which is responsible for the transformation of PMP and PNP into PLP as well as pyridoxine to pyridoxal.[58,62]

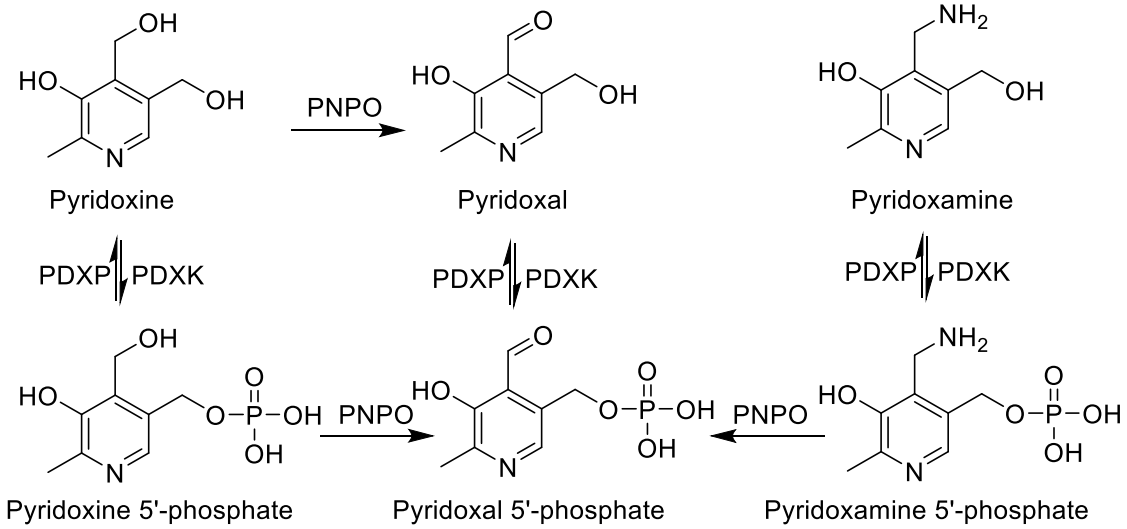

Figure 3. Schematic representation of the interconversion of the vitamers of vitamin B_6 in humans. PDXP, pyridoxal phosphatase; PDXK, Pyridoxal kinase; PNPO, pyridoxamine phosphate oxidase. Modified with permission from the Encyclopedia of food sciences and nutrition.[63]

The vitamin B_6 salvage pathway is used to form the most bioactive form of vitamin B_6, which is PLP.[64] In fact, after being absorbed, the free forms of the vitamers are rapidly transported to the liver[65] from the blood where they are bound to hemoglobin or albumin[66] and converted to PLP by the aforementioned enzymes[65] (the conversion can be done in other tissues as well but occurs mainly in the liver). The liver can release PLP into plasma with binding to albumin[65,67] and PLP can be transported to tissues which absorb the vitamin through dephosphorylation followed by passive diffusion.[61] Pyridoxal is then phosphorylated into its active form and trapped in the cell due to its negative charge. PLP can then act as a coenzyme or get degraded.[68] In humans, PLP is catabolised to 4-pyridoxic acid by a FAD-dependent general aldehyde oxidase,[55,58] and then excreted in urine. The vitamers (mostly pyridoxamine and pyridoxal) can also be excreted directly in urine[69] but this is a minor excretion process.

Part 2.4. Coenzyme activity of vitamin B_6

Once PLP was available widely available for study, a lot of research was done on the role of this new coenzyme in other enzymatic reactions other than decarboxylation. Gunsalus and colleagues, which were the pioneers in PLP activity, demonstrated that it was a crucial coenzyme for transamination reactions,[70,71] which has been confirmed by many other groups.[72,73] They also discovered the pivotal role of the vitamin in the synthesis and degradation of tryptophan by tryptophan synthetase and tryptophanase, respectively.[74,75] In tryptophan synthetase, PLP works as a coenzyme for the condensation of serine and indole which can be seen as a modification of the group at the β-carbon of serine,[76,77] demonstrating again its importance in amino-acid chemistry (as previously described, PLP is the coenzyme for tyrosine decarboxylase). On the other hand, tryptophanase needs the vitamin for the β-elimination of tryptophan to indole and pyruvate.[78] Another role in amino acid chemistry was found for PLP by Umbarger and Brown as well as Phillips and Wood[79,80] with the demonstration that threonine dehydratase uses the vitamin as a coenzyme for the deamination of threonine. In addition, PLP was found to stimulate racemization of amino acids in bacteria by playing a role in alanine racemase and glutamate racemase.[81–83]

Apart from its role as a coenzyme in decarboxylation, transamination, α, β-elimination reactions and racemization of amino-acids, PLP is crucial for hemoglobin synthesis and function. In fact,

PLP serves as a coenzyme for the rate limiting step of hemoglobin synthesis, which is the biosynthesis of δ-aminolevulinic acid by δ-aminolevulinic acid synthase[84,85] and enhances oxygen binding when present in hemoglobin.[86]

Vitamin B_6 also plays in role in other important metabolic aspect which differs from amino acid synthesis and catabolism. First of all, PLP is necessary for the activity of glycogen phosphorylase, the enzyme responsible for the rate-limiting step of the degradation of glycogen into glucose.[87] Another role in metabolism for PLP is fatty acid synthesis. The synthesis of highly unsaturated fatty acids (HUFAs) such as arachidonic acid and docosahexaenoic acid, which are important for multiple functions in humans, requires δ-6-desaturase, which is a PLP-dependant enzyme.[88,89] Finally, PLP plays an important role for sphingolipid metabolism since both serine palmitoyltransferase (SPT) and sphingosine-1-phosphate lyase (SPL) are dependant of the vitamin for their functions which are the synthesis of 3-keto-dihydrosphingosine and the degradation of sphingosine-1-phosphate, respectively.[90]

These are just a few examples of PLP-dependant enzyme. In fact, PLP is a necessary coenzyme in >140 different enzymatic reactions which span into five of the six enzyme classes defined by the Nomenclature Committee of the International Union of Biochemistry and Molecular Biology (https://www.qmul.ac.uk/sbcs/iubmb/enzyme/) and corresponds to about 4% of all the classified enzymes in this database.[21,91,92] These 5 classes are: Oxidoreductase, transferase, hydrolase, lyase and isomerase.[91,92]

Part 2.5. Role of PLP in one-carbon metabolism

Some of the PLP-dependant enzymes that stand out and merits a lot of attention are the enzymes involved in one-carbon metabolism. One-carbon metabolism is a two-phase pathway that involves the exchange of one-carbon groups in homocysteine metabolism.[93,94] The first phase is remethylation, and consists of the transformation of homocysteine into methionine which can then form S-adenosylmethionine (SAM) by activation with ATP.[93] SAM can then be used as a methylation agent for a large amount of molecules such as proteins and DNA,[95] which produces S-adenosylhomocysteine (SAH) as a side product (which is a precursor to homocysteine).[93] The second phase is trans-sulfuration where cystathionine β-synthase, a PLP-dependant enzyme, condenses serine with homocysteine to form cystathionine, which can be hydrolysed, in a PLP-dependant fashion, by γ-cystathionase to form cysteine.[93] It is important to note that N-5-

methyltetrahydrofolate (5-MTHF) is needed for the remethylation since it is the source of the methyl group.[93] 5-MTHF is formed from tetrahydrofolate (THF) through the PLP-dependant enzyme serine hydroxylmethyltransferase (SHMT)[96]

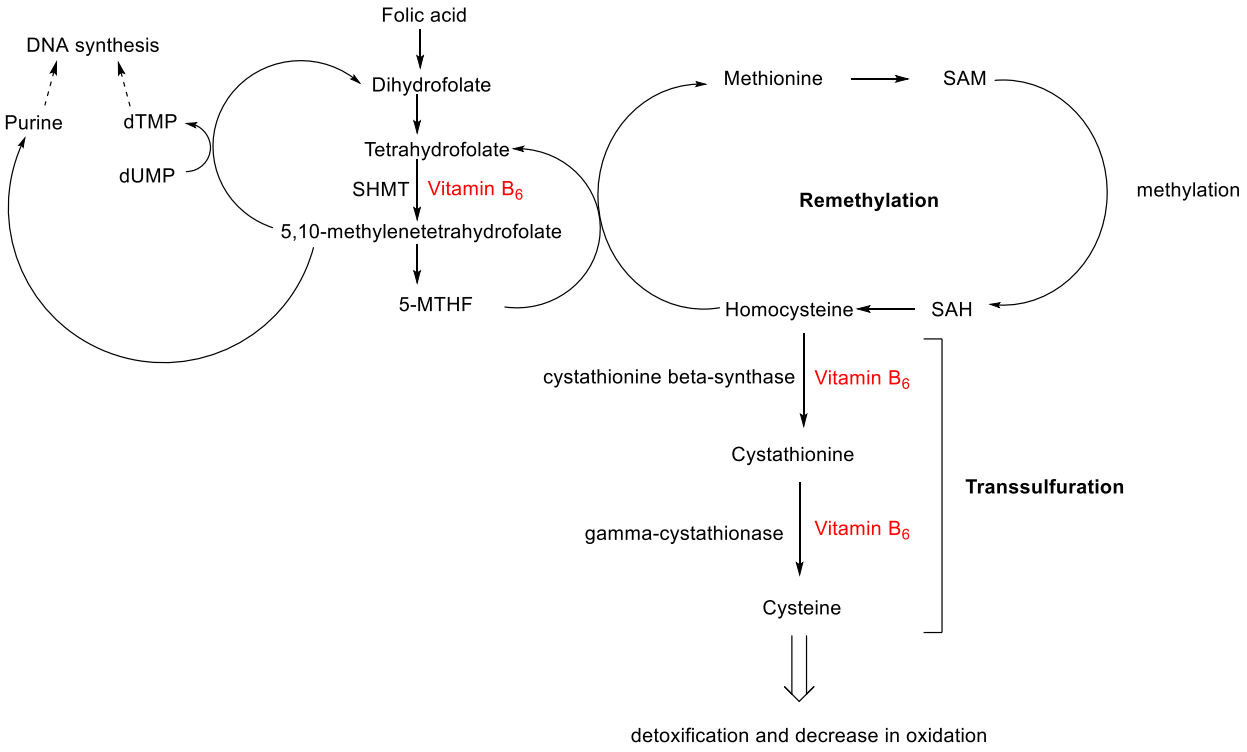

Figure 4. Representation of one-carbon metabolism. A figure representing the role of vitamin B_6 (in red) as a coenzyme in some of the enzymes involved in one-carbon metabolism, which is important for DNA methylation, antioxidation DNA synthesis and protection against carcinogens.[97–99] SHMT, serine hydroxylmethyltransferase; dTMP, deoxythymidylate monophosphate; dUMP, deoxyuridylate monophosphate; 5-MTHF, N-5-methyltetrahydrofolate; SAH, S-adenosylhomocysteine; SAM, S-adenosylmethionine. Modified with permission from Larsson, Giovannucci and Wolk, 2005.[96]

It has been demonstrated that vitamin B_6 deficiency results in an impaired one-carbon metabolism in animals.[100] Along with protection from carcinogens that can come with one carbon metabolism,[96,98,99] DNA methylation and changes in oxidative stress are also related with cancer progression.[101–103] This adds to the relationship between vitamin B_6 and carcinogenesis on top of the role of the vitamin in cellular metabolism.[104] On top of these biochemical functions as

coenzyme that closely links PLP with cancer, it also has been shown that the molecule can have effects in addition to its coenzyme role.

Part 2.6. Preclinical studies on vitamin B_6 and cancer

There is strong evidence that vitamin B_6 plays a role in biochemical functions related to carcinogenesis, such as cellular metabolism (notably one-carbon metabolism), antioxidation and toxic carbonyl reduction. Therefore, it is not surprising that in the early 1950s researchers had started to investigate the hypothesis that a change in vitamin B_6 metabolism could influence tumorigenesis and *vice versa*. In these pioneering preclinical studies, researchers demonstrated the anti-tumor progression effect of low systemic vitamin B_6 levels in immunodeficient rats and mice.[105,106] These observations have been strengthened by the studies conducted by Tryfiates and his colleagues in the 1970s that demonstrated that high proliferating malignant cells require a higher level of PLP due to their high metabolic demands.[107–110] Although antagonist agents of vitamin B_6 for tumor suppression had failed,[21,111–114] Tryfiates still believed and demonstrated that reducing vitamin B_6 could be used as a cancer treatment.[21,115] Researchers continued their efforts to study vitamin B_6 for cancer treatment and different type of evidence of the antineoplastic effect of the vitamin has been published. In the early 80s, Disorbo and colleagues showed that administration of vitamin B_6 *in vitro* can kill cancerous hepatoma rat cells[116] and inhibit the growth of cancerous melanoma cell lines.[117,118] This was followed by studies on *in vivo* administration of vitamin B_6, through injection or dietary addition, in tumor-bearing mice. These studies demonstrated that tumor progression was decreased in response to vitamin B_6 treatment.[119–122] Although this seems to be in contradiction with the observations from Tryfiates,[107-110, 115] these observations are due to the role of vitamin B_6 in immune response.[21] It has been demonstrated that low levels of vitamin B_6 are related to low immune response[123,124] and that diets rich in vitamin B_6 result in a higher immune response in both mice and humans.[125,126] Since an aberrant immune system contributes to tumorigenesis,[127] a highly effective immune response due to high levels of vitamin B_6 leads to decreased tumor formation. To add to these findings, it was demonstrated that in animal models of vitamin B_6 deficiency there is a significant increase in tumor progression and or incidence with virus induced tumors,[120,124] which goes hand in hand with studies that showed an inverse correlation between

levels of PLP and progression of virus induced tumors.[128] Altogether, these findings have led authors to believe that vitamin B_6 is required for immune response.[21]

Furthermore, it has been demonstrated that Pyridoxine works in unison with cisplatin to kill cancer cells *in vitro* and can also increase the sensitivity of cancer cells to different type of stress induced apoptosis.[129] In the same study, low PDXK levels was correlated to a poor prognosis in patients with non-small lung cancer.[129]

Part 2.7. Other roles of vitamin B_6 linked with cancer

Vitamin B_6 does not only play a role as a coenzyme but can also have biological effects on its own. Indeed, researchers have demonstrated that the vitamin can serve as a radical quencher[130,131]and as a scavenger of toxic carbonyl species.[131,132] It is believed that the free OH group on the 3-position of the pyridine ring is part of the reason for this activity.[133] That group can react directly with oxygen radicals and as been shown to be a good antagonist of singlet oxygen.[133] Another chemical property of pyridoxine that indirectly affects redox processes is its capacity to chelate metal ions, such as iron and copper.[134] When these ions are free, they can lead to cellular damage such as lipid peroxidation.[133] Finally, one vitamer of vitamin B_6, pyridoxamine, can play the role of carbonyl scavenger due to the amino group in the compound.[133] The role of free radicals and toxic carbonyl species in cancer is well known and described in many reviews.[101,135,136] One study by Dainin and colleagues demonstrated that hepatoma cells treated with pyridoxamine and H_2O_2 had improved survival rate as well as less carbonylated and aggregated proteins than cells treated with H_2O_2 only, which shows the role vitamin B_6 can play in cancer apart from its coenzyme activity.[137]

Another important role of vitamin B_6 is its capacity to work as a gene expression modulator. In fact, it has been shown that high levels of PLP decrease the transcriptional response usually activated by steroid hormones such as progesterone, estrogen and others.[138] It is known that these steroid hormones lead to changes in gene expression involved in growth and differentiation,[138] which make them directly involved in multiple types of hormone driven neoplasia.[139] Researchers have also shown that vitamin B_6 can change the protein expression in colon,[140] liver and nerve cells.[141] The link between the vitamin's ability to change gene expression and cancer has been shown in colon cancer, where Toya and colleagues found that some genes associated with cancer progression were modulated by vitamin B_6.[140]

In summary, other than its use as a coenzyme, vitamin B_6 can act as a radical quencher and gene expression modulator. These types of biological effects are linked to cancer progression. Therefore, vitamin B_6 doesn't necessarily need to act as a coenzyme to have an impact on carcinogenesis.

Part 2.8. Clinical Studies on vitamin B_6 and cancer

Due to the relationship between vitamin B_6 status and cancer cells demonstrated in preclinical studies, the hypothesis was that vitamin B_6 systemic status in cancer patients should differ from healthy patients. Indeed, as early as in the 1970s[21] researcher studied the levels of PLP or urinary 4-pyridoxic acid in tumor bearing patients. Researcher have been able to demonstrate that there is a vitamin B_6 deficiency in patients affected with cervical cancer,[142] breast cancer,[143] leukemia[144] and in cancer patients with a controlled nutrition (parenteral administration of vitamins, including B_6).[145] Baker and colleagues also demonstrated that vitamin levels are associated with cancer progression.[146] In their study they demonstrated that vitamin B_6 levels were 1.8-3.5-fold higher in colon carcinoma collected from autopsy compared to adjacent healthy tissue, but metastatic liver carcinoma from colon cancer had a 1.2-29 fold lower level of vitamin B_6 than normal healthy liver tissue.[146] This difference between early cancer cells and late-stage cancer cells can potentially be explained by the necessity of advanced cancer cells to avoid cell death (as discussed in figure 5).

Tryfiates and colleagues, which were among of the pioneers of preclinical research on vitamin B_6 and its relationship with cancer (see previous chapter), used their discovery of a new metabolite of pyridoxine in tumor-bearing rats, adenosine-N6-diethylthioether N1-pyridoximine 5' -phosphate,[147] in clinical research. The result of the clinical trials was that adenosine-N6-diethylthioether N1-pyridoximine 50 -phosphate is found in human tumors[148] and that the level is four times higher in the circulation of cancer patients compared to healthy patients.[149] In addition, the same metabolite was also found to differ between patients who respond to therapy compared to ones with progressive tumors by a 3-4 fold factor (higher in active tumors).[150] This is not the only study that demonstrate the difference in vitamin B_6 metabolism in cancer patients versus healthy patients as well as the difference in vitamin B_6 metabolism based on cancer progression. Like previously mentioned, Galluzi and colleagues showed that low PDXK levels was correlated to a poor prognosis in patients with non-small lung cancer.[129] Additionally, Potera

and colleagues found a significant difference in the levels of PLP in plasma between early cancer patients and patients with wide-spread disease.[143]

Part 2.9. Modern hypothesis on the role of vitamin B_6 in carcinogenesis

Some of the pre-clinical and clinical observations may seem contradictory, such as the need of vitamin B_6 in cancer cells because of their increased metabolism but low systemic levels of vitamin B_6 in cancer patients. However, Galluzi and colleagues have described a hypothesis that could explain the different findings[21] which is shown in the following figure.

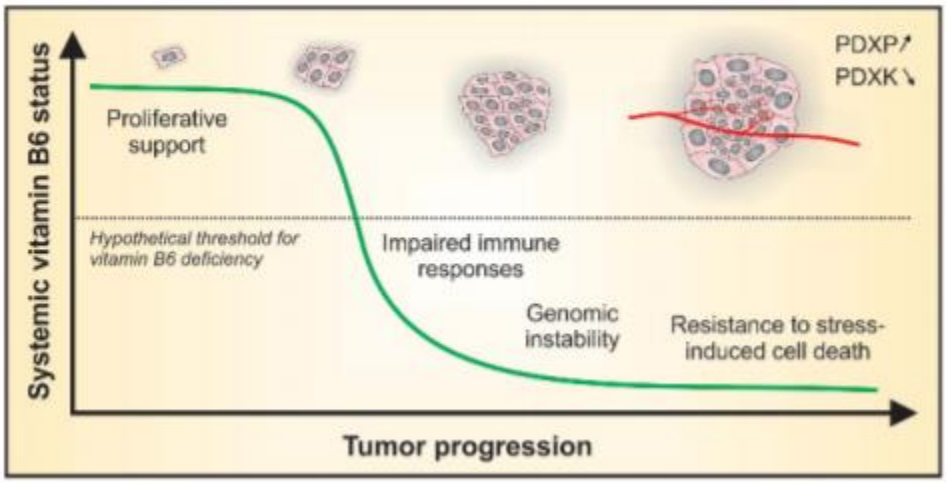

Figure 5. Relationship between vitamin B_6 and cancer. At first, new neoplastic cells need high PLP levels for their metabolic needs which in turn can cause a systemic decrease of vitamin B_6 levels. This can promote the progression of the tumor since vitamin B_6 is necessary for immune response and is important in one-carbon metabolism which is a huge factor in genetic stability. Finally, changes in vitamin B_6 metabolism such as changes in the PDXP and PDXK enzymes changes the ability of cancer cells to die under stress. Which means, more advanced cancers may benefit from less bioactive vitamin B_6 (decreased PDXK) to avoid cell death explaining the change in vitamin status from healthy, to neoplastic, to advanced cancerous cells. Taken from Galluzi and al. with permission.[21]

Further studies need to be done to confirm this hypothesis which makes the research on vitamin B_6 and its relationship with cancer very interesting and promising.

Part 2.10. Vitamin B_6 for cancer treatment and prevention

It shouldn't come as a surprise that with all these studies showing the role of vitamin B_6 in cancer, researchers have tried to use this as a cancer treatment or prevention. However, the studies done so far didn't have the expected results. One of the first example of such an attempt was in 1977 where Pyridoxine administration was tested against bladder cancer patients[151] but the authors did not find a difference between tumor recurrence in the placebo group and PN group. In a recent meta-analysis of randomized controlled trials on vitamin B_6 supplementation effect on cancer risk and death, the only effect of vitamin B_6 supplementation was seen for skin cancer (significant decrease risk with vitamin B_6 supplementation).[152] Although some studies have shown some role of vitamin B_6 for cancer risk reduction, inconsistent findings have led some authors to the conclusion that these results are due to the interaction of vitamin B_6 and other nutrients.[21,153]

Still, one cannot deny the relationship previously discussed between cancer and vitamin B_6 status. Perhaps vitamin B_6 cannot be used exogenously to treat or prevent cancer, but that doesn't necessarily mean that it cannot be used as a biomarker for cancer diagnosis.

Part 2.11. Vitamin B_6 for cancer diagnosis

As of now, even if vitamin B_6 has been studied thoroughly in cancer and has been tried for cancer treatment and prevention, there has been no attempts to use vitamin B_6 as a cancer diagnostic tool. Therefore, the current project aims to study vitamin B_6 as a new cancer diagnostic and possibly staging tool due to the difference of vitamin B_6 metabolism in new cancer cells as well as advance cancer cells compared to each other and healthy cells. The proposed method for this is to synthesize a radioactive analog of the vitamin in order to image it using positron emission tomography (PET). The next chapter will describe this imaging technique and the reasoning for the proposed radiotracers.

Part 3. Positron Emission Tomography (PET) imaging

Positron emission tomography, or PET for short, is a molecular imaging technique that is frequently used to diagnose, monitor and stage disease.[154] It is a powerful tool especially known in its application in cancer and has now become a staple in clinical practices in cancer management due to its reproducibility, sensitivity, lack of side effects and wide range of

information given from a single scan from stage of disease to response to treatment.[155] PET imaging has grown in importance over the last decades due to the large number of possibilities for imaging that comes from new compounds as well as new biochemical pathways to study.

Part 3.1. PET imaging: how it works

PET is an imaging technique that is based on the detection of co-incident photons created from an annihilation event between a positron and an electron.[156] The first and most important aspect of PET imaging is the source of these positrons. Positrons are the antiparticles of electrons and can be understood as electrons with a net positive charge.[157] Positrons are the result of beta (β+) decay which takes place in certain unstable nuclei where the ratio of protons and neutrons is not optimal,[158] also called a radionuclide. In beta decay, a proton releases a positron and a neutrino to become a neutron.[158] This positron is very unstable and if it comes into contact with an electron, it creates an annihilation process in which two photons of the same energy (511 keV) are ideally emitted at an angle of 180°.[157] PET scanners detect these photons based on their energy and have coincidence detectors to detect a pair of photons hitting opposite detectors at the same time.[156] Several other processes are needed to be done to exclude single photons from two different annihilation events or to take into considerations photons that are deflected form their original path as well as other problems encountered.[156] One of the problems with PET imaging is spatial resolution. Modern PET scanners can achieve 4-6 mm spatial resolution which is due to multiple factors such as photon range (distance covered by positron between origin point and annihilation point) amongst others.[156] However, PET imaging is highly sensitive, non-invasive, 3-dimensional and does not cause any side effect[156] and is therefore a very powerful imaging tool.

PET imaging requires the introduction of a radioactive imaging agent into the imaging subject. These agents can span from small chemical compounds, to large proteins[159] and are labeled with radioactive nuclides such as ^{11}C, ^{18}F and others. The most used radionuclide in PET imaging is ^{18}F[159] mostly due to its use in 2-[^{18}F]fluoro-2-deoxy-d-glucose ([^{18}F]FDG) which is by far the most used PET agent.[159] However, ^{18}F is also considered the radionuclide of choice since it has a good half-life of 110 minutes, which is long enough for synthesis purposes but short enough to decay out of the patients bodies in a respectable time,[159] the shortest photon range of all positron emitters giving it the most spatial resolution in PET imaging[159] and a high positron decay ratio

(97%) and low energy (0.635 MeV max).[160] In addition, the C-F bond which is usually implemented in radiolabeling is very strong and fluorine is a good bioisoteric replacement for hydrogen since it has the same size and will unlikely change bioavailability of a known drug.[160]

Part 3.2. Current cancer PET imaging agents and limitations

FDG was synthesized in the late 1970s but wasn't applied for cancer detection until the 1990s.[161]The strength behind FDG PET is largely due to the metabolic trapping of the radiotracer. FDG acts very similarly to glucose in that after injection, it is transported to tissue by a glucose transporter.[159,161] Once in the tissue, it gets phosphorylated by a hexokinase but in contrast with glucose, the FDG-6-phosphate cannot be used in glycolysis since it doesn't have a 2'-hydroxyl group[159,161] and hence is trapped in the cell. The amount of FDG trapped in the cell is correlated to the blood-tissue transport and hexokinase activity, which represents the cellular need for high glucose to power high metabolic rates.[159] Therefore, cancer can be differentiated from healthy tissues due to their increased metabolism, which will result in higher FDG uptake and higher radioactivity in these regions.[162] FDG PET is currently used for detection of recurrent head, neck, colorectal cancer and lymphoma,[163] for staging of breast cancer, advanced melanoma, bladder cancer, NSCLC as well as staging and restaging of lymphoma.[163] However, there are some limitations to the use of FDG. Firstly, FDG cannot differentiate between tissues with high uptake due to cancers versus tissues with high uptake due to other factors such as infection or inflammation.[162] Secondly, not all neoplastic tissue have high metabolic rates and therefore cannot be diagnosed by FDG.[162] Finally, the state of the patient can affect FDG uptake such as fasting and insulin administration before the PET scan.[164]

Because of these pitfalls, several radiotracers for PET carcinogenesis imaging have been developed over the past decades as alternatives or additional tools to FDG.[162] Some examples of the most successful imaging agents are 3′-deoxy-3′-[^{18}F]fluorothymidine (FLT),[161,165] ^{18}F-Fluoroestradiol (FES),[166] ^{11}C-choline[167] and ^{18}F-fluoroetanidazole (FETA)[167] amongst others. These radiotracers all have in common a target associated with cancer. ^{18}F-FLT is a radiotracer analog of thymidine, which measures DNA replication.[161,165] The positive aspects of FLT versus FDG is that it is less affected by inflammation[161] and can be used to measure response to cytostatic treatment of tumors, which are agents that stop growth but may not kill tumors.[167] However, FLT uptake in tumor is low which means that the sensitivity of FLT is also low and

there can be false positives due to sites of high proliferating cells such as active lymph nodes.[167] ^{18}F-FES is an imaging agent used to target estrogen receptors which can be used for treatment decisions and prognosis.[166] Although FES is a very powerful tool since it is specific to the estrogen receptor, it cannot be used for diagnosis of most carcinomas that may not express these receptors.[166] ^{11}C-choline is an agent that tracks lipid synthesis necessary for cell membranes, which is a process that is overactivated in neoplastic cells.[167] This radiotracer is very powerful for the imaging of prostate cancer, especially to differentiate between benign and malignant tumors[168] and has the advantage compared FDG to have low activity in urine, which makes it well-suited for imaging pelvic malignancies.[167,168] However, just like FDG, choline can have high accumulation where there is inflammation.[169] These are just a few examples of the PET agents made in the last decades that have been successful due to their ability to have additional information or different information than a traditional FDG scan. Since cancer is the leading cause of mortality worldwide and the cases of cancer incidence as well as cancer death are expected to grow,[170] it is important to add to the current toolbox of diagnosis, prognosis, staging and treatment management tools in order to limit the number of cancer related death.

Part 3.3. Concepts for the development of new radiotracers

Although new radiotracers for use in PET imaging have been an important field of research recently, the development of new radiotracers is not trivial. There are multiple barriers that need to be overcome when developing a new radiotracer. One of the most important aspects of a radiotracer is its physiochemical properties, which are its Absorption, Distribution, Metabolism and Excretion (ADME)[171] because this will determine how it can reach its biological target *in vivo*. When dealing with new compounds, researchers must be aware and sometimes must measure these properties for the validation of their radiotracers. A great radiotracer *in vitro* can be abandoned because of bad physiochemical properties. The compounds need to have a suitable labelling site and this is usually done by substituting an element in the structure by its radioisotope, but other techniques exist and have been successful, such as substituting a hydrogen for ^{18}F (successful for FDG) since these are conservative substitutions.[172] Once a suitable labelling site has been found, the synthesis of the "cold standard" or the non-radioactive compound, as well as its characterization, is done first.[171] Once this is done, a precursor for radiosynthesis is usually synthesized; a precursor permits the radiolabelling to be at the end of

the synthesis, which can increase yield and decreases radioactivity exposure to chemists.[171] The choice of precursor is usually made in combination with radiosynthesis method.[171] Once the radiotracer is synthesized and characterized, it needs to be tested for its sensitivity and specificity as well as *in vivo* stability and biodistribution.[171,172]

Part 4. Vitamin B_6 modification: synthesis of 6 and 2' derivatives

As discussed previously, in order to transform vitamin B_6 into a radiotracer, it must be modified by replacing one of its hydrogens with fluorine-18. However, before trying to do any radiochemistry (installing fluorine-18), the cold standard must be synthesized. The cold standard is the cold equivalent (containing fluorine-19) of the radiotracer. As discussed in the next section, the proposed radiotracers are [^{18}F]6-Fluoropyridoxine and [^{18}F]6-Fluoropyridoxine. Therefore, the respective cold standards are 6-Fluoropyridoxine and 2'-Fluoropyridoxine. In order to have a better idea on the synthesis methodology which will be used to synthesize these cold standards, the scientific literature was reviewed for syntheses of 6 and 2' pyridoxine derivative, with emphasis on syntheses of 6-Fluoropyridoxine and 2'-Fluoropyridoxine. It was found that 6-Fluoropyridoxine has been previously synthesized in 1973[113] and again in 1998.[173] Both syntheses use the Balz-Schiemann reaction to transform 6-Aminopyridoxine into 6-Fluoropyridoxine, the difference being that the 1998 article uses HF/pyridine instead of HBF_4. Fluorine isn't the only halogen which was added to the 6-position. In fact, in the 1973 article from Korytnyk and Srivastava the authors synthesized 6-Chloropyridoxine and 6-Bromopyridoxine from 6-aminopyridoxine.[113] 6-iodopyridoxine has also been synthesized more recently by Mason and coworkers in one step from pyridoxine hydrochloride.[174] Other research articles have modified the 6 position of pyridoxine but also modified other positions (not a selective modification) which is not useful in the proposed project. For 2'-Fluoropyridoxine, no published synthesis was found. However, there are published methods to modify the 2' position of pyridoxine. For example, Adamczyk and colleagues have synthesized a 2'-alcohol derivative of pyridoxine.[175] The synthesis of this derivative was possible by protecting the three alcohol groups of pyridoxine, followed by oxidation and then a Boekelheide reaction to give the alcohol. There are no published synthesis of common radiochemistry precursors such as tosyl or triflate precursors at the 6 and 2' position.

Part 5. Objectives and hypothesis

The relationship between vitamin B_6 status and carcinogenesis has been explored in depth as well as up-to-date research on the use of vitamin B_6 for treatment and/or prevention of cancer. Although the literature on vitamin B_6 for treatment and prevention of cancer is not consistent, the fact is that the changes in vitamin B_6 status with neoplasia as well as different status based on progression and prognosis of cancers is an important aspect of our understanding of this disease and should be taken advantage of. Fortunately, there exists a powerful molecular imaging tool that we can use to quantitively measure whole body distribution and metabolism of chemical compounds, Positron Emission Tomography (PET). Therefore, the research project proposed consists of the synthesis, characterization and evaluation of radiolabelled analogs of vitamin B_6 for use in PET imaging as cancer diagnostic, staging and prognostic tools.

Part 5.1. Objectives

The following research project has two main objectives:

i) The first objective will be to synthesize the fluorine-18 radiotracer analogs of pyridoxine as well as their respective cold standards shown in the figure below.

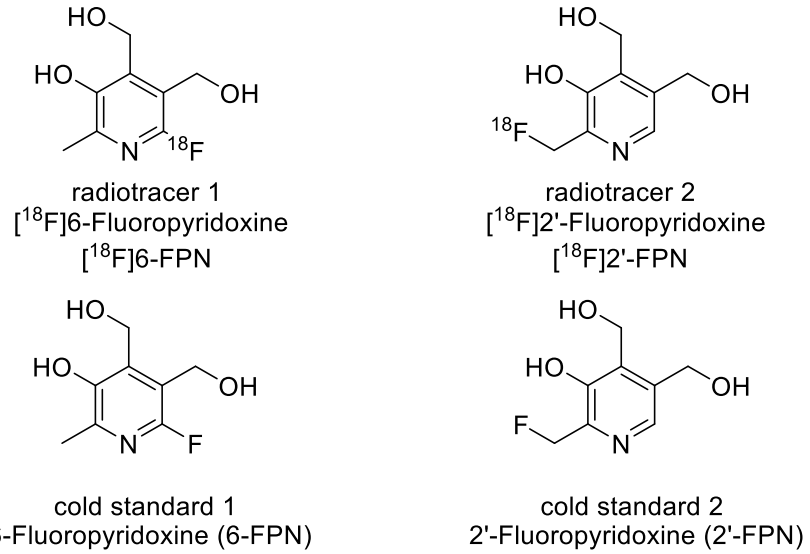

Figure 6. Chemical structures of the proposed radiotracers and their respective cold standards.

The first step in this will be the synthesis, purification and characterization (NMR, mass spec, melting point etc.) of the cold standards. Once the pure characterized cold standards are in hand, an HPLC method for both compounds will be established for further use in radiosynthesis (verification of purity by co-injection).

The second step in this is radiosynthesis, purification and characterization (HPLC co-injection with cold standard, specific activity).

ii) The second objective will be to evaluate the serum stability (human and mice) of the radiotracers. Any metabolites present in substantial amounts will be characterized (NMR, LC-MS).

The first step of this objective would be to evaluate the radiotracer *in vivo* with healthy mice to determine the biodistribution, areas of high background, clearance route and rate, and unwanted activity such as bone uptake.

The second step will be to evaluate the radiotracers ability to distinguish tumor sites in mice models of breast and lung cancer.

The last step will be to evaluate the radiotracers ability to distinguish between tumor stage and aggressiveness in mice models of breast and lung cancer.

Part 5.2. Proposed methodology and hypothesis

The proposed methodology and expected results for the previously listed objectives are as follow

i) The synthesis of the cold standard can be done following already published methods or standard fluorination techniques (scheme 1). 6-Fluoropyridoxine (cold standard 2) has already been synthesized by Korytnyk and Srivastava[113] from vitamin B_6 and other methods have been showed for fluorination of the 6-position of pyridoxine compounds.[176] Suitable 6-halogen precursors for radiochemistry can be synthesized following the same chemistry[113] or can be modified to a trimethylammonium precursor using known chemistry (scheme 2).[177] 2'-Fluoropyridoxine has not been reported in the literature but there is known chemistry to modify the 2' position of

pyridoxine[178] in order to make a suitable precursor for cold and radiochemistry (scheme 3, scheme 4).

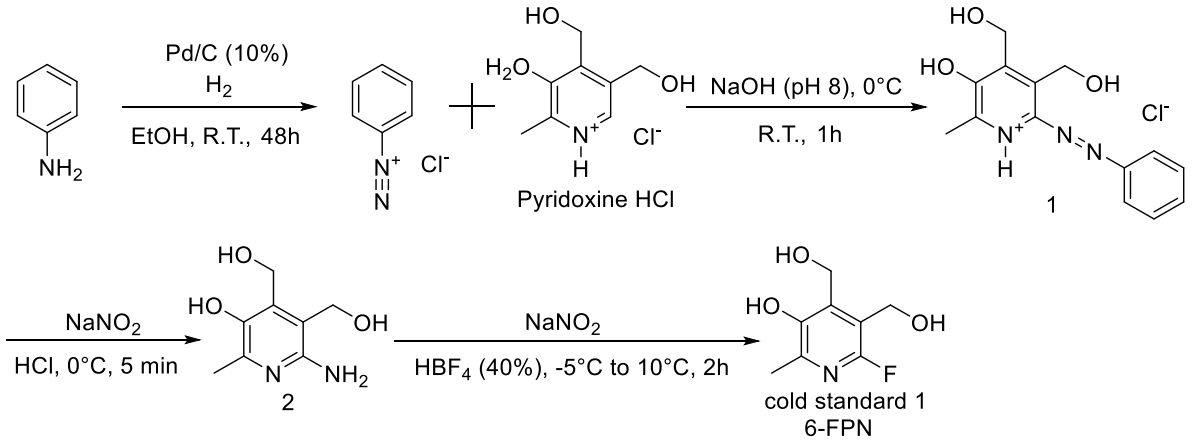

Scheme 1. Proposed synthesis of cold standard 1, 6-Fluoropyridoxine (6-FPN). The synthesis and characterization of compound 1 and 2 has been recorded by Culbertson and colleagues.[179] The fluorination of compound 2 to 6-FPN has been previously published by Korytnyk and Srivastava.[113]

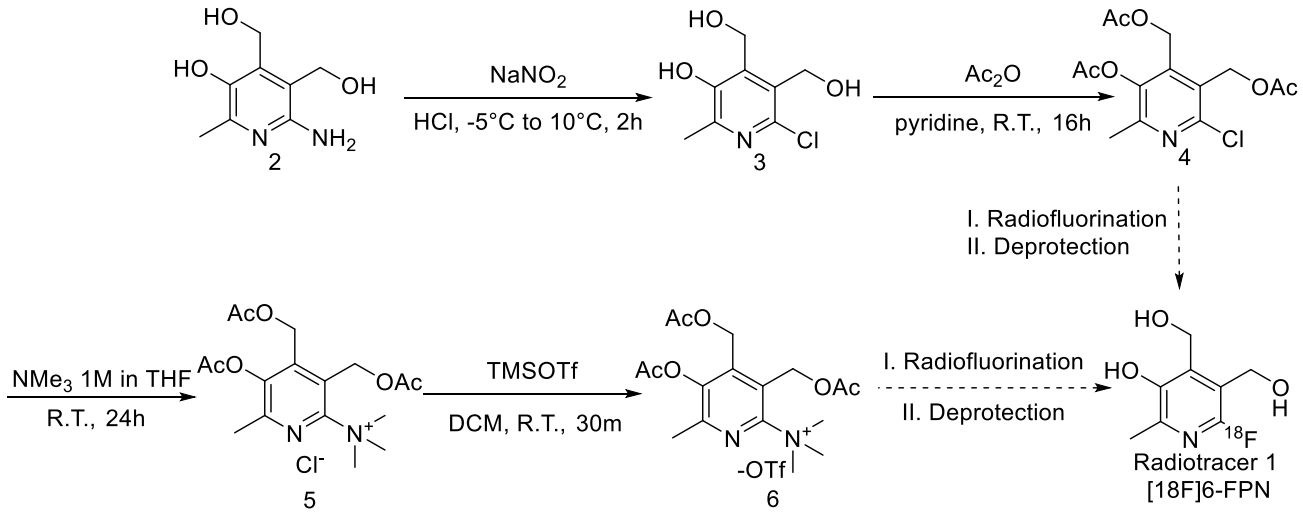

Scheme 2. Proposed synthesis of radiotracer 1, [^{18}F]6-Fluoropyridoxine ([^{18}F]6-FPN). Compound 2 synthesized as shown in scheme 1 can be chlorinated following a similar methodology to fluorination.[113] Compound 4 can be obtained by simple acetic anhydride protection. Compound 4 can be used directly as a precursor or can be modified using known procedures to compound 6[177] which is another possible precursor for radiotracer 2. Multiple radiofluorination methods could be explored starting with typical methods already successful for the radiofluorination of the 6-position of pyridine rings from chloro or trimethylamine salt precursors such as K_2CO_3/Kryptofix 222 in DMSO[180] at high temperatures or $TBAHCO_3$ in MeCN/t-BuOH at moderate temperatures[181] amongst others. The radiofluorination would be followed by deprotection, which usually consist of stirring with base (NaOH) or acid (HCl) at high temperature for a short period of time.[182]

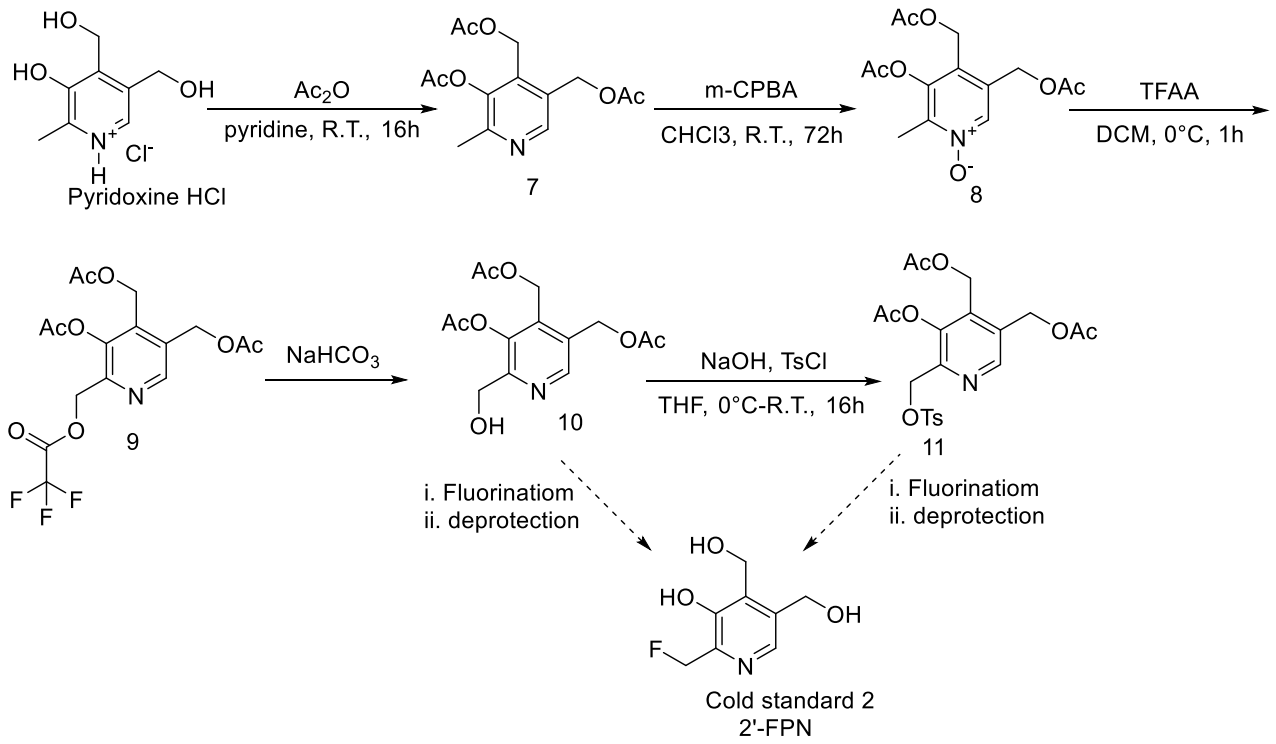

Scheme 3. Proposed synthesis of cold standard 2, 2'-Fluoropyridoxine (2'-FPN). Compound 9 can be synthesized following the described steps. Compound 10 could be fluorinated using known chemistry such as DAST.[183] Compound 11 can be fluorinated by standard fluorination techniques such as KF/Kryptofix 2.2.2 and CsF.[184] Deprotection of the acetyl group can be done using acid at high temperatures.[182]

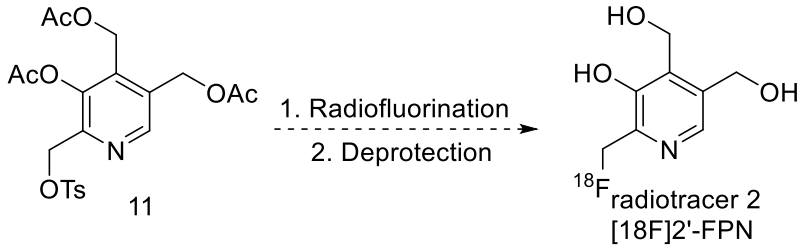

Scheme 4. Proposed synthesis for radiotracer 2 [^{18}F]2'-Fluoropyridoxine ([^{1}8F]2'-FPN). Radiotracer 1 can be synthesized from precursor 11 (synthesis shown above in scheme 3). Standard radiofluorination methods such as K^{18}F and Kryptofix at high temperatures can be used and followed by acid at high temperature for the deprotection.[182,184]

Chapter 2. Experimental procedures

Part 1. General information

Materials: Trifluoromethanesulfonic acid, Trifluoromethanesulfonic anhydride and Sodium Fluoride (II) were purchased from Alfa Aesar. PBSF, Tetrabutylammonium fluoride hydrate and Trimethyl amine (2 M in THF) were purchased from Oakwood. 4-methoxybenzyl chloride (95% with potassium carbonate added as stabiliser) was purchased from Matrix Scientific. TMAF was purchased from Synquest. 2-adamantanone, 1,2-dichloroethane, malonic acid, sodium cyanoborohydride, sodium triacetoxy borohydride and TBDMSCl were borrowed from other labs. All other chemicals were obtained from Sigma Aldrich and Fisher scientific.

Instrumentation: Proton Nuclear Magnetic Resonance (^{1}H NMR) spectra, Fluorine Nuclear Magnetic resonance (^{19}F NMR) and Carbon Nuclear Magnetic resonance (^{13}C NMR) were recorded on a Bruker Advance 300 equipped with a cryoprobe (300, 282 and 75 MHz respectively) or a Bruker Advance 600 equipped with a cryoprobe (600, 282 and 150 Mhz respectively). Chemical shifts for protons are reported in parts per million and are referenced to residual protium in the NMR solvent ($CHCl_3$ = δ 7.26 ppm, D_6-DMSO = δ 2.50 ppm, CD_3OD = δ 3.31 ppm). Chemical shifts for carbon are reported in parts per million downfield from and are referenced to the carbon resonances of the solvent residual peak (CDCl3 = δ 77.16 ppm, D_6-DMSO = δ 39.52 ppm, CD_3OD = δ 49 ppm). Chemical shifts for fluorine are reported in parts per million and are referenced to $CFCl_3$ (δ 0 ppm). NMR data are represented as follows: chemical shift (δ ppm), multiplicity (s = singlet, d = doublet, t = triplet, q = quartet, p = pentet, hept = heptet, m = multiplet,). All NMR spectra were taken at 25 °C. High-resolution mass spectra were obtained on the Kratos Concept Mass Spectrometer for electron impact (EI) mass spectrometry or an Micromass Q-TOF I Mass Spectrometer for electrospray ionisation (ESI) mass spectrometry. High-performance liquid chromatography (HPLC) was performed on a Shimadzu LC-20 instrument with a binary pump and a diode array detector.

Part 2. Radiochemistry attempt on 6-Chloropyridoxine triacetate

HPLC analysis (appendix 1) - For the HPLC analysis a Luna Omega 5µm polar C18 100A LC column 150x4.6 mm was used. The oven temperature was set at 40 °C oven and the flow rate at 2 mL/min. A gradient elution starting at 100% water (solvent A) and 0% acetonitrile (solvent B)

for the first 30 minutes was used, then increased to 50% of acetonitrile in 7 minutes followed by 5 minutes at 50% then dropped back down to 0% acetonitrile, at which it stayed for the remaining 10 minutes.

^{18}F-TEAF radiofluorination General procedure

Using 3-5 mg of precursor, we use standard KF methodology in order to make [^{18}F]TEAF. Waters QMA light was preconditioned with 10 mL Ethanol, 10 mL 0.5 M $NaHCO_3$, 10 mL H_2O. GE PETtrace cyclotron $^{18}O(p,n)^{18}F$ reaction was run with 2.5 mL of [^{18}O]H_2O in target irradiated at 55 micro Amps for 2-5 minutes (82-394 mCi). After trapping on QMA fluoride was eluted with a solution of 10 mg of NEt_4HCO_3 in 0.5 mL H_2O. 1 mL MeCN was added and the solution was heated at 100 °C for 5 minutes with vacuum. Then, it was heated another 5 minutes with vacuum and argon flow. Then, the precursor dissolved in 0.5 mL DMF was added and the reaction was stirred at 130 °C for 30 minutes.

^{18}F-TEAF radiofluorination with HCl deprotection

The general procedure for ^{18}F-TEAF radiofluorination was followed with 4.1 mg of precursor, using 162 mCi of radioactivity. After the 30 minutes, a solution of 2 M HCl in H_2O was added and stirring at 110 °C for 20 minutes was followed. The solution was then transferred to the product vial. The reactor was washed with 2 mL of water and this wash water was also transferred to the product vial.

^{18}F-TEAF radiofluorination without deprotection

The general procedure for ^{18}F-TEAF radiofluorination was followed with 3.2 mg of precursor, using 82 mCi of radioactivity. The reactor was washed with 2 mL of MeCN and this wash MeCN was also transferred to the product vial.

Part 3. Fluorination attempts of compounds 11 and 21

Fluorination using $TBAF(Pin)_2$ general procedure: Compound 11 (23.2 mg, 0.05 mmol, 1 equiv.) was added to an oven dried microwave reaction vial equipped with a stir bar with $TBAF(Pin)_2$ (55.1 mg, 0.1 mmol, 2 equiv.). The solids were degassed under nitrogen and then dissolved in anhydrous MeCN (0.157 M, 0.32 mL). The solution was stirred under nitrogen at 80 or 50 °C for 16 hours. The mixture was transferred to a round bottom flask and the solvents were removed

with rotary evaporation. The crude product (30% of the reaction mixture) was dissolved in $CDCl_3$ and was analysed by HPLC and ^{19}F NMR (64 scans).

Fluorination using TBAF general procedure: Compound 11 (23.2 mg, 0.05 mmol, 1 equiv.) was added to an oven dried microwave reaction vial equipped with a stir bar. The solid was degassed under nitrogen and then TBAF 1 M solution in THF (3 equiv., 0.15 mmol, 0.15 mL) was added. The solution was stirred at 50, 80 or 110 °C for 16 hours. The mixture (whole) was dissolved in $CDCl_3$ and was analysed by HPLC and ^{19}F NMR (64 scans).

Fluorination using KF general procedure: Compound 11 (23.2 mg, 0.05 mmol, 1 equiv.) was added to an oven dried microwave reaction vial equipped with a stir bar. KF (3 equiv., 0.15 mmol, 8.7 mg) and Kryptofix (3 equiv., 0.15 mmol, 56.5 mg) were added to the flask. The solids were degassed under nitrogen and then dissolved in anhydrous DMSO (0.1 M, 0.5 ml). The solution was stirred at 100 or 120 °C for 16 hours. The mixture (50% of the solution) was dissolved in D_6-DMSO and analysed with HPLC and ^{19}F NMR (64 scans).

Fluorination using CsF general procedure: Compound 21 was put in an oven dried microwave reaction vial equipped with a stir bar along with CsF. The solids were degassed under nitrogen, and dissolved with tBuOH (0.1 M). The reaction was stirred for 20 minutes under nitrogen at high temperature (90, 120 or 150 °C). The mixture was transferred to a round bottom flask and the solvent removed by rotary evaporation. The resulting black solid was analysed by ^{19}F NMR (64 scans) in $CDCl_3$ and HPLC.

Fluorination using KF general procedure: Compound 21 was put in an oven dried microwave reaction vial equipped with a stir bar along with KF. The solids were degassed under nitrogen, and dissolved with DMSO (0.1 M). The reaction was stirred for 60 minutes under nitrogen at high temperature (80, 100 or 120 °C). The mixture (50% of the solution) was dissolved in D_6-DMSO and analysed by ^{19}F NMR (64 scans) and HPLC.

Part 4. Fluorination attempt of alcohol 25

Compound 25 (1 equiv.) was dissolved in anhydrous solvent (0.2 M). The solution was cooled down in an ice bath. Triethyl amine (1.5 equiv.) was added along with either Tosyl Chloride (1.5 equiv.) or Tosyl Fluoride (1.5 equiv.) and an additive in some cases. The reaction mixture was warmed to an established temperature. The reaction was stirred for several hours. HCl (1 M, 6

mL) was added and the organic layer was extracted out. The aqueous layer was extracted with DCM (6x8 mL). The combined organic layers were washed with 2x35 mL brine. The combined organic layers were dried with Na_2SO_4, filtered, and evaporated to dryness.

Experiment with TsF at room temperature: The solvent used was DCM. DMAP (5 mol%) was added as additive. The reaction was stirred at room temperature 16 hours.

Experiment with TsF at 70 °C: The solvent used was chloroform. No additives were added. The reaction was stirred at reflux (70 °C) for 5 hours.

Experiment with TsF at 100 °C: The solvent used was DMF. No additives were added. The reaction was stirred at 100 °C for 5 hours.

Experiment with TsCl at room temperature: The solvent used was DCM. TBAF (1.5 equiv.) was added as the fluorination agent. The reaction was stirred at room temperature 16 hours.

Part 5. HPLC methods for analysis of reactions

HPLC general procedure: For the HPLC analysis a Luna Omega 5µm polar C18 100A LC column 250x4.6 mm was used. The oven temperature was set at 40 °C and the flow rate at 1 mL/min. HPLC grade water (containing 0.1% Trifluoroacetic acid) and HPLC grade acetonitrile (containing 0.1% trifluoroacetic acid) were the solvents A and B, respectively.

Method 1 (polar short method): The starting concentration of solvent A and B were equal (50/50). The concentration of solvent B was increased over 20 minutes to 100% (linearly) and kept at 100% for 2 minutes afterwards dropping immediately back to 50% (total 22 minutes)

Method 2 (polar long method): Solvent B starting concentration was 30% and increased to 100% over 30 minutes (linearly) and was kept at 100% for 5 minutes afterwards dropping immediately back to 30%, staying at this concentration for 5 more minutes (total 40 minutes)

Method 3 (non-polar): Solvent B starting concentration was 1% and was increased to 100% over 25 minutes (linearly) and was kept at 100% for 5 minutes afterwards dropping immediately back to 1% and staying at 1% for another 5 minutes (total 35 minutes)

Part 6. Experimental procedure for synthesis (and optimization) of chemical compounds

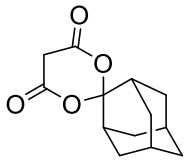

Spiroadamantyl-1,3-dioxane-4,6-dione (SPIAd): Procedure based on a literature report.[185] Malonic acid (360.5 mg, 2.4 mmol, 1 equiv.) and 2-adamantanone (250 mg, 2.4 mmol ,1 equiv.) were dissolved in acetic anhydride (0.31 mL). Sulfuric acid (4.8 µL) was added and the mixture was stirred at room temperature for 8 hours. The crude oil was dissolved in a minimum amount of EtOAc, then cold hexanes was added. Crystals were filtered and the solid was dried under vacuum. The yield of crystals was 60%. ^{1}H NMR (300 MHz, $CDCl_3$) δ 1.75-1.82 (m, 6H); 1.92 (s, 2H); 2.12-2.20 (m, 6H); 3.61(s, 2H). ^{13}C NMR (75 MHz, $CDCl_3$) δ 26.2, 33.6, 36.6, 36.8, 37.8, 109.8, 163.2 MS (ESI) Mass calc for $[C_{13}H_{15}O_4]^-$: 235.0971, found: 235.23

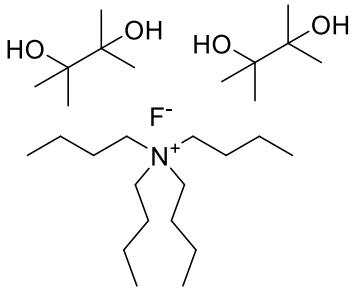

Tetrabutylammonium fluoride bispinacol (TBAF(Pin)$_2$) : Synthesis using the procedure describe by the Gouverneur group.[186] 315.5 mg of tetrabutylammonium fluoride trihydrate (1 mmol, 1 equiv.) and 236.3 mg of pinacol (2 mmol, 2 equiv.) were added to an oven dried round bottom flask equipped with a stir bar. The solids were degassed under nitrogen and were then dissolve in anhydrous hexanes (30 mL). The solution was stirred under hard reflux (90 °C) for 2 hours. The solution was cooled to room temperature and the solution was filtered. The solids were washed with excess hexanes and dried under high pressure. The salt was a white solid and the yield obtained was 65%. ^{1}H NMR ($CDCl_3$, 300 MHz) δ 0.97 (t, 12H, J= 7.4 Hz); 1.16 (s, 24H); 1.41 (sx, 8H, J= 7.3 Hz); 1.56-1.66 (m, 8H); 3.25-3.30 (m, 8H). ^{13}C NMR ($CDCl_3$, 75 MHz) δ 13.8, 19.8, 24.1, 25.3, 58.7, 74.7

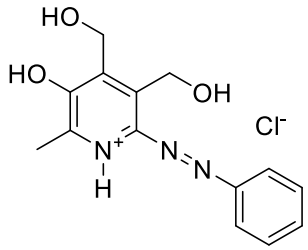

6-Phenylazopyridoxine hydrochloride, 1 – Synthesized using a similar procedure described by Culbertson, Enright and Ingold.[179] 2.118 g (10.3 mmol, 1 equiv.) of Pyridoxine hydrochloride was dissolved in 50 mL deionized water in a 250 mL Erlenmeyer. The solution was adjusted to pH 8 with 2.5 M NaOH, equipped with a stir bar, then placed in an ice bath. In a 25 mL round bottom flask equipped with a stir bar, 1 equivalent of aniline (0.94 mL) was combined with 10 mL 6 M HCl and cooled down to 0 °C. In a separate 10 mL flask, $NaNO_2$ was dissolved in 2 mL deionized water and the solution was cooled down to 0 °C. The cooled down $NaNO_2$ was added portion wise to the aniline solution at 0 °C to perform diazotization. The diazotized aniline solution was then added portion wise to the pyridoxine solution at 0 °C while maintaining pH 8 by subsequent additions of 2.5 M NaOH. Once addition was finished, the solution was allowed to warm up to room temperature and was stirred 2 hours, protected from light. Once the reaction was done, the pH was adjusted to 3 with 6 M HCl and the solution was placed on ice to crystallise. The reaction mixture was filtered and the precipitate was washed with ethanol. The precipitate was then dried under vacuum to give pure compound 1 as a red solid in 69% yield. ^{1}H NMR (300 MHz, CD_3OD) δ 2.50 (s, 3H); 5.24 (s, 2H); 5.21 (s, 3H); 7.50-7.57 (m, 3H); 7.97-7.98 (m, 2H) ^{13}C NMR (75 MHz, D_6-DMSO) δ 19.4, 54.7, 56.9, 122.6, 129.4, 131.1, 133.1, 133.8, 146.0, 150.9, 152.6, 152.9 MS (EI) Mass calc for $[C_{14}H_{15}N_3O_3]^+$: 273.113, found: 273.1113

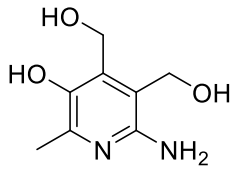

6-Aminopyridoxine hydrochloride, 2- Synthesized using a similar procedure described by Culbertson, Enright and Ingold.[179] 1.161 g of 6-Phenylazopyridoxine hydrochloride (compound 1, 3.75 mmol, 1 equiv.) was dissolved in 90 mL 99% EtOH in a 200 mL round bottom flask equipped with a stir bar. 150 mg of palladium on carbon (10 weight %) was added to the

solution. The solution was put under vacuum for 20 minutes, then put under hydrogen using a balloon. The solution was stirred under hydrogen in the dark for 20 hours. The solution was filtered through celite and the celite bed was washed with warm ethanol/water 8:2 (several washes, around 150 mL total). Collection of the product was followed by UV (blue fluorescence). The solvent was removed by rotary evaporation to give a dark brown solid. The crude solid was purified by silica column chromatography using 90/9/1 CH_2Cl_2:MeOH:NH_4OH (90 mL silica), the fractions containing product combined and the s olvent removed by rotary evaporation to give the pure amine product as a yellow solid in 95% yield. ^{1}H NMR (300 MHz, d_6-DMSO) δ 2.18 (s, 3H); 4.39 (d, 2H, J=5.18 Hz); 4.60 (s, 2H); 4.81 (t, 1 H, J= 5.36 Hz); 5.03 (s, 2H); 5.22 (bs, <1H); 7.96 (bs, <1H). ^{13}C NMR (75 MHz, d_6-DMSO) δ 19.0, 55.7, 56.1, 115.9, 135.8, 141.2, 142.9, 151.6. MS (EI) Mass calc for $[C_8H_{12}N_2O_3]^+$: 184.0848, found: 184.08496

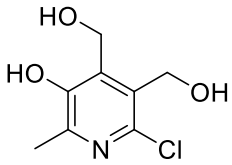

6-Chloropyridoxine, 3 – 107.8 mg of compound 4 (0.327 mmol, 1 equiv.) was dissolved into 3 mL of 2 M HCl and stirred at reflux for 2 hours. The reaction was quenched with water and the solvent was removed by rotary evaporation to give a yellow oil. The product was purified by silica column using 9:1 dichloromethane/methanol. The fractions containing product were combined and the solvent removed by rotary evaporation to give the pure compound as a white solid in a 60% yield. ^{1}H NMR (600 MHz, d_6-DMSO) δ 2.32 (s, 3H); 4.57 (s, 2H); 4.78 (s, 2H); 5.09 (s, 1H). ^{13}C NMR (150 MHz, d_6-DMSO) δ 19.0, 56.7, 56.5, 130.6, 136.7, 139.4, 146.3, 149.6. HRMS (ESI) Mass calcd for $[C_8H_{11}NO_3]^+$: 204.0427, found: 204.0421

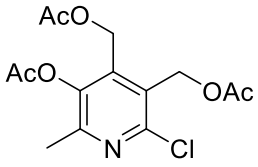

6-Chloropyridoxine triacetate, 4 – 264.8 mg of compound 2 (1.2 mmol, 1 equiv.) was dissolved in 12 M HCl (10 mL) and the solution was cooled to -10 °C. Sodium Nitrite (1.2 equiv., 1.44 mmol, 99.4 mg) was added slowly. The reaction was stirred at 4 °C for 2 hours. The solution was neutralised to pH 7 using NaOH 10 M and freeze dried to give crude compound 3. The resulting

solid was dissolved in 5 mL pyridine and 1.2 mL (12 mmol) of acetic anhydride was added. The reaction was stirred 16 hours in the dark at room temperature. The solution was transferred to an Erlenmeyer with 25 mL of ice. The mixture was warmed to room temperature and transferred to a separatory funnel. The aqueous mixture was extracted with 6x10 mL EtOAc. The combined organic fractions were washed with 3x20 mL brine. The combined organic layers were dried with Na_2SO_4, filtered, and the solvent was removed by rotary evaporator. The crude product was purified by silica column chromatography using 2:1 hexanes/EtOAc as the solvent (80 mL silica). The fractions containing product combined and the solvent removed by rotary evaporation to give the pure product as a white solid in 46% yield from 6-Aminopyridoxine. ^{1}H NMR (300 MHz, $CDCl_3$) δ 2.02 (s, 3H); 2.08 (s, 3H); 2.38 (s, 3H); 2.39 (s, 3H); 5.17 (s, 2H); 5.26 (s, 2H) ^{13}C NMR (75 MHz, $CDCl_3$) δ 19.6, 20.6, 20.7, 20.8, 57.2, 60.5, 127.9, 139.6, 144.1, 149.0, 153.6, 168.5, 170.2, 170.6 MS (ESI-pos) calcd for $[C_{14}H_{16}ClNNaO_6]^+$: 352.0564, found: 352.0575

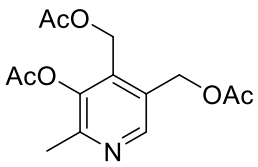

Pyridoxine triacetate, 7 – Pyridoxine HCl (1.8 g, 8.75 mmol, 1 equiv.) was dissolved in 3 mL pyridine in a round bottom flask equipped with a stir bar. Acetic anhydride (8.2 mL, 87 mmol, 10 equiv.) was added to the solution and the reaction was stirred overnight at room temperature in the dark. The solution was transferred onto ice (100 mL, in a 250 mL beaker). After the ice melted and the water reached room temperature, the aqueous mixture was extracted with 5x20 mL EtOAc. The combined organic phases were washed with 3x20 mL brine. The combined organic phases were dried with Na_2SO_4, filtered, and evaporated to dryness. The crude product was purified by silica column chromatography with 7/4 EtOAc:Hexanes (100 mL silica). The fractions containing product were combined and the solvent was removed by rotary evaporation to give the product as a white solid in 90% yield. ^{1}H NMR (300 MHz, $CDCl_3$) δ 2.03 (s, 3H); 2.08 (s, 3H); 2.38 (s, 3H); 2.42 (s, 3H); 5.14 (s, 2H); 5.26 (s, 2H); 8.44 (s, 1H). ^{13}C NMR (300 MHz, $CDCl_3$) δ 19.6 (s), 20.6 (s), 20.6 (s), 20.9 (s), 56.9 (s), 61.2 (s), 129.5 (s), 135.7 (s). 144.7 (s), 147.8 (s), 153.1 (s), 168.6 (s), 170.3 (s), 170.4 (s). MS (ESI-pos) calcd for $[C_{14}H_{17}NNaO_6]^+$: 318.0954, found: 318.0968.

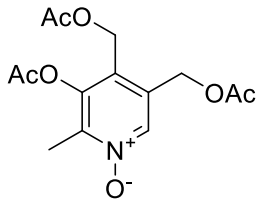

Pyridoxine triacetate N-oxide, 8 – Compound 7 (1 g, 3.39 mmol, 1 equiv.) was dissolved in 40 mL glacial acetic acid then 0.7 mL of 30% H_2O_2 (1.7 equiv.) was added. The solution was stirred at 80 °C in the dark for 16 hours. The mixture was put under rotary evaporation until there was 5 mL left, 5 mL water was then added and the solvents were removed by rotary evaporation. The pale oil was dissolved in 20 mL DCM and transferred to a separatory funnel. The organic layer was washed with 3x10 mL water. The combined aqueous layers were washed with 6x10 mL DCM. The combined organic layers were then dried with Na_2SO_4, filtered and evaporated to dryness. The crude product was purified by silica column chromatography with 6/5 Acetone:Hexanes (200 mL silica). The fractions containing product were combined and the solvent was removed by rotary evaporation to give the product as a white solid in a 68% yield. ^{1}H NMR (400 MHz, $CDCl_3$) δ 2.02 (s, 3H); 2.12 (s, 3H); 2.33 (s, 3H); 2.39 (s, 3H); 5.06 (s, 2H); 5.21 (s, 2H); 8.29 (s, 1H) ^{13}C NMR (75 MHz, $CDCl_3$) δ 11.9, 20.4, 20.5, 20.7, 56.2, 60.2, 125.1, 131.3, 137.1, 144.4, 146.7, 167.9, 170.1, 170.2. MS (EI) calcd for $[C_{14}H_{17}NO_7]^+$: 311.1005, found: 311.10306.

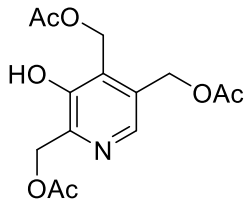

2,4,5-tri(((acetyl)oxy)methyl)-pyridin-3-ol, 10 – Compound 8 (830.0 mg, 2.67 mmol, 1 equiv.) was weighted and transferred to an oven dried round bottom flask equipped with a stir bar. The solid was degassed and dissolved in anhydrous DCM (3 mL). The solution was cooled to 0 °C. Trifluoroacetic anhydride (0.78 mL, 5.5 mmol, 2 equiv.) was added dropwise. The solution was warmed to room temperature and stirred in the dark for 2 hours under nitrogen. The solvents were removed by rotary evaporation, the pink oil was dissolved in 10 mL DCM and extracted

with 4x10 mL saturated $NaHCO_3$. The combined aqueous layers were extracted with 3x8 mL DCM. The combined organic layers were dried with Na_2SO_4, filtered, and evaporated to dryness. The crude product was purified by silica column chromatography with 6/4 EtOAc:Hexanes (100 mL silica). The fractions containing product were combined and the solvent was removed by rotary evaporation to give the product as a brown solid in a 80% yield. ^{1}H NMR (300 MHz, $CDCl_3$) δ 2.09 (s, 3H); 2.10 (s, 3H); 2.16 (s, 3H); 5.21 (s, 2H); 5.26 (s, 2H); 5.28 (s, 2H); 8.25 (s, 1H), 8.66 (bs, 1H) ^{13}C NMR (100 MHz, $CDCl_3$) δ 20.9, 20.96, 20.97, 57.4, 61.3, 64.2, 130.4, 132.4, 142.6, 144.3, 150.9, 170.6, 172.2, 173.3 MS (EI) calcd for $[C_{14}H_{17}NO_7]^+$: 311.1005, found: 311.10289

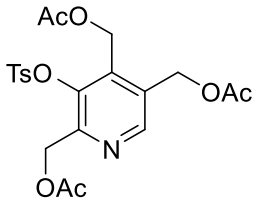

3-(p-toluenesulfonyl)- 2,4,5-tri(((acetyl)oxy)methyl)-pyridine, 11 – Compound 10 (124.4 mg, 0.4 mmol, 1 equiv.) was dissolved in 2 mL anhydrous DCM and the solution was cooled to 0 °C. Triethyl amine (0.08 mL, 0.6 mmol, 1.5 equiv.), TsCl (114.4 mg, 0.6 mmol, 1.5 equiv.) and DMAP (3.67 mg, 0.003 mmol, 5 mol%) was added. The reaction mixture was warmed to room temperature then stirred 16 hours in the dark under nitrogen. HCl (1 M, 5 mL) was added and the organic layer was extracted out. The aqueous layer was extracted with DCM (3x8 mL). The combined organic layers were washed with 2x10 mL brine. The combined organic layers were dried with Na_2SO_4, filtered, and evaporated to dryness. The crude product was purified by silica column chromatography with 5/4 Hexanes:EtOAc (40 mL silica), the fractions containing product were combined and the solvent was removed by rotary evaporation to give the product as a white solid in a 85% yield. ^{1}H NMR (400 MHz, $CDCl_3$) δ 2.03 (s, 3H); 2.09 (s, 3H); 2.11 (s, 3H); 2.50 (s, 3H); 5.13 (s, 2H); 5.18 (s, 2H); 5.23 (s, 2H); 7.42-7.44 (m, 2H); 7.87-7.90 (m, 2H); 8.60 (s, 1H) ^{13}C NMR (100 MHz, $CDCl_3$) δ 20.6, 20.8, 21.9, 57.6, 61.1, 62.2, 128.5, 130.4, 131.9, 132.3, 138.4, 141.9, 146.8, 148.8, 151.0, 170.1, 170.4, 170.6 MS (ESI-Pos) calcd for $[C_{21}H_{23}NNaO_9S]^+$: 488.0991, found: 488.1005

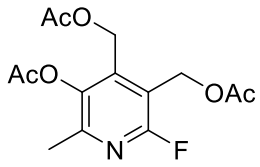

6-Fluoropyridoxine triacetate, 12 - Pyridoxine triacetate (7, 0.25 mmol, 1 equiv., 73.8 mg) was put into an oven dried round bottom flask equipped with a stir bar and degassed under N_2. The solid was dissolved in HPLC grade acetonitrile (5 ml, 0.5 M) then AgF_2 was added in a single portion. The solution was stirred overnight under nitrogen in the dark. The solution was filtered through celite and the celite bed was washed with EtOAc. The liquid filtrate was transferred to a separatory funnel and washed with 20 mL saturated $NaHCO_3$. The aqueous layer was extracted with 4x10 mL Et_2O. The combined organic layer was dried with $MgSO_4$, filtered and evaporated to dryness. The crude material was purified with silica column chromatography using 1/1 hexanes:EtOAc (20 mL silica). The fractions containing product were combined and the solvent was removed by rotary evaporation to give the product as a white solid in 9% yield. ^{1}H NMR (300 MHz, $CDCl_3$) δ 2.02 (s, 3H); 2.06 (s, 3H); 2.34 (s, 3H); 2.37 (s, 3H); 5.16 (s, 2H); 5.26 (s, 2H) ^{13}C NMR (75 MHz, $CDCl_3$) δ 19.6, 20.6, 20.6, 20.9, 56.9, 61.2, 129.4, 135.6, 144.7, 147.9, 153.2, 168.6, 170.3, 170.4 ^{19}F NMR (282 Hz, $CDCl_3$) δ -73.12 (s). MS (ESI-Pos) calc for $[C_{14}H_{16}FNNaO_6]^+$: 336.0859, found: 336.0861.

Optimisation - Pyridoxine triacetate (7, 0.25 mmol, 1 equiv., 73.8 mg) was put into an oven dried round bottom flask equipped with a stir bar and degassed under N_2. The solid was dissolved in HPLC grade acetonitrile (2.5 mL-10 mL, 0.1 M-0.025 M) then AgF_2 (3-6 equiv.) was added in a single portion unless otherwise noted. The solution was stirred overnight under nitrogen in the dark unless otherwise noted. The solution was filtered through celite and the celite bed was washed with EtOAc. The liquid filtrate was transferred to a separatory funnel and washed with 20 mL saturated $NaHCO_3$. The aqueous layer was extracted with 4x10 mL Et_2O. The combined organic layer was dried with $MgSO_4$, filtered and evaporated to dryness. The crude material was purified with silica column chromatography using 1/1 hexanes:EtOAc (20 mL silica). The fractions containing product were combined and the solvent was removed by rotary evaporation to give the product as a white solid.

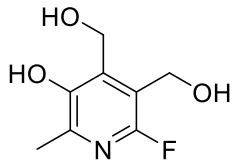

6-Fluoropyridoxine (6-FPN) - compound 12 (81.5 mg, 0.,26 mmol) was dissolved in 0.15 mL 2 M HCl and stirred at reflux for 2 hours. The solution was cooled to room temperature and 5 mL of water was added. The solution was evaporated to dryness then purified by silica column chromatography with 95:5 DCM:MeOH (20 mL silica). The fractions containing product were combined and the solvent was removed by rotary evaporation to give the product as a clear oil in 54% yield. ^{1}H NMR (300 MHz, CD_4OD) δ 2.35 (s, 3H); 4.62 (s, 2H); 4.98 (s, 2H) ^{13}C NMR (75 MHz, CD_4OD) δ 18.3 (s), 55.1 (s), 59.2 (d, J=3.4 Hz), 118.2 (d, J=30.2 Hz), 139.7 (d, J=3.3 Hz), 144.7 (d, J= 13.7 Hz), 150.0 (d, J= 4.0 Hz), 154.4 (d, J= 230.8 Hz) ^{19}F NMR (282 MHz, CD_4OD) δ -88.45 (s) MS (ESI-Pos) calcd for $[C_8H_{10}FNNaO_3]^+$: 210.0542, found: 210.0552

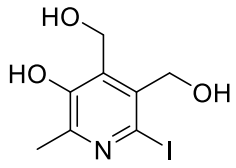

6-Iodopyridoxine, 13 – Synthesis following the procedure by Mason and coworkers.[174] Pyridoxine HCl (1.233 g, 6 mmol, 1 equiv.) was dissolve in a aqueous 10% solution of K_2CO_3 (18 mL). Iodine was added (1.523 g, 12 mmol, 2 equiv.). The solution was stirred in the dark for 3 hours. The reaction was quenched with a saturated solution of sodium thiosulfate followed by 12 M HCl until pH 3 was reached. A precipitate was formed, which was filtered and dried under vacuum to give the pure product as a yellow solid in a 53% yield. ^{1}H NMR (400 MHz, d_6-DMSO) δ 2.30 (s, 3H); 4.55 (s, 2H); 4.78 (s, 2H); 5.08 (bs, 1H); 5.83 (bs, 1H); 9.51 (s, 1H) ^{13}C NMR (100 MHz, $CDCl_3$) δ 18.9, 57.0, 63.9, 112.0, 134.9, 136.2, 148.2, 150.4 MS (EI) calcd for $[C_8H_{10}INO_3]^+$: 294.9705, found: 294.96834.

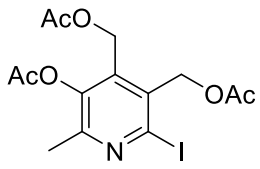

6-Iodopyridoxine triacetate, 14. Synthesis following the procedure by Mason and coworkers.[174] 6-Iodopyridoxine, 13 (885 mg, 3 mmol, 1 equiv.) was dissolved in 4 mL pyridine and acetic anhydride (9 mL, 90 mmol, 30 equiv.) was added at 0 °C. The reaction was stirred 16 hours in the dark. 40 mL of toluene was added and the solvent was removed by rotary evaporation. The azeotropic drying was repeated. The crude oil was purified by silica column chromatography using 2:1 hexanes/EtOAc (100 mL silica). The fractions containing product were combined and the solvent was removed by rotary evaporation to give the product as a white solid in a 79% yield. ^{1}H NMR (400 MHz, $CDCl_3$) δ 2.02 (s, 3H); 2.09 (s, 3H); 2.37 (s, 3H); 2.39 (s, 3H), 5.15 (s, 2H); 5.33 (s, 2H) ^{13}C NMR (75 MHz, $CDCl_3$) δ 19.6, 20.6, 20.7, 20.8, 57.3, 66.2, 76.7, 77.2, 77.6, 121.5, 133.8, 137.7, 154.8, 168.4, 170.2, 170.5 MS (ESI-Pos) calc for $[C_{14}H_{16}INNaO_6]^+$: 443.9920, found: 443.9910.

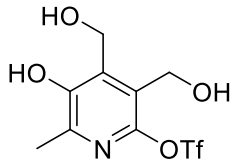

6-Tiflatepyridoxine, 15: Trifluoromethanesulfonic acid (0.11 mL, 1.2 mmol, 3 equiv.) was added to DMSO (0.5 mL) in a round bottom flask equipped with a stir bar. The solution was cooled down to 0 °C. 6-Aminopyridoxine (88.3 mg, 0.4 mmol, 1 equiv.) and $NaNO_2$ (69 mg, 1 mmol, 2.5 equiv.) were added subsequently while stirring the solution. The solution was stirred 10 minutes at 0 °C, then warmed up to room temperature and stirred 2 hours protected from light. The reaction mixture was quenched with water (10 mL) then the aqueous mixture was extracted with butanol (3x10 mL). The combined organic phases were dried with Na_2SO_4, filtered and evaporated by rotary evaporation (azeotrope drying with toluene). The crude product was purified by silica column chromatography with 95:5 DCM/MeOH. The fractions containing product were combined and the solvent were removed by rotary evaporation to give the pure product as a pale-yellow oil with a 37% yield. ^{1}H NMR (MeOD4, 400 MHz) δ 2.38 (s, 3H); 4.64 (s, 2H); 4.997 (s, 2H). ^{19}F NMR (MeOD4, 282.6 MHz) δ -79.94. ^{13}C NMR (MeOD4, 150.9 MHz) δ 18.7, 56.1, 59.4, 120.1 (q, J= 320.1 Hz), 123.9, 138.1, 146.6, 147.1, 152.8. HRMS (ESI) Mass calcd for $[C_9H_{12}F_3NNaO_4S]^+$: 340.0079, found: 340.0107

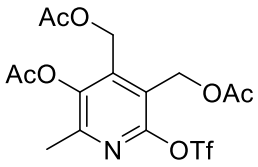

Triacetoxy-6-Triflatepyridoxine, 16: 6-Trilfylpyridoxine (50 mg, 0.19 mmol, 1 equiv.) was dissolved in pyridine (1 mL) and add acetic anhydride (0.18 mL, 1.9 mmol, 10 equiv.). The solution was stirred protected from light for 16 hours at room temperature. The solution is then quenched with water (10 mL). This mixture is extracted with EtOAc (4x 10 mL). The combined organic phases were then washed with brine (2x20 mL). The combined organic layers were dried with Na_2SO_4, filtered and evaporated to dryness by rotary evaporation. The crude oil was purified by silica column chromatography with 3:1 Hexanes/Acetone. The fractions containing product were combined and the solvent removed by rotary evaporation to give the pure product as a pale-yellow oil with a 74% yield. ^{1}H NMR ($CDCl_3$, 300 MHz) δ 2.02 (s, 3H); 2.07 (s, 3H); 2.37 (s, 3H); 2.39 (s, 3H); 5.22 (s, 2H); 5.27 (s, 2H). ^{19}F NMR (CDCl3, 282.4 MHz) δ -72.63. ^{13}C NMR (CDCl3, 150 MHz) δ 19.4, 20.6, 20.6, 20.7, 56.9, 57.3, 118.7 (q, J= 320.7 Hz), 120.9, 141.2, 144.7, 151.7, 152.8, 168.3, 170.2, 170.6 HRMS (ESI) Mass calcd for $[C_{15}H_{18}F_3NNaO_9S]^+$: 466.0396, found: 466.0405

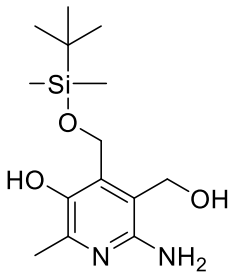

6-Aminopyridoxine-α4-tert-butyldimethylsilyl ether, 17. Synthesis following the procedure by Culbertson, Enright and Ingold.[179] 6-Aminopyridoxine (2, 172 mg, 0.78 mmol, 1 equiv.) and imidazole (109 mg, 1.6 mmol, 2 equiv.) were added to a oven dried round bottom flask equipped with a stir bar. The solids were degassed with N_2 then dissolved in anhydrous DMF (2 mL). The solution was cooled to 10 °C. TBDMSCl was added (120.6 mg, 0.78 mmol, 1 equiv.) and the reaction was stirred at 10 °C for 4 hours in the dark. A small amount of water was added and the reaction was stirred a few minutes before transferring to a separatory funnel with 25 mL brine. The aqueous layer was extracted with 6x10 mL dichloromethane. The combined organic phases

were washed with 2x60 mL brine. The combined organic phases were dried with Na_2SO_4, filtered, and evaporated to dryness. The crude product was purified by silica column chromatography with 95/5 DCM:MeOH (75 mL silica). The fractions containing product were combined and the solvent was removed by rotary evaporation to give the product as a yellowish solid in a 28% yield. ^{1}H NMR (400 MHz, d_6-DMSO) δ 0.05 (s, 6H); 0.85 (s, 9H); 2.20 (s, 3H), 4,43 (d, 2H, J = 5.3 Hz); 4.73 (s, 2H); 4.81 (t, 1H, J=5.3 Hz); 5.08 (s, 2H); 7.72 (s, 1H) ^{13}C NMR (75 MHz, d_6-DMSO) δ 18.0, 19.3, 25.8, 56.3, 56.4, 116.6, 135.5, 140.4, 143.1, 151.9 MS (EI) calcd for $[C_{14}H_{26}N_2O_3Si]^+$: 298.1713, found: 298.1692

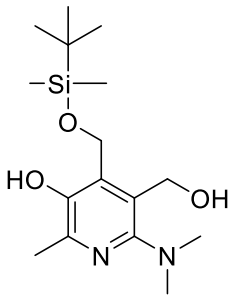

6-Dimethylaminopyridoxine-α4-tert-butyldimethylsilyl ether, 18. Synthesis following the procedure by Culbertson, Enright and Ingold.[179] Compound 17 (217.6 mg, 0.73 mmol, 1 equiv.) was dissolved in 1,2-dichloroethane (4.3 mL) and 37% aqueous formaldehyde (5 eq, 218 µL) was added followed by stirring at room temperature for 10 minutes. Sodium triacetoxyborohydride was then added (2 eq, 209.4 mg) and the solution was stirred 2 hours at room temperature in the dark. The solvent was removed by rotary evaporation. The crude oil was redissolved in 4.3 mL MeOH and sodium cyanoborohydride was added (6 eq, 275.2 mg). The resulting solution was stirred 24 hours at room temperature in the dark. The solvent was removed by rotary evaporation. The crude oil was resuspended in water, the pH was then adjusted to 9 using a K_2CO_3 aqueous solution. The aqueous mixture was extracted with EtOAc (5x10 mL). The combined organic phases were dried with Na_2SO_4, filtered, and evaporated to dryness. The crude product was purified by silica column chromatography with 95/5 DCM:MeOH (75 mL silica). The fractions containing product were combined and the solvent was removed by rotary evaporation to give the product as a yellowish solid in a 49% yield. ^{1}H NMR (400 MHz, d_6-DMSO) δ 0.09 (s, 6H); 0.87 (s, 9H); 2.30 (s, 3H), 2.64 (s, 6H), 4,57 (s, 2H); 4.90 (s, 2H); 8.36 (s, 1H) ^{13}C NMR (75 MHz, d_6-DMSO) δ 17.9, 19.5, 25.7, 43.7, 56.4, 57.8, 124.4, 135.6, 142.8, 145.4, 154.6 MS. MS (EI) Mass calc for $[C_{16}H_{30}N_2O_3Si]^+$: 326.2026, Mass found: 326.20378

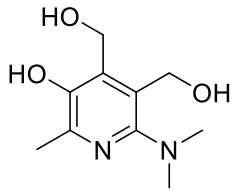

6-Dimethylaminopyridoxine, 19. Synthesis following the procedure by Culbertson, Enright and Ingold.[179] Compound 18 (250 mg, 0.76 mmol, 1 equiv.) was put into a oven dried round bottom flask equipped with a stir bar and dissolved in anhydrous THF (4.8 mL, 0.16 M). TBAF (1 M solution in THF, 2.5 equiv., 1.9 mL) was added and the solution was stirred in the dark at room temperature for 30 minutes. The solvent was removed by rotary evaporation to give a pale oil. The oil was purified by silica column chromatography with 9/1 DCM:MeOH (150 mL silica). The fractions containing product were combined and the solvent was removed by rotary evaporation to give the product as a pale oil with 86% crude yield (taken immediately to next steps without further purification or characterisation)

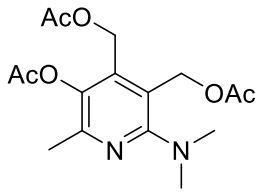

6-Dimethylaminepyridoxine triacetate, 20. Compound 19 (0.66 mmol, 139 mg, 1 equiv.) was dissolved in 1 mL pyridine and acetic anhydride (7 mmol, 0.66 mL, 10 equiv.) was added then the reaction was stirred in the dark at room temperature for 16 hours. The solvent was removed by rotary evaporation. The product was purified by silica column chromatography with 4/1 Hexane:Acetone (15 mL silica). The fractions containing product were combined and the solvent was removed by rotary evaporation to give the product as a pale oil in a 85% yield. ^{1}H NMR (400 MHz, $CDCl_3$) δ 2.03 (s, 3H); 2.07 (s, 3H); 2.30 (s, 3H); 2.33 (s, 3H), 2.83 (s, 6H), 5.05 (s, 2H); 5.26 (s, 2H). ^{13}C NMR ($CDCl_3$, 75 MHz) δ 19.6, 20.7, 20.8, 21.1, 43.3, 57.7, 60.6, 118.8, 138.6, 139.8, 150.2, 169.2, 170.5, 170.8 MS (ESI-Pos) Mass calc for $[C_{16}H_{23}N_2O_6]^+$: 339.1556, found: 339.1566

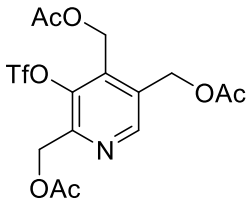

2,4,5-tri(((acetyl)oxy)methyl)-pyridin-3-yl trifluoromethanesulfonate, 21. Compound 10 (112 mg, 0.36 mmol, 1 equiv.) was added to an oven dried round bottom flask equipped with a stir bar. The solid was degassed under nitrogen and dissolved in anhydrous DCM (0.1 M, 4 mL). The solution was cooled down to -10 °C. Trifluoromethanesulfonic anhydride (0.076 mL, 0.45 mmol, 1.25 mmol) was added drop wise under nitrogen. The reaction mixture was warmed to room temperature and stirred in the dark under nitrogen for 2 hours. The reaction was quenched with 5 mL water. The mixture was transferred to a separatory funnel. The water layer was separated and extracted with DCM (3 x 8 mL). The combined organic layers were washed with 10% H_2SO_4 in water (2 x 15 mL) and water (2x15 mL). The combined organic phases were dried with Na_2SO_4, filtered, and evaporated to dryness to give the product as a white solid in a 89% yield. ^{1}H NMR (400 MHz, $CDCl_3$) δ 2.09 (s, 3H); 2. 11 (s, 3H); 2.15 (s, 3H); 5.26 (s, 2H); 5.27 (s, 2H); 5.33 (s, 2H); 8.70 (s, 1H) ^{13}C NMR (150 MHz, $CDCl_3$) δ 20.55, 20.73, 20.84, 57.07, 60.73, 62.23, 118.56 (q, J= 319.2 Hz), 133.07, 137.97, 141.59, 150.28, 150.31, 170.11, 170.38, 170.57 ^{13}C NMR ($CDCl_3$, 150 MHz) δ 20.5, 20.7, 20.8, 57.1, 60.7, 62.2, 118.6 (q, J= 320.5 Hz), 133.1, 138.0, 141.6, 150.3, 150.3, 170.1. 170.4, 170.6 ^{19}F NMR (283 MHz, $CDCl_3$) δ -72.77 (s) MS ESI-Pos) Mass calculated for $[C_{15}H_{16}F_3NNaO_9S]^+$: 466.0396, found: 466.0391

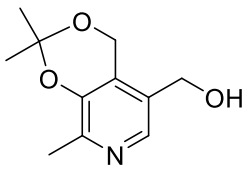

(2,2,8-Trimethyl-4H-[1,3]dioxino[4,5-c]pyridin-5-yl)methanol , 22. Synthesis following literature procedure.[187] Pyridoxine HCl (1.645 g, 8 mmol, 1 equiv.) was suspended in 27 mL of acetone. 2,2-dimethoxypropane (7.9 mL, 64 mmol, 8 equiv.) followed by p-toluenesulfonic acid monohydrate (6.9 g, 40 mmol, 5 equiv.). was added and the reaction mixture was stirred for 24 hours in the dark at room temperature. The mixture was quenched slowly with $NaHCO_3$ then the acetone was removed by rotary evaporation. The resulting aqueous mixture was quenched again (slowly) with $NaHCO_3$. The aqueous mixture was extracted with DCM (5x25 mL). The

combined organic layers were washed with water (2x50 mL) and brine (2x50 mL). The combined organic phases were dried with Na_2SO_4, filtered, and evaporated to dryness to give a crude off-white solid. The product was purified by silica column chromatography with 1/1 Hexanes:Acetone (200 mL silica). The fractions containing product were combined and the solvent was removed by rotary evaporation to give the product as a white solid in a 66% yield. ^{1}H NMR (400 MHz, CDCl3) δ 1.54 (s, 6H); 2.36 (s, 3H); 4.54 (s, 2H); 4.93 (s, 2H); 7.79 (s, 1H) ^{13}C NMR (75 MHz, $CDCl_3$) δ 147.8 (s), 146.2 (s), 138.7 (s), 129.6 (s), 126.6 (s), 99.9 (s), 60.3 (s), 58.7 (s), 24.9(s), 18.4(s) MS (EI) calcd for $[C_{11}H_{15}NO_3]^+$:209.1052, found: 209.10689

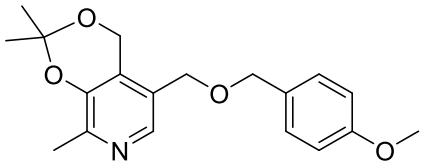

5-{[(4-Methoxybenzyl)oxy]methyl}-2,2,8-trimethyl-4H-[1,3]dioxino[4,5-c]pyridine, 23. Synthesis following literature procedure.[175] Compound 22 (836.9 mg, 4 mmol, 1 equiv.) was added to an oven dried round bottom flask equipped with a stir bar, degassed under nitrogen and dissolved in 12 mL anhydrous DMF. In a sperate oven dried round bottom flask equipped with a stir bar, NaH (60% dispersion in oil, 679.4 mg, 17 mmol, 4 equiv.) was added, degassed under nitrogen and dissolved in 24 mL anhydrous DMF. The NaH mixture was heated to 70 °C and the DMF solution of compound 22 was added drop wise. The reaction mixture was stirred at 70 °C for 1 hour under nitrogen. The flask was removed from heat to cool down until 40 °C and then was placed in an ice bath. Once the solution was cooled to 0 °C, p-methoxybenzyl chloride (0.65 ml, 4.8 mmol, 1.2 equiv.) was added drop wise. The reaction mixture was warmed to room temperature and stirred 16 hours in the dark under nitrogen. The flask was put on ice and the mixture was quenched slowly with water (50 mL total). The mixture was extracted with Ether (5x25 mL). The combined organic phases were dried with $MgSO_4$, filtered, and evaporated to dryness to give a crude pale oil. The product was purified by silica column chromatography with 1/1 Hexanes:EtOAc (200 mL silica). The fractions containing product were combined and the solvent was removed by rotary evaporation to give the product as a pale-yellow oil in a 63% yield. ^{1}H NMR (400 MHz, CDCl3) δ 1.55 (s, 6H); 2.42 (s, 3H); 3.812 (s, 3H); 4.40 (s, 2H); 4.43 (s, 2H); 4.86 (s, 2H); 6.88 (m, 2H); 7.33 (m, 2H); 7.95 (s, 1H) ^{13}C NMR (75 MHz, $CDCl_3$) δ 158.5(s), 148.2(s), 146.2 (s), 139.8 (s), 129.7, 126.6 (s), 126.3 (s), 114.0 (s), 99.6 (s), 72.0 (s),

67.2 (s), 58.8(s), 55.4 (s), 24.9(s), 18.6(s) MS (ESI-Pos) calcd for $[C_{19}H_{24}NO_4]^+$: 330.1705, found: 330.1717

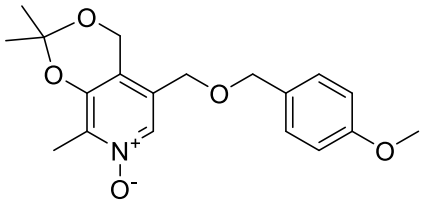

5-{[(4-Methoxybenzyl)oxy]methyl}-2,2,8-trimethyl-4H-[1,3]dioxino[4,5-c]pyridine-N-oxide, 24. Synthesis following literature procedure.[175] Compound 23 (1011 mg, 3.07 mmol, 1 equiv.) was dissolved in 25 mL chloroform and m-CPBA (815 mg, 3.4 mmol, 1.1 equiv.) was added in portions over a few minutes. The reaction was stirred at room temperature in the dark for 2 hours. The mixture was quenched with sodium thiosulfate pentahydrate (7 g, 30 mmol, 10 eq, in 20 mL water). The organic layer was separated and washed with $NaHCO_3$(3x20 mL). The combined aqueous layers were extracted with chloroform (8x15 mL). The combined organic phases were dried with Na_2SO_4, filtered, and evaporated to dryness to give a crude pale oil. The product was purified by silica column chromatography with 95:5 DCM:MeOH (250 mL silica). The fractions containing product were combined and the solvent was removed by rotary evaporation to give the product as a white solid in a quantitative yield. No characterisation done, directly taken to next step.

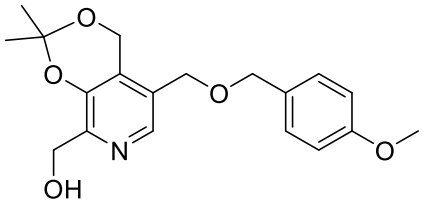

(5-{[(4-Methoxybenzyl)oxy]methyl}-2,2-dimethyl-4H-[1,3]dioxino[4,5-c]pyridin-8-yl)methanol, 25. Synthesis following literature procedure.[175] Compound 24 (848 mg, 2.46 mmol, 1 equiv.) was added to an oven dried round bottom flask equipped with a stir bar, degassed with nitrogen and dissolved in anhydrous DCM (0.3 M, 8.2 mL). The solution was cooled to 0 °C and 0.5 equiv. (1.23 mmol, 0.17 mL) of trifluoroacetic anhydride was added drop wise. The solution was stirred 5 minutes at 0 °C under nitrogen after which more trifluoroacetic anhydride (0.44 mL, 3.2 mmol, 1.3 equiv.) was added drop wise. The mixture was warmed to room temperature

and stirred 16 hours under nitrogen in the dark. The reaction mixture was then placed into an ice bath and quenched with MeOH. The solvent was evaporated under rotary evaporation. The pale oil was redissolved in chloroform and washed with saturated aqueous $NaHCO_3$ (4x20 mL). The combined aqueous layers were extracted with chloroform (5x15 mL). The combined organic phases were dried with Na_2SO_4, filtered, and evaporated to dryness to give a crude pale oil. The product was purified by silica column chromatography with 7/1 DCM:Acetone (200 mL silica). The fractions containing product were combined and the solvent was removed by rotary evaporation to give the product as a off white solid in a 70% yield (from compound 23). ^{1}H NMR (300 MHz, CDCl3) δ 1.54 (s, 6H); 3.81 (s, 3H); 4.42 (s, 2H); 4.44 (s, 2H); 4.69 (s, 2H); 4.87 (s, 2H); 6.88 (m, 2H); 7.23 (m, 2H); 8.02 (s, 1H) ^{13}C NMR (75 MHz, $CDCl_3$) δ 159.6 (s), 147.7 (s), 144.9 (s), 138.9 (s), 129.7 (s), 129.5 (s), 128.0 (s), 126.9(s), 100.3 (s), 72.2 (s), 67.1 (s), 59.7 (s), 58.9(s), 55.4 (s), 24.8(s) MS (ESI-Pos) calcd for $[C_{19}H_{24}NO_5]^+$: 346.1654, found: 346.1682

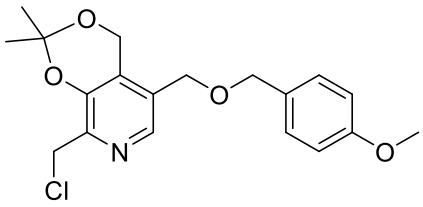

5-{[(4-Methoxybenzyl)oxy]methyl}-2,2-dimethyl-4H-[1,3]dioxino[4,5-c]pyridine-8-chloride, 26: Compound 25 (192 mg, 0.556 mmol, 1 equiv.) was dissolved in 2.8 mL anhydrous DCM and the solution was cooled to 0 °C. Triethyl amine (0.12 mL, 0.84 mmol, 1.5 equiv.), TsCl (160.1 mg, 0.84 mmol, 1.5 equiv.) and DMAP (3.4 mg, 0.028 mmol, 5 mol%) were added. The reaction mixture was warmed to room temperature then stirred 16 hours in the dark under nitrogen. HCl (1 M, 6 mL) was added and the organic layer was extracted out. The aqueous layer was extracted with DCM (6x8 mL). The combined organic layers were washed with 2x35 mL brine. The combined organic layers were dried with Na2SO4, filtered, and evaporated to dryness. The crude product was purified by silica column chromatography with 3/1 Hexanes:Acetone (25 mL silica), the fractions containing product were combined and the solvent was removed by rotary evaporation to give the product as a white solid in a 35% yield. ^{1}H NMR (300 MHz, $CDCl_3$) δ 1.57 (s, 6H); 3.80 (s, 3H); 4.42 (s, 2H); 4.45 (s, 2H); 4.68 (s, 2H); 4.86 (s, 2H); 6.88 (m, 2H); 7.23 (m, 2H); 8.06 (s, 1H). ^{13}C NMR (150 MHz, $CDCl_3$) δ 24.8, 41.5, 55.4, 58.8, 66.9, 72.4,

100.6, 114.1, 128.1, 129.4, 129.6, 129.7, 140.2, 145.0, 146.5, 159.6 MS (ESI-Pos) calcd for $[C_{19}H_{23}NO_4Cl]^+$: 364.1316, found: 364.1317

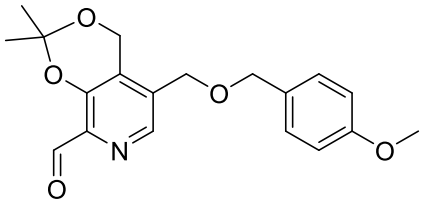

5-{[(4-Methoxybenzyl)oxy]methyl}-2,2-dimethyl-4H-[1,3]dioxino[4,5-c]pyridine-8-carbaldehyde, 27. Synthesis following literature procedure.[175] Compound 25 (589.1 mg, 1.70 mmol, 1 equiv.) was dissolved in chloroform (0.06 M, 28 mL) and MnO_2 (85% activated, 2.27 g, 22.2 mmol, 13 equiv.) was added. The reaction mixture was stirred in the dark at room temperature under nitrogen for 21 hours. The reaction mixture was filtered through celite, the celite bed was washed with DCM and the resulting filtrate was concentrated under rotary evaporation. The crude oil was purified by silica column chromatography with 14/1 DCM:Acetone (100 mL). The fractions containing product were combined and the solvent was removed by rotary evaporation to give the product as a white solid in a 76% yield (kept in the fridge). ^{1}H NMR (400 MHz, CDCl3) δ 1.62 (s, 6H); 3.82 (s, 3H); 4.47 (s, 2H); 4.49 (s, 2H); 4.91 (s, 2H); 6.89 (m, 2H); 7.25 (m, 2H); 8.27 (s, 1H), 10.32 (s, 1H) ^{13}C NMR (75 MHz, $CDCl_3$) δ 189.3 (s), 159.7 (s), 151.2 (s), 141.4 (s), 139.7 (s), 133.8 (s), 129.8 (s), 129.4 (s), 129.2 (s), 114.2 (s), 101.2 (s), 72.8 (s), 66.8 (s), 58.8 (s), 55.4 (s), 24.9 (s) MS (ESI-Pos) calcd for $[C_{19}H_{21}NNaO_5]^+$: 366.1317, found: 366.1313

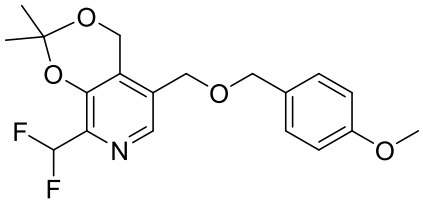

5-{[(4-Methoxybenzyl)oxy]methyl}-2,2-dimethyl-4H-[1,3]dioxino[4,5-c]pyridine-8,8-difluoride, 28. Compound 27 (0.092 mmol, 1 eq, 31.6 mg) was weighted into an oven dried microwave vial equipped with a stir bar and transferred into a glovebox. TMAF (0.276 mmol, 3 eq, 25.7 mg) was added and the solids were dissolved in anhydrous Ether (0.46 mL, 0.2 M). After 30 second stirring, PBSF (0.33 mmol, 3.6 eq, 0.06 mL) was added. The reaction mixture was stirred in the glovebox in the dark at room temperature for 24 hours. The mixture was dissolved in ether and

filtered through a silica plug which was washed with 9:1 ether/acetone. The solvent was removed by rotary evaporation and the product was purified by P-TLC using 96:4 DCM/Ethyl acetate as the eluent. The silica containing the product was removed by scrapping and washed with ethyl acetate. The solvent was removed by rotary evaporation to give a yellow oil in a 55/6% yield. ^{1}H NMR (600 MHz, CDCl3) δ 1.57 (s, 6H); 3.82 (s, 3H); 4.45 (s, 2H); 4.47 (s, 2H); 4.89 (s, 2H); 6.84 (t, J= 54 Hz); 6.9 (m, 2H), 7.25 (m, 2H); 8.15 (s, 1H). ^{13}C NMR (75 MHz, $CDCl_3$) δ 159.7 (s), 147.1 (s), 140.4 (s), 140.4 (s), 131.6 (s), 129.8 (s), 129.3 (s), 128.8 (s), 114.1 (s), 111.0 (t, J= 239 Hz), 100.9 (s), 72.5 (s), 66.8 (s), 58.8 (s), 55.4 (s), 24.8 (s) ^{19}F NMR (282 MHz) $CDCl_3$) δ 119.6 (d, J= 54.2 Hz) MS (ESI-Pos) calcd for $[C_{19}H_{22}F_2NO_4]^+$: 366.1517, found: 366.1533

For optimisation: Compound 27 (0.092 mmol, 1 eq, 31.6 mg) was weighted into an oven dried microwave vial equipped with a stir bar and transferred into a glovebox. TMAF was added and the solids were dissolved into an anhydrous solvent. After 30 second of stirring, PBSF was added. The reaction mixture was stirred in the glovebox in the dark at room temperature for 24 hours. The mixture was dissolved in ether (2 mL) and filtered through a silica plug which was washed with 9:1 ether/acetone. The solvent was removed by rotary evaporation and the product was purified by P-TLC using 96:4 DCM/Ethyl acetate as the eluent. The silica containing the product was removed by scrapping and washed with ethyl acetate. The solvent was removed by rotary evaporation.

For TMAF screening: Compound 27 (0.092 mmol, 1 eq, 31.6 mg) was weighted into an oven dried microwave vial equipped with a stir bar and transferred into a glovebox. TMAF (0.5 equiv. or 1 equiv.) was added and the solids were dissolved into an anhydrous ether (0.2 M, 0.46 mL). After 30 second stirring, PBSF (0.33 mmol, 3.6 eq, 0.06 mL) was added. The reaction mixture was stirred in the glovebox in the dark at room temperature for 24 hours. The mixture was dissolved in ether (2 mL) and filtered through a silica plug which was washed with 9:1 ether/acetone. The solvent was removed by rotary evaporation and the product was purified by P-TLC using 96:4 DCM/Ethyl acetate as the eluent. The silica containing the product was removed by scrapping and washed with ethyl acetate. The solvent was removed by rotary evaporation.

For short reaction time screening: Compound 27 (0.092 mmol, 1 eq, 31.6 mg) was weighted into an oven dried microwave vial equipped with a stir bar and transferred into a glovebox. TMAF

(0.276 mmol, 3 eq, 25.7 mg) was added and the solids were dissolved into an anhydrous solvent. After 30 second stirring, PBSF (0.33 mmol, 3.6 eq, 0.06 mL) was added. The microwave vial was sealed and transferred out of the glove box. The reaction was stirred for one hour at either room temperature or under heat. The mixture was dissolved in ether (2 mL) and filtered through a silica plug which was washed with 9:1 ether/acetone. The solvent was removed by rotary evaporation and the resulting oil was dissolved in $CDCl_3$ with added 2-Fluorobenzoic acid and analysed by ^{19}F NMR.

Chapter 3. Results and discussion

Part 1– Synthesis of cold standard 1: 6-Fluoropyridoxine (6-FPN)

1.1. Attempted synthesis using the Balz-Schiemann reaction

The first attempt at synthesizing 6-Fluoropyridoxine was done following the previously reported scheme by Korytnyk and Srivastava[113] which consisted of hydrogenating 6-Phenylazopyridoxine hydrochloride (compound 1) to 6-Aminopyridoxine (compound 2) and then fluorinating using the Balz-Schiemann reaction[188] (scheme 5).

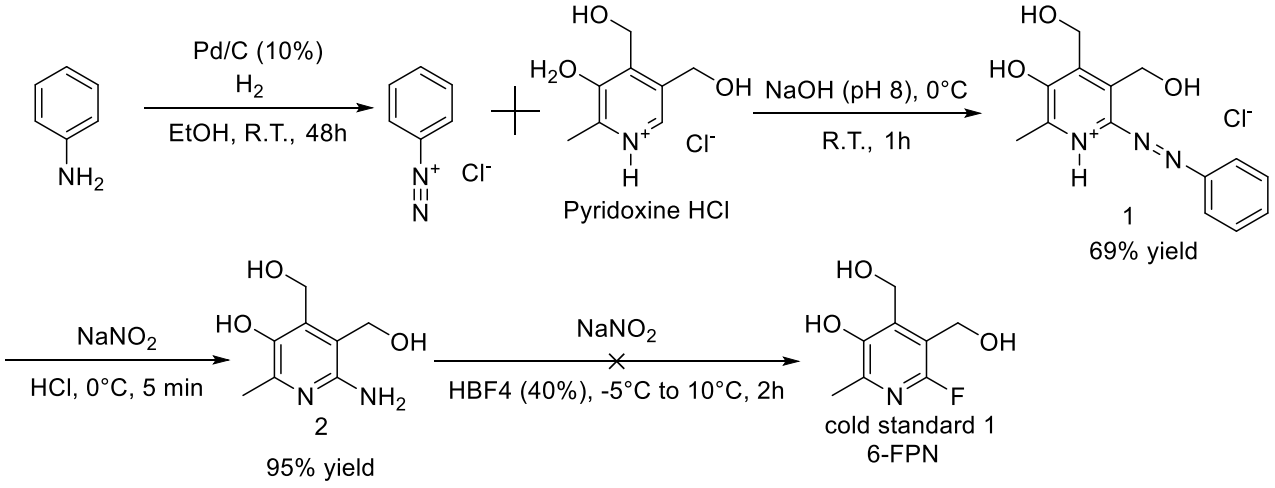

Scheme 5. Attempted synthesis of 6-FPN from 6-Aminopyridoxine following the procedure by Korytnyk and Srivastava. Compound 2 (6-Aminopyridoxine hydrochloride) was successfully synthesized in two steps from pyridoxine HCl with a 65% yield with a modified literary procedure.[179] Diazotization of aniline followed by coupling with pyridoxine HCl to form compound 1 (6-Phenylazopyridoxine hydrochloride) was first perform with a 69% yield followed by hydrogenation to form the amine with a 95% yield. The Balz-Schielmann fluorination of amine 2 did not result in any formation of cold standard 2.

The first step of the synthesis consisted of hydrogenating 6-Phenylazopyridozine (synthesized from pyridoxine HCl using the method described by Colbertson and colleagues,[179] scheme 5). The resulting product from the reduction is 6-Aminopyridoxine (compound 2). This product was formed in two steps from pyridoxine HCl in a 65% yield (scheme 5). The final step of the synthesis reported by Korytnyk and Srivastava[113] consist of the fluorination of 6-Aminopyridoxine via the Balz-Schiemann reaction.[188] When this reaction was attempted, it did not result in formation of 6-Fluoropyridoxine. In the procedure reported in the 1973 article, the

authors used ether extraction to isolate their product from the aqueous solution of HBF_4 (which was treated with NaOH until pH 3-4).[113] However, 6-Fluoropyridoxine has 3 free OH groups which might make it stay in the aqueous layer. Therefore, the experiment was repeated but before doing any extraction a crude ^{19}F NMR was done in order to evaluate if the fluorination was taking place. The ^{19}F NMR of the crude reaction show that the only fluorine present is the BF_4 fluorine (155 ppm; figure 7). We suggest that this reaction did not work because although solutions of HBF_4 does release HF in situ[206] and the BF_4- ion can act as a source of F- in the reaction,[187] the BF_4- anion can hydrolyze to hydroboric acid (H_3BO_2) after long storage time and hydroboric acid can quickly react with 3 equivalents of HF to form $HBF_3OH_2O_7$ which will be inert in this reaction. Therefore, an old solution of HBF_4 could be unreactive. Using a more recent solution of HBF_4 might have led to formation of product, however, we decided to pursue another route due to potential problems with the purification of the compound (extraction only possible with t-BuOH and most likely low yielding due to the high polarity of 6-Fluoropyridoxine).

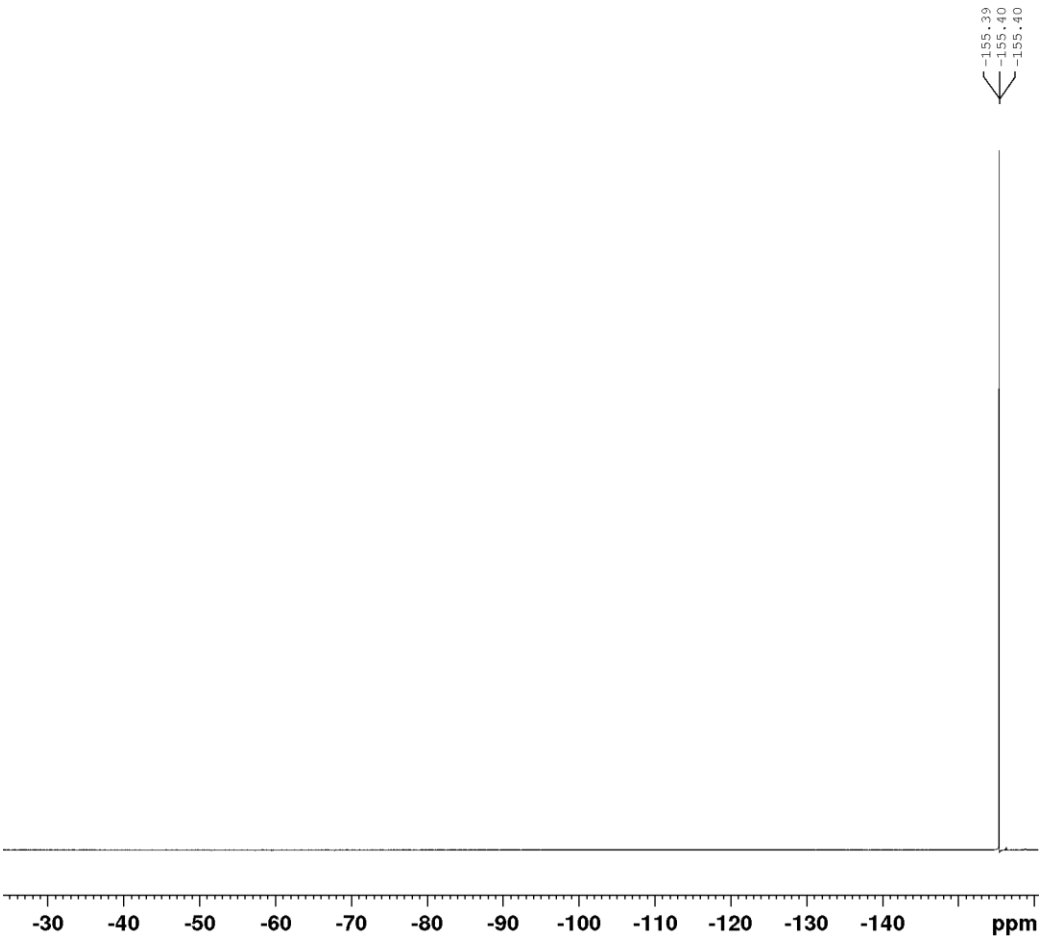

Figure 7. ^{19}F NMR of Balz-Schielmann reaction with 6-Aminopyridoxine. 6-Aminopyridoxine (110 mg, 0.5 mmol, 1 equiv.) was dissolved in 2.3 mL 48% HBF_4 in water, cooled down to -5 °C and 1.2 equivalents (43 mg) of $NaNO_2$ was added slowly. The solution was stirred 2 hours at 4 °C. A drop of the solution was dissolved in deuterated methanol and analysed by ^{19}F NMR.

1.2.Synthesis of cold standard using silver difluoride

After studying the literature for methods to fluorinate the 6 position of pyridine derivatives, the C-H fluorination of pyridines using silver difluoride as described by Hartwig and coworkers[176] was found to be an appropriate solution to the problem at hand. This methodology developed by Fier and Hartwig occurs at room temperature and has been successful for the fluorination of multiple substituted pyridines. This fluorination can occur without modification of the 6 position and therefore simplifies the synthetic scheme. This reaction is very susceptible to water and labile hydrogens which means pyridoxine needs to be protected before proceeding. One previously reported method to protect the 3 OH groups of pyridoxine is the acetylation of all of the groups by reacting pyridoxine with acetic anhydride in the presence of a base.[201] Therefore,

this method was very interesting since the cold standard 6-Fluoropyridoxine could be synthesized in 3 steps: protection of pyridoxine with acetyl groups, fluorination, deprotection to give the cold standard. To begin, triacetoxy pyridoxine (compound 7) was synthesized in 89% yield from pyridoxine HCl (scheme 6). Then, the first attempt at the fluorination of pyridoxine triacetate was done using the optimized conditions reported by Fier and Hartwig (Acetonitrile 0.05 M, 3 equivalents AgF_2, stir at room temperature)[173] and resulted in a 10% yield (scheme 6). With the protected cold standard in hand (compound 12), the cold standard was easily accessible by acid deprotection (scheme 6, 6-FPN).

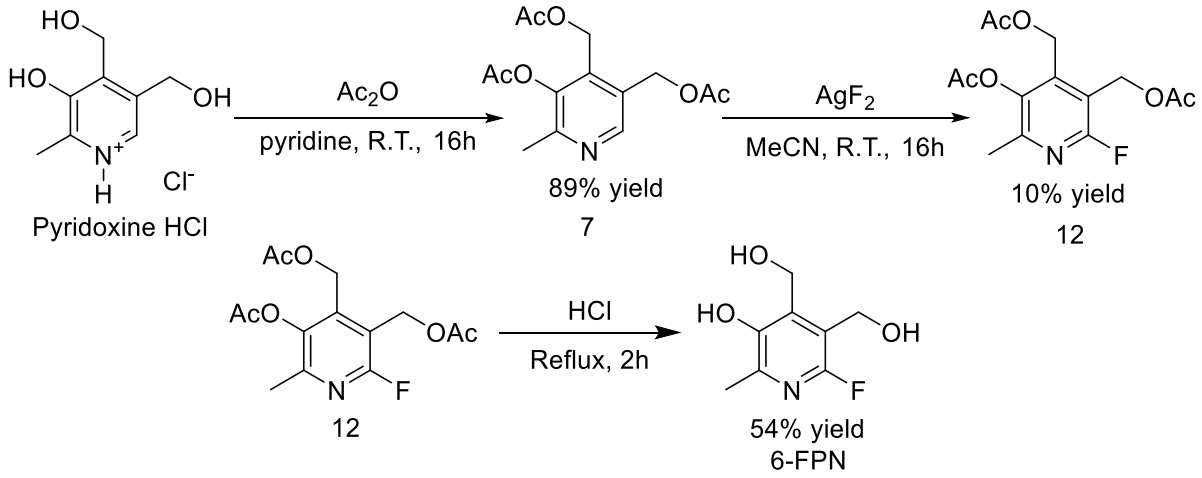

Scheme 6. Synthesis of cold standard (6-FPN) 1 using silver II fluorination. Cold standard 1 was synthesized from pyridoxine HCl in 3 steps with a 4% total yield. Pyridoxine HCl was first protected using a modified literature procedure[189] with a 89% yield, then was fluorinated using direct C-H activation following the method described by the Hartwig group[176] with a 10% yield. The cold standard was obtained from this compound by HCl deprotection with a 54% yield.

The fluorination yield much lower than the reported yields for the pyridines (ranging from 41 to 94%).[176] Due to this result, the experiment was repeated with different conditions to look for ways to increase the yield (table 1). All of the experiments tried resulted in a lower yield (changing the concentration, changing the temperature, changing the amount of AgF_2; table 1). Therefore the conditions from the Hartwig paper[176] were the best one with a yield of 9%. In all of the conditions, there was a large amount of the triacetoxy pyridoxine starting material left. We suggest that the reactivity of the compound is low due to the acetyl group potentially coordinating with the silver difluoride. The proposed mechanism by Hartwig and colleagues[176] starts with the coordination of AgF_2 to the pyridine ring. The acetyl groups, being close in

proximity could potentially coordinate with AgF_2. There are no examples in the Hartwig paper with carbonyl groups in close proximity to each other. In addition, the acetyl group add steric hinderance to the compound which could also decrease the reactivity.

Table 1. Optimization of the fluorination of pyridoxine triacetate using silver difluoride. The fluorination of pyridoxine triacetate using silver difluoride was tested using several conditions. The conditions were based on the optimisation described by Hartwig and his colleagues[176] in which the optimal condition were found to be 3 equivalents of silver difluoride at room temperature in acetonitrile. All experiments were done in an oven dried round bottom flask under nitrogen atmosphere using a nitrogen balloon. All experiments were protected from light unless otherwise noted. In all experiments, pyridoxine triacetate was still present (followed by TLC) after 16 hours of stirring.

Experiment	Concentration (M)	AgF_2 equivalents	Temperature (°C)	Yield
1	0.025	3	Room temp.	5%
2	0.05	3	Room temp.	10%
3	0.083	3	Room temp.	6%
4	0.1	3	Room temp	4%
5	0.025	3	40	2%
6	0.05	3	40	2%
7	0.083	3	40	7%
8	0.1	3	40	4%
9	0.05	3	4	5%
10[a]	0.05	3	Room Temp.	3%
11	0.05	4	Room Temp	6%
12[b]	0.05	6	Room Temp.	7%

a. The reaction was done with lights on
b. 3 equivalents were added, the reaction was stirred one hour, then 3 equivalents were added again

The cold standard can be successfully synthesized with the key step being the direct C-H fluorination with AgF_2. However, AgF_2 is produced by the reaction between AgCl or AgF and fluorine gas at 200 °C for several hours.[190,191] Therefore, the only synthesis of ^{18}F-labelled AgF_2 described in the literature was done by heating a silver-plated target liner in the presence of F_2 gas at 350 °C to create a AgF_2 coated liner which was exposed to Neon gas and was then irradiated with 14 MeV deuterons.[192] F_2 gas needs special handling due to its high corrosivity[193] and targetry using the 20Ne reaction is low yielding.[194] This makes ^{18}F-labelled AgF_2

inaccessible. Therefore, the procedure cannot be repeated in radiochemistry. Hence, the reaction was tested with AgF under several conditions. These experiments are described in table 2.

Table 2. Attempted direct C-H fluorination of pyridoxine triacetate using AgF. The fluorination of pyridoxine triacetate using silver fluoride was tested with and without the use of an additive. The experiments were run using the optimised conditions found with silver difluoride (table 1). All experiments were done in an oven dried round bottom flask under nitrogen atmosphere using a nitrogen balloon. All experiments were protected from light. In all experiments., there was no conversion of pyridoxine triacetate.

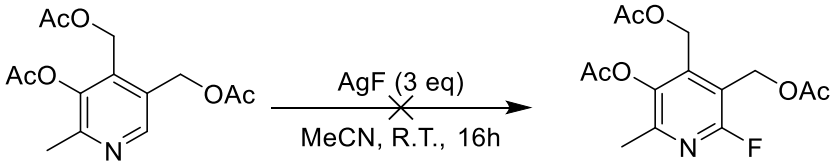

Experiment	Additive	Additive equivalents
1	none	N/A
2	DBU	2
3	TBAF (1 M in THF)	2

Without any success from silver fluoride, there was no possibilities that this chemistry could be transferable to radiochemistry.

1.3. Synthesis of chlorine precursor, attempted radiofluorination

With the cold standard in hand, a route to the radiotracer was needed. Since direct radiofluorination of chloropyridine derivatives has been reported,[180] the synthesis and attempted fluorination of a protected 6-Chloropyridoxine was the first methodology that was tested. The synthesis of 6-Chloropyridoxine was previously reported in the literature[113] and since acetyl protection is successful with pyridoxine it should also work with the chlorine derivative. Therefore, the 6-Chloropyridoxine triacetate (compound 4) was synthesized in two steps from 6-Aminopyridoxine (compound 2) as shown in scheme 7 and could be tested for radiofluorination.

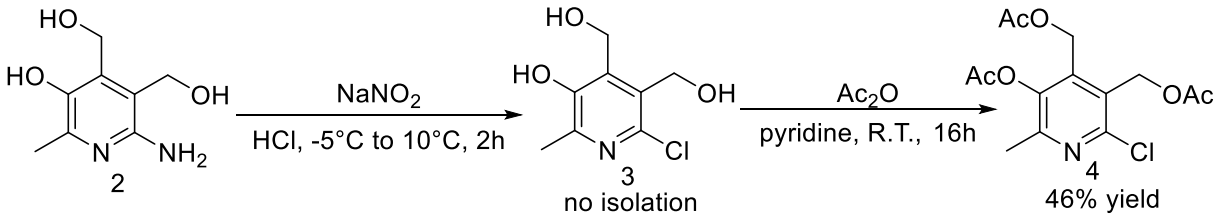

Scheme 7. Synthesis of 6-Chloropyridoxine triacetate. Compound 4 (6-Chloropyridoxine triacetate) was synthesized in two steps from 6-Aminopyridoxine (compound 2). 6-Aminopyridoxine was chlorinated by using diazotization and the reaction mixture was neutralised, freeze dried then acetylated to give the wanted product.

With the chlorine precursor in hand, direct radiofluorination was attempted. The first attempts were made using a standard S_NAr procedure (^{18}F-TBAF nucleophilic substitution)[195] along with HCl deprotection (Table 3). Several conditions for radiofluorinations were tested on the 6-Chloropyridoxine triacetate precursor (table 3, table 4). Before attempting any radiofluorinations, the precursor, cold standard and deprotected precursor were analysed by HPLC (appendix 1).

Table 3. Radiofluorination attempts on 6-Chloropyridoxine triacetate. Standard KF methodology was used in order to make [^{18}F]TEAF. The chlorine precursor was stirred 30 minutes at 130 °C in DMF. In one experiment, this step was followed by deprotection. In one experiment, the reaction mixture was directly transfer into a vial. Experiments were monitored by HPLC analysis.

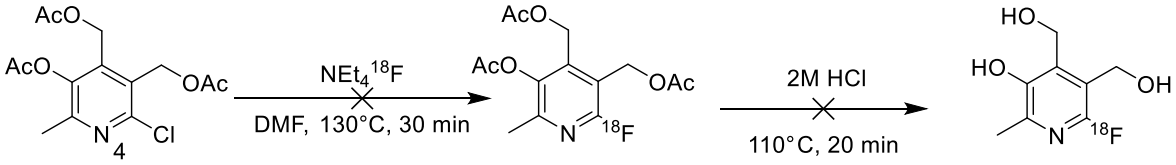

Experiment	Starting activity (mCi)	Deprotection method	Final activity (mCi)	Remaining precursor	Product formation
1	162	HCl[a]	61.4	No	No
2	82	N/A	27.2	No	No

a. 2 M HCl (H_2O) for 20 minutes 110 °C

Experiment 1: There was no trace of the precursor, product and only a little trace of Chloropyridoxine (deprotected precursor) in the final mixture which indicates that in these conditions the precursor is being broken down. A possible explanation is that once all the precursor is deprotected to the Chloropyridoxine, this compound is susceptible to radical scavenging which may lead to its degradation. As discussed in the introduction, pyridoxine is

known as a radical scavenger[130,131] and it would not be surprising that this would also be the case for Chloropyridoxine.

Experiment 2: The last attempt using [^{18}F]TEAF was done without deprotection in the module in order to attempt manual deprotection with citric acid and or ethanol as radical scavengers (table 3, line 3). After stirring 30 minutes at 130 °C in DMF in the presence of [^{18}F]TEAF, the solution was transferred to the product vial. The final activity was 27.2 mCi (initial: 82 mCi). When the reaction mixture was analysed by HPLC, there was no gamma signal except for the free fluoride one. In addition, there was no trace of the precursor and a little trace of the Chloropyridoxine (5.6 minutes, figure 19 and 21). Due to these observations, no manual deprotections were attempted because there was no sign of any fluorination on the pyridoxine. This indicates that the precursor may be susceptible to deprotection and complete degradation just by stirring with [^{18}F]TEAF in DMF at 130 °C for 30 minutes.

Experiment 1:

UV-Detector Ch.1

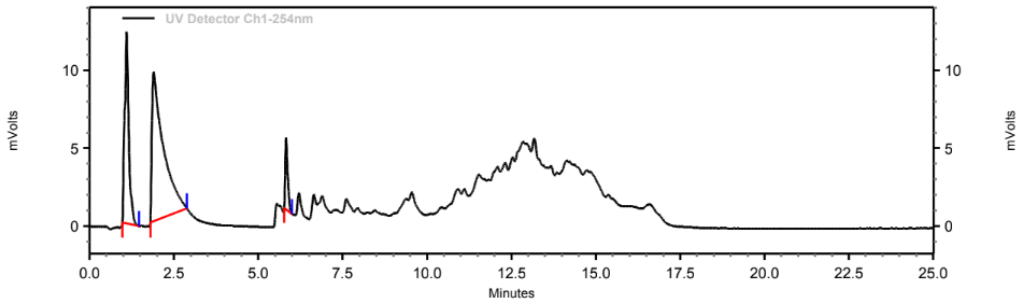

UV Detector
Ch1-254nm Results

Retention Time	Area	Area Percent	Height	Height Percent
1.100	103407	29.327	12271	46.377
1.900	225302	63.897	9579	36.203
5.825	23894	6.776	4609	17.419
Totals	352603	100.000	26459	100.000

Figure 8. HPLC-UV analysis of the crude reaction mixture from the standard SNAr radiochemistry with HCl deprotection of the 6-Fluoropyridoxine precursor.

Gamma

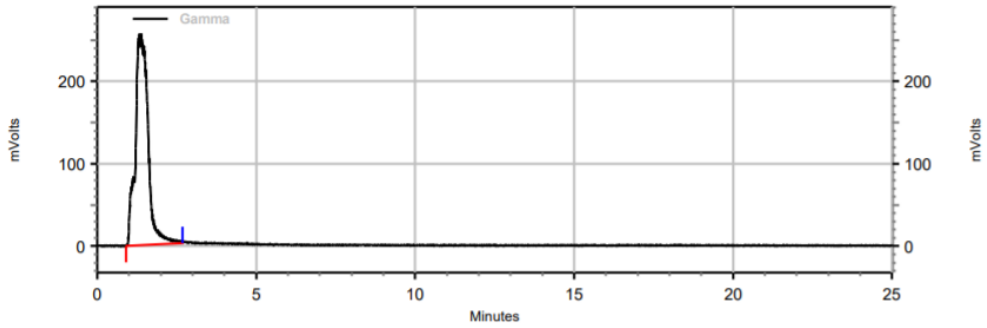

Gamma Results

Retention Time	Area	Area %	Height	Height %
1.333	7115117	100.00	256748	100.00
Totals	7115117	100.00	256748	100.00

Figure 9. Radio-HPLC analysis of the crude reaction mixture from the standard S_NAr radiochemistry with HCl deprotection of the 6-Fluoropyridoxine precursor.

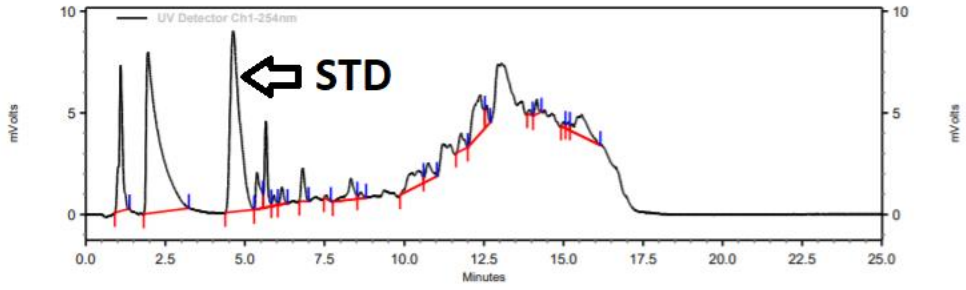

UV Detector
Ch1-254nm Results

Retention Time	Area	Area Percent	Height	Height Percent
1.092	54806	8.200	7195	16.987
1.950	219058	32.775	7971	18.820
4.625	183067	27.390	8896	21.003
5.375	17417	2.606	1809	4.271
5.658	25601	3.830	4254	10.044
5.908	3456	0.517	515	1.216
6.158	5916	0.885	852	2.012
6.808	12405	1.856	1635	3.860
7.533	1227	0.184	176	0.416
8.325	14673	2.195	1041	2.458
8.633	2647	0.396	285	0.673
10.433	22840	3.417	726	1.714
10.750	11043	1.652	856	2.021
11.783	9037	1.352	844	1.993
12.383	41526	6.213	1890	4.462
12.592	6020	0.901	1043	2.463
13.925	1387	0.208	225	0.531
14.158	4644	0.695	728	1.719
15.000	1446	0.216	234	0.552
15.142	2194	0.328	334	0.789
15.442	27958	4.183	846	1.997

Figure 10. HPL-UV analysis of the crude reaction mixture from the standard S_NAr radiochemistry with HCl deprotection of the 6-Fluoropyridoxine precursor with Co-inject of cold standard (STD, shown by arrow).

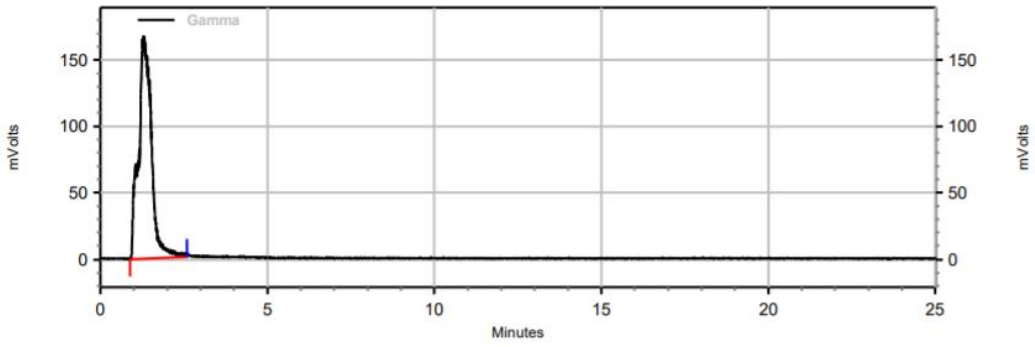

Gamma Results

Retention Time	Area	Area %	Height	Height %
1.295	4440458	100.00	167674	100.00
Totals	4440458	100.00	167674	100.00

Figure 11. Radio-HPLC analysis of the crude reaction mixture from the standard S_NAr radiochemistry with HCl deprotection of the 6-Fluoropyridoxine precursor with Co-inject of cold standard.

Experiment 2:

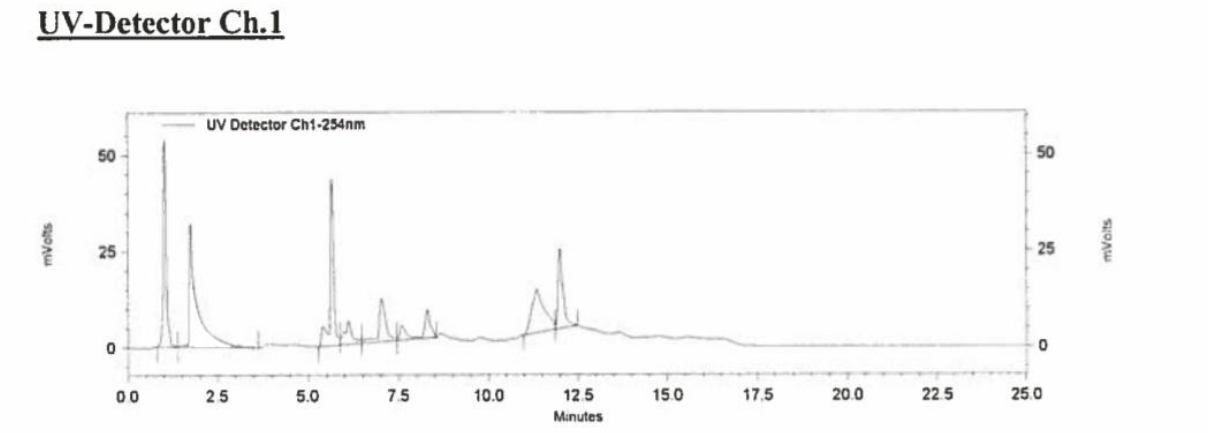

UV Detector
Ch1-254nm Results

Retention Time	Area	Area Percent	Height	Height Percent
1.033	289884	15.258	53875	28.970
1.750	458820	24.150	31934	17.172
5.642	313945	16.524	43453	23.366
6.125	88843	4.676	5991	3.222
7.025	151556	7.977	11176	6.010
8.300	126825	6.675	7475	4.020
11.358	274797	14.464	11364	6.111
12.000	195218	10.275	20699	11.130
Totals	1899888	100.000	185967	100.000

Figure 12. HPLC-UV analysis of the crude reaction mixture from the standard S_NAr radiochemistry without deprotection of the 6-Fluoropyridoxine precursor.

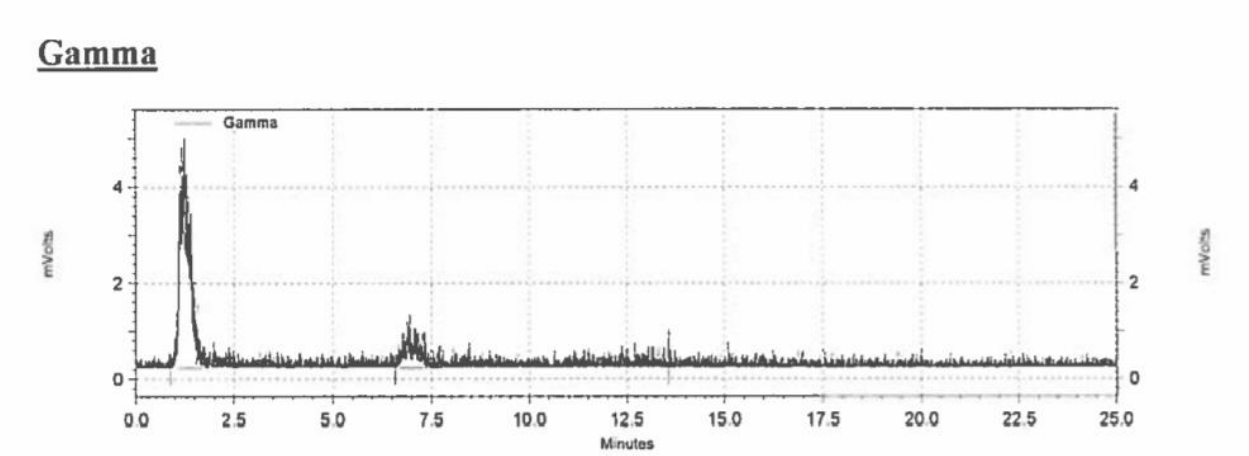

Gamma Results

Retention Time	Area	Area %	Height	Height %
1.260	77517	80.32	4772	71.64
6.948	18159	18.82	1097	16.47
13.582	830	0.86	792	11.89
Totals	96506	100.00	6661	100.00

Figure 13. Radio-HPLC analysis of the crude reaction mixture from the standard S_NAr radiochemistry without deprotection of the 6-Fluoropyridoxine precursor.

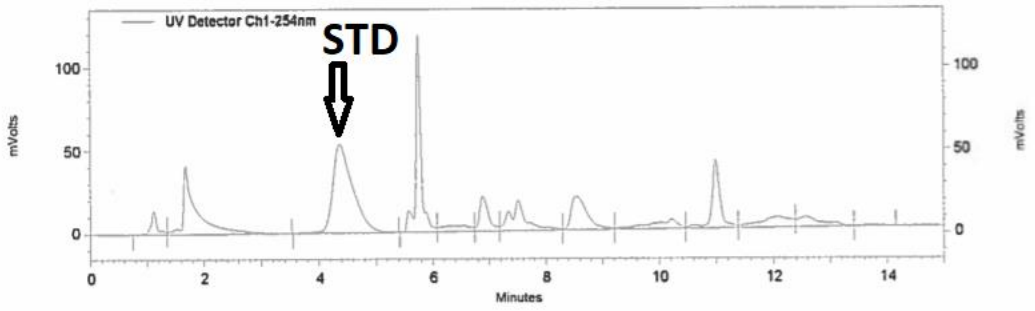

UV Detector
Ch1-254nm Results

Retention Time	Area	Area Percent	Height	Height Percent
1.117	105985	2.137	14274	4.080
1.675	675899	13.626	41201	11.777
4.367	1289026	25.986	53115	15.182
5.750	762626	15.374	118948	34.000
6.367	121942	2.458	3460	0.989
6.883	232063	4.678	20894	5.972
7.508	348285	7.021	18088	5.170
8.533	393461	7.932	20046	5.730
10.217	181092	3.651	5702	1.630
10.983	412095	8.308	40988	11.716
12.083	235112	4.740	6295	1.799
12.567	182360	3.676	6109	1.746
13.733	20448	0.412	727	0.208
Totals	4960394	100.000	349847	100.000

Figure 14. HPL-UV analysis of the crude reaction mixture from the standard S_NAr radiochemistry without deprotection of the 6-Fluoropyridoxine precursor with co-injection of cold standard (STD, shown by arrow).

.

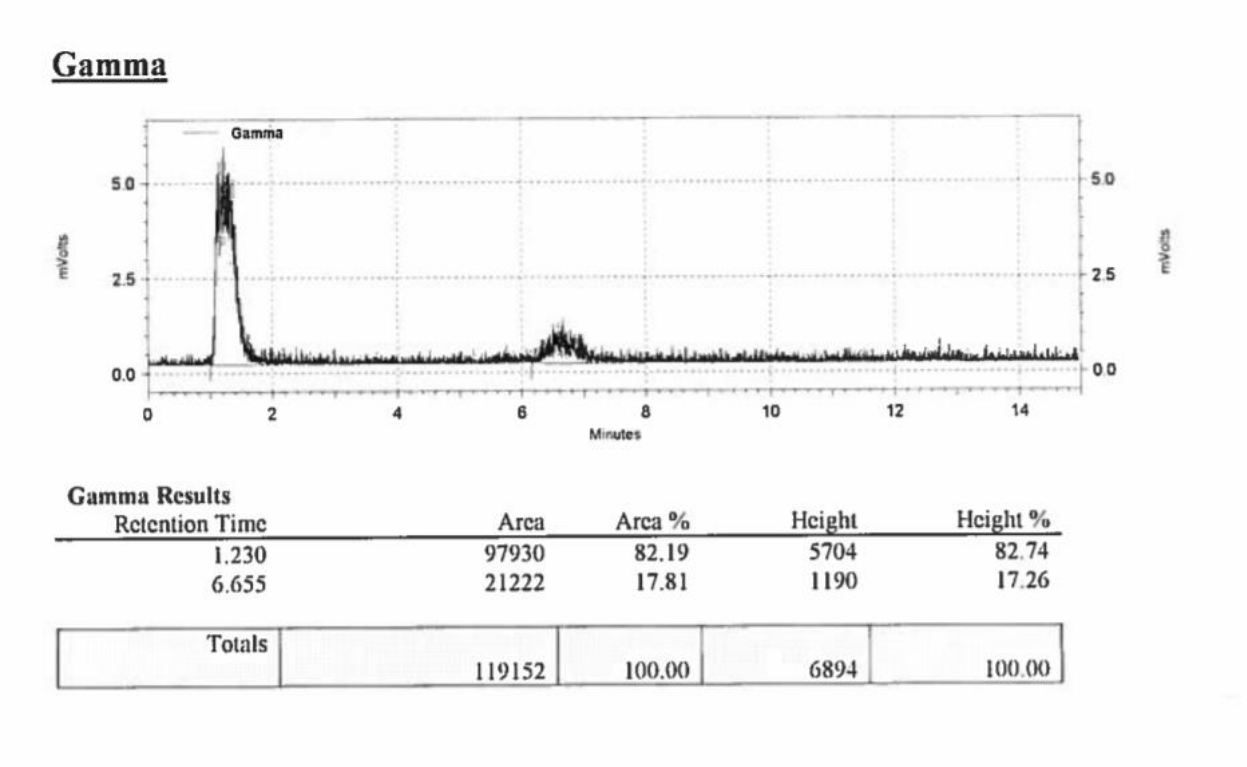

Gamma Results

Retention Time	Area	Area %	Height	Height %
1.230	97930	82.19	5704	82.74
6.655	21222	17.81	1190	17.26
Totals	119152	100.00	6894	100.00

Figure 15. Radio-HPLC analysis of the crude reaction mixture from the standard S_NAr radiochemistry without deprotection of the 6-Fluoropyridoxine precursor with co-injection of cold standard.

Due to the lack of success of fluorinations, a stability test was performed with the precursor. 3.2 mg of precursor was heated at 130 °C in pure DMF for 30 minutes and in DMF with NEt_4HCO_3. There was no recovery of the precursor at 130 °C with tetraethylammonium bicarbonate and some decomposition in pure DMF at high temperature. This shows that the precursor is in fact not stable in DMF at high temperature with the presence of base. These observations fit with previous studies on the stability of pyridoxine. For example, Yessaad and colleagues demonstrated that 30% of vitamin B_6 gets decomposed after stirring at 80 °C for one hour in an aqueous solution of 0.1 M NaOH.[196] Thus, we concluded that the precursor is not stable under the conditions used and that standard S_NAr should not be used for this compound.

Since none of the attempted experiments using [^{18}F]TEAF resulted in the formation of the product or any radiofluorination of the pyridoxine, this methodology was dropped and, a different methodology was approached. The new methodology consisted of using tetraethylammonium bicarbonate with K^{18}F/K2.2.2 in DMF at high temperatures (table 4). This

methodology was previously successful for the radiofluorination of chloroquinoline (unpublished results from the Scott lab). In addition, the method was done at lower temperature (100 °C). In order to test several conditions at the same time, the reactions were done in batch manually. (table 4).

Table 4. Manual radiofluorinations attempts of 6-Chloropyridoxine triacetate. Waters QMA light was preconditioned with 10 mL Ethanol, 10 mL 0.5 M $NaHCO_3$, 10 mL H_2O. GE PETtrace cyclotron $^{18}O(p,n)^{18}F$ reaction was run with 2.5 mL of $[^{18}O]H_2O$ in target irradiated at 55 micro Amps for 2 minutes. After trapping on QMA fluoride was eluted with a solution of KOTf (10 mg) and K_2CO_3 (50 micrograms) in H_2O (0.5 mL). Then acetonitrile (1 mL) was added and the mixture was azeotropically dried at 100 °C under vacuum for 5 minutes and an additional 5 minutes under vacuum and a stream of Argon. Resulting $[^{18}F]KF$ was dissolved in DMF (3 mL) and removed from the hot cell for use in batch reactions manually. 100 µL or about 1 mCi of the solution was added to each 500µL reaction (DMF only) containing the precursor and tetraethylammonium bicarbonate.

Mass of precursor (mg)/µmol	Mass $TEAHCO_3$[a]/µmol	Ratio (precursor/$TEAHCO_3$)	Temperature (°C)
3.3/10	0.8/4.9	2	100
3.3/10	1.9/10	1	100
3.3/10	3.8/20	0.5	100
3.3/10	0.8/4.9	2	110
3.3/10	1.9/10	1	110
3.3./10	3.8/20	0.5	110
6.6/20	0.8/4.9	4	100
6.6/20	3.8/20	1	100
6.6/20	7.6/40	2	100
6.6/20	0.8/4.9	4	110
6.6/20	3.8/20	1	110
6.6/20	7.6/40	2	110

a. $TEAHCO_3$ = tetraethylammonium bicarbonate (NEt_4HCO_3)

None of these trials gave any of the 6-Fluoropyridoxine triacetate (radio-TLC analysis) and all had remaining starting material left (TLC analysis). These results show that the precursor is degraded easily in the presence of base at high temperatures (100 °C and above) and cannot be fluorinated with $[^{18}F]TEAF$ of $K^{18}F$/Kryptofix under the conditions tested. Again, this might be due to the instability of pyridoxine in presence of base at high temperature and its susceptibility to ionizing radiation. In addition, the presence of the acetyl group may increase that instability since there is the possibility of creating an acetyl anion or radical which can increase the rate of degradation. Due to this lack of success for fluorination and high susceptibility of degradation of

triacetoxy chloropyridoxine, this indicates that this precursor may not be a good precursor for the formation of the radiotracer.

1.4. Synthesis of 6-Iodopyrdoxine triacetate and attempted work

Following a similar idea, the next methodology for fluorination of the 6 position of pyridoxine was based on the conversion of a 6-halide pyridoxine. In this methodology, instead of using chlorine, the 6-Iodopyridoxine was synthesized. Direct fluorination of 6-Iodopyridines derivatives has been reported[197] as well as formation of spirocyclic hypervalent iodine(III) complexes from 6-Iodopyridines derivatives which can also be used to incorporate the fluorine.[198] Therefore, 6-Iodopyridoxine triacetate was synthesized in two steps from pyridoxine HCl as described by Mason and coworkers[174] (scheme 8) with a 42% total yield.

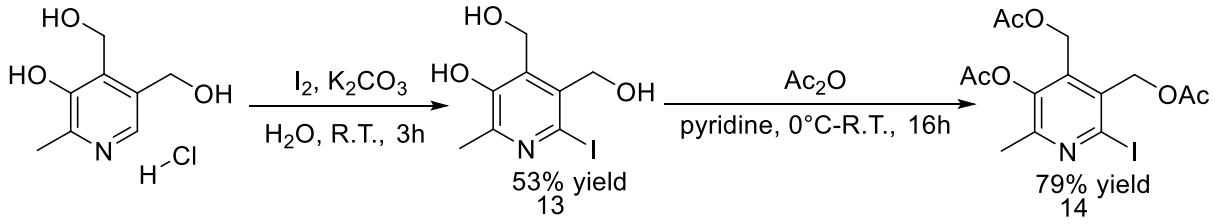

Scheme 8. Synthesis of 6-Iodopyridoxine triacetate from pyridoxine HCl. Pyridoxine HCl was iodinated in basic conditions with a 53% yield and the resulting 6-Iodopyridoxine was acetylated on all oxygens with a 79% yield.

With this product in hand, two standard direct fluorinations methods were tested: TBAF at high temperature and KF/Kryptofix at high temperature (table 5). In both experiments, the starting material was completely gone after 25 minutes. There was no sign of the fluorine peak for triacetoxy-6-Fluoropyridoxine (figure 16 and 17, -73.22 ppm: previously synthesized). This shows this precursor is very sensitive to high heat in the presence of fluorine sources. This instability in presence of fluorine maybe due to elimination of the acetyl groups by fluorine. This could lead to acetyl ions which are capable of degrading a compound. It has been demonstrated that NaF can lead to deacetylation of histones[199] and that fluorine can act as nucleophilic catalyst for hydrolysis and acyl migration.[200]

Table 5. Direct fluorination attempts on 6-Iodopyridoxine triacetate

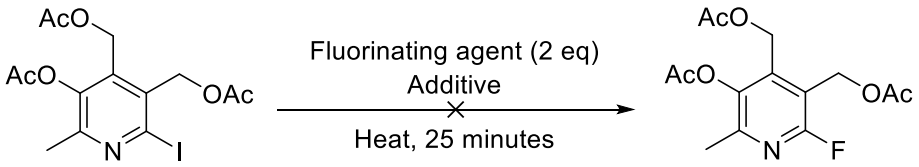

Experiment	Fluorinating agent	Additive	Temperature (°C)	Solvent	Concentration (M)	Remaining SM[b]
1	TBAF[a]	N/A	80	THF	0.5	No
2	KF	Kryptofix (2 equiv.)	90	DMSO	0.5	No

a. TBAF 1 M in THF
b. SM: Starting material

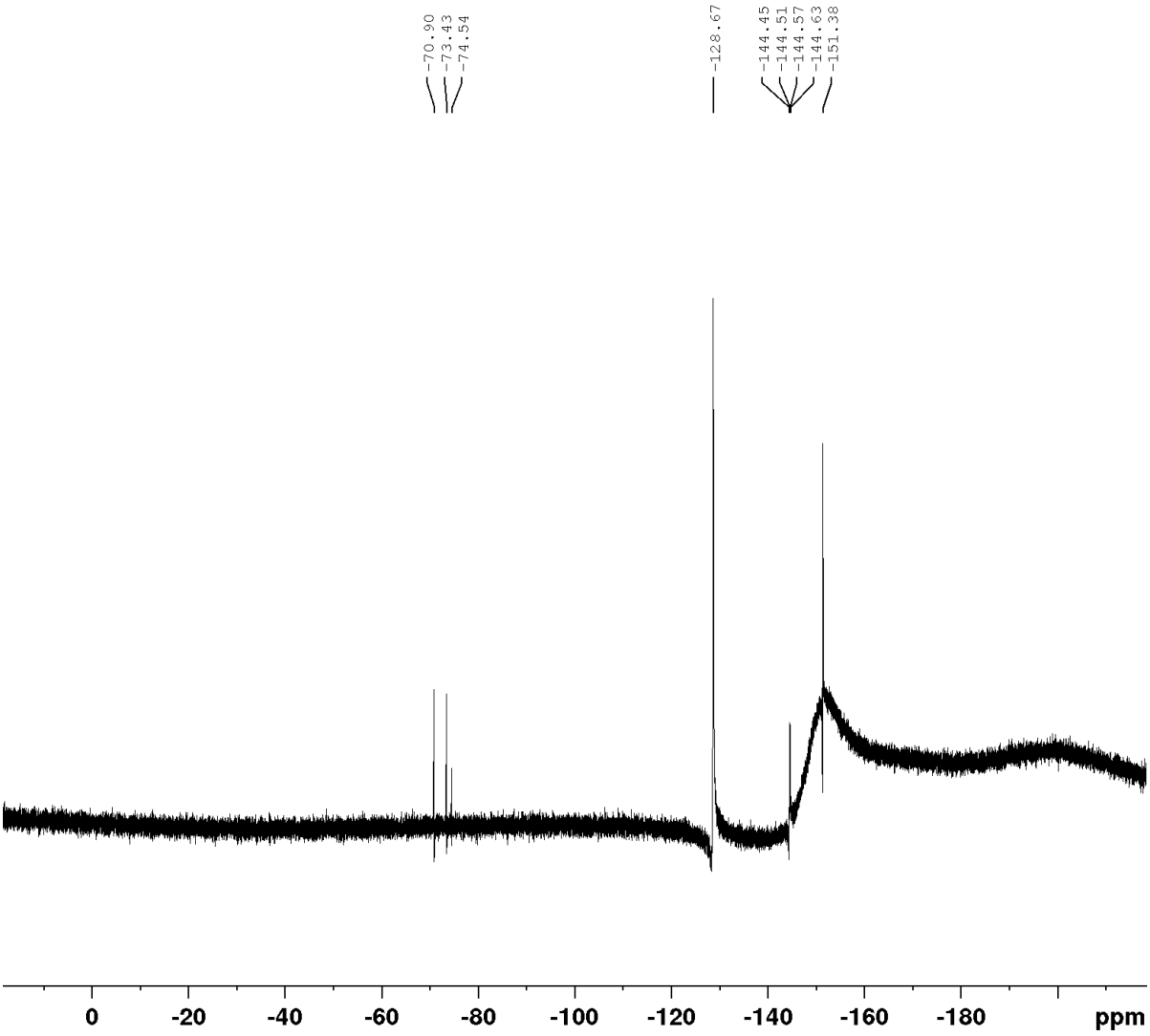

Figure 16. Crude ^{19}F NMR of the direct fluorination attempt on 6-Iodopyridoxine triacetate with TBAF.

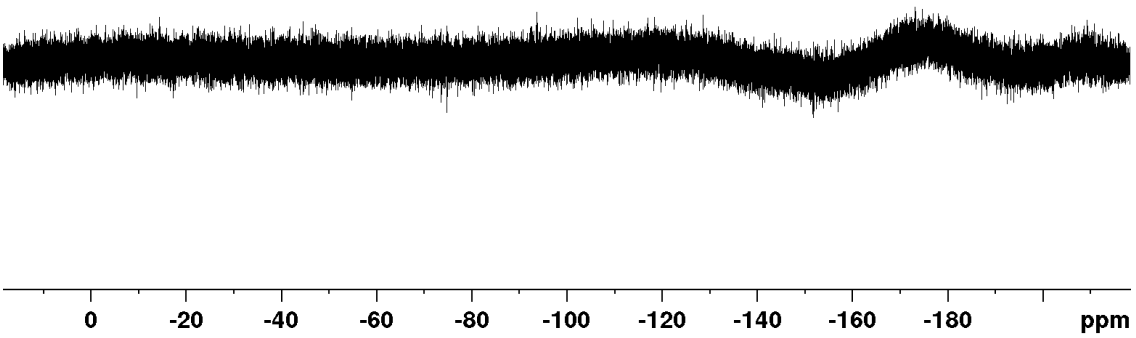

Figure 17. Crude ^{19}F NMR of the direct fluorination attempt on 6-iodopyridoxine triacetate with KF/Kryptofix.

Direct fluorination of the iodine did not work. Therefore, the conversion to the spirocyclic hypervalent iodine (III) precursor was attempted. Spirocyclic iodonium ylides have been synthesized from non-activated heteroarenes and have been used to incorporate ^{18}F into these compounds[196] Rotstein and coworkers demonstrated that Spiroadamantyl-1,3-dioxane-4,6-dione is an effective auxiliary to generate iodonium ylides which can be fluorinated at high temperatures in DMF.[182] Interestingly, they were able to make the iodonium ylide of pyridine and fluorinate it. Thus, the methodology used to synthesize the pyridine iodonium ylide was tested on 6-Iodopyridoxine triacetate (scheme 9).

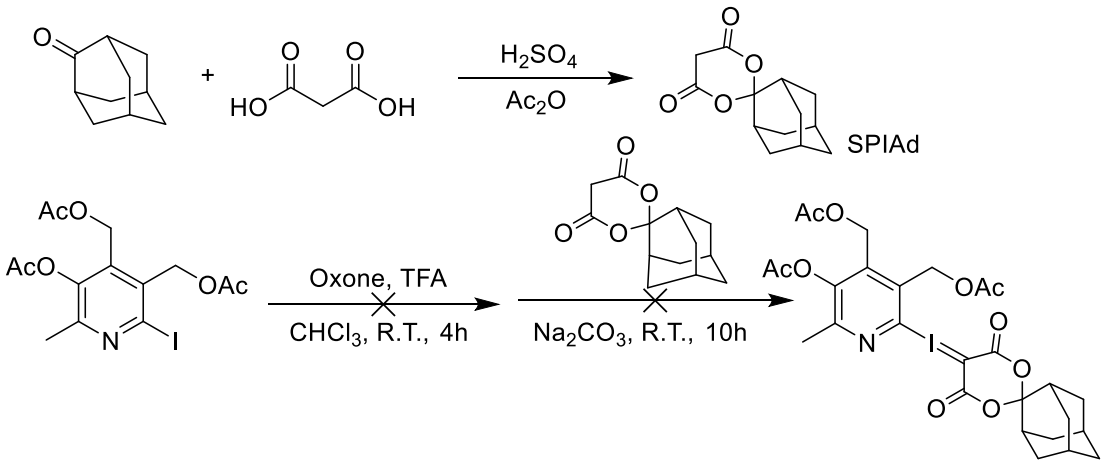

Scheme 9. Synthesis of spiroadamantyl-1,3-dioxane-4,6-dione (SPIAd) and attempted synthesis of pyridoxine iodonium (III) ylide. SPIAd was synthesized from 2-adamantanone and malonic acid based on a previous literature procedure.[185] 6-Iodopyridoxine triacetate (0.25 mmol, 105.3 mg, 1 equiv.) was treated with trifluoroacetic acid (0.76 mL) and Oxone (0.4 mmol, 120 mg, 1.2 equiv.) in chloroform (0.25 mL) and the reaction stirred for 4 hours. The mixture was dried with rotary evaporation. The crude oil was resuspended in ethanol (0.7 mL) and SPIAd was added (1 eq, 0.25 mmol in 0.5 mL 10% Na_2CO_3) then stirred 5-10 hours until full conversion. The mixture was diluted with H_2O and extracted with chloroform. The organic layer was washed with water (4x) and brine (1x). The organic layer was dried with $MgSO_4$, filtered and evaporated to dryness.

Unfortunately, this methodology did not lead to the desired product. The methodology consists of oxidizing the iodine using Oxone and adding the auxiliary to make the iodonium halide. An important part of the methodology is the use of trifluoroacetic acid which provides an acidic environment that is good for oxidation but also results in the protonation of the nitrogen in the pyridine ring in order to prevent oxidation at that position. However, the use of such a strong acid is probably the reason why the conditions failed since this sort of acidic conditions can lead to deprotection of the acetyl groups. Once the acetyl groups are deprotected, the resulting Iodopyridoxine or oxidized derivative will favor the aqueous layer in the final extraction. This can explain why this methodology did not work. One methodology that could make this work would be modifying the protecting groups. As previously observed, the acetyl protected pyridoxine is not only very susceptible to free fluoride decomposition but can also hinder the synthesis of the spirocyclic hypervalent iodine precursor. Therefore, potential future work could involve protecting the 6-Iodopyridoxine with other groups. One potential protection strategy would be benzyl groups (CH_2-C_6H_5). This strategy could be interesting since there is already

published methodology to synthesize the benzyl protected 6-Iodopyridoxine[174] and the benzyl protecting group is much more robust than the acetyl group[201] and will not have any electronic effect of the pyridine ring.

1.5. Attempted synthesis of the trimethyl ammonium precursor

The previous attempts at fluorination of the 6-Chloropyridoxine triacetate (compound 4) and 6-Iodopyridoxine triacetate (compound 14) showed that the acetylated derivatives of pyridoxine are sensitive to fluorine sources at high temperatures and bases at high temperatures. There seems to be some sort of mechanism by which base or fluorine can decompose these derivatives very fast (less than 20 minutes) at high temperatures (80 °C and above). The AgF_2 method used for the synthesis of the cold standard was low yielding but did result in fluorination and did not result in complete degradation of starting material. Three things can explain these observations: the experiment was done at room temperature, AgF_2 is not a source of free fluoride and is less aggressive than other fluoride sources. Therefore, the methodology used for radiofluorination of pyridoxine must follow one of these rules: done at low temperatures or done using less harsh fluorine sources.

Interestingly, although most radiofluorination labelling is done in harsh conditions (80 °C and above) there are some examples of radiofluorination done at low temperature (50 °C) and even at room temperature.[177,202] In the examples found in the literature, the authors used trimethylammonium salts as precursors for radiofluorination.[177,202] In addition, in both of these article, the authors show that this chemistry can be used on pyridine derivatives.[177,202] Therefore, the use of a trimethylammonium salt precursor might be the answer for the fluorination of the 6 position of pyridoxine. Several methods exist in order to synthesize a trimethylammonium salt on the 6 position of pyridine rings.[177,202,203] A few of these methods consists of the nucleophilic substitution of a leaving group by trimethyl amine.[177,203] Interestingly, one of these methods consist of doing the substitution of chlorine[177] and 6-Chloropyridoxine triacetate (compound 4) is already in hand so the experimental conditions to substitute the chlorine to the

trimethylammonium salt was attempted on this compound (scheme 10).

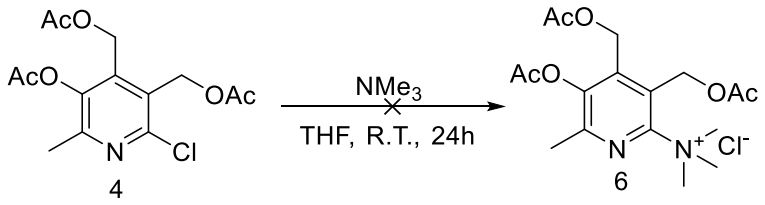

Scheme 10. Attempted synthesis of the trimethyl ammonium precursor by S_NAr reaction. 6-Chloropyridoxine triacetate (4) was dissolved in THF at room temperature. Trimethyl amine (2 M in THF) was added and the reaction was stirred 24 hours at room temperature. There was no formation of product and no conversion of the starting material.

Unfortunately, the conditions did not lead to the desired product nor to any consumption of the starting material. This may be explained by the fact that the acetyl groups block the 6 position for nucleophilic attack because of steric hinderance. In addition, this reaction is uphill thermodynamically due to the ionic and hindered nature of the product, which makes it a very difficult reaction to achieve. Still, in order to make sure that direct substitution was not possible with the acetyl group present, the activating group was changed.

One activating group that has been used for the synthesis of trimethyl ammonium pyridinium salt is the trifluoromethanesulfonic acid group.[202,203] This is a very good electron withdrawing group and a better leaving group than chlorine so it should theoretically react better than the chlorine. Therefore, the next attempt at direct substitution with trimethyl amine would be done with triacetoxy-6-Triflatepyridoxine. 6-Triflatepyridoxine (compound 15) was synthesized by a modified Balz-Schiemann procedure adapted from Kassanova and colleagues[204] by reacting 6-Aminopyridoxine with trifluoromethanesulfonic acid in the presence of sodium nitrite (scheme 11). The acetyl protection was done next to give the triacetoxy-6-triflatepyridoxine (compound 16) in two steps from 6-Aminopyridoxine (compound 2) in a 27% yield (figure 28).

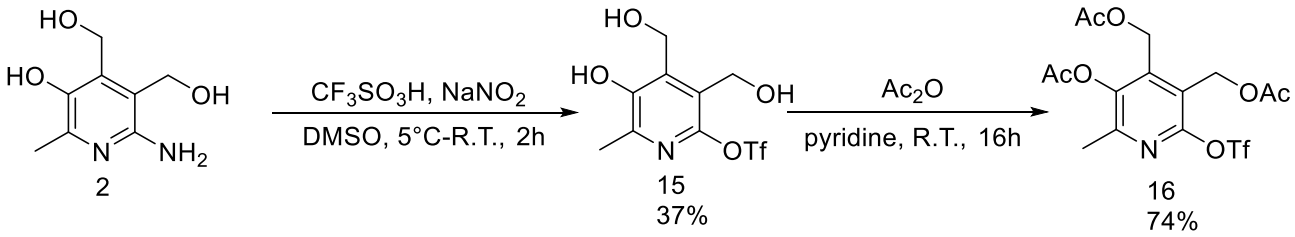

Scheme 11. Synthesis of triacetoxy-6-trifllatepyridoxine. 6-Aminopyridoxine (2) was modified to the pyridoxine triflate (15) by one-pot diazotization in the presence of triflic acid with a 37% yield. The 6-Trifllate pyridoxine was protected by acetyl groups to the corresponding triacetyl-6-triflatepyridoxine with a 74% yield.

With the 6-Triflate compound in hand, the synthesis of the 6-Trimethylammonium precursor was attempted with a direct S_NAr approach as previously reported.[202] This approach consists of stirring the 6-Triflate compound in the presence of NMe_3. Several conditions were attempted without any success. The experiments attempted are summarized in table 6.

Table 6. Attempted synthesis of the trimethylammonium precursor by direct addition of trimethyl amine to triacetoxy-6-triflatepyridoxine.

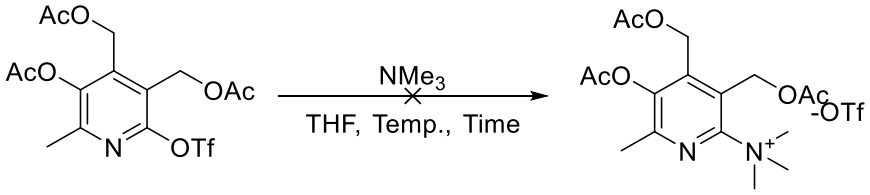

Temperature (°C)	Time (h)	Product formation	SM[a] conversion
4	24	None	None
R.T.	24	None	None
60	4	None	None

a. SM=Starting Material

Several conditions ranging from 0 °C to 60 °C were tested but none of them led to the desired product and none of them led to any consumption of the starting material (table 6, appendices 3-5). These results show that acetylated pyridoxine is not suitable for direct substitution with trimethylamine. As hypothesized before, this might be due to the steric effects of the acetyl protecting groups. In order to test this hypothesis, the substitution of the leaving group for the

trimethyl amine was attempted on the unprotected 6-Triflate pyridoxine (scheme 12) but without any success.

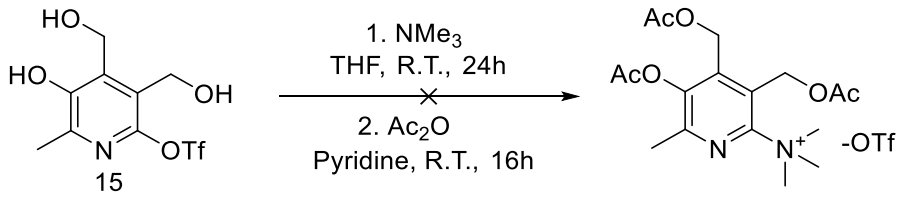

Scheme 12. Attempted formation of the trimethylammonium salt from the triflate precursor. After stirring compound 15 in presence of NMe_3 at room temperature in THF, the mixture was washed with water and extracted with tBuOH. The extract was evaporated to dryness and subjected to acetyl protection. The crude mixture was analysed by HPLC.

The only difference between the unprotected and protected triflate precursor was that there was some conversion of the starting material when using the unprotected triflate but the side products were not identified (appendix 7). This demonstrates that the acetyl groups can hinder reactivity but even without them, the formation of the trimethyl ammonium salt cannot be done by substitution on this position of pyridoxine. This might be due in part by the uphill nature of the reaction due to the product being ionic and the starting material being neutral.

A different approach to S_NAr to synthesize aryltrimethylammonium salts is by methylation of the corresponding dimethylamine.[203] This methodology has been used to synthesize 6—trimethylammonium pyridine triflate by Reeves and colleagues[203] and consists of the methylation of the corresponding N,N-dimethylamine pyridine with Methyl triflate at room temperature. This could be a very interesting pathway since 6-Dimethylpyridoxine can be accessible from pyridoxine HCl such as reported by Culbertson and colleagues.[179] Therefore, 6-Dimethylamine pyridoxine was synthesized as described by Culbertson, Enright and Ingold[179] and protected with acetyl groups as shown in scheme 13.

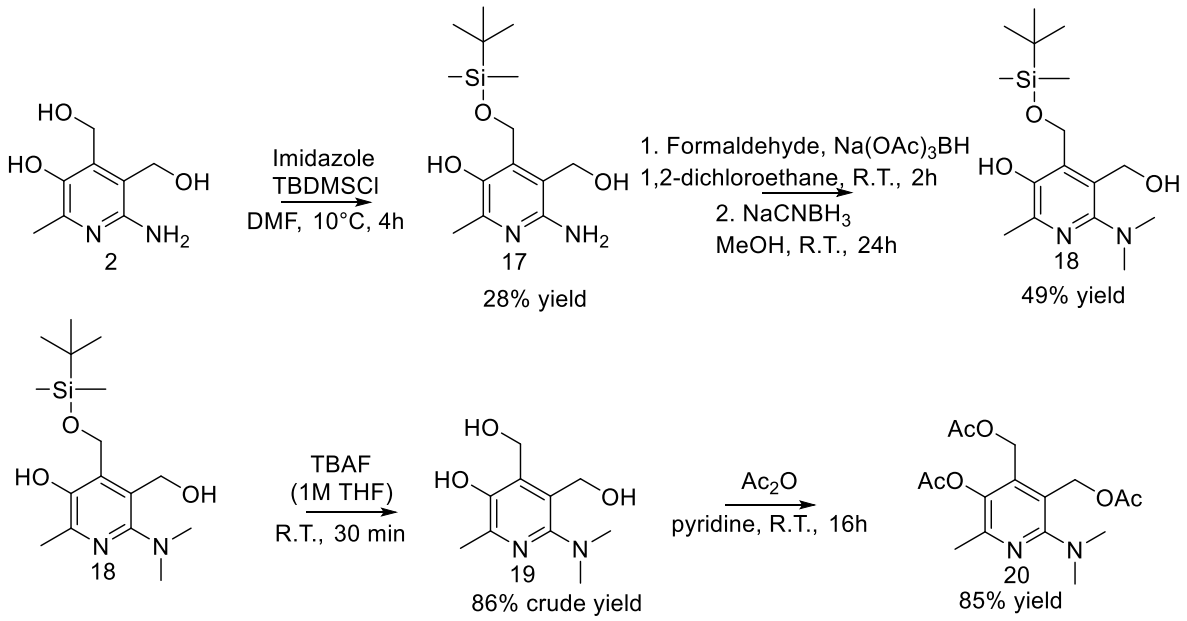

Scheme 13. Synthesis of 6-Dimethylaminopyridoxine triacetate from 6-Aminopyridoxine (compound 2). 6-Aminopyridoxine was protected on the α^4oxyen with TBDMSCl with a 28% yield, then the following compound was dimethylated to make compound 18 with a 49% yield which was transformed to 6-Dimethylpyridoxine with TBAF (86% crude yield, product not purified). The following crude compound (19) was protected with acetic anhydride with an 85% (from precursor 18).

6-Dimethylaminepyridoxine (compound 19) was synthesized according to the scheme from Culbertson and colleagues[179] in a 12% yield from 6-Aminopyridoxine (compound 2) in 3 steps. Next, 6-Dimethylaminepyridoxine was acetylated in an 85% yield (scheme 13). The resulting 6-Dimethylaminopyridoxine triacetate (compound 20) was subjected to two methylation procedures (table 7). One procedure was done at room temperature as described by Reeves and colleagues[203] and the other was done at 50 °C. None of these methods resulted in methylation of the dimethylamine.

Table 7. Attempted methylation of the 6-Dimethylaminopyridoxine triacetate.

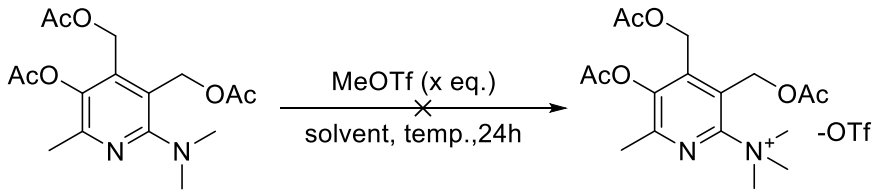

Experiment	MeOTf equivalents (x)	Solvent	Concentration (M)	Temperature
1	1.1	DCM	0.667	Room temperature
2	5	Toluene	0.1	50

In contrast to the substitution attempts, there was some consumption of the starting material in both procedures. The compounds made were not characterize but may be due to side reactions. The lack of reactivity can probably be explained due to the steric hinderance of the acetyl groups, or it can be due to the electron withdrawing effect of the acetyl groups which could be lowering the nucleophilicity of the nitrogen and decreasing the chances of nucleophilic attack. This demonstrates that the presence of acetyl groups may be an issue for the formation of the trimethylammonium salt precursor. Again, in this case, changing the protection strategy could lead to better reactivity. For example, using methoxymethyl ether instead of acetyl groups would potentially lead to better reactivity since this group would not have any electron withdrawing effect decreasing the nucleophilicity of the dimethylamine. However, the formation of the product is still unfavored due to it being ionic which makes this reaction uphill. Therefore, chances are that additional conditions would drive the formation of the product. For example, if a soluble Ag^+ source was added to the reaction, the formation of product would lead to an insoluble silver salt which would precipitate and drive the reaction forward.

Part 2 – Synthesis of cold standard 2: 2'-Fluoropyridoxine (2'-FPN)

The first steps for the synthesis of 2'-Fluoropyridoxine is the formation of a suitable precursor. For this purpose, the OTs leaving group is a prime example of a good precursor for fluorination.[182,184] The OTs leaving group can be easily accessible from an alcohol[205] and the formation of a 2'-Hydroxypyridoxine derivative has been previously reported in the literature.[178] In this report, the modification of the 2' carbon is done by a key reaction which is the Boekelheide reaction[206] which consist of the rearrangement of the pyridine N-oxide to the trifluoroacetylated methylpyridoxine. This compound can be readily hydrolysed to the corresponding 2'-OH. The synthesis of the 2'-alcohol was attempted following a similar methodology. The first step of the synthesis being the acetylation of the pyridoxine, followed by oxidation and then the Boekelheide reaction to give the alcohol in 49% yield (scheme 14, compound 10). This alcohol was thought to be the 2'-alcohol (compound 10', figure 18) but turned out to be the 3-alcohol due to an acyl migration (compound 10, figure 18). However, before making the tosyl and triflate precursor and attempting fluorination this was not known. Therefore, an acetylated tosylpyridoxine (compound 11, initially thought to be 2'-O-Tosylpyridoxine triacetate) was synthesized (scheme 14) and tested with various fluorination methodology.

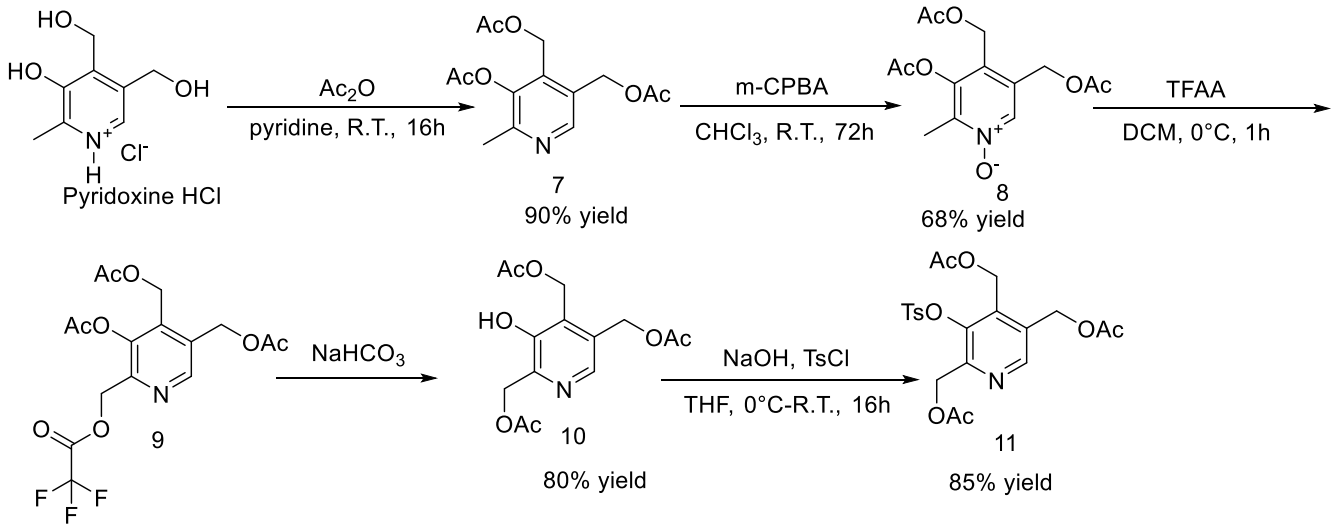

Scheme 14. Synthesis of 3-(p-toluenesulfonyl)-2,4,5-tri(((acetyl)oxy)methyl)-pyridine (compound 11). Pyridoxine HCl was first protected using a similar procedure described by Korytnyk and colleagues[191] with an 89% yield. The triacetylated N-oxide was prepared from compound 7 with hydrogen peroxide in acetic acid with a 67% yield. Compound 10 was synthesized using a modified previously reported procedure[178] from compound 8 in 80% yield. Finally, the alcohol was tosylated with an 85% yield to form compound 11.

Standard fluorination procedures were tested on the tosyl precursor (table 8) such as KF/Kryptofix and TBAF.[182] In addition, TBAF(pinacol)$_2$ was also tested. This alcohol coordinated TBAF was found to be very effective for the fluorination of primary tosylates[207] and is milder than the uncoordinated TBAF. To verify if any desired fluorination occurred, a crude ^{19}F NMR of the reaction mixture was analysed.

2.1.Fluorination of triacetate tosyl precursor (compound 11)

Standard fluorination procedure were tested on the tosyl precursor such as KF/Kryptofix and TBAF.[182] Also, an alcohol coordinated fluorine (TBAF(pinacol)$_2$) was also tested. In a recent article by the Scott group, this mild fluorinating agent was found to be very effective for the fluorination of primary tosylates.[207] The initial hypothesis was that these fluorinations were tested on the 2'-OTs precursor as shown in scheme 15, but the precursor was actually the 3-tosyl.

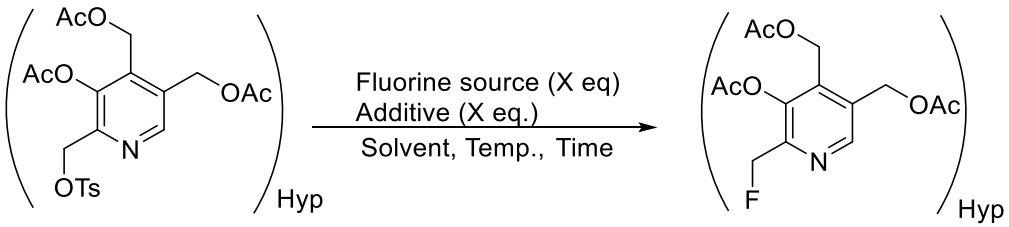

Scheme 15. Initial hypothesis for the fluorination of the tosyl precursor.

Originally, based on the chemical shift of -221 ppm found in the ^{19}F NMR of 2-(fluoromethyl)pyridine,[208] the chemical shift of triacetoxy-2-fluoropyridoxine was expected around 200 ppm. In addition, because it is a primary fluorine, it was expected to form a triplet due to the interaction with the two hydrogens present on the 2' carbon. In all of the experiments, there was no sign of any peak in the 200 ppm region nor any sign of a triplet in the crude ^{19}F NMR (appendices 8-14).

After determining the real structure of the compound, the crude ^{19}F NMR spectra from the experiments which were run were analysed to look for the presence of the 3 position fluorine. The fluorine signal of 3-Fluoropyridine has been demonstrated to be at -126.7 ppm in d_6-DMSO[209] and -125.7 ppm in $CDCl_3$ (114.2 in the protonated N-H+ form)[210] so this was used as a reference to analyse the spectra. There was no fluorine signal in that region in any of the experiment other than the signal from TBAF.

Table 8. Attempted fluorination of the tosyl precursor. The tosyl precursor previously synthesized and thought to be the 2'-OTs precursor (scheme 15) was fluorinated using different conditions. The formation of product was followed by ^{19}F NMR and HPLC-UV spectrum were analyse to look for remaining starting material.

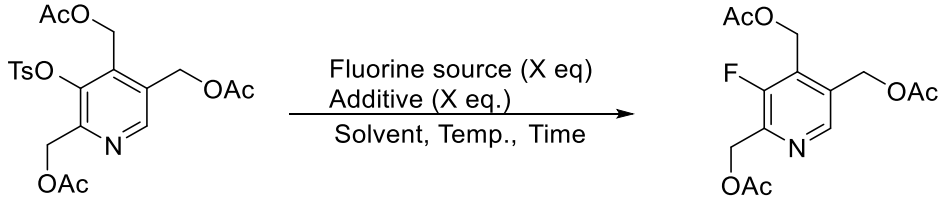

Fluorine source	Equivalents of fluorine (x)	Additive (x equiv.)	Solvent	Temperature (°C)	Time (h)	Product formation[a]	Remaining SM[b]
TBAF	3	N/A	THF (0.33 M)	50	16	No	No
				80	16	No	Yes
				110	16	No	Yes
$TBAF(Pin)_2$	2	N/A	MeCN (0.157 M)	80	16	No	No
				50	16	No	No
KF	3	3 (Kryptofix)	DMSO (0.1 M)	100	16	No	No
				120	16	No	No

a. Analysed by HPLC-UV and fluorine NMR

b. Analysed by HPLC-UV

In the experiments with KF, there was a peak at 145 ppm which is the peak for KF (appendices 13-14). In the experiments with TBAF and $TBAF(Pinacol)_2$ there was also fluorine signals other than TBAF (appendices 8-12). In all of these experiments, the TBAF fluorine signal was evident at 128 ppm (TBAF fluorine signal in $CDCl_3$ previously measured at 129.36 ppm[211]). In both experiments with $TBAF(Pinacol)_2$ and in the experiments with TBAF at 50 °C and 80 °C there is a fluorine peak at 66 ppm (appendices 8-11). This is a very unusual chemical shift for fluorine; hence this was a strange observation. One possible reason for the observation of that peak would

be that there is formation of p-toluenesulfonyl fluoride. In fact, the fluorine peak for p-toluenesulfonyl fluoride has a chemical shift of 66.2 ppm in chloroform[212] which is exactly the chemical shift seen in these experiments. Since the precursor is a p-toluenesulfonyl ether this is very likely since the fluoride could attack the sulfur and create p-toluenesulfonyl fluoride. The lack of this peak in the experiment with TBAF at 110 °C (appendix 12) might be due to other mechanism happening at that temperature instead of formation of tosyl fluoride. Another interesting observation is the presence of multiple fluorine peaks at around 150 ppm in all the experiments conducted with TBAF (appendices 10-12) but not with TBAF(Pinacol)$_2$ (appendices 8-9). This might be due to the fact that TBAF is a harsher fluorine source than TBAF(Pinacol)$_2$. It is unclear what these fluorine peaks represent. These results show that there is some reaction of the starting material but none that leads to the desired product.

In order to verify if all the starting material is consumed through side reaction or decomposition, an HPLC was conducted on the crude reaction to observe if there was remaining starting material (appendices 22-28; HPLC of the starting material in appendix 21). In most of the experiments, no starting material was left in the reactions. Surprisingly, in the experiments conducted with TBAF at 80 °C and 110 °C there was still some starting material in the reaction mixture (appendices 25-26) in contrast to the experiment conducted at 50 °C (appendix 24). These contradicting results may be due to remaining starting material on the side walls of the reaction vessels which did not dissolve in the solvent or react with the TBAF. This is probably the case since in all of the experiments the final crude mixture resembles a black tar like substance which may be due to the decomposition of the starting material (it is important to note that a lot of black solid present in that tar like substance is not soluble in any common solvents such as chloroform, methanol, acetone, ethyl acetate, hexanes or water). Therefore, the starting material is completely consumed in all of the experiments conducted.

2.2. Synthesis of triflate precursor and attempted fluorination.

Due to the failure to fluorinate the tosyl precursor, a new precursor needed to be synthesized. A very well known precursor for radiochemistry is the OTf precursor due to its use in the synthesis of ^{18}F-FDG.[213] By following a very similar synthesis to the one for tosylpyridoxine (compound 11), triflatepyridoxine (compound 21) was synthesized from pyridine HCl in 4 steps with a 44% yield with the crucial step being protection of the alcohol (compound 10) with

trifluoromethanesulfonic anhydride (scheme 14, scheme 16).

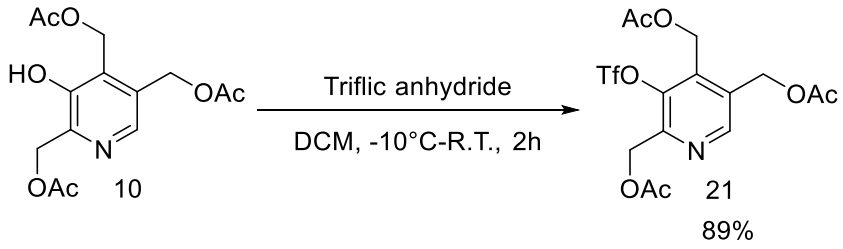

Scheme 16. Synthesis of 2,4,5-tri(((acetyl)oxy)methyl)-pyridin-3-yl trifluoromethanesulfonate (compound 21).

Standard fluorination procedures were tested on the triflate precursor such as KF/Kryptofix and CsF (table 9).[182] However, the experiments with KF and CsF were conducted for 60 minutes and 20 minutes, respectively. This relatively short reaction time was due to the fact that the solutions turned into a black tar rapidly in these reactions, indicating that the reactions are not proceeding as desired. Similarly, to the experiments conducted with the tosyl precursor, the crude reaction was analysed by fluorine NMR for the presence of product. Originally, the expected fluorine signal was expected to be a triplet showing up around -200 ppm. This type of signal was not observed in any of the reactions. As stated above (section 2.1), after determining the real structure of the compound, the crude ^{19}F NMR spectra from the experiments which were run were analysed to look for the presence of the 3 position fluorine (-126.7 ppm in d_6-DMSO[209] and -125.7 ppm in $CDCl_3$, 114.2 in the protonated N-H+ form).[210] There was no fluorine signal in that region in any of the experiment other than the signal from TBAF.

Table 9. Fluorination attempts on 2,4,5-tri(((acetyl)oxy)methyl)-pyridin-3-yl trifluoromethanesulfonate (compound 21). The triflate precursor previously synthesized and thought to be the 2'-OTf precursor was fluorinated using different conditions. The formation of product was followed by ^{19}F NMR and HPLC-UV spectrum were analyse to look for remaining starting material.

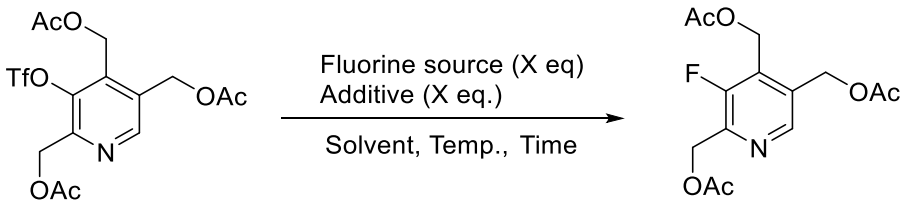

Fluorine source	Experiment	Solvent	Additive	Temperature (°C)	Time (min)	Remaining SM[a]	Fluorination of the 2' position[b]
CsF	1	TbuOH (0.1 M)	N/A	90	20	No	No
	2			120	20	No	No
	3			150	20	No	No
KF	1	DMSO (0.1 M)	Kryptofix	80	60	No	No
	2			100	60	No	No
	3			120	60	No	No

a. Analyse by HPLC-UV

b. Analysed by ^{19}F NMR

In the experiments with CsF, there was no fluorine signal at all in the NMR (appendices 15-17). In the experiments with KF there was the presence of a fluorine signal at -77 to78 ppm (appendices 18-20). This signal is very close to the fluorine signal of the starting material (-72.8 ppm) but based on the HPLC experiments there is no starting material left (appendices 34-36). Therefore, this could the signal for some sort of triflate derivative (CF_3SO_2R) but unlike with the tosyl precursor, there is no signal in the positive region which means that there is no formation of CF_3SO_2F (the fluorine attached to the sulfur should have a chemical shift pf 37.7 ppm).[214] It is unclear what kind of triflate derivative is being formed. In the experiments with KF, there is also the presence of a peak at -86 ppm (appendices 18-20), which seems to get larger as the temperature of the experiment increases (largest peak in the experiment at 120 °C). It is unclear from what sort of product this fluorine signal is derived. It could be some sort of SO_2CF_3 derivative or decomposition product for example.

In order to verify if all starting material is consumed through side reaction or decomposition, an HPLC was conducted on all of the reaction to observe if there was remaining starting material. In all of the experiments, there was no remaining starting material (appendices 31-36; HPLC UV of the starting material in appendix 29 and appendix 30).

Due to these results, the stability of the starting material was tested. The triflate starting material was stirred at 120 °C for 20 minutes in tBuOH and DMSO and there was no decomposition (the solution stayed clear and the compound was still present as observed by TLC and HPLC: appendix 37 and appendix 38). This shows that the precursor is stable at high temperatures in the solvents used and therefore, it is the presence of the free fluoride source that leads to decomposition.

Initially, after failing all the fluorination attempts, the literature was searched for alternatives and a paper from 1976 from Underwood and colleagues was discovered.[215] In this publication, the authors attempted to synthesize the same alcohol as the one presented here: triacetoxy 2'-hydroxypyridoxine. However, in the article triacetoxy 2'-hydroxypyridoxine was not successfully synthesized following the same synthesis steps due to an acyl migration which results in the formation of the triacetoxy 3-hydroxypyridoxine instead (figure 18 below).

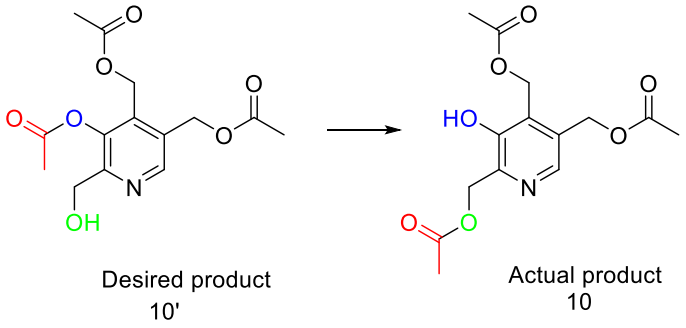

Figure 18. Acyl migration of triacetoxy-2'-hydroxypyridoxine. The acetyl group in red is being transferred from the oxygen in blue (3-OH) to the oxygen in green (2'-OH).

In the article, the authors stirred their trifluoroacetic ester in methanol for 24 hours in order to hydrolyse to the corresponding 2'-alcohol, providing the time necessary for the acyl migration to occur. In contrast, the ester was hydrolysed by extraction (DCM/$NaHCO_3$) in our methodology which makes it less likely that there was migration during purification. There should not be any

trace of the alcohol before purification because the reaction is running in anhydrous conditions. However, because this rearrangement would change the position that is being modified and the pyridoxine moiety itself, some additional NMR experiments were conducted on the alcohol compound to analyse if the alcohol synthesized was the 2' or 3-OH.

The 2D NMR experiments (figure 21) show that all protons from the CH_2 present are coupling to the carbonyls carbon from the acetyl groups (figure 19) and that all protons from the acetyl CH_3 groups are coupling to the carbons from the CH_2 group (figure 20). This clearly shows that the compound in hand is in fact the 3-OH compound such as reported by Underwood and colleagues[215].

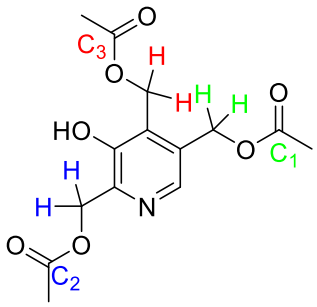

Figure 19. Structure of the 3-OH (compound 10) compound highlighting the long-range coupling between protons from the CH_2 groups and carbons from the acetyl groups. The protons in blue red and green are coupling with C2, C3 and C1, respectively.

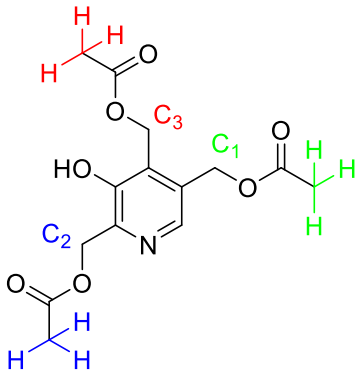

Figure 20. Structure of the 3-OH (compound 10) compound highlighting the long-range coupling between protons from the acetyl groups and carbons from the CH_2 groups. The carbon 1, 2 and 3 are coupling with the protons in green, blue and red, respectively.

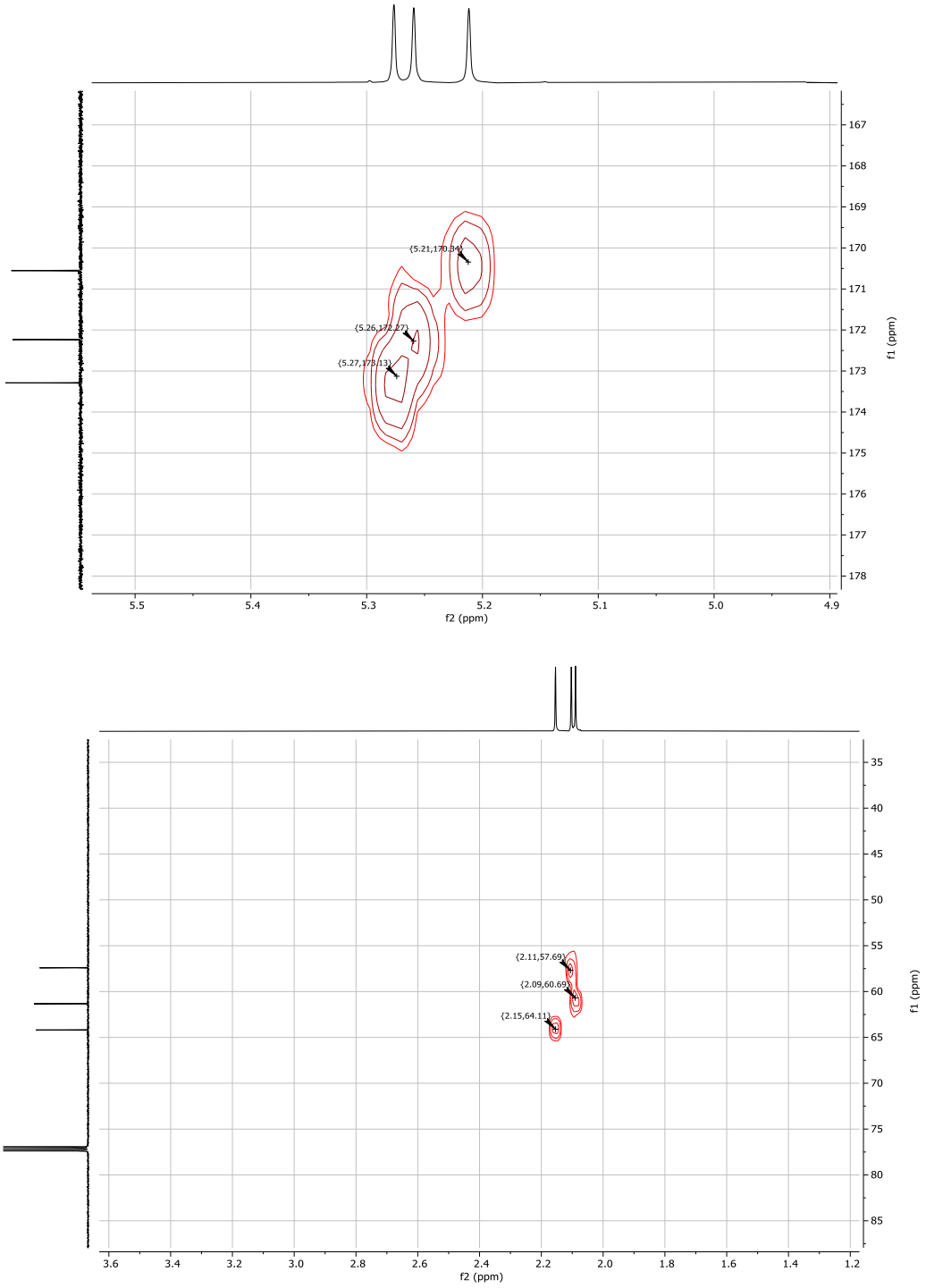

Figure 21. ^{1}H-^{13}C HMBC long-range coupling 2D NMR of compound 10. The top spectrum represents the region in the ^{1}H NMR (x-axis) representing the CH_2 of compound 10 (refer to figure 19) and the region in the ^{13}C NMR (y-axis) representing the carbonyls carbon (C=O, refer to figure 19). As shown, the carbons are doing long-range coupling with the protons. The lower spectrum represents the region in the ^{1}H NMR (x-axis) representing the CH_3 groups of the acetyl (refer to figure 20) and the region in the ^{13}C NMR (y-axis) representing the carbons of the CH_2 (refer to figure 20). As shown, the carbons are doing long-range coupling with the protons.

The failure to fluorinate the 3 position of pyridoxine can be explained by the difficulty of doing a S_NAr compared to doing a S_N2. Since the substitution led to the aromaticity being broken, this becomes a much harder reaction to do compared to the fluorination at the 2' position. In addition, the reaction intermediate for the substitution on the 3 position would be much more unstable because, unlike the reaction intermediate for the S_N2 on the 2' position, there is no stabilisation of the partial negative charge by the nitrogen in the ring. Due to these differences, the fluorination on the 3 position would most likely need slower and would need very harsh conditions in order to drive the formation of product.

Part 3. Different protection strategy leading to interesting chemistry

3.1. Synthesis of a real 2'-alcohol and attempted fluorinations

The previously reported experiments made it clear that fluorination of pyridoxine is extremely challenging. The only successful fluorination was done by direct C-H activation of pyridoxine triacetate using AgF_2 (part 1.2). It seems that with the presence of any kind of fluorinating agent at high temperature the pyridoxine triacetate moiety is rapidly destroyed. In addition, the synthesis of the 2'-alcohol with the acetyl protection strategy does not work due the possibility of acetyl migration. Therefore, the synthesis plan must be modified in order to incorporate milder fluorination methods and to incorporate different protecting groups which could sustain the conditions previously tried and are suitable for the synthesis of the 2' alcohol.

By looking at the previously synthesized fully protected pyridoxine derivatives present in the literature, the synthesis of (5-{[(4-Methoxybenzyl)oxy]methyl}-2,2-dimethyl-4H-[1,3]dioxino[4,5-c]pyridin-8-yl)methanol (compound 25) by Adamczyk and colleagues stands out from the others.[175] This 2'-alcohol is exactly the compound needed to synthesized the tosyl and triflate precursor and no acetyl groups are used in the approach. The synthesis was lightly modified and the alcohol was synthesized in 4 steps from pyridoxine HCl in a 29% yield (scheme 17).

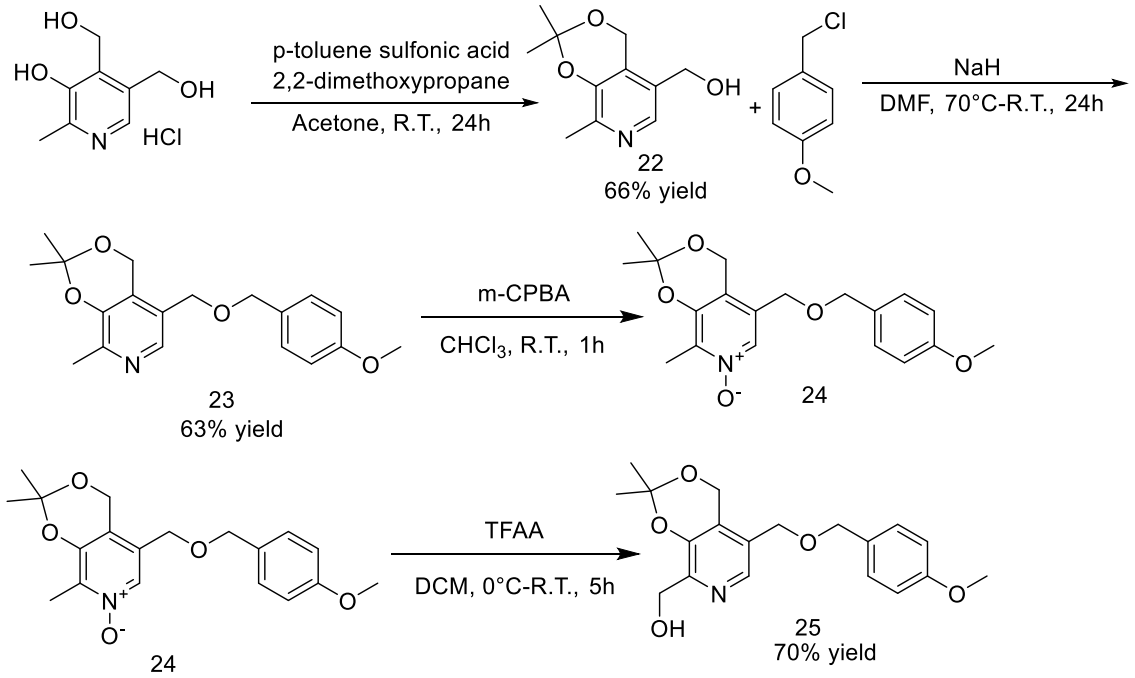

Scheme 17. Synthesis of (5-{[(4-Methoxybenzyl)oxy]methyl}-2,2-dimethyl-4H-[1,3]dioxino[4,5-c]pyridin-8-yl)methanol (compound 25) from pyridoxine HCl. The alcohol (compound 25) was synthesized in a total of 4 steps with a total 42% yield following a previously recorded synthesis.[175] Pyridoxine was first protected with an acetal to make compound 22 which is subjected to NaH and p-methoxybenzyl chloride at high temperature to get compound 23. The fully protected pyridoxine is then oxidized with m-CPBA to form the N-oxide which is transformed into the alcohol using TFAA.

With the alcohol in hand, the synthesis of the triflate and tosyl precursors was attempted. Neither the tosyl nor triflate precursor was synthesized using standard conditions (scheme 18). Interestingly, the conditions used for the tosylation of the alcohol resulted in the formation of the corresponding 2'-chlorine (compound 26) in a 35% yield (scheme 18).

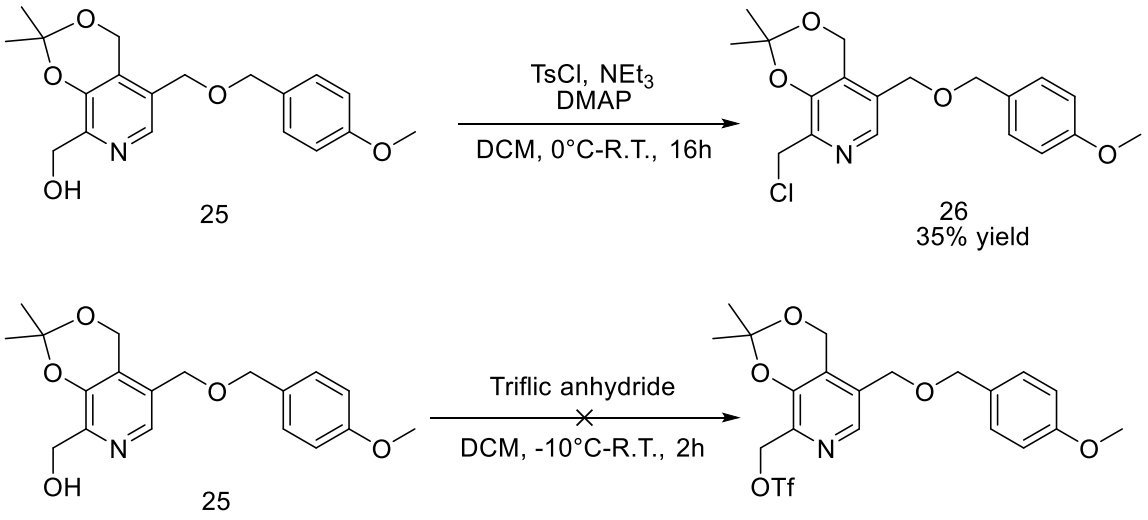

Scheme 18. Attempted synthesis of 2'-triflate (bottom) and 2'-tosyl (top) on the acetonide/benzyl protected pyridoxine. A standard tosylation procedure was attempted on alcohol 25 with no formation of the desired tosyl protected alcohol but formation of the 2'-chlorine compound with a 35% yield (top). A standard procedure for addition of triflate was attempted on compound 25 with no formation of the desired compound (bottom).

This type of reactivity is not new, where Ding and colleagues in 2011 demonstrated that treatment of several benzyl alcohols and pyridine methanol derivatives with tosyl chlorides leads to the formation of the corresponding chlorides.[216] Based on their proposed mechanism, there is formation of the tosylate but the resulting HCl by-product coordinates with triethyl ammine to make triethylammonium hydrochloride, and this nucleophilic chloride can displace the tosyl group.[216] This reactivity was very interesting since based on the proposed mechanism, tosyl fluoride could potentially be used to make the corresponding fluorine from the alcohol precursor. Thus, the reaction conditions were tested with tosyl fluoride instead of tosyl chloride (table 10, line 1). This did not yield in any formation of the desired fluorinated product nor in any conversion of the starting material. The experiment was repeated in harsher conditions (in chloroform at reflux and in DMF at 100 °C) with the same results (table 10, line 2 and line 3).

Table 10. Direct fluorination attempts of (5-{[(4-Methoxybenzyl)oxy]methyl}-2,2-dimethyl-4H-[1,3]dioxino[4,5-c]pyridin-8-yl)methanol (compound 25) using tosyl fluoride.

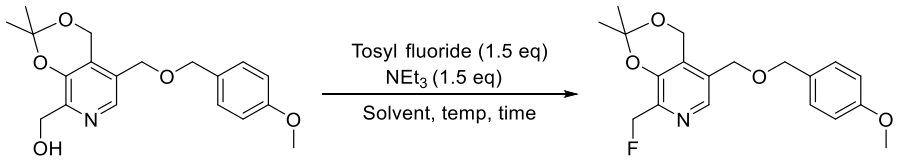

Solvent	Additive	Temperature (°C)	Time	Product formation	SM conversion[a]
DCM	DMAP (5 mol%)	Room temp.	16	N/A	None
Chloroform	None	70	5	N/A	None
DMF	None	100	5	N/A	None

a. SM = starting material (compound 25)

Based on these experiments, it seems that tosyl fluoride is highly unreactive compared to tosyl chloride. We suggest that this is due to fluorine being a worse leaving group than the chlorine and since the first step of the reaction is displacement of the halogen, tosyl fluoride would be less reactive because it is a poorer leaving group. In fact, it has been shown that in SO_2F_2, the S-F bond is 40 kcal/mol stronger than the S-Cl bond in SO_2Cl_2[217] which could explain the much higher stability towards electrophilic substitution. Therefore, an experiment using tosyl chloride in the presence of TBAF as an external F- source was attempted (scheme 19). In this experiment, there was a small conversion of the starting material (0.4% of the chlorine product synthesized) but no formation of the fluorine product. In the ^{19}F NMR there was the characteristic peak for tosyl fluoride at 66 ppm[212] (appendix 39) which indicates that the tosyl chloride was converted to tosyl fluoride due to the TBAF. Since the TBAF was added in the same amount as the tosyl chloride (1.5 equivalents), chances are that most of the tosyl chloride was converted into tosyl fluoride. These experiments show that the interesting conversion of the 2'-alcohol to the corresponding chloride using tosyl chloride cannot be used for the formation of the corresponding fluoride using tosyl fluoride under standard conditions.

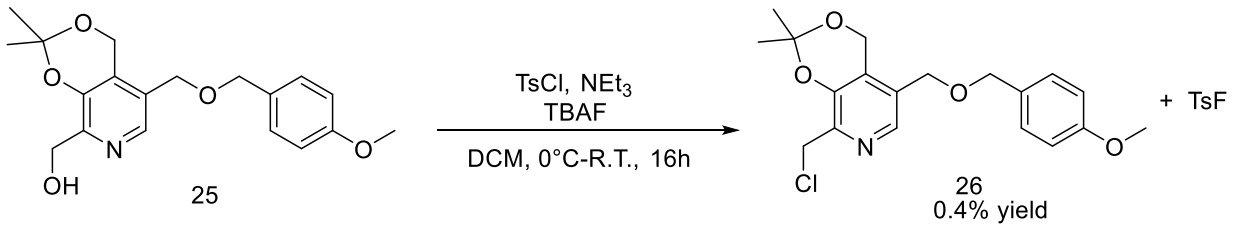

Scheme 19. Reaction between alcohol compound 25 and tosyl chloride in the presence of TBAF.

In addition of the strong S-F bond in tosyl fluoride, this SN_2 reaction is disfavored because the partial positive charge it forms during the transition stage would be destabilised by the presence of the nitrogen in the ring. Also, SN_2 reactions are favored in polar aprotic solvent and the experiments above do not use the best solvents for SN_2 such as DMSO or acetone.

Based on the proposed mechanism from Ding and colleagues,[216] it is clear that the formation of the chlorine product is pushed by the presence of the free chlorine which replaces the tosyl group. Therefore, switching to another base such as NaOH that can trap the chlorine in the from of NaCl could potentially lead to the formation of the tosyl compound. Therefore, doing a tosylation with NaOH could potentially lead to the tosyl compound.

Part 3.2. Difluorination of the pyridoxine

The interesting formation of the 2'-chlorine product from the alcohol with the tosylation procedure could not be used for fluorination using tosyl fluoride or by adding a fluorine source (table 10). In addition, the 2'-tosyl or 2'-triflate precursors could not be formed with the new protection strategy (scheme 18). Although the new protection strategy did not seem to have any utility for the formation of the 2'-fluorine, the synthesized alcohol could be transformed into an aldehyde using MnO_2 as previously reported by Adamczyk.[175] Interestingly, the Sanford group from the University of Michigan recently reported the deoxyfluorination of heteroaldehydes at room temperature[218] in which pyridine derivatives with aldehyde groups on the 2' carbon were transformed to the corresponding 2'-difluorinated product (ex: 5-bromo-2-pyridinecarboxaldehyde). This methodology was very interesting since not only was it perfect for the new protection strategy (no presence of other aldehydes such as acetyl protecting groups) but it is done at room temperature and would be less harsh on the material. 5-{[(4-

Methoxybenzyl)oxy]methyl}-2,2-dimethyl-4H-[1,3]dioxino[4,5-c]pyridine-8-carbaldehyde (aldehyde 27) was synthesized from alcohol compound 25 with a 72% yield using the previously reported procedure[175] (scheme 20).

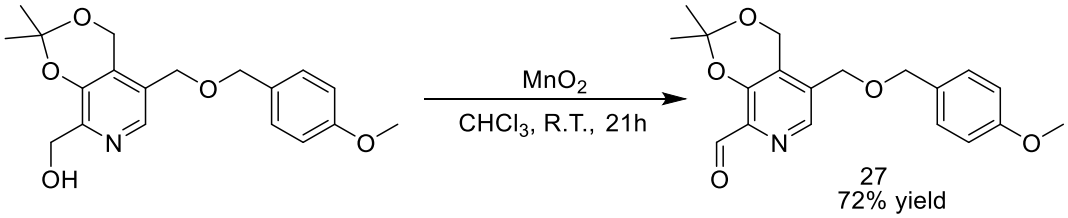

Scheme 20. Synthesis of 5-{[(4-Methoxybenzyl)oxy]methyl}-2,2-dimethyl-4H-[1,3]dioxino[4,5-c]pyridine-8-carbaldehyde (27) from alcohol compound 25.

With this 2' aldehyde precursor in hand, the optimised conditions for deoxyfluorination of heteroaldehydes (THF, 0.3 M, 3 equivalents of TBAF, 1.2 equivalents of PBSF) as demonstrated by Ferguson and colleagues was tested[218] (table 11). This reaction led to a 9% yield of the desired difluorinated product. This yield was much lower than the yields reported in the paper (ranging from 27% to 90%), therefore the conditions were modified in order to increase the yield (table 11).

Table 11. Difluorination of 5-{[(4-Methoxybenzyl)oxy]methyl}-2,2-dimethyl-4H-[1,3]dioxino[4,5-c]pyridine-8-carbaldehyde (27) using TMAF and PBSF. The difluorination of the aldehyde precursor (compound 27) was done using the optimal conditions described by Sanford and coworkers[218] and with alternate conditions to observe the effect on the yield.

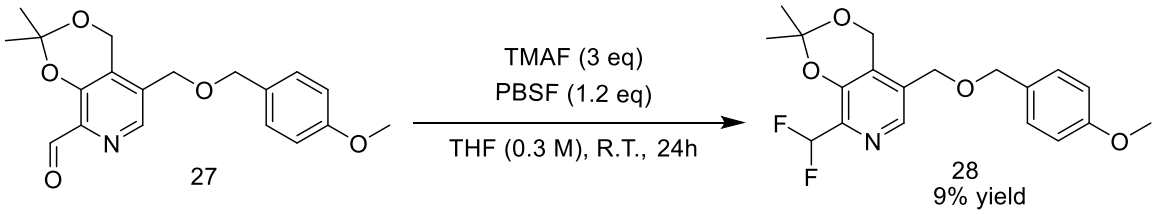

TMAF equivalents	PBSF equivalents	Solvent	Concentration (M)	Temperature (°C)	Yield (%)
3	1.2	DMF	0.3	Room temp.	N/A
3	1.2	DCM	0.3	Room temp.	N/A
3	1.2	Ether	0.3	Room temp.	32
4.5	1.2	Ether	0.3	Room temp.	25
4.5	1.8	Ether	0.3	Room temp.	26
3	1.8	Ether	0.3	Room temp.	39
3	1.8	Ether	0.5	Room temp.	17
3	1.8	Ether	0.2	Room temp.	41
2	1.8	Ether	0.3	Room temp	28
3	3.6	Ether	0.3	Room temp.	46
3	3.6	Ether	0.2	Room temp.	56
3	6.0	Ether	0.2	Room temp.	48
3	3.6	1,4-dioxane	0.2	Room temp.	20
3	3.6	MTBE[a]	0.2	Room temp.	37

a. MTBE: methyl tert-butyl ether

The solvents tested were the best three solvents, excluding THF, tested by Ferguson and colleagues[218]: Ether, DCM and DMF. Although DCM and DMF failed to produce any of the product, using ether substantially increased the yield to 32%. The second screening was the screening of TMAF and PBSF equivalents. From this screening, it was clear that 3 equivalents of TMAF was the best ratio as increasing or decreasing that ratio led to lower yields. Secondly, using a higher amount of PBSF (up to 3.6 equivalents) led to a higher yield as well, however

using more than 3.6 equivalents did not lead to better results. Finally, the concentration of ether in the reaction was tested. From these experiments it was found that a slightly lower concentration of ether (0.2 M) also led to a small increase in yield. Ether derivatives such as 1,4-dioxane and methyl tert-butyl ether were tested with the best conditions but were not as successful. The best yield obtained was 56% when the reaction was conducted in ether at 0.2 M using 3 equivalents of TMAF and 3.6 equivalents of PBSF.

This result was very good and although this exact reaction has not been used for radiofluorination, it has the potential for it. Indeed, ^{18}F-TMAF has been previously reported in the literature[219] and was made by using the standard $^{18}O(p, n)^{18}F$ cyclotron produced aqueous ^{18}F. Although the transition to radiochemistry is theoretically possible, there are some experiments which can give an idea of the feasibility of the transfer to radiochemistry. First, the reaction should be tested on a time scale which is more appropriate for radiochemistry. Due to the half-life of fluorine of 109 minutes,[159] reactions in fluorine radiochemistry should be kept to a minimal amount of time. Second, the reaction should be tested with an excess of the precursor versus the fluorine source, since the precursor is usually in large excess compared to the radionuclide.[220] Analysis of the crude mixture of these reactions is also very important to understand if any side product (monofluorination) is forming and if the desired product can be separated from the side product/starting material using HPLC in a reasonable time frame.

Therefore, we evaluated the difluorination reaction after 60 min (table 13) and we evaluated the difluorination reaction without using excess precursor (table 13). Both experiments were done separately to see how each effect the yield of the reaction. In addition, a test HPLC was conducted with both product and starting material to analyse the differential elution time between the two (appendix 43). The reaction mixture was analysed by HPLC in the TMAF screening and halfway in the short reaction time screening (30 minutes) to look for potential side products (appendix 40- appendix 42).

Table 12. Screening of the TMAF amount effect on the difluorination reaction of 5-{[(4-Methoxybenzyl)oxy]methyl}-2,2-dimethyl-4H-[1,3]dioxino[4,5-c]pyridine-8-carbaldehyde (27). The difluorination of compound 27 was done using either 0.5 or 1 equivalents of TMAF in ether for 24 hours. The crude reaction mixture was analysed by HPLC.

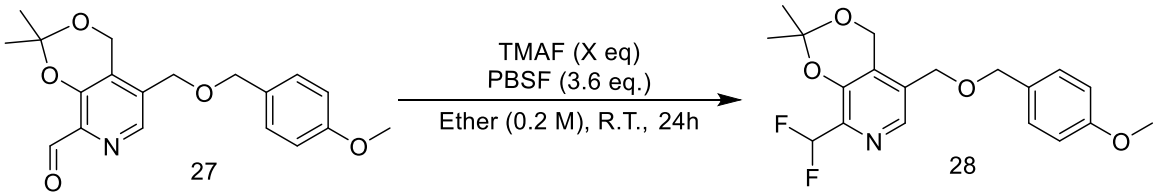

TMAF equivalents (X)	Yield (%)
0.5	1
1	11

Table 13. Difluorination reaction of aldehyde 27 with TMAF and PBSF in 60 minutes. The difluorination of 5-{[(4-Methoxybenzyl)oxy]methyl}-2,2-dimethyl-4H-[1,3]dioxino[4,5-c]pyridine-8-carbaldehyde (27) was done using the optimized amount of TMAF (3 equiv.) and PBSF (3.6 equiv.) previously established for this reaction (table 11) and the reaction was analysed after 60 minutes. The reaction was done in ether at room temperature and in MTBE or 1,4-dioxane with heat. The yield was calculated by fluorine NMR using 2-Fluorobenzoic acid as internal standard. The reaction mixture was also analysed by HPLC after 30 minutes of reaction time.

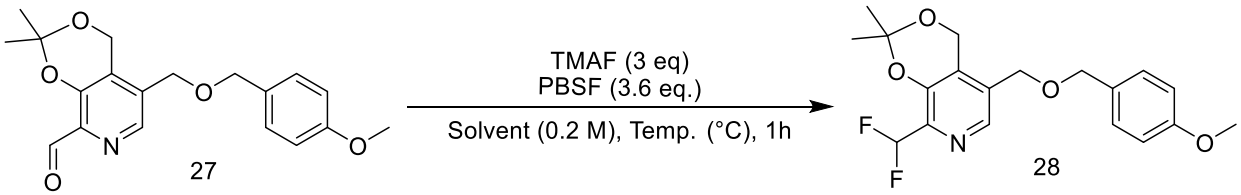

Solvent	Temperature (°C)	Yield (%)[a]
Ether	Room temp.	0.2
MTBE	45	0.2
1,4-dioxane	45	29
1,4-dioxane	80	10

a. NMR yield

The first observation is that the product can easily separate from the starting material. In the HPLC experiment, the product came out at 10.14 minutes and the starting material at 5.26

minutes (appendix 43). The second observation is that there doesn't seem to be any major side product present in the reaction mixture in any of the experiments conducted.

The results from the TMAF screening demonstrate that using less TMAF leads to a drop in the yield of the product as expected with a yield of only 1% at 0.5 equivalents of TMAF.

The results from the short reaction time experiments show that a bit of heat can push the reaction to react faster. The yield of the product using the ether, the best solvent used so far, was only 0.2%. In addition, there was the presence of an unknown compound in the HPLC at 11.7 minutes (appendix 42). Since that compound is decently separated from the product, it should not create any problem and therefore it was not analysed. The reaction was tested at 45 °C in MTBE and 1,4-dioxane, as well as 80 °C in 1,4-dioxane (table 13). After one hour, the product was only 0.2% in the MTBE at 45 °C but was 29% in the 1,4-dioxane at 45 °C. At 80 °C, the product yield was 10% which was not as good as the one at 45 °C. This could be due to decomposition of the starting material or side reactions occurring at this higher temperature compared to 45 °C. This result demonstrates that the reaction can be done in a short time frame (one hour) if heated a bit in 1,4-dioxane. No experiments with heat were tested with ether due to its low boiling point (34 °C).[221]

Chapter 4. Conclusion and future work

Part 1. Conclusion

Although there is an evident link between vitamin B_6 and cancer there is no successful approach to use Vitamin B_6 in the fight against this terrible disease. Based on the higher concentration of Vitamin B_6, the alternate trapping mechanism of vitamin B_6 by phosphorylation found in cancer cells, as well as a link between these factors and cancer progression, Vitamin B_6 looks like a great candidate to be used as a nuclear medicine cancer diagnostic. One of the most used tools to detect and stage cancer is PET. More and more research is focused on the synthesis of new PET radiotracers in order to increase the diagnostic arsenal and be able to detect, stage and plan the treatment all types of cancers. Therefore, the purpose of this thesis was to synthesize a radiotracer base on Vitamin B_6 which could potentially be used in PET imaging. Two potential radiotracers were identified as target compounds: 6-Fluoropyridoxine (6-FPN) and 2'-Fluoropyridoxine (2'-FPN). 6-Fluoropyridoxine was synthesised from pyridoxine hydrochloride in 3 steps and a total 4% yield with the key step being the direct C-H fluorination using silver difluoride. Unfortunately, the methodology used to synthesize the cold standard was not transferable to radiochemistry. Many attempts were made to fluorinate the 6 position of pyridoxine using a methodology transferable to radiochemistry with no success. Even the synthesis of possible precursors such as 6-Trimethylammonium pyridoxine did not succeed. There was no successful synthesis of the second tracer, 2'-FPN. The synthesis of a triacetylated 2'-tosyl and triflate precursor was attempted but due to acyl migration, only 3-tosyl and 3-triflate precursors were obtained. These compounds were subjected to several standard fluorination conditions without any success and with degradation of the starting material in almost all conditions. A different protection methodology resulted in the successful synthesis of a 2'-alcohol pyridoxine derivative. However, this derivative could not be successfully transformed into a good precursor (tosyl or triflate). Due to the failure to make any good precursor for the formation of 2'-FPN, the alcohol was converted into an aldehyde which was successfully difluorinated using TMAF and PBSF. Therefore, this methodology was optimised and tested for its potential to be transferred to radiochemistry. The difluorination of the 2'-aldehyde derivative of pyridoxine reached a yield of 56% and was successful using short reaction times and non stochiometric amounts of fluorine source (although in much lower yield). This work

demonstrated that this difluorination approach was successful for the cold difluorination of pyridoxine and may still hold promise for use in radiochemistry.

Part 2. Future work

From the experiments attempted to synthesize 6-Fluoropyridoxine or potential precursor for the fluorination of the 6 position of pyridoxine we have only attempted acetyl protection as the protection strategy. We suggest that there are several problems with this protection strategy. First of all, the acetyl groups are not very robust protection groups and might be partially responsible for the decomposition of the acetyl protected 6-chloro precursor (compound 4). It is also responsible for the failure to synthesize the spirocyclic hypervalent iodine precursor since the conditions use to make this precursor are too harsh. Another problem with the acetyl group is its electron withdrawing effect. This is especially unhelpful when attempting to make the 6-Trimethyl ammonium precursor by methylation of the 6-Dimethylamine. Therefore, changing the protection strategy would be the next step to take. For example, 6-Iodopyridoxine could be protected with benzyl group which are more robust and this compound could be subjected to the conditions necessary to make the spirocyclic hypervalent iodine. Another example would be to protect the dimethyl amine using methoxymethyl ether which would not have electron withdrawing effects. In addition, perhaps changing the protection strategy will change the stability of the compound in presence of free fluoride at high temperature, which will be very helpful. In addition, for the synthesis of the trimethylammonium salt, the addition of an Ag^+ source could drive the reaction forward since the formation of the product would lead to the formation of an insoluble silver salt.

The different protection strategy for the modification of the 2' position was very successful. With this protection strategy, the 2'-alcohol (compound 25) was synthesized but we were unable to transform it into a tosyl or triflate precursor. We suggest that the formation of the tosyl precursor is possible. In the reaction attempted, the 2'-chlorine product was formed due to a substitution from free chlorine on the in situ created tosyl compound (as discussed previously). Therefore, using conditions which would block this reaction such as changing the base to NaOH and quenching the free chlorine by formation of NaCl could potentially lead to isolation of the tosyl precursor. This tosyl precursor could be used for fluorination of the 2' position. With the 2'-alcohol, we were also able to create a precursor for difluorination. We succeeded in forming

the 2’-aldehyde (compound 27) which was successfully difluorinated. We also determined that the difluorination is potentially transferable to radiofluorination since the reaction could be done in a short time frame and could be done without using excess fluorine.

References

(1) Combs, G. F.; McClung, J. P. What Is a Vitamin? In *The Vitamins*; Academic Press: Westborough, MA, 2017; pp 3–6.

(2) Carpenter, K. J. The Discovery of Thiamin. *Ann. Nutr. Metab.* **2012**, *61*, 219–223.

(3) Maurer, K. J.; Quimby, F. W. Chapter 34 - Animal Models in Biomedical Research. In *Laboratory Animal Medicine: Third Edition*; Fox, J. G., Anderson, L. G., Otto, G. M., Pritchett-Corning, K. R., Whary, M. T., Eds.; Elsevier Inc., 2015; pp 1497–1526.

(4) Combs, G. F.; McClung, J. P. Discovery of the Vitamins. In *The Vitamins*; Academic Press: Westborough, MA, 2017; pp 7–31.

(5) Mccollum, E. V; Simmonds, N.; Pitz, W. The Relation of the Unidentified Dietary Factors, the Fat-Soluble A, and Water-Soluble B, of the Diet to the Growth Promoting Properties of Milk. *J. Biol. Chem.* **1916**, *27*, 33–43.

(6) Marks, J. *The Vitamins in Health and Disease: A Modern Reappraisal*; Churchill: London, 1948.

(7) Combs, G. F.; McClung, J. P. Vitamin Deficiency. In *The Vitamins*; Academic Press: Wesetborough, MA, 2017; pp 59–78.

(8) Harden, A.; Young, W. J. The Alcoholic Ferment of Yeast-Juice. *Source B. Chem. 1900–1950* **2014**, *77*, 369–375.

(9) Combs, G. F.; McClung, J. P. General Properties of Vitamins. In *The Vitamins*; Academic Press: Wesetborough, MA, 2017; pp 33–58.

(10) Clarke, R. Homocysteine, B Vitamins, and the Risk of Cardiovascular Disease. *Clin. Chem.* **2011**, *57*, 1201–1202.

(11) Greenwald, P.; Anderson, D.; Nelson, S. A.; Taylor, P. R. Clinical Trials of Vitamin and Mineral Supplements for Cancer Prevention. *Am. J. Clin. Nutr.* **2007**, *85*, 314–317.

(12) Camarena, V.; Wang, G. The Epigenetic Role of Vitamin C in Health and Disease. *Cell. Mol. Life Sci.* **2016**, *73*, 1645–1658.

(13) Bird, R. P. The Emerging Role of Vitamin B6 in Inflammation and Carcinogenesis. *Adv. Food Nutr. Res.* **2018**, *83*, 151–194.

(14) Holmes, F. F. Vitamins and Cancer. *Adv. Biosci.* **1985**, *50*, 127–137.

(15) Moreno, F. S.; Wu, T. S.; Penteado, M. V.; Rizzie, M. B.; Jordao Junior, A. A.; Almeida-Muradian, L. B.; Dagli, M. L. A Comparison of Beta-Carotene and Vitamin A Effects on a Hepatocarcinogenis Model. *Int. J. Vit. Nutr. Res.* **1995**, No. 65, 87–94.

(16) Key, T. J.; Appleby, P. N.; Travis, R. C.; Albanes, D.; Alberg, A. J.; Barricarte, A.; Black, A.; Boeing, H.; Bueno-De-Mesquita, H. B.; Chan, J. M.; Chen, C.; Cook, M. B.; Donovan, J. L.; Galan, P.; Gilbert, R.; Giles, G. G.; Giovannucci, E.; Goodman, G. E.; Goodman, P. J.; Gunter, M. J.; Hamdy, F. C.; Heliövaara, M.; Helzlsouer, K. J.; Henderson, B. E.; Hercberg, S.; Hoffman-Bolton, J.; Hoover, R. N.; Johansson, M.;

Khaw, K. T.; King, I. B.; Knekt, P.; Kolonel, L. N.; Le Marchand, L.; Männistö, S.; Martin, R. M.; Meyer, H. E.; Mondul, A. M.; Moy, K. A.; Neal, D. E.; Neuhouser, M. L.; Palli, D.; Platz, E. A.; Pouchieu, C.; Rissanen, H.; Schenk, J. M.; Severi, G.; Stampfer, M. J.; Tjønneland, A.; Touvier, M.; Trichopoulou, A.; Weinstein, S. J.; Ziegler, R. G.; Zhou, C. K.; Allen, N. E. Carotenoids, Retinol, Tocopherols, and Prostate Cancer Risk: Pooled Analysis of 15 Studies. *Am. J. Clin. Nutr.* **2015**, *102*, 1142–1157.

(17) Musa-Veloso, K.; Card, J. W.; Wong, A. W.; Cooper, D. A. Influence of Observational Study Design on the Interpretation of Cancer Risk Reduction by Carotenoids. *Nutr. Rev.* **2009**, *67*, 527–545.

(18) Mills, J. P.; Furr, H. C.; Tanumihardjo, S. A. Retinol to Retinol-Binding Protein (RBP) Is Low in Obese Adults Due to Elevated Apo-RBP. *Exp. Biol. Med.* **2008**, *233*, 1255–1261.

(19) Sun, L.; Qi, Q.; Zong, G.; Ye, X.; Li, H.; Liu, X.; Zheng, H.; Hu, F. B.; Liu, Y.; Lin, X. Elevated Plasma Retinol-Binding Protein 4 Is Associated with Increased Risk of Type 2 Diabetes in Middle-Aged and Elderly Chinese Adults. *J. Nutr.* **2014**, *144*, 722–728.

(20) Hak, A. E.; Stampfer, M. J.; Campos, H.; Sesso, H. D.; Gaziano, J. M.; Willett, W.; Ma, J. Plasma Carotenoids and Tocopherols and Risk of Myocardial Infarction in a Low-Risk Population of US Male Physicians. *Circulation* **2003**, *108*, 802–807.

(21) Galluzzi, L.; Vacchelli, E.; Michels, J.; Garcia, P.; Kepp, O.; Senovilla, L.; Vitale, I.; Kroemer, G. Effects of Vitamin B6 Metabolism on Oncogenesis, Tumor Progression and Therapeutic Responses. *Oncogene* **2013**, *32*, 4995–5004.

(22) Cairns, R. A.; Harris, I. S.; Mak, T. W. Regulation of Cancer Cell Metabolism. *Nat. Rev. Cancer* **2011**, *11*, 85–95.

(23) Goldberger, J. The Relation of Diet to Pellagra. *J. Am. Med. Assoc.* **1922**, *78*, 1676–1680.

(24) Rosenberg, I. H. A History of the Isolation and Idenfication of Vitamin B6. *Ann. Nutr. Metab.* **2012**, *61*, 236–238.

(25) Kuhn, R.; Gyorgi, P.; Wagner-Juregg, T. Über Eine Neue Klass von Naturefarbstoffen (Vorläufige Mitteilung). *Ber. Dtsch. Chem. Ges.* **1933**, *66*, 567–580.

(26) Elvehjem, C. A.; Madden, R. J.; Strong, F. M.; Wolley, D. W. The Isolation and Identification of the Anti-Black Tongue Factor. *J. Biol. Chem.* **1938**, *123*, 137–149.

(27) Reader, V. The Assay of Vitamin B(4). *Biochem J.* **1930**, *24*, 1827–1831.

(28) Kinnersley, H. W.; O'Brien, J. R.; Peters, R. A.; Reader, V. Large Scale Preparations of Vitamin B 1 and Vitamin B 4 Concentrates. *Biochem J.* **1933**, *27*, 225–231.

(29) Kinnersley, H. W.; O'Brien, J. R.; Peters, R. A. Crystalline Vitamin B1. *Biochem J.* **1935**, *29*, 701–715.

(30) Lepkovsky, S. Crystalline Factor I. *Science (80-.).* **1938**, *87*, 169–170.

(31) Keresztesy, J. C.; Stevens, J. R. Vitamin B-6. *J. Am. Chem. Soc.* **1938**, *60*, 1267–1268.

(32) Kuhn, R.; Wendt, G. Über Das Aus Reiskleie Und Hefe Isolierte Adermin (Vitamin B 6).

Beritcht Atsch Chem Ges **1938**, *71B*, 1118.

(33) Tchiba, A.; Michi, K. Crystalline Vitamin B-6. *Sci Pap. Inst Phys Chem Res* **1938**, *34*, 1014.

(34) Folkers, K.; Harris, S. A. Synthesis of Vitamin B-6. *J. Am. Med. Soc.* **1939**, *61*, 1245–1247.

(35) Kuhn, R.; Westphal, K.; Wendt, G.; Westphal, O. Synthesis of Adermin. *Naturwissenschaften* **1939**, *27*, 469.

(36) Gyorgi, P.; Eckhardt, R. E. Vitamin B-6 and Skin Lesions in Rats. *Nature* **1939**, *144*, 512.

(37) Snell, E. E.; Guirard, B. M.; Williams, R. J. Occurence in Natural Products of a Physiologically Active Metabolite of Pyridoxine. *J. Biol. Chem.* **1942**, *143*, 519–530.

(38) Snell, E. E. Effect of Heat Sterilization on Growth Promoting Activity of Pyridoxine for Streptococcus Lactis. *Proc Soc Exp Biol Med* **1942**, *51*, 356–358.

(39) Snell, E. E. The Vitamin Activities of "pyridoxal" and "Pyridoxamine." *J. Biol. Chem.* **1944**, *154*.

(40) Snell, E. E. The Vitamin B6 Group. I. Formation of Additional Members from Pyridoxine and Evidence Concerning Their Structure. *J. Am. Chem. Soc.* **1944**, *66*, 2082–2088.

(41) Bellamy, D. W. The Funcitons of Vitamin B6: A Beginning. *Biochem. Biophys. Res. Commun.* **2003**, *312*, 49–50.

(42) Gale, E. F. The Production of Amines by Bacteria. II. The Production of Tyramine by Streptococcus Faecalis. *Biochem J.* **1940**, *34*, 846–852.

(43) Gunsalus, I. C.; Bellamy, W. D. The Function of Pyridoxine and Pyridoxine Derivatives in the Decarboxylation of Tyrosine. *J. Biol. Chem.* **1944**, *155*, 557–563.

(44) Bellamy, W. D.; Gunsalus, I. C. Tyrosine Decarboxylase by Streptococci. I. Growth Requirement for Active Cell Production. *J. Bacteriol.* **1944**, *48*, 191–199.

(45) Harris, S. A.; Heyl, D.; Folkers, K. The Vitamin B6 Group. II. The Structure and Synthesis of Pyridoxine and Pyridoxal. *J. Am. Chem. Soc.* **1944**, *66*, 2088–2092.

(46) Gunsalus, I. C.; Bellamy, W. D. A Function of Pyridoxal. *J. Biol. Chem.* **1944**, *155*, 357–358.

(47) Bellamy, W. D.; Gunsalus, I. C. Tyrosine Decarboxylase. II. Pyridoxine Deficient Media for Apo-Enzyme Production. *J. Bacteriol.* **1945**, *50*, 95–103.

(48) Umbreit, W. W.; Bellamy, W. D.; Gunsalus, I. C. The Function of Pyridoxine Derivatives: Comparison of Natural and Synthetic Codecarboxylase. *Arch. Biochem. Biophys.* **1945**, *7*, 185–199.

(49) Gunsalus, I. C.; Bellamy, W. D.; Umbreit, W. W. A Phosphorylated Derivative of Pyridoxal as the Coenzyme of Tyrosine Decarboxylase. *J. Biol. Chem.* **1944**, *155*, 685–686.

(50) Bellamy, W. D.; Umbreit, W. W.; Gunsalus, I. C. The Funciton of Pyridoxine: Conversion of Members of the Vitamin B6 Group into Codecarboxylase. *J. Biol. Chem.* **1945**, *160*, 461–472.

(51) Gunsalus, I. C.; Umbreit, W. W.; Bellamy, W. D.; Foust, C. E. Some Properties of Synthetic Codecarboxylase. *J. Biol. Chem.* **1945**, *161*, 743–744.

(52) Gunsalus, I. C.; Umbreit, W. W. Codecarboxylase Not the 3-Phosphate of Pyridoxal. *J. Biol. Chem.* **1947**, *170*, 415–416.

(53) Umbreit, W. W.; Gunsalus, I. C. Codecarboxylase Not Pyridoxal-3-Phosphate. *J. Biol. Chem.* **1949**, *179*, 279–281.

(54) McCormick, D. B.; Gregory, M. E.; Snell, E. E. Pyridoxal Phosphokinases. *J. Biol. Chem.* **1961**, *236*, 2076–2084.

(55) Wilson, G. R.; Davis, R. E. Clinical Chemistry of Vitamin B6. *Adv. Clin. Chem.* **1983**, *23*, 1–68.

(56) Roth-Maier, D. A.; Kettler, S. I.; Kirchgessner, M. Availability of Vitamin B6 from Different Food Sources. *Int. J. Food Sci. Nutr.* **2002**, *53*, 171–179.

(57) Henderson, L. M. Intestinal Absorption of B6 Vitamers. In *Vitamin B6: Its role in Health and Disease*; Reynols, R. D., Leklem, J. E., Eds.; Liss: New York, 1985; pp 25–33.

(58) Snell, E. E.; Haskell, B. E. The Metabolism of Vitamin B6. *Compr. Biochem.* **1971**, *21*, 47–71.

(59) Fonda, M. L. Purification and Characterization of Vitamin B6-Phosphate Phosphatase from Human Erythrocytes. *J. Biol. Chem.* **1992**, *267*, 15978–15983.

(60) Hanna, M. C.; Turner, A. J.; Kirkness, E. F. Human Pyridoxal Kinase cDNA cloning, expression, and modulation by ligands of the benzodiazepine receptor. *J. Biol. Chem.* **1997**, *272*, 10756–10760.

(61) Di Salvo, M. L.; Constetabile, R.; Safo, M. K. Vitamin B 6 Salavage Enzymes: Mechanism, Structure and Regulation. *BBA - proteins proteomics* **2011**, *1814*, 1597–1608.

(62) McCormick, D. B.; Chen, H. Update on Interconversions of Vitamin B-6 with Its Coenzyme. *J. Nutr.* **1999**, *129*, 325–327.

(63) Bender, D. A. Vitamin B6/Physiology. In *Encyclopedia of Food Sciences and Nutrition*; Caballero, B., Ed.; Academic Press: Baltimore, 2003; pp 6020–6032.

(64) Snell, E. E. Vitamin B6 and Decarboxylation of Histidine. *Ann. N.Y. Acad. Sci.* **1990**, *585*, 1–12.

(65) Merrill, A. H.; Henderson, J. M.; Wang, E.; McDonald, B. W.; Milikan, W. J. Metabolism of Vitamin B-6 by Human Liver. *J. Nutr.* **1984**, *114*, 1664–1674.

(66) Mehansho, H.; Henderson, L. M. Transport and Accumulation of Pyridoxine and Pyridoxal by Erythrocytes. *J. Biol. Chem.* **1980**, *255*, 11901–11907.

(67) Bohney, J. P.; Fonda, M. L.; Feldhoff, R. C. Identification of Lys190 as the Primary

Binding Site for Pyridoxal 5′-Phosphate in Human Serum Albumin. *FEBS Lett.* **1992**, *298*, 266–268.

(68) Whittaker, J. W. Intracellular Trafficking of the Pyridoxal Cofactor. Implications for Health and Metabolic Disease. *Arch. Biochem. Biophys.* **2016**, *592*, 20–26.

(69) Kelsay, J.; Baysal, A.; Linkswiler, H. Effect of Vitamin B6 Depletion on the Pyridoxal, Pyridoxamine, and Pyridoxine Content in the Blood and Urine of Men. *J. Nutr.* **1968**, *94*, 490–494.

(70) Lichstein, H. C.; Gunsalus, I. C.; Umbreit, W. W. Function of the Vitamin B6 Group, Pyridoxal Phosphate (Codecarboxylase) in Transamination. *J. Biol. Chem.* **1945**, *161*, 311–320.

(71) Umbreit, W. W.; O'Kane, D. J.; Gunsalus, I. C. Function of the Vitamin B6 Group: Mechanism of Transamination. *J. Biol. Chem.* **1948**, *176*, 629–637.

(72) Cheney, M. C.; Curry, D. M.; Beaton, G. H. Blood Transaminase Activities in Vitamin B6 Deficiency: Specificity and Sensitivity. *Can. J. Physiol. Pharmacol.* **1965**, *43*, 579–589.

(73) Ames, S. R.; Sarma, P. S.; Elvehjem, C. A. Transaminase and Pyridoxine Deficiency. *J. Biol. Chem.* **1947**, *167*, 135–141.

(74) Wood, W. A.; Gunsalus, I. C.; Umbreit, W. W. Function of Pyridoxal Phosphate: Resolution and Purification of the Tryptophanase Enzyme of Escherichia Coli. *J. Biol. Chem.* **1947**, *170*, 313–321.

(75) Umbreit, W. W.; Wood, W. A.; Gunsalus, I. C. The Activity of Pyridoxal Phosphate in Tryptophane Formation by Cell-Free Enzyme Preparations. *J. Biol. Chem.* **1946**, *165*, 731–732.

(76) John, R. A. Pyridoxal Phosphate-Dependant Enzymes. *Biochim. Biophys. Acta.* **1995**, *1248*, 81–96.

(77) Lane, A. N.; Kirschner, K. The Catalytic Mechanisme of Tryptophan Synthase from Escherichia Coli. *Eur. J. Biochem.* **1983**, *129*, 571–582.

(78) Shimada, A.; Fujii, N.; Saito, T. Tryptophanase Activity on D-Tryptophan. In *Progress in Biological Chiraliry*; Pàlyi, G., Zucchi, C., Caglioti, L., Eds.; Elsevier Inc.: Oxford, 2004; pp 321–327.

(79) Umbarger, H. E.; Brown, B. Threonine Deamination in Escherichia Coli. II. Evidence for Two L-Threonine Deaminases. *J. Bacteriol.* **1957**, *73*, 105–112.

(80) Phillips, A. T.; Wood, W. A. The Mechanism of Action of 5'-Adenylic Acid-Activated Threonine Dehydrase. *J. Biol. Chem.* **1965**, *240*, 4703–4709.

(81) Wood, W. A.; Gunsalus, I. C. D-Alanine Formation: A Racemase in Streptococcus Faecalis. *J. Biol. Chem.* **1951**, *190*, 403–415.

(82) Wood, W. A. The Discovery, Synthesis, and Role of Pyridoxal Phosphate: Phase I of Many Phases in the Gunsalus Odyssey. *Biochem. Biophys. Res. Commun.* **2003**, *312*, 185–189.

(83) Narrod, S. A.; Wood, W. A. Evidence for a Glutamic Acid Racemase in Lactobacillus Arabinosus. *Arch. Biochem. Biophys.* **1952**, *35*, 462–463.

(84) Nandi, D. L. Delta-Aminolevulinic Acid Synthase of Rhodopseudomonas Spheroides. Binding of Pyridoxal Phosphate to the Enzyme. *Arch. Biochem. Biophys.* **1978**, *188*, 266–271.

(85) Cheltsov, A. V.; Guida, W. C.; Ferreira, G. C. Circular Permutation of 5-Aminolevulinate Synthase: Effect on Folding, Conformational Stability, and Structure. *J. Biol. Chem.* **2003**, *278*, 27945–27955.

(86) Schnackers, K. D.; Benesch, R. E.; Kwong, S.; Benesch, R.; Helmreich, E. J. Specific Receptor Sites for Pyridoxal 5'-Phosphate and Pyridoxal 5'-Deoxymethylenephosphonate at the Alpha and Beta NH2-Terminal Regions of Hemoglobin. *J. Biol. Chem.* **1983**, *258*, 872–875.

(87) Chang, Y. C.; Scott, R. D.; Graves, D. J. Function of Pyridoxal 5'-Phosphate in Glycogen Phosphorylase: A Model Study Using 6-Fluoro-5'-Deoxypyridoxal- and 50 -Deoxypyridoxal-Reconstituted Enzymes. *Biochemistry* **1987**, *26*, 360–367.

(88) Nakamura, M. T.; Nara, T. Y. Structure, Function, and Dietary Regulation of Delta-6, Delta-5, and Delta-9 Desaturases. *Annu. Rev. Nutr.* **2004**, *24*, 345–376.

(89) Horrobin, D. F. Fatty Acid Metabolism in Health and Disease: The Role of Delta-6-Desaturase. *Am. J. Clin. Nutr.* **1993**, *57*, 732S-736S.

(90) Bourquim, F.; Capitani, G.; Grutter, M. G. PLP-Dependant Enzymes as Entry and Exit Gates of Sphingolipid Metabolism. *Protein Sci.* **2011**, *20*, 1492–1508.

(91) Bairoch, A. The ENZYME Data Bank. *Nucleic Acids Res.* **1994**, *22*, 3626–3627.

(92) Percudani, R.; Peracchi, A. A Genomic Overview of Pyridoxal-Phosphate Dependant Enzymes. *EMBO Rep.* **2003**, *4*, 850–854.

(93) Selhub, J. Homocysteine Metabolism. *Annu. Rev. Nutr.* **1999**, *19*, 217–246.

(94) Mason, J. B. Biomarkers of Nutrient Exposure and Status in One-Carbon (Methyl) Metabolism. *J. Nutr.* **2003**, *133*, 941S-947S.

(95) Kerins, D. M.; Koury, M. J.; Capdevilla, A.; Rana, S.; Wagner, C. Plasma S-Adenosylhomocysteine Is a More Sensitive Indicator of Cardiovascular Disease than Plasma Homocysteine. *Am. J. Clin. Nutr.* **2001**, *74*, 723–729.

(96) Larsson, S. C.; Giovannucci, E.; Wolk, A. Vitamin B6 Intake, Alcohol Consumption, and Colorectal Cancer: A Longitudinal Population-Based Cohort of Women. *Gastroenterology* **2005**, *128*, 1830–1837.

(97) Kim, Y. I. Folate and DNA Methylation (a Mechanistic Link between Folate Deficiency and Colecteral Cancer?). *Cancer Epidemiol. Biomarkers Prev.* **2004**, *13*, 511–519.

(98) Hayes, J. D.; McLellan, L. I. Glutathione and Glutathione-Dependent Enzymes Represent a Co-Ordinately Regulated Defence against Oxidative Stress. *Free Radic. Res.* **1999**, *31*, 273–300.

(99) Hayes, J. D.; Pulford, D. J. The Glutathione S-Transferase Supergene Family (Regulation of GST and the Contribution of the Isoenzymes to Cancer Chemoprotection and Drug Resistance). *Crit. Rev. Biochem. Mol. Biol.* **1995**, *30*, 445–600.

(100) Martinez, M.; Cuskelly, G. J.; Williamson, J.; Toth, J. P.; Gregory, J. F. Vitamin B-6 Deficiency in Rats Reduces Hepatic Serine Hydroxymethyltransferase and Cystathionine Beta-Synthase Activities and Rates of in Vivo Protein Turnover, Homocysteine Remethylation and Transsulfuration. *J. Nutr.* **2000**, *130*, 1115–1123.

(101) Gorlach, A.; Dimova, E. Y.; Petry, A.; Martinez-ruiz, A.; Hernansanz-Agustin, P.; Rolo, A. P.; Palmeira, C. M.; Kietzmann, T. Reactive Oxygen Species, Nutrition, Hypoxia and Diseases: Problems Solved? *Redox. Biol.* **2015**, *6*, 372–385.

(102) Zhang, Z.; He, Y.; Tu, X.; Huang, S.; Chen, Z.; Wang, L.; Song, J. Mapping of DNA Hypermethylation and Hypomethylation Induced by Folate Deficiency in Sporadic Colorectal Cancer and Clinical Implication Analysis of Hypermethylation Pattern in CBS Promoter. *Clin. Lab.* **2017**, *63*, 733–748.

(103) Yang, J. .; Hongjia, L.; Deng, H.; Wang, Z. Association of One-Carbon Metabolism-Related Vitamins (Folate, B6, B12), Homocysteine and Methionine With the Risk of Lung Cancer: Systematic Review and Meta-Analysis. *Front Oncol.* **2018**, *8*, 493.

(104) Dang, C. V. Links between Metabolism and Cancer. *Genes&Dev.* **2012**, *26*, 877–890.

(105) Stoerk, H. C. Growth Retardation of Lymphosarcoma Implants in Pyridoxine Deficient Rats by Testosterone and Cortisone. *Proc Soc Exp Biol Med* **1950**, *74*, 798–800.

(106) Mihich, E. Host Defense Mechanisms in the Regression of Sarcoma 180 in Pyridoxine-Deficient Mice. *Cancer Res.* **1962**, *22*, 218–227.

(107) Tryfiates, G. P.; Morris, H. P. Effect of Pyridoxine Deficiency on Tyrosine Transaminase Activity and Growth of Four Morris Hepatomas. *J. Natl. Cancer Inst.* **1974**, *52*, 1259–1262.

(108) Tryfiates, G. P.; Shuler, J. K.; Hefner, M. H.; Morris, H. P. Effect of B6 Deficiency on Hepatoma 7794A Growth Rate: Activities of Tyrosine Transaminase and Serine Dehydratase before and after Induction by Hydrocortisone. *Eur. J. Cancer* **1974**, *10*, 147–154.

(109) Tryfiates, G. P. Effect of Pyridoxine Availability on the Activity of Serine Dehydratase of Normal Liver, Host Liver, and Three Morris Hepatomas. *J. Natl. Cancer Inst.* **1975**, *54*, 171–172.

(110) Tryfiates, G. P. P. Effect of Pyridoxine on the Growth of Morris Hepatoma No. 7288Ctc and Enzyme Activity. *Oncology* **1976**, *33*, 209–211.

(111) Korytnyk, W.; Angelino, N. Vitamin B6 Antagonists Obtained by Replacing or Modifying the 2-Methyl Group. *J. Med. Chem.* **1977**, *20*, 745–749.

(112) Korytnyk, W.; Ghosh, A. C.; Potti, P. G.; Srivastava, S. C. Synthesis and Biological Properties of 4-Amino- and 4-Bromo-4-Norpyridoxol. New Approaches for the Modification of the 4 Position of Vitamin B6. *J. Med. Chem.* **1976**, *19*, 999–1002.

(113) Korytnyk, W.; Srivastava, S. C. Synthesis and Physicochemical and Biological Properties of 6-Halogen-Substituted Vitamin B 6 Analogs. *J. Med. Chem.* **1973**, *16*, 638–642.

(114) Grimaldi, T.; La Pesa, M.; Curci, E.; Semeraro, N. Latest Research on the Effect of Desoxypyridoxine on the Formation and Development of Experimental Neoplasms. I. Ascitic Tumors in Mice. *Pathologica* **1971**, *63*, 89–91.

(115) Tryfiates, G. P. Control of Tumor Growth by Pyridoxine Restriction or Treatment with an Antivitamin Agent. *Cancer Detetct. Prev.* **1981**, *4*, 159–164.

(116) DiSorbo, D. M.; Litwack, G. Vitamin B6 Kills Hepatoma Cells in Culture. *Nutr. Cancer* **1982**, *3*, 216–222.

(117) DiSorbo, D. M.; Nathanson, L. High-Dose Pyridoxal Supplemented Culture Medium Inhibits the Growth of a Human Malignant Melanoma Cell Line. *Nutr. Cancer* **1983**, *5*, 10–15.

(118) DiSorbo, D. M.; Wagner, J. R.; Nathanson, L. In Vivo and in Vitro Inhibition of B16 Melanoma Growth by Vitamin B6. *Nutr. Cancer* **1985**, *7*, 43–52.

(119) Trebukhnia, R. V.; Mikhal'tsevich, G. N. Vitamin B6 Metabolism in Mice with Ehrlich Ascites Tumor. *Vopr. Pitan.* **1982**, *1*, 40–44.

(120) Gridley, D. S.; Stickney, D. R.; Nutter, R. L.; Slater, J. M.; Shultz, T. D. Suppression of Tumor Growth and Enhancement of Immune Status with High Levels of Dietary Vitamin B6 in BALB/c Mice. *J. Natl. Cancer Inst.* **1987**, *78*, 951–959.

(121) Nikonova, T. V.; Draudin-Krylenko, V. A.; Bukin, I. V.; Turusov, V. S. Protective Action of Nicotinamide and Pyridoxine on the Initiation Stage of Carcinogenesis Induced in Mice by Procarbazine. *Eksp. Onkol.* **1988**, *10*, 17–19.

(122) Draudin-Krylenko, V. A.; Bukin, I. V.; Nikonova, T. V. Anticarcinogenic Action of Vitamins PP and B6 in the Natulan Initiation of Malignant Growth in Mice. *Vopr. Onkol.* **1989**, *35*, 34–38.

(123) Ha, C.; Miller, L. T.; Kerkvliet, N. I. The Effect of Vitamin B6 Deficiency on Cytotoxic Immune Responses of T Cells, Antibodies, and Natural Killer Cells, and Phagocytosis by Macrophages. *Cell. Immunol.* **1984**, *85*, 318–329.

(124) Ha, C.; Kerkvliet, N. I.; Miller, L. T. The Effect of Vitamin B-6 Defiency on Host Susceptibility to Moloney Sarcoma Virus-Induced Tumor Growth in Mice. *J. Nutr.* **1984**, *114*, 938–948.

(125) Gebhard, K. J.; Gridley, D. S.; Stickney, D. R.; Shultz, T. D. Enhancement of Immune Status by High Levels of Dietary Vitamin B-6 without Growth Inhibition of Human Malignant Melanoma in Athymic Nude Mice. *Nutr. Cancer* **1990**, *14*, 15–26.

(126) Folkers, K.; Morita, M.; Mcree, J. The Activities of Coenzyme Q10 and Vitamin B6 for Immune Responses. *Biochem. Biophys. Res. Commun.* **1993**, *193*, 88–92.

(127) Gonzalez, H.; Hagerling, C.; Werb, Z. Roles of the Immune System in Cancer: From Tumor Initiation to Metastatic Progression. *Genes&Dev.* **2018**, *32*, 1267–1284.

(128) Meisler, N. T.; Nutter, L. M.; Thanassi, J. W. Vitamin B6 Metabolism in Liver and Liverderived Tumors. *Cancer Res.* **1982**, *42*, 3538–3543.

(129) Galluzzi, L.; Vitale, I.; Senovilla, L.; Olaussen, K. A.; Pinna, G.; Eisenberg, T.; Goubar, A.; Martins, I.; Michels, J.; Kratassiouk, G. Prognostic Impact of Vitamin B6 Metabolism in Lung Cancer. *Cell Rep.* **2012**, *2*, 257–269.

(130) Matxain, J. M.; Ristilla, M.; Strid, A.; Eriksson, L. A. Theoretical Study of the Antioxidant Properties of Pyridoxine. *J. Phys. Chem. A* **2006**, *110*, 13068–13072.

(131) Jain, S. K.; Lim, G. Pyridoxine and Pyridoxamine Inhibits Superoxide Radicals and Prevents Lipid Peroxidation, Protein Glycosylation, and (Na+ + K+)-ATPase Activity Reduction in High Glucose-Treated Human Erythrocytes. *Free Radic. Biol. Med.* **2001**, *30*, 232–237.

(132) Amarnath, V.; Amarnath, K.; Amarnath, K.; Davies, S.; Roberts, L. J. Pyridoxamine: An Extremely Potent Scavenger of 1,4-Dicarbonyls. *Chem. Res. Toxicol.* **2004**, *17*, 410–415.

(133) Wondrak, G. T.; Jacobson, E. L. Vitamin B6: Beyond Coenzyme Functions. *Subcell. Biochem.* **2012**, *56*, 291-300.

(134) Williams, V. R.; Neilands, J. B. Apparent Ionization Constants, Spectral Properties and Metal Chelation of the Cotransaminases and Related Compounds. *Arch. Biochem.* **1954**, *53*, 56–70.

(135) Liou, G.-Y.; Storz, P. Reactive Oxygen Species in Cancer. *Free Radic. Res.* **2010**, *44*, 479–496.

(136) Semchyshyn, H. M. Reactive Carbonyl Species *In Vivo*: Generation and Dual Biological Effects. *Sci. World J.* **2014**, *2014*, 417842.

(137) Dainin, K.; Ide, R.; Maeda, A.; Suama, K.; Akagawa, M. Pyridoxamine Scavenges Protein Carbonyls and Inhibits Protein Aggregation in Oxidative Stress-Induced Human HepG2 Hepatocytes. *Biochem. Biophys. Res. Commun.* **2017**, *486*, 845–851.

(138) Tully, D. B.; Allgood, V. E.; Cidlowski, J. A. Modulation of Steroid Receptor-Mediated Gene Expression by Vitamin B6. *FASEB J.* **1994**, *8*, 342–349.

(139) Capper, C. .; Rae, J. M.; Auchus, R. J. The Metabolism, Analysis, and Targeting of Steroid Hormones in Breast and Prostate Cancer. *Horm. Cancer* **2016**, *7*, 149–164.

(140) Toya, K.; Hirata, A.; Ohata, T.; Sanada, Y.; Kato, N.; Yanaka, N. Regulation of Colon Gene Expression by Vitamin B6supplementation. *Mol. Nutr. Food Res.* **2012**, *56*, 641–652.

(141) Oka, T. Modulation of Gene Expression by Vitamin B6. *Nutr. Res. Rev.* **2001**, *14*, 257–265.

(142) Ramaswamy, P. G.; Natarajan, R. Vitamin B6 Status in Patients With Cancer of the Uterine Cervix. *Nutr. Cancer* **1984**, *6*, 176–180.

(143) Potera, C.; Rose, D. P.; Brown, R. R. Vitamin B6 Defiency in Cancer Patients. *Am. J. Clin. Nutr.* **1977**, *30*, 1677–1679.

(144) Pais, R. C.; Vanous, E.; Hollins, B.; Faraj, A.; Davis, R.; Camp, V. M.; Ragab, A. H. Abnormal Vitamin B6 Status in Childhood Leukemia. *Cancer* **1990**, *66*, 2421–2428.

(145) Inculet, R. I.; Norton, J. A.; Nichoalds, G. E.; Naher, M. M.; White, D. E.; Brennan, M. F. Water-Soluble Vitamins in Cancer Patients on Parenteral Nutrition: A Prospective Study. *J. Parenter. Enter. Nutr.* **1987**, *11*, 243–249.

(146) Baker, H.; Frank, O.; Chen, T.; Feingold, S.; DeAngelis, B.; Baker, E. R. Elevated Vitamin Levels in Colon Adenocarcinoma as Compared with Metastatic Liver Adenocarcinoma from Colon Primary and Normal Adjacent Tissue. *Cancer* **1981**, *47*, 2883–2886.

(147) Tryfiates, G. P. Metabolic Interconversions of Pyridoxine by Morris Hepatoma No. 7777 Cells. Synthesis of a Novel Metabolite. *Anticancer Res* **1983**, *3*, 53–58.

(148) Tryfiates, G. P.; Bishop, R. E.; Murgo, A. J. Vitamin B6 and Cancer: A Novel Pyridoxal 5-Phosphate Conjugate in Tumor Cells and Blood of Cancer Patients. *Anticancer Res* **1991**, *11*, 1281–1284.

(149) Tryfiates, G. P.; Bishop, R. E. Vitamin B6 and Cancer: Adenosine-N6-Diethylthioether N1-Pyridoximine 50 -PO4, a Circulating Human Tumor Marker. *Anticancer Res* **1995**, *15*, 379–383.

(150) Tryfiates, G. P.; Gannett, P. M.; Bishop, R. E.; Shastri, P. K.; Ammons, J. R.; Arbogast, J. G. Vitamin B6 and Cancer: Synthesis and Occurrence of Adenosine-N6-Diethylthioether-N-Pyridoximine-5′-Phosphate, a Circulating Human Tumor Marker. *Cancer Res.* **1996**, *56*, 3670–3677.

(151) Byar, D.; Blackard, C. Comparisons of Placebo, Pyridoxine, and Topical Thiotepa in Preventing Recurrence of Stage I Bladder Cancer. *Urology* **1977**, *10*, 556–561.

(152) Zhang, S.-L.; Chen, T.-S.; Ma, C.-Y.; Meng, Y.-B.; Zhang, Y.-F.; Chen, Y.-W.; Zhou, Y.-H. Effect of Vitamin B Supplementation on Cancer Incidence, Death Due to Cancer, and Total Mortality. *Med.* **2016**, *95*, 3485.

(153) Mocellin, S.; Briarava, M.; Pilati, P. Vitamin B6 and Cancer Risk: A Field Synopsis and Meta-Analysis. *J. Nationak Cancer Inst.* **2017**, *109*, 1–9.

(154) Parodi, K. Vision 20/20: Positron Emission Tomography in Radiation Therapy Planning, Delivery, and Monitoring. *Med. Phys.* **2015**, *42*, 7153–7168.

(155) Jones, T. The Role of Positron Emission Tomography within the Spectrum of Medical Imaging. *Eur. J. Nucl. Med.* **1996**, *23*, 207–211.

(156) Lameka, K.; Farwell, M. D.; Ichise, M. Positron Emission Tomography. In *Handbook of Clinical Neurology: Neuroimaging Part 1*; Masdeu, J. C., Gilberto Gonzalez, R., Aminoff, M. J., Boller, F., Swaab, D. F., Eds.; Shirley Decker-lucke, ELSEVIER: Amsterdam, 2016; pp 209–227.

(157) Konya, J.; Nagy, N. M. Interaction of Radiation with Matter. In *Nuclear and Radiochemistry*; Elsevier Inc.: Amsterdam, 2018; pp 85–131.

(158) Konya, J.; Nagy, N. M. Radioactive Decay. In *Nuclear and Radiochemistry*; Elsevier Inc.: Amsterdam, 2018; pp 49–84.

(159) Miller, P. W.; Long, N. J.; Vilar, R.; Gee, A. D. Synthesis of 11C, 18F, 15O, and 13N Radiolabels for Positron Emission Tomography. *Angew Chem Int Ed Engl* **2008**, *47*, 8998–9033.

(160) Jacobson, O.; Kiesewetter, D. O.; Chen, X. Fluorine-18 Radiochemistry, Labeling Strategies and Synthetic Routes. *Bioconjug. Chem.* **2015**, *26*, 1–18.

(161) Gambhir, S. S. Molecular Imaging of Cancer with Positron Emission Tomography. *Nat. Rev. Cancer* **2002**, *2*, 683–693.

(162) Chen, K.; Chen, X. Positron Emission Tomography Imaging of Cancer Biology: Current Status and Future Prospects. *Semin Oncol.* **2011**, *38*, 70–86.

(163) Kayani, I.; Groves, A. M. 18F-Fluorodeoxyglucose PET/CT in Cancer Imaging. *Clin. Med.* **2006**, *6*, 240–244.

(164) Shreve, P. D.; Anzai, Y.; Wahl, R. L. Pitfalls in Oncologic Diagnosis with FDG PET Imaging: Physiologic and Benign Variants. *Radiohraphics* **1999**, *19*, 61–77.

(165) Shields, A. F.; Grierson, J. R.; Dohmen, B. M.; Machulla, H. J.; Stayanoff, J. C.; Lawhorn-Crews, J. M.; Obradovich, J. E.; Muzik, O.; Mangner, T. J. Imaging Proliferation in Vivo With [F-18]FLT and Positron Emission Tomography. *Nat. Med.* **1998**, *4*, 1334–1336.

(166) Liao, G. J.; Clark, A. S.; Schubert, E. K.; Mankoff, D. A. 18F-Fluoroestradiol PET: Current Status and Potential Future Clinical Applications. *J. Nucl. Med.* **2016**, *57*, 1269–1275.

(167) Farwell, M. D.; Pryma, D. A.; Mankoff, D. A. PET/CT Imaging in Cancer: Current Applications and Future Directions. *Cancer* **2014**, *120*, 3433–3445.

(168) Tian, M.; Zhang, H.; Oriuchi, N.; Higuchi, T.; Endo, K. Comparison of 11C-Choline PET and FDG PET for the Differential Diagnosis of Malignant Tumors. *Eur. J. Nucl. Med. Mol. Imaging* **2004**, *31*, 1064–1072.

(169) Welle, C. L.; Cullen, E. L.; Peller, P. J.; Lowe, V. L.; Murphy, R. C.; Johnson, G. B.; Binkovitz, L. A. 11C-Choline PET/CT in Recurrent Prostate Cancer and Nonprostatic Neoplastic Processes. *Radiographics* **2016**, *36*, 279–292.

(170) Torre, L. A.; Siegel, R. L.; Ward, E. M.; Jemal, A. Global Cancer Incidence and Mortality Rates and Trends—An Update. *Cancer Epidemiol. Biomarkers Prev.* **2016**, *25*, 16–27.

(171) Lever, S. Z.; Fan, K.-H.; Lever, J. R. Tactics for Preclinical Validation of Receptor-Binding Radiotracers. *Nucl. Med. Biol.* **2017**, *44*, 4–30.

(172) Sharma, R.; Aboagye, E. Development of Radiotracers for Oncology – the Interface with Pharmacology. *Br. J. Pharmacol.* **2011**, *16*, 1565–1585.

(173) He, S.; Mason, R. P.; Hunjan, S.; Mehta, V. D.; Arora, V.; Katipally, R.; Kulkarni, P. V.; Antich, P. P. Development of Novel 19F NMR PH Indicators: Synthesis and Evaluation of

a Series of Fluorinated Vitamin B6 Analogues. *Bioorg. Med. Chem* **1998**, *6*, 1631–1639.

(174) Yu, J. X.; Cui, W.; Bourke, V. A.; Mason, R. P. 6-Trifluoromethylpyridoxine: Novel 19F NMR PH Indicator for in Vivo Detection. *J. Med. Chem.* **2012**, *55*, 6814–6821.

(175) Adamczyk, M.; Akireddy, S. R.; Reddy, R. E. Transformation of Vitamin B6 to (+)-Deoxypyridinoline, a Useful Biochemical Marker for Diagnosis of Bone Diseases. *Tetrahedron* **2000**, *56*, 2379–2390.

(176) Fier, P. S.; Hartwig, J. F. Selective C-H Fluorination of Pyridines and Diazines Inspired by a Classic Amination Reaction. *Science (80-.).* **2013**, *342*, 956–960.

(177) Basuli, F.; Zhang, X.; Jagoda, E. M.; Choyke, P. L.; Swenson, R. E. Rapid Synthesis of Maleimide Functionalized Fluorine-18 Labeled Prosthetic Group Using "Radio-fluorination on the Sep-Pak" Method. *J. Label. Compd. Radiopharm.* **2018**, *61*, 599–605.

(178) Morisawa, Y.; Kataoaka, M.; Watanabe, T.; Kitano, N.; Matsuzawa, T. Studies on Anticoccidial Agents. 1. Synthesis and Anticoccidial Activity of 4-Deoxypyridoxol and Its Esters. *J. Med. Chem.* **1974**, *17*, 1083–1086.

(179) Culbertson, S. M.; Enright, G. D.; Ingold, K. U. Synthesis of a Novel Radical Trapping and Carbonyl Group Trapping Anti-AGE Agent: A Pyridoxamine Analogue for Inhibiting Advanced Glycation (AGE) and Lipoxidation (ALE) End Products. *Org. Lett.* **2003**, *5*, 2659–2662.

(180) Kugler, F.; Sihver, W.; Ermert, J.; Hubner, H.; Gmeiner, P.; Prante, O.; Coenen, H. H. Evaluation of 18F-Labeled Benzodioxine Piperazine-Based Dopamine D4 Receptor Ligands: Lipophilicity as a Determinate of Nonspecific Binding. *J.Med.Chem* **2011**, *54*, 8343–8352.

(181) Yue, X.; Yan, X.; Wu, C.; Niu, G.; Ma, Y.; Jacobson, O.; Shen, B.; Kiesewetter, D. O.; Chen, X. One-Pot Two-Step Radiosynthesis of a New 18F-Labeled Thiol Reactive Prosthetic Group and Its Conjugate for Insulinoma Imaging. *Mol. Pharm.* **2014**, *11*, 3875–3884.

(182) Cole, E. L.; Stewart, M. N.; Littich, R.; Hoareau, R.; Scott, P. J. H. Radiosyntheses Using Fluorine-18: The Art and Science of Late Stage Fluorination. *Curr. Top. Med. Chem.* **2014**, *14*, 875–900.

(183) Middleton, W. J. New Fluorinating Reagents. Dialkylaminosulfur Fluorides. *J.Org.Chem.* **1975**, *40*, 574–578.

(184) Tiwari, A. D.; Wu, C.; Zhu, J.; Zhang, S.; Zhu, J.; Wang, W. R.; Zhang, J.; Tatsuoka, C.; Matthews, P. M.; Miller, R. H.; Wang, Y. Design, Synthesis, and Evaluation of Fluorinated Radioligands for Myelin Imaging. *J. Med. Chem.* **2016**, *59*, 3705–3718.

(185) Rotstein, B. H.; Wang, L.; Liu, R. Y.; Patteson, J.; Kwan, E. E.; Vasdev, N.; Liang, S. H. Mechanistic Studies and Radiofluorination of Structurally Diverse Pharmaceuticals with Spirocyclic Iodonium(III) Ylides. *Chem. Sci.* **2016**, *7*, 4407–4417.

(186) Engle, K. M.; Pfeifer, L.; Pidgeon, G. W.; Giuffredi, G. T.; Thompson, A. L.; Paton, R. S.; Brown, J. M.; Gouverneur, V. Coordination Diversity in Hydrogen-Bonded Homoleptic

Fluoride-Alcohol Complexes Modulates Reactivity. *Chem. Sci.* **2015**, *6*, 5293–5302.

(187) Bachmann, T.; Rychlik, M. Chemical Glucosylation of Pyridoxine. *Carbohydr. Res.* **2020**, *489*, 107929.

(188) Balz, G.; Schiemann, G. Aromatic Fluorine Compounds. I. A New Method for Their Preparation. *Chem. Ber.* **1927**, *60*, 1186–1190.

(189) Korytnyk, W.; Srivastava, S. C.; Angelino, N.; Potti, P. G. G.; Paul, B. A General Method for Modifying the 2-Methyl Group of Pyridoxol. Synthesis and Biological Activity of 2-Vinyl- and 2-Ethynylpyridoxols and Related Compounds†. *J. Med. Chem.* **1973**, *16*,

(190) Priest, H. F.; Swinehart, C. F. Anhydrous Metal Fluorides. In *Inorganic synthesis*; Audrieth, L. F., Ed.; McGraw-Hill Book Company: New York, 1950; Vol. 1, pp 162–175.

(191) Meshri, D. T. Silver. *Encyclopedia of Chemical Technology*; 1991; pp 235–236.

(192) Clark, J. C.; Goulding, R. W.; Palmer, A. J. Preparation of 18F-Labelled Fluorocarbons for Use in Pharmacodynamics Studies. In *New developments Radiopharmaceuticals and Labelled Compounds*; IAEA, Ed.; Vienna, 1973; pp 411–421.

(193) Compressed gas association. Fluorine. In *Handbook of Compressed Gases*; Springer: Boston, MA, 1999; pp 364–371.

(194) Barnhart, T. E.; Nickles, R. J.; Roberts, A. D. Revisiting Low Energy Deuteron Production of [18F] Fluoride and Fluorine for PET. *AIP Conf. Proc.* **2003**, *680*, 1086–1089.

(195) BoschiS, S.; Lodi, F. Chemistry of PET Radiopharmaceuticals: Labelling Strategies. In *Basic Science of PET Imaging*; Khalil, M., Ed.; Springer International Publishing, 2017; pp 73–103.

(196) Yessaad, M.; Bernard, L.; Bourdeaux, D.; Chennell, P.; Sautou, V. Development of a Stability Indicating Method for Simultaneous Analysis of Five Water-Soluble Vitamins by Liquid Chromatography. *Pharm. Technol. Hosp. Pharm.* **2018**, *3*, 207–218.

(197) Koren, A. O.; Horti, A. G.; Mukhin, A. G.; Gündisch, D.; Kimes, A. S.; Dannals, R. F.; London, E. D. 2-, 5-, and 6-Halo-3-(2(S)-Azetidinylmethoxy)Pyridines: Synthesis, Affinity for Nicotinic Acetylcholine Receptors, and Molecular Modeling. *J. Med. Chem.* **1998**, *41*, 3690–3698.

(198) Rotstein, B. H.; Stephenson, N. A.; Vasdev, N.; Liang, S. H. Spirocyclic Hypervalent Iodine(III)-Mediated Radiofluorination of Non-Activated and Hindered Aromatics. *Nat. Commun.* **2014**, *5*, 1–7.

(199) Ming, J.; Wu, S.; You, T.; Wang, X.; Yu, C.; Luo, P.; Zhang, A.; Pan, X. Histone Deacetylation in the Promoter of P16 Is Involved in Fluoride-Induced Human Osteoblast Activation via the Inhibition of Sp1 Binding. *Biol. Trace Elem. Res.* **2019**, *188*, 373–383.

(200) Craig, R.; Litvajova, M.; Cronin, S. A.; Connon, S. J. Enantioselective Acyl-Transfer Catalysis by Fluoride Ions. *Chem. Commun.* **2018**, *54*, 10108–10111.

(201) Green, T. W.; Wuts, P. G. M. *Protective Groups in Organic Synthesis*; Willey-

Interscience: New York, 1999.

(202) Richard, M.; Specklin, S.; Roche, M.; Hinnen, F.; Kuhnast, B. Original Synthesis of Radiolabeling Precursors for Batch and on Resin One-Step/Late-Stage Radiofluorination of Peptides. *Chem. Commun.* **2020**, *56*, 2507–2510.

(203) Reeves, J. T.; Fandrick, D. R.; Tan, Z.; Song, J. J.; Lee, H.; Yee, N. K.; Senanayake, C. H. Room Temperature Palladium-Catalyzed Cross Coupling of Aryltrimethylammonium Triflates with Aryl Grignard Reagents. *Org. Lett.* **2010**, *12*, 4388–4391.

(204) Kassanova, A. Z.; Krasnokutskaya, E. A.; Beisembai, P. S.; Filimonov, V. D. A Novel Convenient Synthesis of Pyridinyl and Quinolinyl Triflates and Tosylates via One-Pot Diazotization of Aminopyridines and Aminoquinolines in Solution. *Synth.* **2016**, *48*, 256–262.

(205) Kabalka, G. W.; Varma, M.; Varma, R. S.; Srivastava, P. C.; Knapp, F. F. Tosylation of Alcohols. *J. Org. Chem.* **1986**, *51*, 2386–2388.

(206) Boekelheide, V.; Linn, W. V. Rearrangements of N-Oxides. A Novel Synthesis of Pyridyl Carbinols and Aldehydes. *J. Am. Chem. Soc.* **1954**, *76*, 1286–1291.

(207) Winton, W. P.; Brooks, A. F.; Wong, K. K.; Scott, P. J. H.; Viglianti, B. L. Synthesis of 6-(Fluoromethyl)-19-Norcholest-5(10)-En-3-Ol, a Fluorinated Analogue of NP-59, Using the Mild Fluorinating Reagent, TBAF(Pinacol)2. *SynOpen* **2019**, *03*, 55–58.

(208) Le Guen, C.; Mazzah, A.; Penhoat, M.; Melnyk, P.; Rolando, C.; Chausset-Boissarie, L. Direct and Regioselective C(Sp 3)-H Bond Fluorination of 2-Alkylazaarenes with Selectfluor. *Synth.* **2021**, *53*, 1157–1162.

(209) Brugarolas, P.; Freifelder, R.; Cheng, S. H.; Dejesus, O. Synthesis of: Meta -Substituted [18F]3-Fluoro-4-Aminopyridine via Direct Radiofluorination of Pyridine N -Oxides. *Chem. Commun.* **2016**, *52*, 7150–7152.

(210) Hartman, J. S.; Shoemaker, J. A. W.; Janzen, A. F.; Ragogna, P. J.; Szerminski, W. R. The Coordination Chemistry of (Py)2BF2+ and Related Difluoroboron Cations. *J. Fluor. Chem.* **2003**, *119*, 125–139.

(211) Lin, Q.; Zhu, X.; Fu, Y. P.; Zhang, Y. M.; Fang, R.; Yang, L. Z.; Wei, T. B. Rationally Designed Anion-Responsive-Organogels: Sensing F-via Reversible Color Changes in Gel-Gel States with Specific Selectivity. *Soft Matter* **2014**, *10*, 5715–5723.

(212) Tang, L.; Yang, Y.; Wen, L.; Yang, X.; Wang, Z. Catalyst-Free Radical Fluorination of Sulfonyl Hydrazides in Water. *Green Chem.* **2016**, *18*, 1224–1228.

(213) Hamacher, K.; Coenen, H. H.; Stocklin, G. Efficient Stereospecific Synthesis of No-Carrier-Added 2-[18F]-Fluoro-2-Deoxy D-Glucose Using Aminopolyether Supported Nucleophilic Substitution. *J. Nucl. Med.* **1986**, *27*, 235–238.

(214) Satori, P.; Junger, C. Die Elektrochemische Fluorierung von Alkansulfonamiden Und Alkandisulfonamiden. *J. Fluor. Chem.* **1996**, *79*, 71–75.

(215) Underwood, G. R.; Paul, B.; Becker, M. A. Selective Modification of the 2-position of

Pyridoxol. *J. Het. Chem.* **1976**, *13*, 1229–1232.

(216) Ding, R.; He, Y.; Wang, X.; Xu, J.; Chen, Y.; Feng, M.; Qi, C. Treatment of Alcohols with Tosyl Chloride Does Not Always Lead to the Formation of Tosylates. *Molecules* **2011**, *16*, 5665–5673.

(217) Kiang, T.; Zare, R. N. Stepwise Bond Dissociation Energies for the Removal of Fluorine from Thionyl Fluoride and Sulphuryl Fluoride. *J. Chem. Soc. Chem. Commun.* **1980**, No. 24, 1228–1229.

(218) Ferguson, D. M.; Melvin, P. R.; Sanford, M. S. Deoxyfluorination of (Hetero)Aryl Aldehydes Using Tetramethylammonium Fluoride and Perfluorobutanesulfonyl Fluoride or Trifluoromethanesulfonic Anhydride. *Isr. J. Chem.* **2020**, *60*, 398–401.

(219) Feliu, A. L.; Rottenberg, D. A. Synthesis and Evaluation of Fluorine-18 21-Fluoroprednisone as a Potential Ligand for Neuro-PET Studies. *J. Nucl. Med.* **1987**, *28*, 998–1005.

(220) Wadsak, W.; Mitterhauser, M. Basics and Principles of Radiopharmaceuticals for PET/CT. *Eur. J. Radiol.* **2010**, *73*, 461–469.

(221) Brown, R. L.; Stein, S. E. Boiling Point Data. In *NIST Chemistry WebBook, NIST Standard Reference Database Number 69*; Lindstrom, P. J., Mallard, W. G., Eds.; National Institute of Standards and Technology: Gaithersburg MD; p 20899.

Appendices

Appendix 1. HPLC-UV traces of relevant compounds for radiofluorination of 6-Chloropyridoxine triacetate.

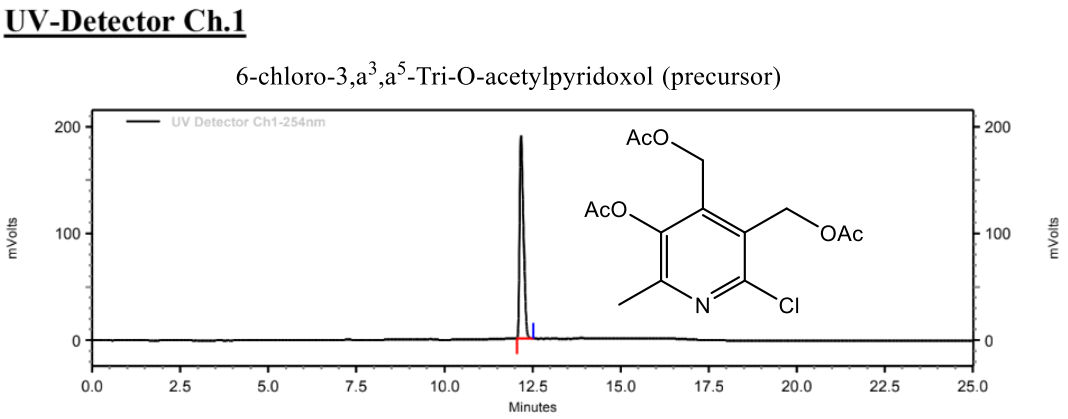

UV Detector
Ch1-254nm Results

Retention Time	Area	Area Percent	Height	Height Percent
12.175	1447537	100.000	189724	100.000

Figure A1. HPLC analysis of 6-Chloropyridoxine triacetate.

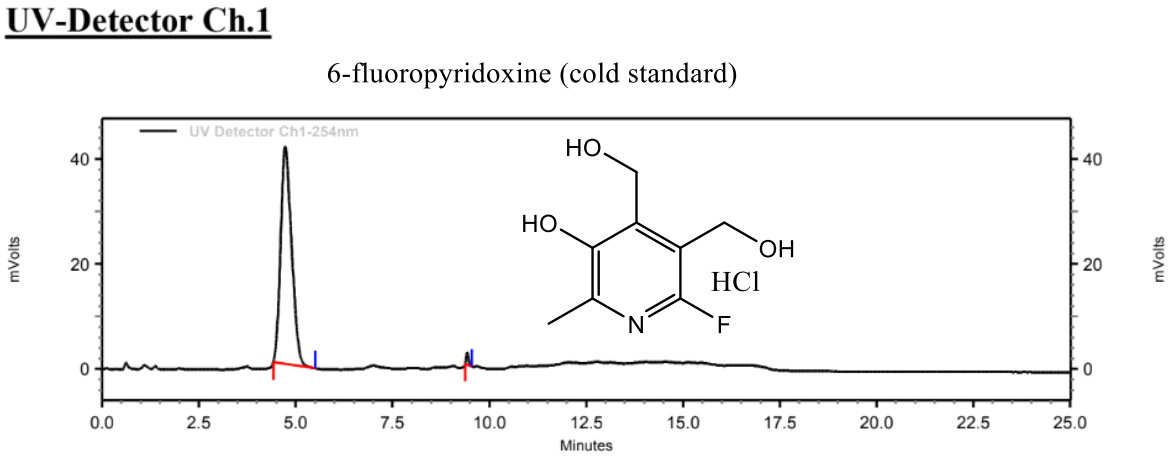

UV Detector
Ch1-254nm Results

Retention Time	Area	Area Percent	Height	Height Percent
4.733	816999	98.743	41419	94.460
9.425	10403	1.257	2429	5.540
Totals	827402	100.000	43848	100.000

Figure A2. HPLC analysis of 6-Fluoropyridoxine.

UV-Detector Ch.1

6-chloropyridoxine (side product)

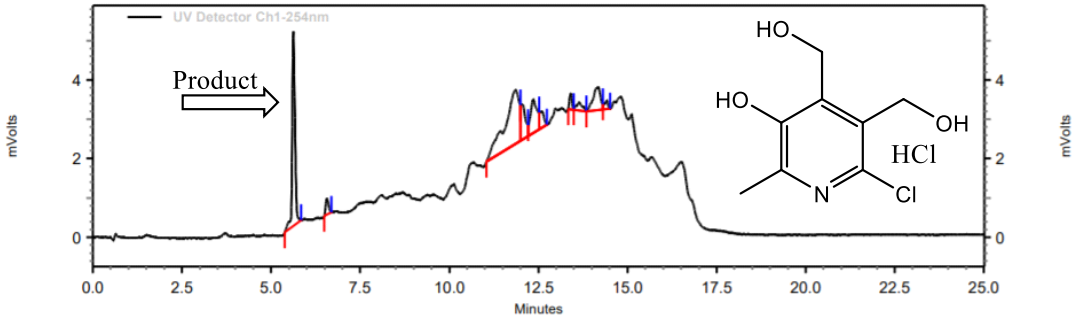

UV Detector
Ch1-254nm Results

Retention Time	Area	Area Percent	Height	Height Percent
5.625	27034	25.567	4943	47.657
6.567	2326	2.200	421	4.059
11.858	38881	36.771	1375	13.257
12.042	8081	7.642	907	8.745
12.350	10933	10.340	870	8.388
12.600	3822	3.615	422	4.069
13.408	1943	1.838	420	4.049
13.642	2479	2.344	214	2.063
14.183	8698	8.226	577	5.563
14.417	1541	1.457	223	2.150
Totals	105738	100.000	10372	100.000

Figure A3. HPLC analysis of 6-Chloropyridoxine.

Appendix 2. HPLC-UV trace of the triacetoxy-6-triflatepyridoxine (compound 16)

SHIMADZU LabSolutIons **Analysis Report**

<Sample Information>

Sample Name	: epm-4-25		
Sample ID	: March 3		
Data Filename	: epm-4-25.lcd		
Method Filename	: Emile standard.lcm		
Batch Filename	:		
Vial #	: 1-1	Sample Type	: Unknown
Injection Volume	: 1000 uL		
Date Acquired	: 03/03/2021 1:10:31 PM	Acquired by	: ShimadzuHPLC
Date Processed	: 03/03/2021 1:45:34 PM	Processed by	: ShimadzuHPLC

<Chromatogram>

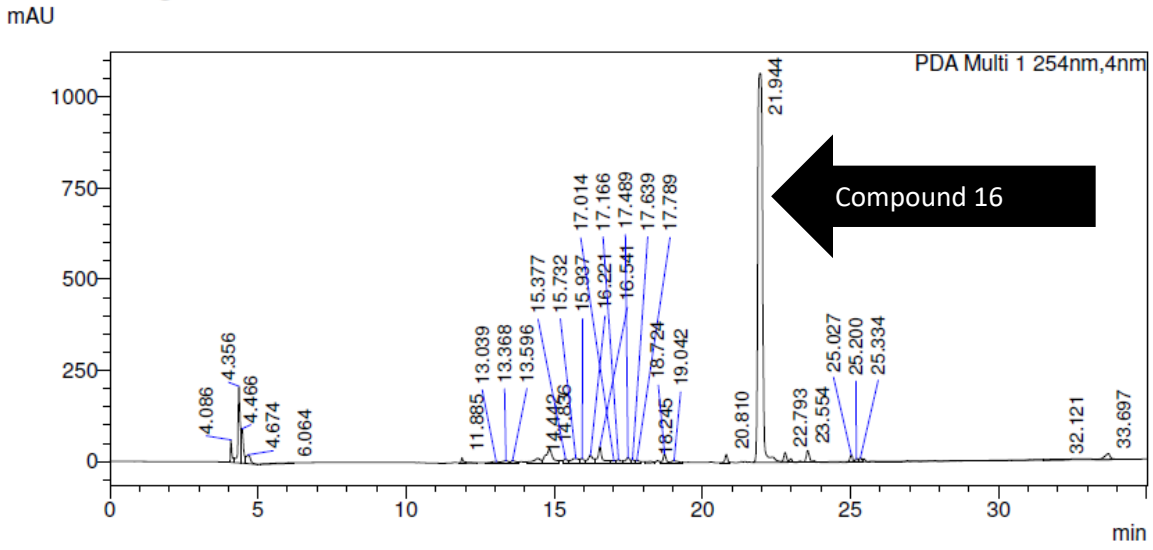

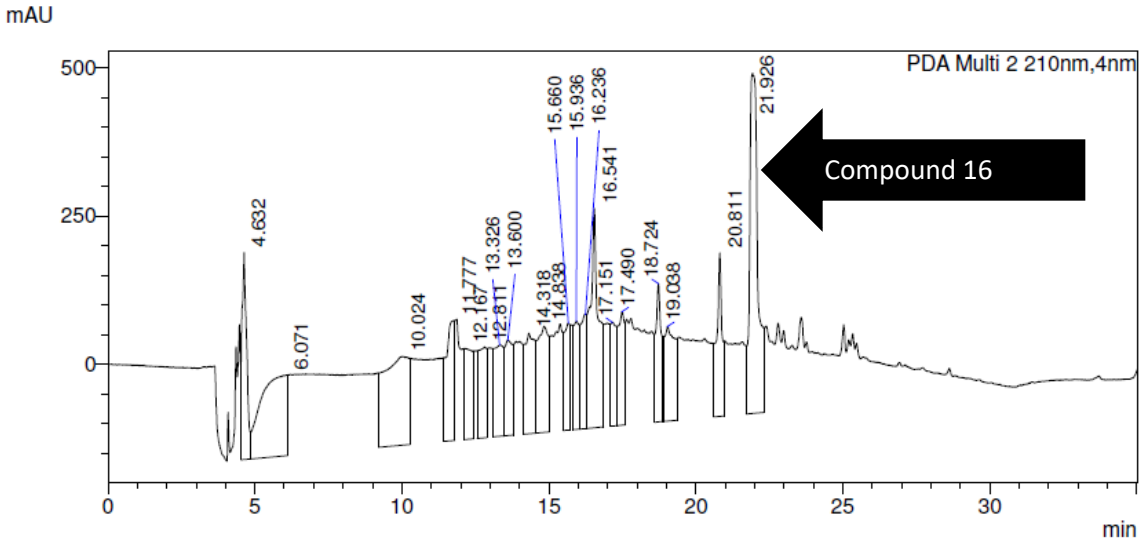
mAU
PDA Multi 2 210nm,4nm
Compound 16
500
250
0
4.632
6.071
10.024
12.167
12.777
12.811
13.326
13.600
14.318
14.838
15.660
15.936
16.236
16.541
17.151
17.490
18.724
19.038
20.811
21.926
0
5
10
15
20
25
30
min

PDA Ch1 254nm

Peak#	Ret. Time	Area	Height	Area%	Height%
1	4.086	202867	61039	1.153	3.261
2	4.356	1122944	209002	6.384	11.167
3	4.466	434965	93829	2.473	5.013
4	4.674	237718	24006	1.351	1.283
5	6.064	101858	1686	0.579	0.090
6	11.885	114720	15024	0.652	0.803
7	13.039	91868	4608	0.522	0.246
8	13.368	93846	6484	0.534	0.346
9	13.596	81555	7078	0.464	0.378
10	14.442	225774	13297	1.284	0.710
11	14.836	630418	38151	3.584	2.038
12	15.377	104254	11529	0.593	0.616
13	15.732	231340	12898	1.315	0.689
14	15.937	117898	13154	0.670	0.703
15	16.221	257992	21080	1.467	1.126
16	16.541	442329	44667	2.515	2.387
17	17.014	80227	7013	0.456	0.375
18	17.166	94989	8897	0.540	0.475
19	17.489	149853	15456	0.852	0.826
20	17.639	66312	9275	0.377	0.496
21	17.789	72365	7714	0.411	0.412
22	18.245	62514	4282	0.355	0.229
23	18.724	170208	25042	0.968	1.338
24	19.042	95523	6758	0.543	0.361
25	20.810	135670	23092	0.771	1.234
26	21.944	11225025	1067092	63.817	57.015
27	22.793	162223	25491	0.922	1.362
28	23.554	238139	32229	1.354	1.722
29	25.027	128752	20855	0.732	1.114
30	25.200	65635	10552	0.373	0.564
31	25.334	75357	12538	0.428	0.670
32	32.121	69434	1894	0.395	0.101
33	33.697	204709	15878	1.164	0.848
Total		17589282	1871591	100.000	100.000

PDA Ch2 210nm

Peak#	Ret. Time	Area	Height	Area%	Height%
1	4.632	3911797	348258	4.471	8.027
2	6.071	8340751	135889	9.532	3.132
3	10.024	8872804	149362	10.141	3.443
4	11.777	3894509	202429	4.451	4.666
5	12.167	2817101	153272	3.220	3.533
6	12.811	2950505	152853	3.372	3.523
7	13.326	3121507	154027	3.567	3.550
8	13.600	2980714	161057	3.407	3.712
9	14.318	3951248	169260	4.516	3.902
10	14.838	4545315	178565	5.195	4.116
11	15.660	2572259	180429	2.940	4.159
12	15.936	2565218	182474	2.932	4.206
13	16.236	2665348	192947	3.046	4.448
14	16.541	7584682	369933	8.668	8.527
15	17.151	2463932	175031	2.816	4.035
16	17.490	2720436	191411	3.109	4.412
17	18.724	2893187	233328	3.307	5.378
18	19.038	3964345	159475	4.531	3.676
19	20.811	3408235	275268	3.895	6.345
20	21.926	11274641	573054	12.886	13.209
Total		87498533	4338321	100.000	100.000

Appendix 3. HPLC-UV trace of the crude reaction mixture from the reaction between compound 16 and trimethyl amine at 4 °C.

SHIMADZU LabSolutIons **Analysis Report**

<Sample Information>

Sample Name	: epm-4-29		
Sample ID	: March 11		
Data Filename	: epm-4-29-lowtemp1.lcd		
Method Filename	: Emile standard.lcm		
Batch Filename	:		
Vial #	: 1-1	Sample Type	: Unknown
Injection Volume	: 1000 uL		
Date Acquired	: 11/03/2021 9:07:22 AM	Acquired by	: ShimadzuHPLC
Date Processed	: 11/03/2021 9:42:25 AM	Processed by	: ShimadzuHPLC

<Chromatogram>

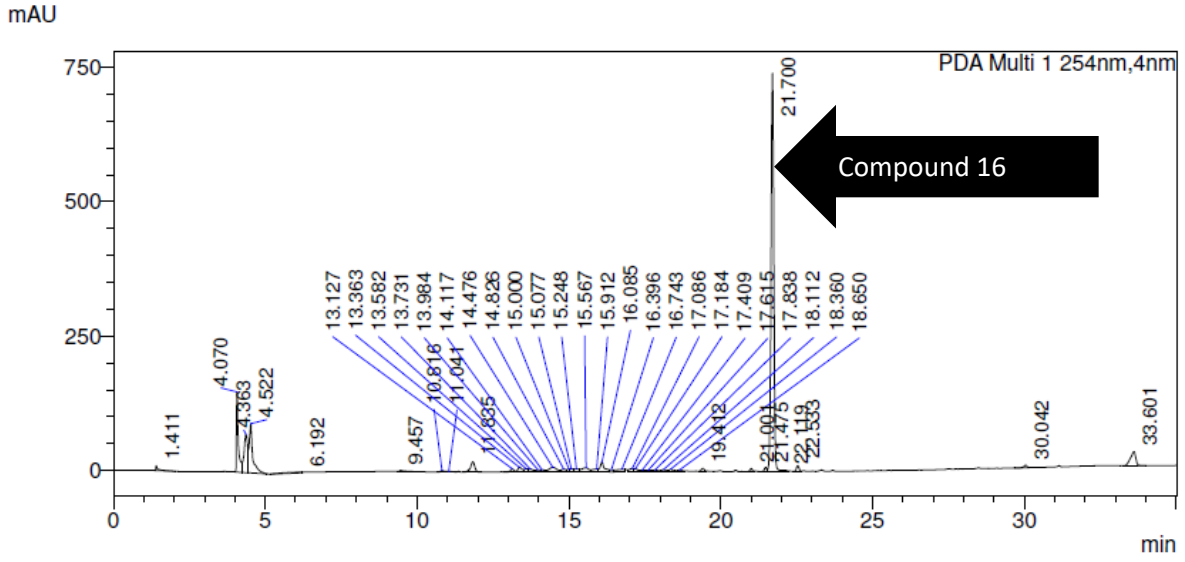

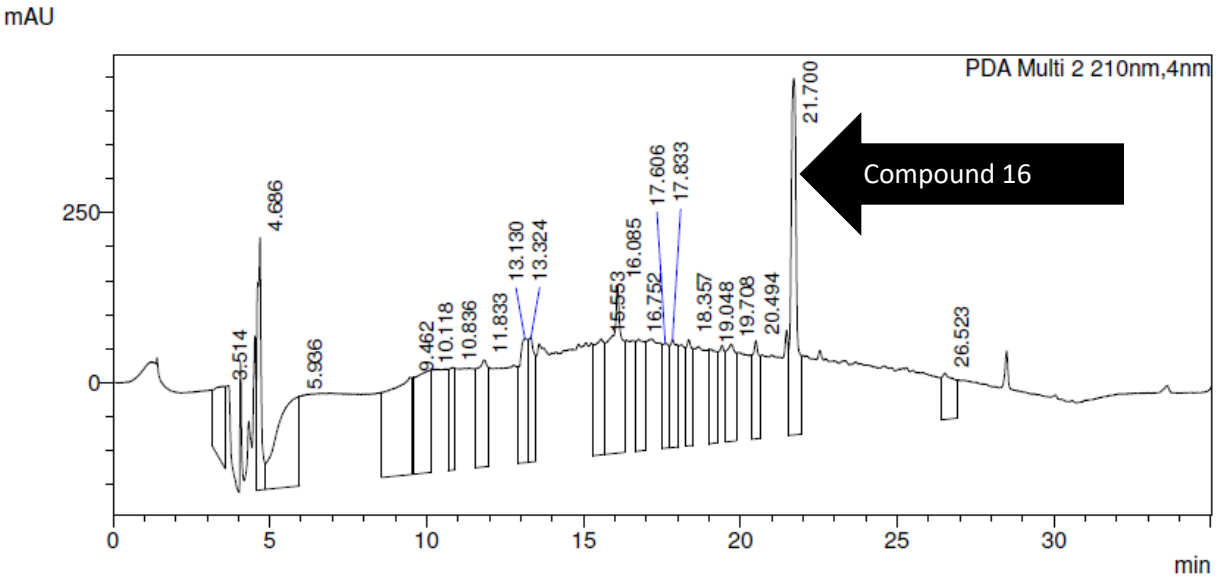

PDA Ch2 210nm

Peak#	Ret. Time	Area	Height	Area%	Height%
1	3.514	2532177	115860	3.473	3.166
2	4.686	3227105	371289	4.426	10.147
3	5.936	6260316	131943	8.585	3.606
4	9.462	7593548	143390	10.414	3.919
5	10.118	4859901	150626	6.665	4.117
6	10.836	2015846	150990	2.765	4.127
7	11.833	3816122	157638	5.233	4.308
8	13.130	3182818	183040	4.365	5.002
9	13.324	2632390	182899	3.610	4.999
10	15.553	3586825	170638	4.919	4.663
11	16.085	7016179	246938	9.622	6.749
12	16.752	3104710	164405	4.258	4.493
13	17.606	2054923	155034	2.818	4.237
14	17.833	2708803	158569	3.715	4.334
15	18.357	2068052	156244	2.836	4.270
16	19.048	2354104	138694	3.228	3.790
17	19.708	3011450	143036	4.130	3.909
18	20.494	2127013	144865	2.917	3.959
19	21.700	6766026	524857	9.279	14.344
20	26.523	1999173	68058	2.742	1.860
Total		72917481	3659016	100.000	100.000

PDA Ch1 254nm

Peak#	Ret. Time	Area	Height	Area%	Height%
1	1.411	51778	8745	0.556	0.673
2	4.070	638276	148106	6.856	11.401
3	4.363	609470	71286	6.546	5.488
4	4.522	737281	90845	7.919	6.993
5	6.192	81435	1484	0.875	0.114
6	9.457	26263	2109	0.282	0.162
7	10.816	25220	3052	0.271	0.235
8	11.041	28064	1755	0.301	0.135
9	11.835	198447	19512	2.132	1.502
10	13.127	60405	6587	0.649	0.507
11	13.363	92280	9455	0.991	0.728
12	13.582	61228	6680	0.658	0.514
13	13.731	60369	6080	0.648	0.468
14	13.984	45880	4439	0.493	0.342
15	14.117	41099	4282	0.441	0.330
16	14.476	170036	8927	1.826	0.687
17	14.826	61954	5648	0.665	0.435
18	15.000	32707	5623	0.351	0.433
19	15.077	48326	6062	0.519	0.467
20	15.248	61029	6119	0.656	0.471
21	15.567	138143	8102	1.484	0.624
22	15.912	63618	5783	0.683	0.445
23	16.085	206069	18585	2.213	1.431
24	16.396	35917	4336	0.386	0.334
25	16.743	100149	5321	1.076	0.410
26	17.086	67243	5981	0.722	0.460
27	17.184	47605	5922	0.511	0.456
28	17.409	36817	3314	0.395	0.255
29	17.615	34660	3251	0.372	0.250
30	17.838	47391	3857	0.509	0.297
31	18.112	47826	4316	0.514	0.332
32	18.360	44694	5220	0.480	0.402
33	18.650	52073	3583	0.559	0.276
34	19.412	50693	6620	0.544	0.510
35	21.001	32912	5750	0.354	0.443
36	21.475	44861	7642	0.482	0.588
37	21.700	4668344	739233	50.143	56.908
38	22.119	29004	2933	0.312	0.226
39	22.533	66714	10760	0.717	0.828
40	30.042	38231	5157	0.411	0.397
41	33.601	325570	26542	3.497	2.043
Total		9310080	1299007	100.000	100.000

Appendix 4. HPL-UV trace of the crude reaction mixture from the reaction between compound 16 and trimethyl amine at room temperature.

SHIMADZU LabSolutions Analysis Report

<Sample Information>

Sample Name	: epm-4-29		
Sample ID	: March 11		
Data Filename	: epm-4-29-roomtemp1.lcd		
Method Filename	: Emile standard.lcm		
Batch Filename	:		
Vial #	: 1-1	Sample Type	: Unknown
Injection Volume	: 1000 uL		
Date Acquired	: 11/03/2021 9:46:33 AM	Acquired by	: ShimadzuHPLC
Date Processed	: 11/03/2021 10:21:36 AM	Processed by	: ShimadzuHPLC

<Chromatogram>

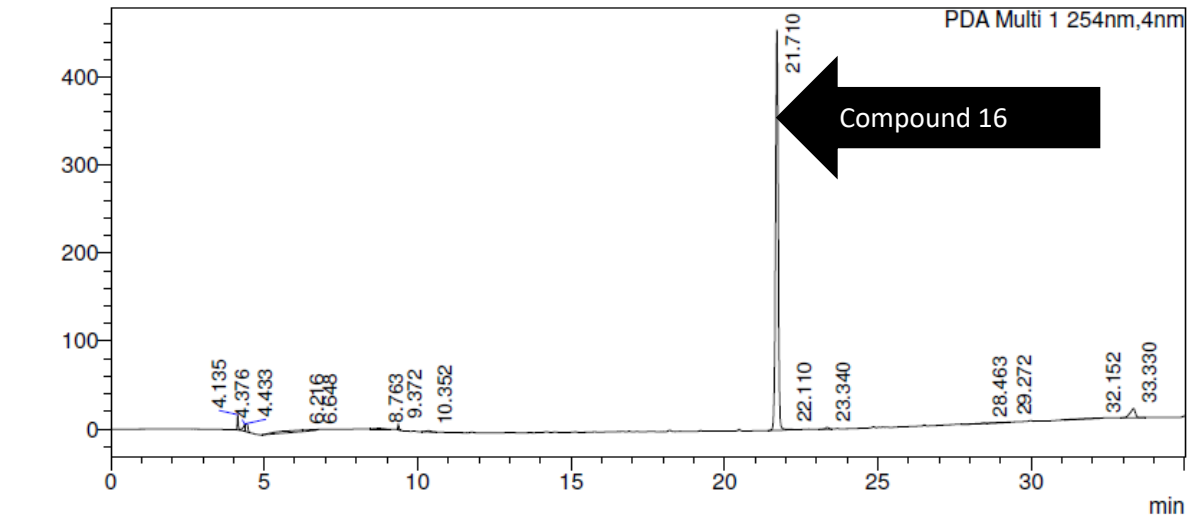

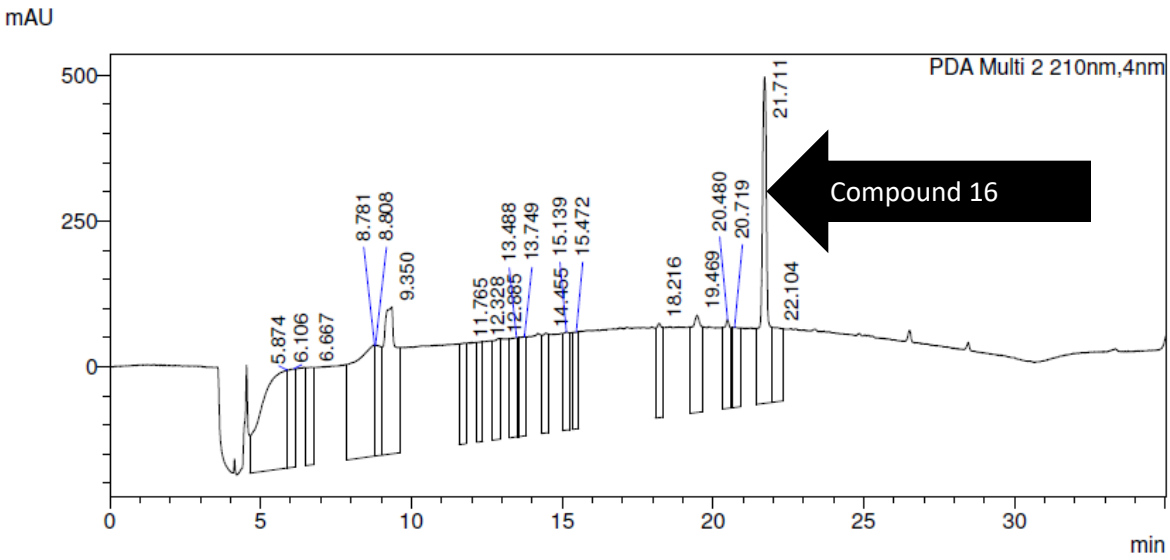

PDA Ch1 254nm

Peak#	Ret. Time	Area	Height	Area%	Height%
1	4.135	37513	17033	1.141	3.304
2	4.376	45112	8168	1.373	1.585
3	4.433	40172	9298	1.222	1.804
4	6.216	128485	1527	3.909	0.296
5	6.648	28150	782	0.856	0.152
6	8.763	33494	1289	1.019	0.250
7	9.372	16025	6409	0.488	1.243
8	10.352	14963	1268	0.455	0.246
9	21.710	2727328	454529	82.981	88.179
10	22.110	15412	1208	0.469	0.234
11	23.340	17675	2121	0.538	0.412
12	28.463	13904	610	0.423	0.118
13	29.272	13769	397	0.419	0.077
14	32.152	28984	352	0.882	0.068
15	33.330	125689	10475	3.824	2.032
Total		3286675	515465	100.000	100.000

PDA Ch2 210nm

Peak#	Ret. Time	Area	Height	Area%	Height%
1	5.874	9757199	168097	12.929	4.413
2	6.106	2500866	168463	3.314	4.423
3	6.667	2804852	167059	3.717	4.386
4	8.781	9807428	190669	12.996	5.006
5	8.808	2799206	190547	3.709	5.002
6	9.350	7278783	251919	9.645	6.614
7	11.765	2405069	173337	3.187	4.551
8	12.328	2056168	171329	2.725	4.498
9	12.885	2634604	172909	3.491	4.539
10	13.488	2530765	170648	3.354	4.480
11	13.749	2608755	170132	3.457	4.466
12	14.455	2360894	171567	3.128	4.504
13	15.139	2410676	169045	3.194	4.438
14	15.472	2232385	166795	2.958	4.379
15	18.216	2412419	161706	3.197	4.245
16	19.469	3840155	166952	5.089	4.383
17	20.480	2336516	152541	3.096	4.005
18	20.719	2290378	137753	3.035	3.616
19	21.711	7731691	560030	10.245	14.702
20	22.104	2666855	127626	3.534	3.351

Appendix 5. HPLC-UV trace of the crude reaction mixture from the reaction between compound 16 and trimethyl amine at high temperature.

SHIMADZU LabSolutions **Analysis Report**

<Sample Information>

Sample Name	: epm-4-29		
Sample ID	: March 16		
Data Filename	: epm-4-29-hightemp1.lcd		
Method Filename	: Emile standard.lcm		
Batch Filename	:		
Vial #	: 1-1	Sample Type	: Unknown
Injection Volume	: 1000 uL		
Date Acquired	: 16/03/2021 2:56:49 PM	Acquired by	: ShimadzuHPLC
Date Processed	: 16/03/2021 3:31:51 PM	Processed by	: ShimadzuHPLC

<Chromatogram>

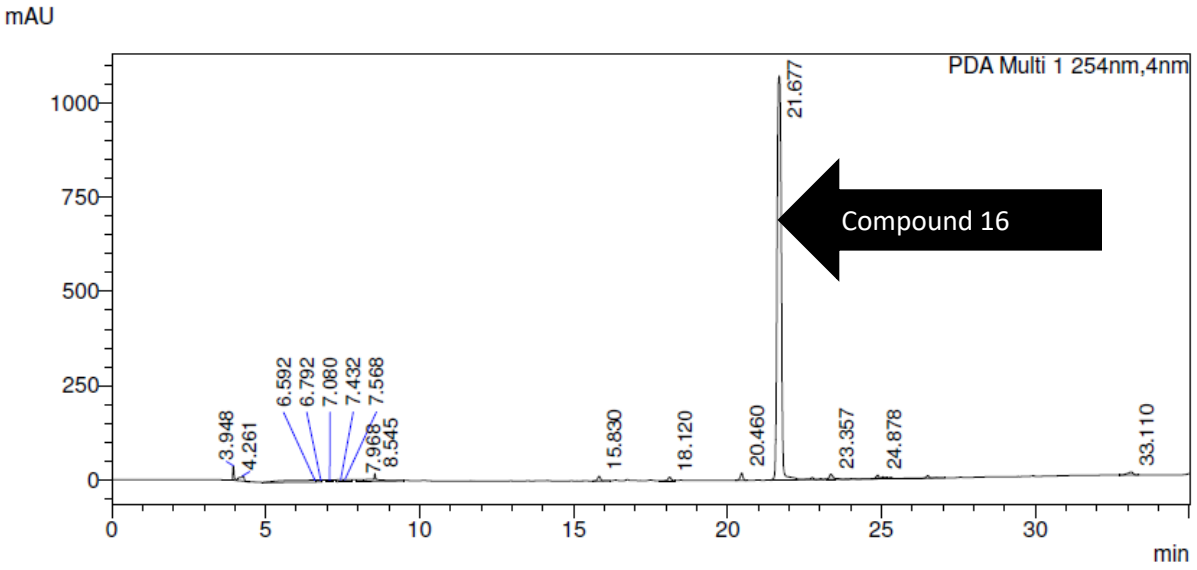

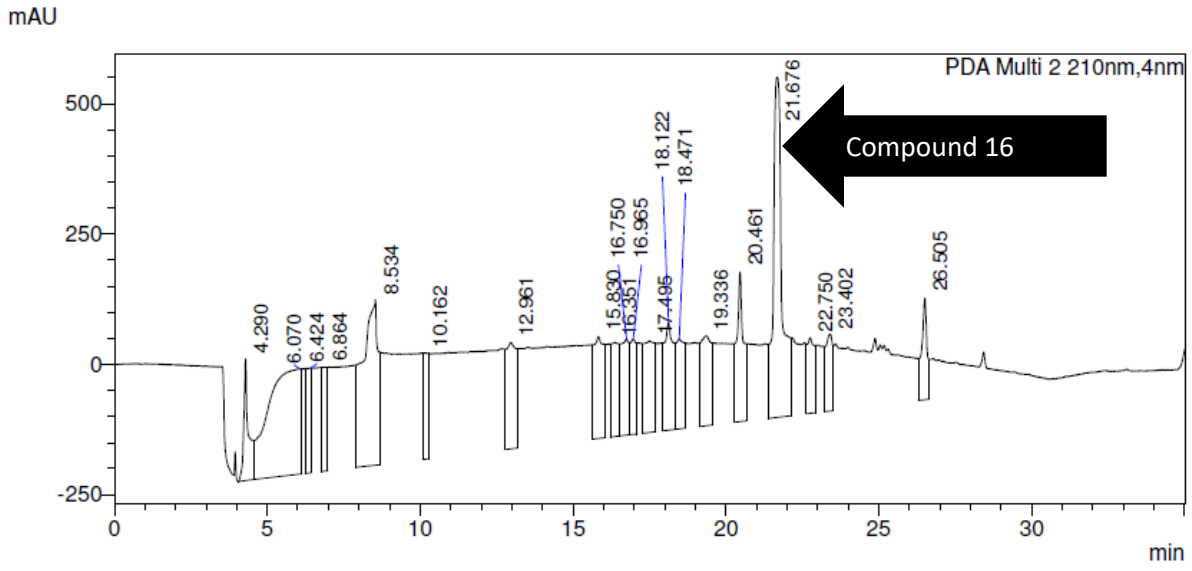

PDA Ch1 254nm

Peak#	Ret. Time	Area	Height	Area%	Height%
1	3.948	106003	37855	0.903	3.032
2	4.261	135188	14356	1.152	1.150
3	6.592	401027	5063	3.417	0.406
4	6.792	60462	5072	0.515	0.406
5	7.080	71817	5012	0.612	0.401
6	7.432	70664	4939	0.602	0.396
7	7.568	73468	4870	0.626	0.390
8	7.968	58259	4571	0.496	0.366
9	8.545	266423	20138	2.270	1.613
10	15.830	88913	12502	0.758	1.001
11	18.120	63729	9508	0.543	0.762
12	20.460	116590	19296	0.993	1.546
13	21.677	9941125	1072914	84.699	85.947
14	23.357	113100	13990	0.964	1.121
15	24.878	70125	10447	0.597	0.837
16	33.110	100164	7817	0.853	0.626
Total		11737057	1248350	100.000	100.000

PDA Ch2 210nm

Peak#	Ret. Time	Area	Height	Area%	Height%
1	4.290	2494897	231281	2.599	5.195
2	6.070	15115604	201853	15.745	4.534
3	6.424	2409110	200871	2.509	4.512
4	6.864	2483851	199367	2.587	4.479
5	8.534	11362108	316878	11.835	7.118
6	10.162	2339791	203949	2.437	4.581
7	12.961	4618093	203952	4.810	4.582
8	15.830	4593630	195246	4.785	4.386
9	16.351	3258545	180512	3.394	4.055
10	16.750	3433963	183830	3.577	4.129
11	16.965	2567320	182592	2.674	4.102
12	17.495	4387654	175555	4.570	3.944
13	18.122	4354656	206137	4.536	4.631
14	18.471	3293206	172572	3.430	3.877
15	19.336	4426632	172008	4.611	3.864
16	20.461	4540257	286693	4.729	6.440
17	21.676	13094730	651904	13.640	14.644
18	22.750	2339129	144766	2.437	3.252
19	23.402	2395916	147097	2.496	3.304
20	26.505	2491931	194582	2.596	4.371
Total		96001024	4451644	100.000	100.000

Appendix 6. HPLC-UV trace of 6-Triflatepyridoxine (compound 15).

SHIMADZU LabSolutions **Analysis Report**

<Sample Information>

Sample Name	: epm-3-78		
Sample ID	: November 17		
Data Filename	: epm-3-78_HS.lcd		
Method Filename	: Emile standard.lcm		
Batch Filename	:		
Vial #	: 1-1	Sample Type	: Unknown
Injection Volume	: 1000 uL		
Date Acquired	: 19/11/2020 1:57:46 PM	Acquired by	: ShimadzuHPLC
Date Processed	: 19/11/2020 2:32:49 PM	Processed by	: ShimadzuHPLC

<Chromatogram>

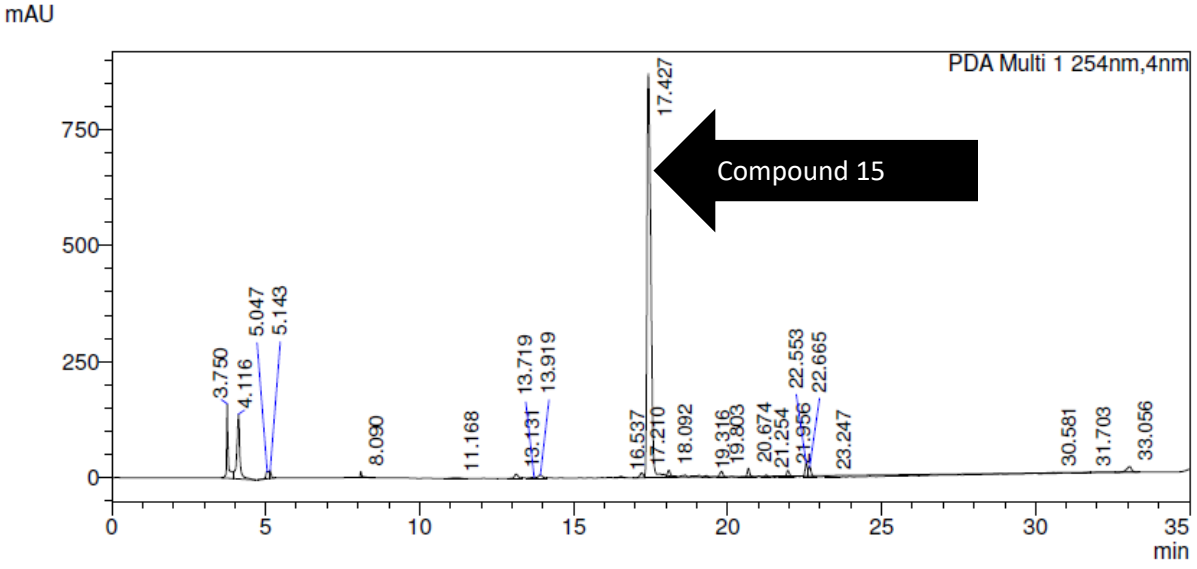

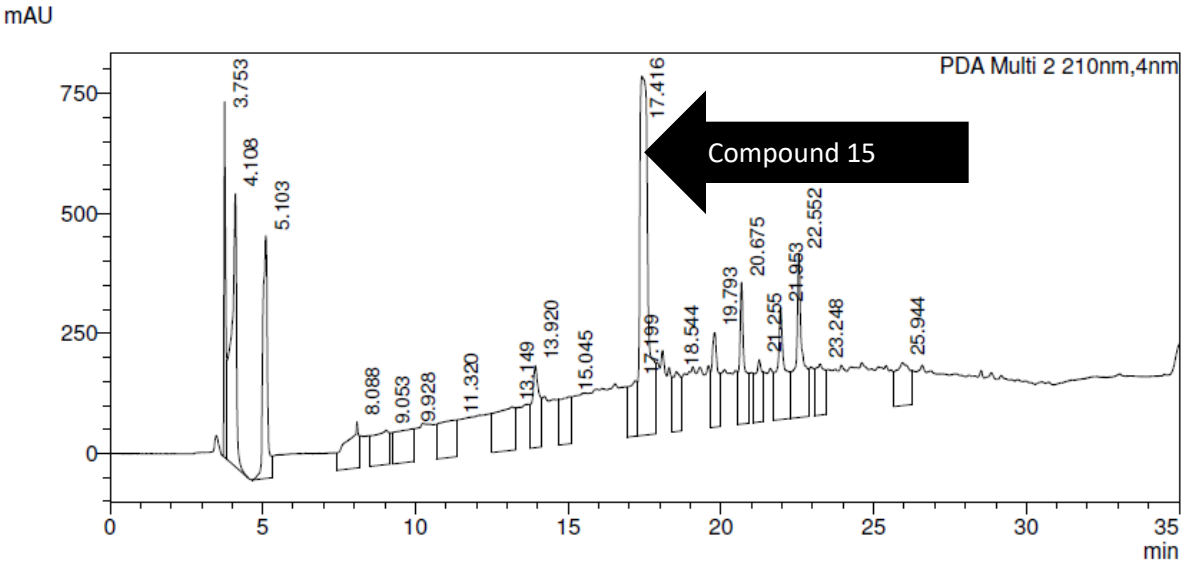
mAU
PDA Multi 2 210nm,4nm
Compound 15
3.753
4.108
5.103
8.088
9.053
9.928
11.320
13.149
13.920
15.045
17.199
17.416
18.544
19.793
20.675
21.255
21.953
22.552
23.248
25.944
750
500
250
0
0
5
10
15
20
25
30
35
min

PDA Ch1 254nm

Peak#	Ret. Time	Area	Height	Area%	Height%
1	3.750	588782	159261	6.640	11.475
2	4.116	944697	138382	10.654	9.971
3	5.047	103188	16242	1.164	1.170
4	5.143	77803	17392	0.877	1.253
5	8.090	54533	12548	0.615	0.904
6	11.168	36993	1811	0.417	0.131
7	13.131	88232	9536	0.995	0.687
8	13.719	42409	3002	0.478	0.216
9	13.919	76365	7479	0.861	0.539
10	16.537	33862	3514	0.382	0.253
11	17.210	78053	10351	0.880	0.746
12	17.427	5684967	868280	64.111	62.560
13	18.092	72624	12355	0.819	0.890
14	19.316	28682	3437	0.323	0.248
15	19.803	97506	12650	1.100	0.911
16	20.674	118378	19304	1.335	1.391
17	21.254	38107	5282	0.430	0.381
18	21.956	104849	14892	1.182	1.073
19	22.553	177579	30828	2.003	2.221
20	22.665	141091	22988	1.591	1.656
21	23.247	34075	2762	0.384	0.199
22	30.581	65029	2252	0.733	0.162
23	31.703	36881	1383	0.416	0.100
24	33.056	142765	11977	1.610	0.863
Total		8867448	1387907	100.000	100.000

PDA Ch2 210nm

Peak#	Ret. Time	Area	Height	Area%	Height%
1	3.753	2922545	732932	3.816	15.094
2	4.108	6470836	567567	8.448	11.688
3	5.103	5139442	504892	6.710	10.398
4	8.088	2644619	96141	3.453	1.980
5	9.053	2667814	71500	3.483	1.472
6	9.928	2890131	68439	3.773	1.409
7	11.320	3032465	76615	3.959	1.578
8	13.149	4064995	90423	5.307	1.862
9	13.920	2881545	171350	3.762	3.529
10	15.045	2392165	98290	3.123	2.024
11	17.199	2201464	115804	2.874	2.385
12	17.416	14484614	748242	18.911	15.409
13	18.544	2088382	124581	2.727	2.566
14	19.793	2744283	196623	3.583	4.049
15	20.675	3419162	294397	4.464	6.063
16	21.255	2013755	129871	2.629	2.675
17	21.953	4127668	231966	5.389	4.777
18	22.552	5141872	340451	6.713	7.011
19	23.248	2319648	106249	3.028	2.188
20	25.944	2947285	89456	3.848	1.842
Total		76594689	4855788	100.000	100.000

Appendix 7. HPLC-UV of the crude reaction mixture from the reaction between compound 15 and trimethyl amine at room temperature after acetyl protection.

SHIMADZU LabSolutions **Analysis Report**

<Sample Information>

Sample Name	: epm-4-40		
Sample ID	: April 13		
Data Filename	: epm-4-40-crude.lcd		
Method Filename	: Emile standard.lcm		
Batch Filename	:		
Vial #	: 1-1	Sample Type	: Unknown
Injection Volume	: 1000 uL		
Date Acquired	: 19/04/2021 11:31:56 AM	Acquired by	: ShimadzuHPLC
Date Processed	: 19/04/2021 12:06:59 PM	Processed by	: ShimadzuHPLC

<Chromatogram>

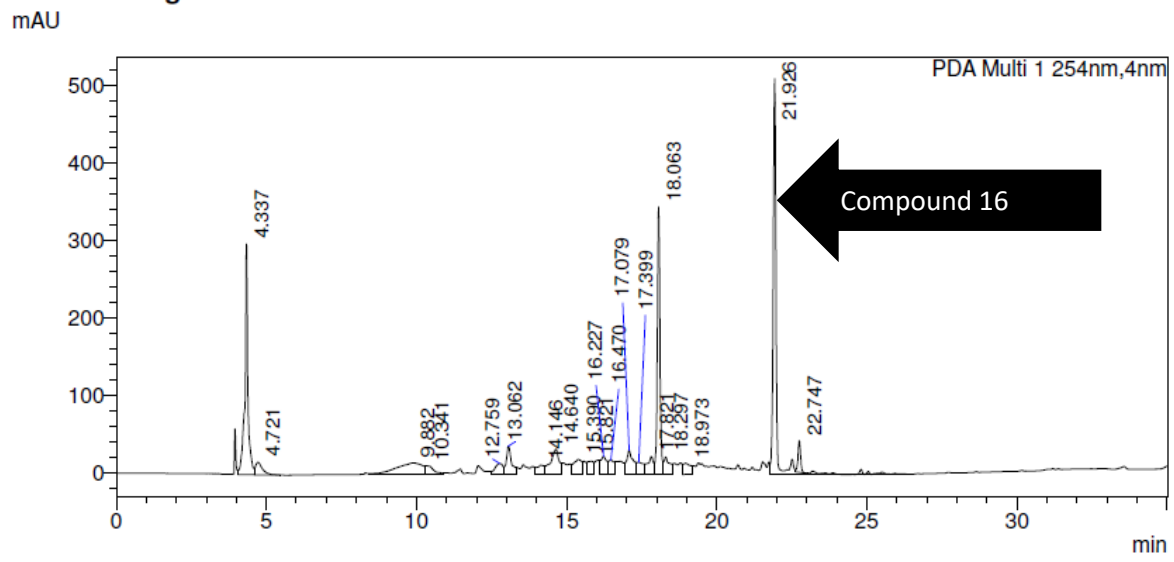

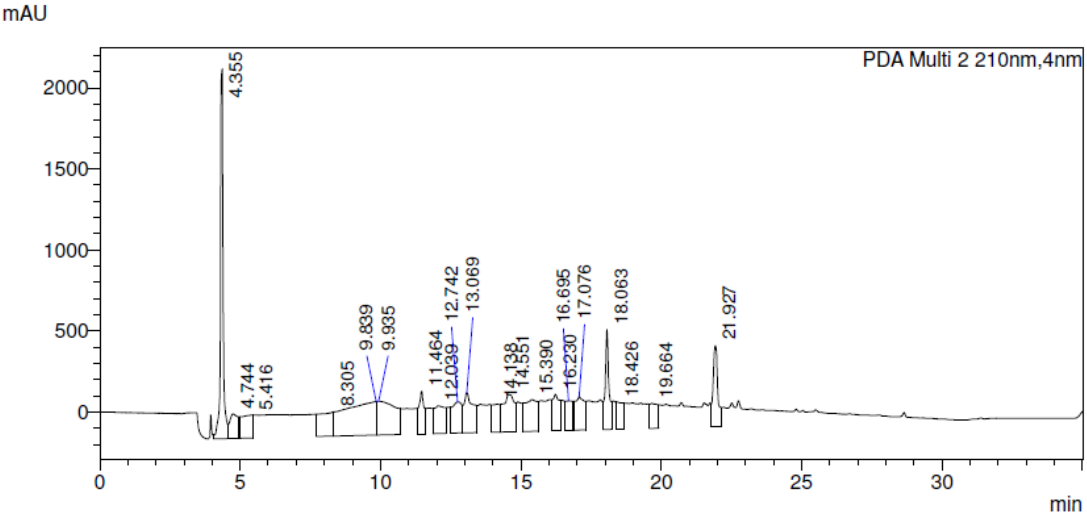

PDA Ch1 254nm

Peak#	Ret. Time	Area	Height	Area%	Height%
1	4.337	2015779	294723	14.967	19.466
2	4.721	264739	16196	1.966	1.070
3	9.882	909494	14778	6.753	0.976
4	10.341	232207	11389	1.724	0.752
5	12.759	257438	14084	1.911	0.930
6	13.062	441865	36809	3.281	2.431
7	14.146	202578	11987	1.504	0.792
8	14.640	648658	32567	4.816	2.151
9	15.390	356023	19581	2.643	1.293
10	15.821	251995	17177	1.871	1.135
11	16.227	338271	23446	2.512	1.549
12	16.470	217671	18982	1.616	1.254
13	17.079	505489	31367	3.753	2.072
14	17.399	244182	15669	1.813	1.035
15	17.821	296493	23082	2.201	1.525
16	18.063	2166716	344692	16.088	22.766
17	18.297	286039	22177	2.124	1.465
18	18.973	247965	14367	1.841	0.949
19	21.926	3334070	510218	24.755	33.699
20	22.747	250333	40748	1.859	2.691
Total		13468005	1514040	100.000	100.000

PDA Ch2 210nm

Peak#	Ret. Time	Area	Height	Area%	Height%
1	4.355	15382294	2276283	13.182	34.173
2	4.744	2963093	151055	2.539	2.268
3	5.416	3735011	140688	3.201	2.112
4	8.305	5186851	149205	4.445	2.240
5	9.839	16399797	206699	14.054	3.103
6	9.935	9568632	207084	8.200	3.109
7	11.464	3444188	262431	2.951	3.940
8	12.039	4528652	171572	3.881	2.576
9	12.742	4467946	191941	3.829	2.882
10	13.069	5963646	247689	5.110	3.718
11	14.138	3021918	173476	2.590	2.604
12	14.551	6651893	231958	5.700	3.482
13	15.390	6170113	196779	5.287	2.954
14	16.230	4031072	224480	3.454	3.370
15	16.695	2879669	183821	2.468	2.760
16	17.076	4676490	207106	4.007	3.109
17	18.063	5744790	615702	4.923	9.243
18	18.426	2824679	167896	2.421	2.521
19	19.664	3010094	154221	2.579	2.315
20	21.927	6043958	500917	5.179	7.520
Total		116694786	6661003	100.000	100.000

Appendix 8. Crude ^{19}F NMR of the fluorination attempt of compound 11 using $TBAF(Pin)_2$ at 80 °C.

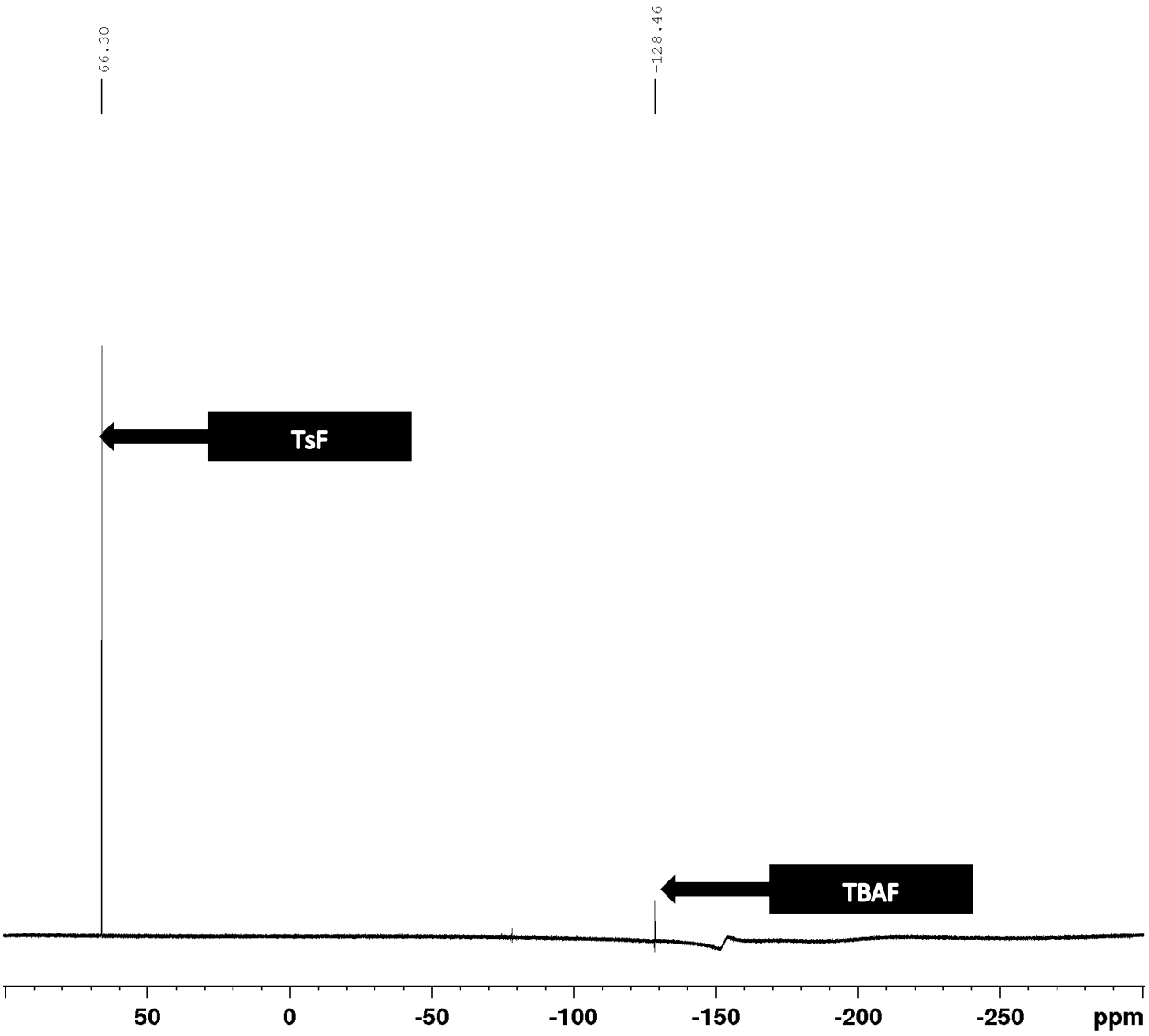

Appendix 9. Crude ^{19}F NMR of the fluorination attempt of compound 11 using $TBAF(Pin)_2$ at 50 °C

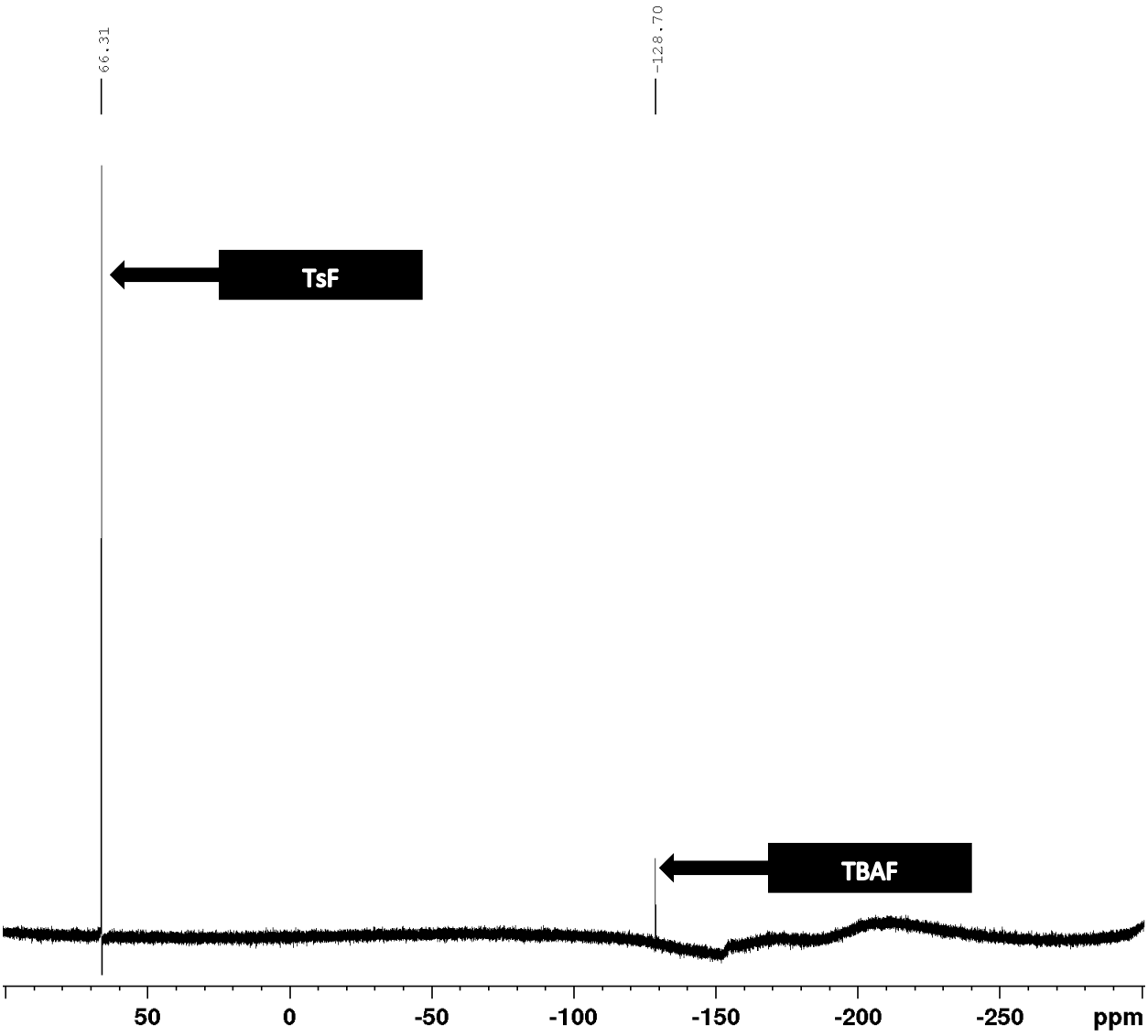

Appendix 10. Crude ^{19}F NMR of the fluorination attempt of compound 11 using TBAF at 50 °C

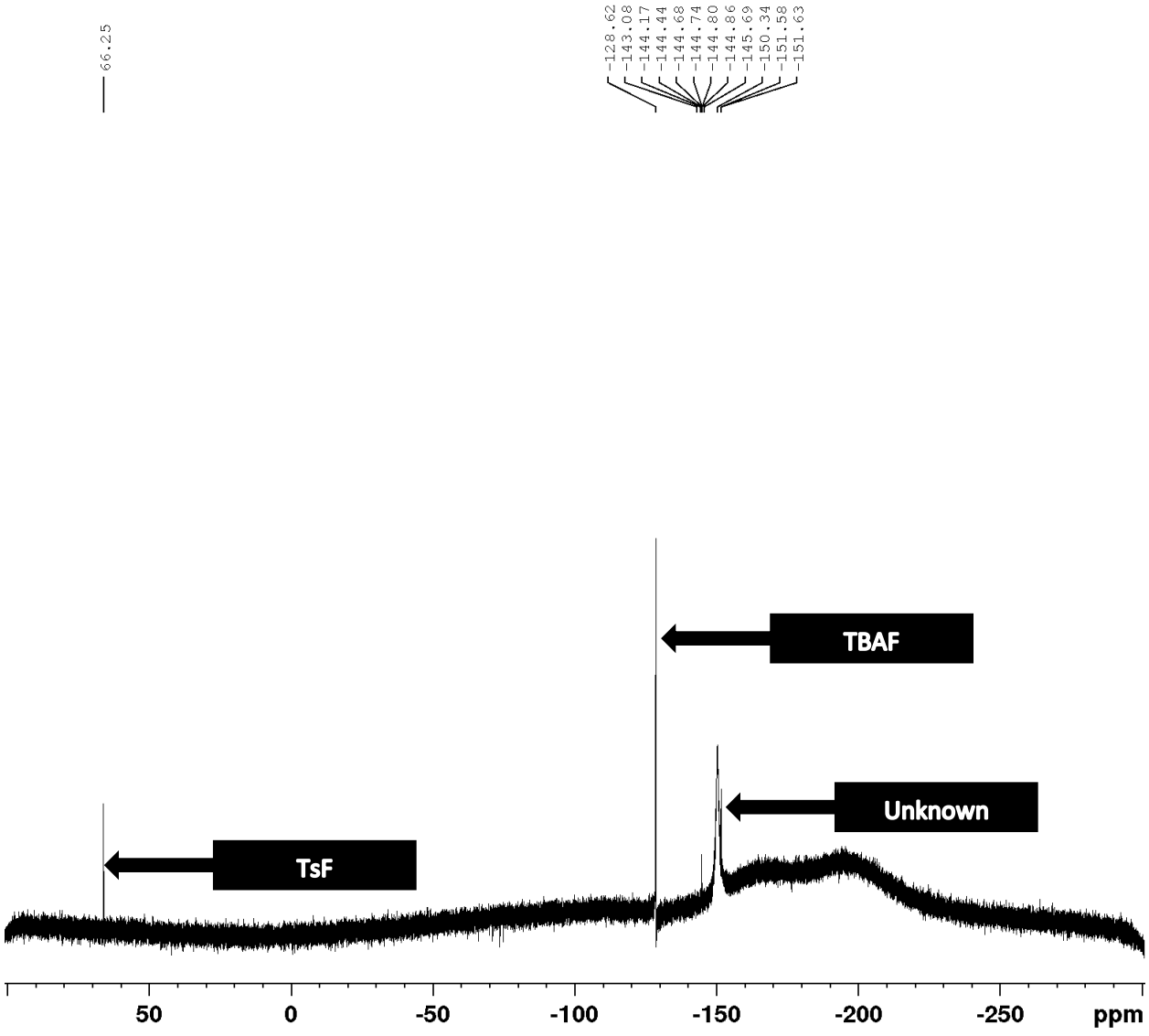

Appendix 11. Crude ^{19}F NMR of the fluorination attempt of compound 11 using TBAF at 80 °C

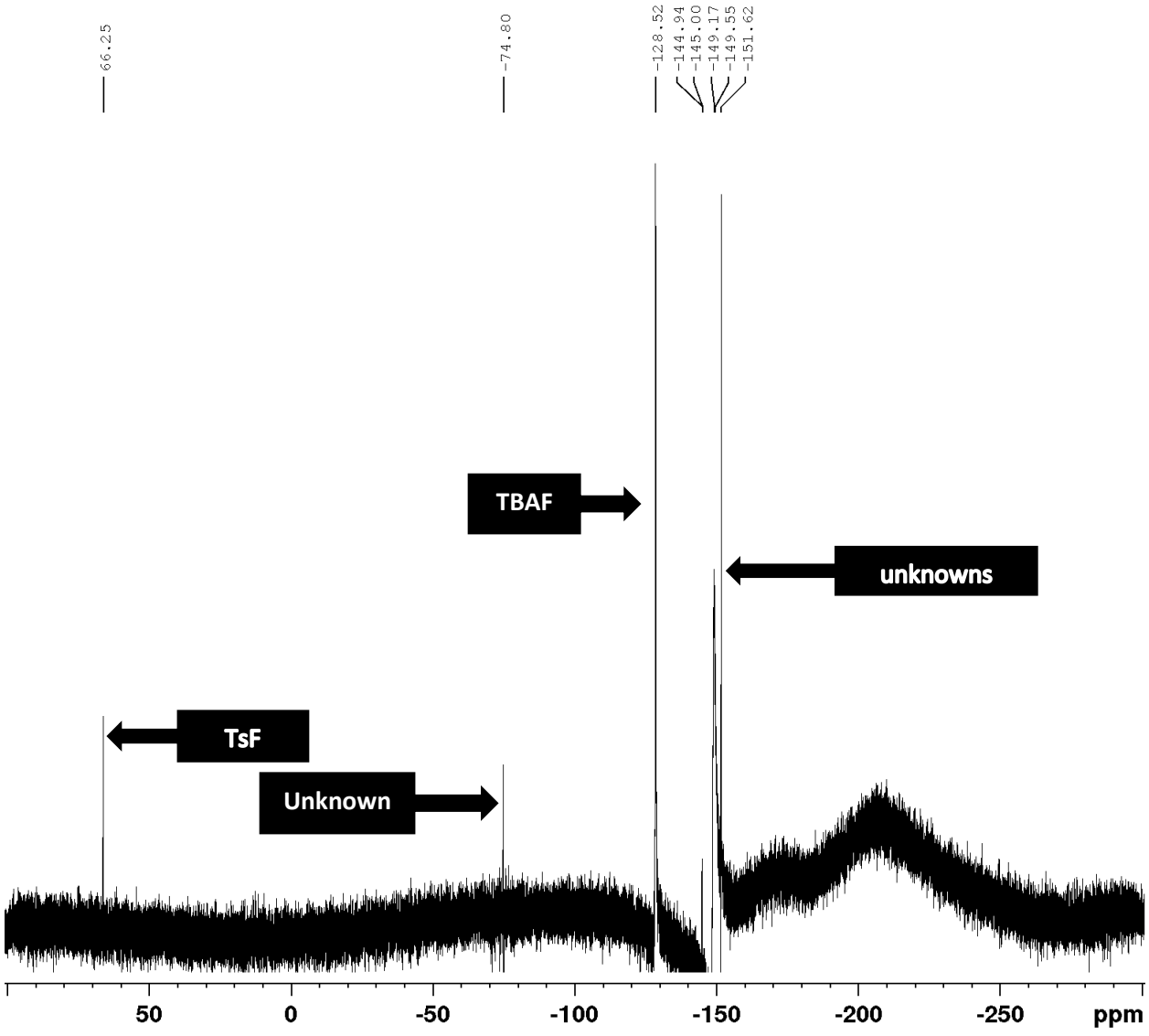

Appendix 12. Crude ^{19}F NMR of the fluorination attempt of compound 11 using TBAF at 110 °C

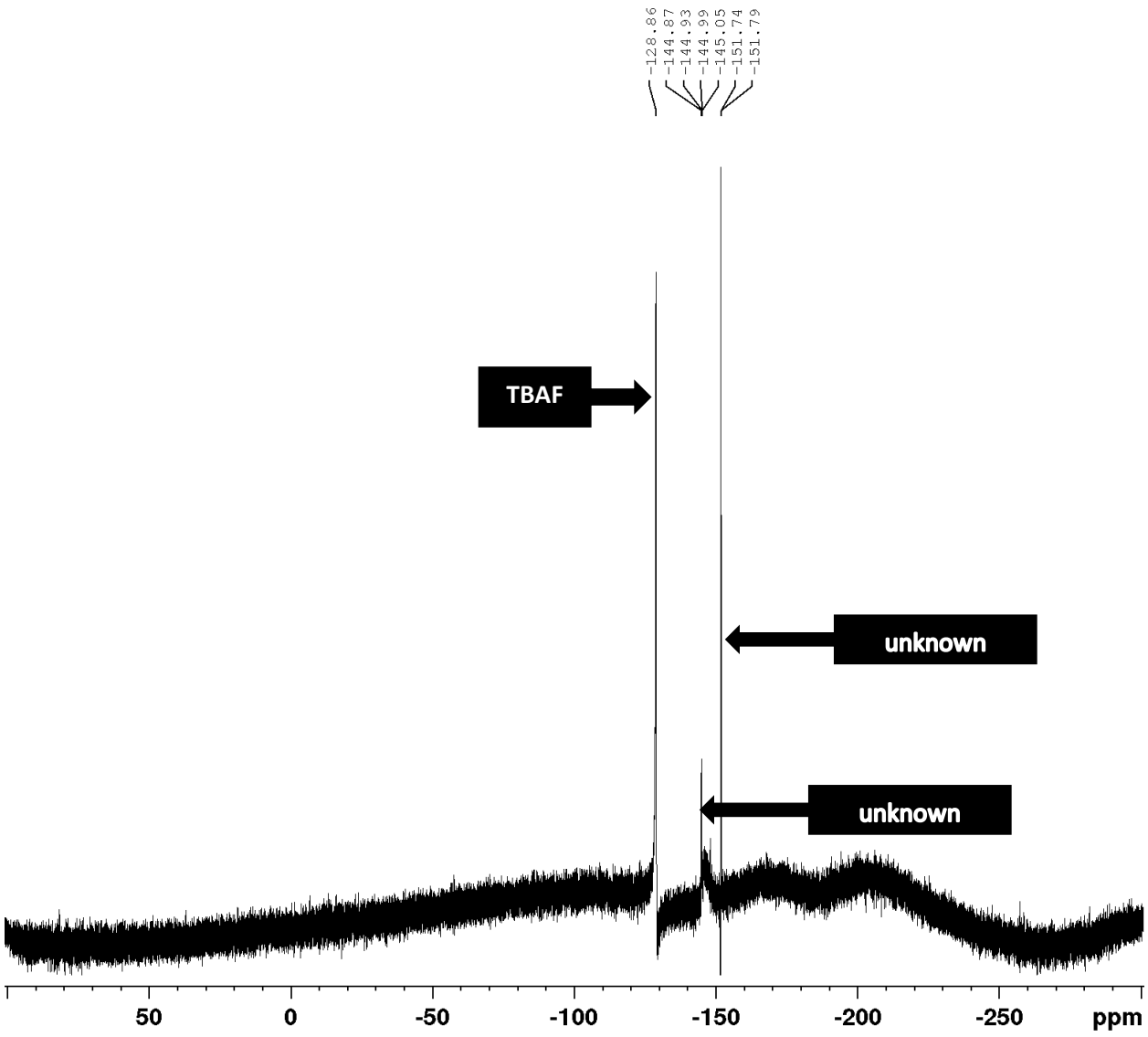

Appendix 13. Crude ^{19}F NMR of the fluorination attempt of compound 11 using KF/Kryptofix at 100 °C

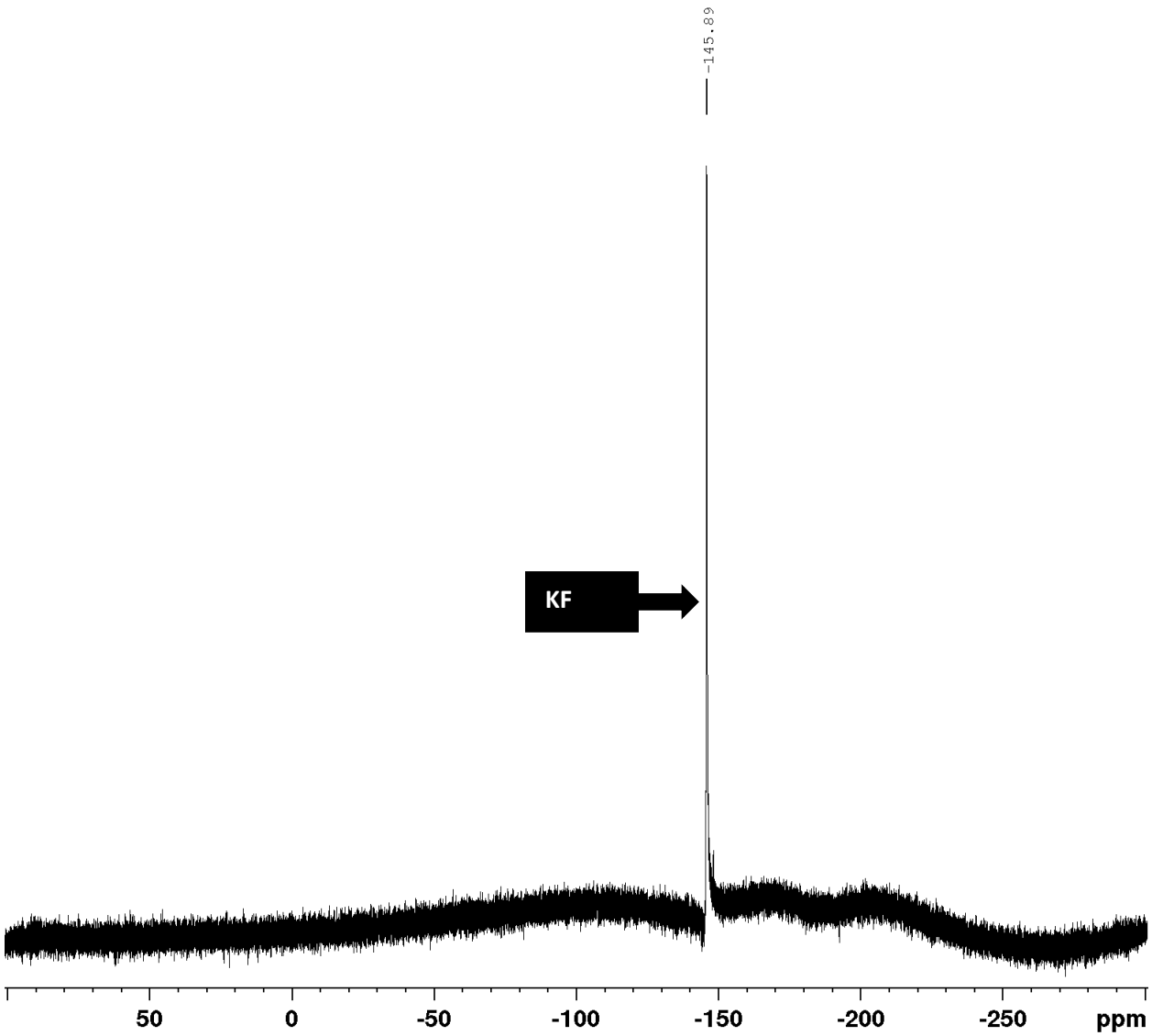

Appendix 14. Crude ^{19}F NMR of the fluorination attempt of compound 11 using KF/Kryptofix at 120 °C

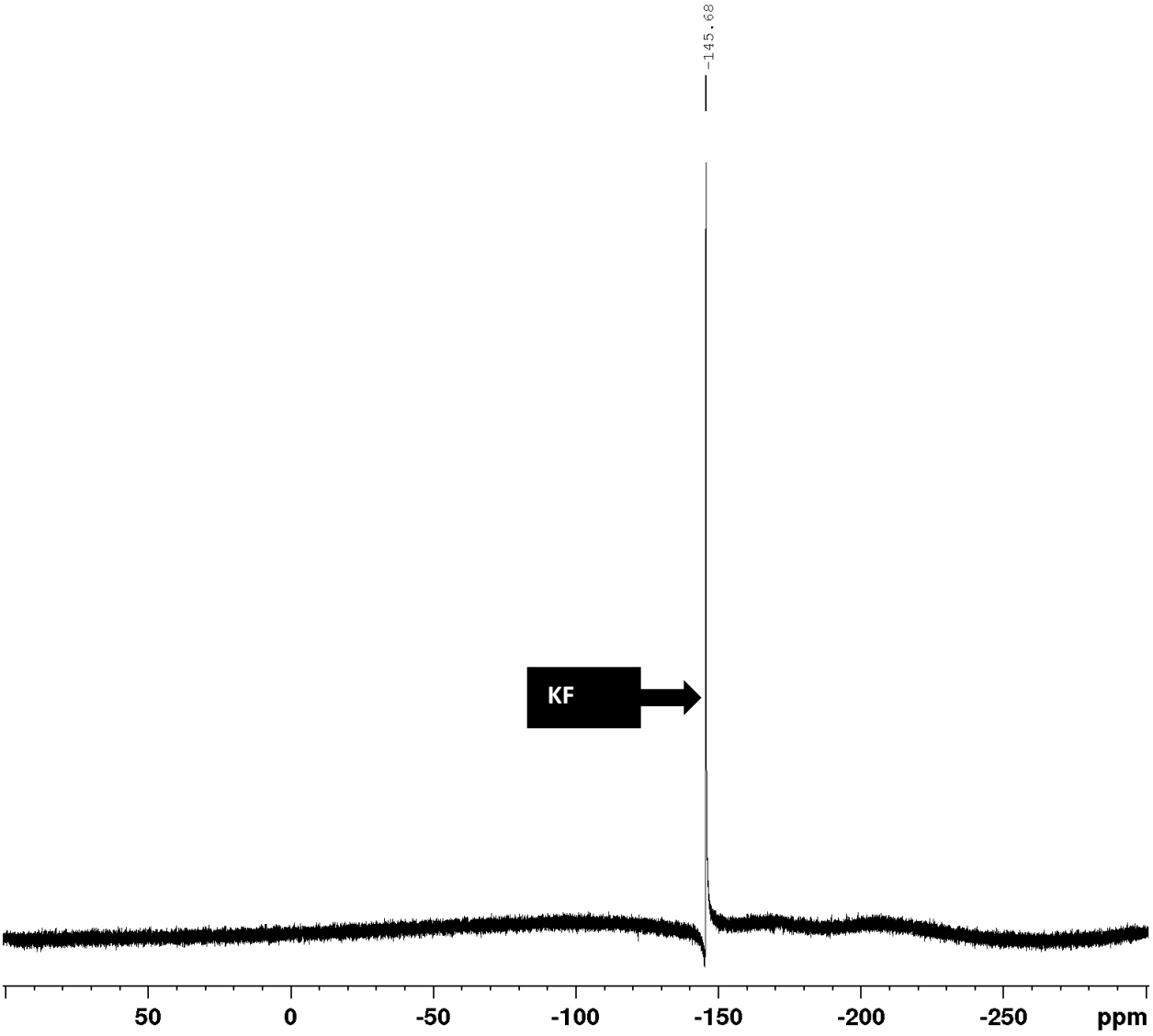

Appendix 15. ^{19}F NMR of the crude reaction mixture from the fluorination attempt of compound 21 with CsF at 150 °C.

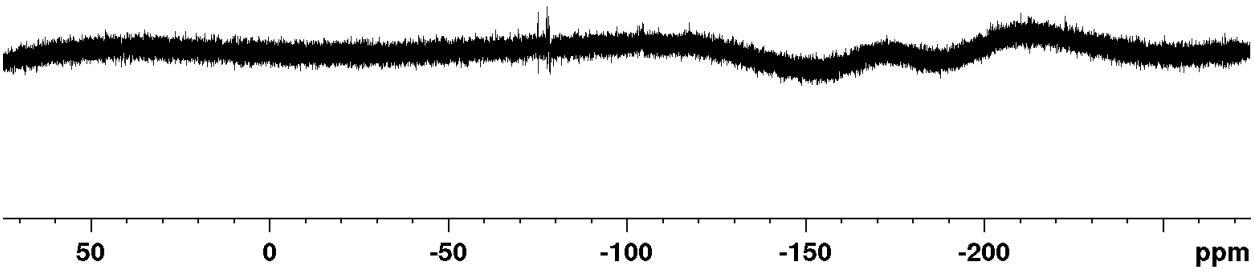

Appendix 16. **^{19}F NMR of the crude reaction mixture from the fluorination attempt of compound 21 with CsF at 90 °C**

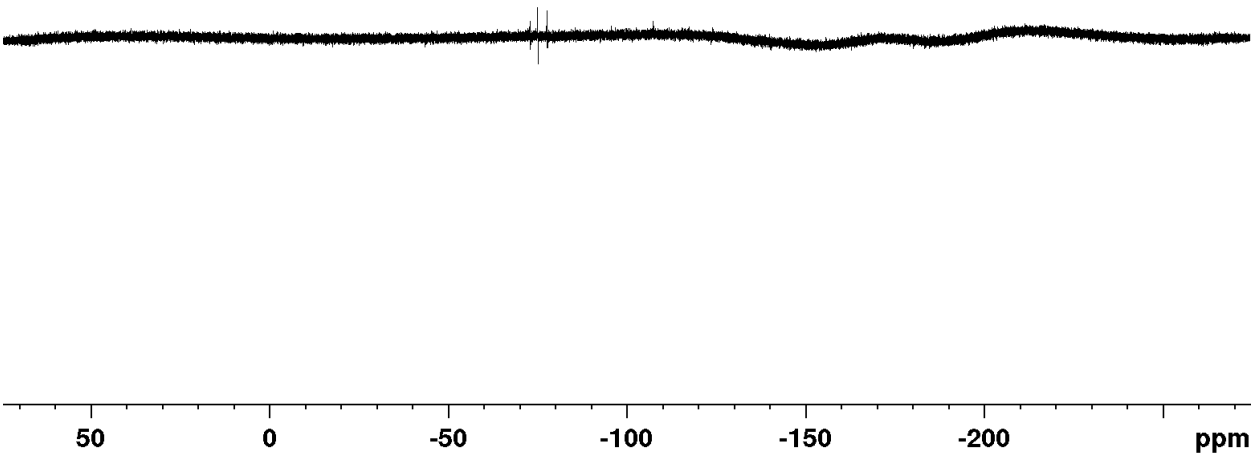

Appendix 17. ^{19}F NMR of the crude reaction mixture from the fluorination attempt of compound 21 with CsF at 120 °C.

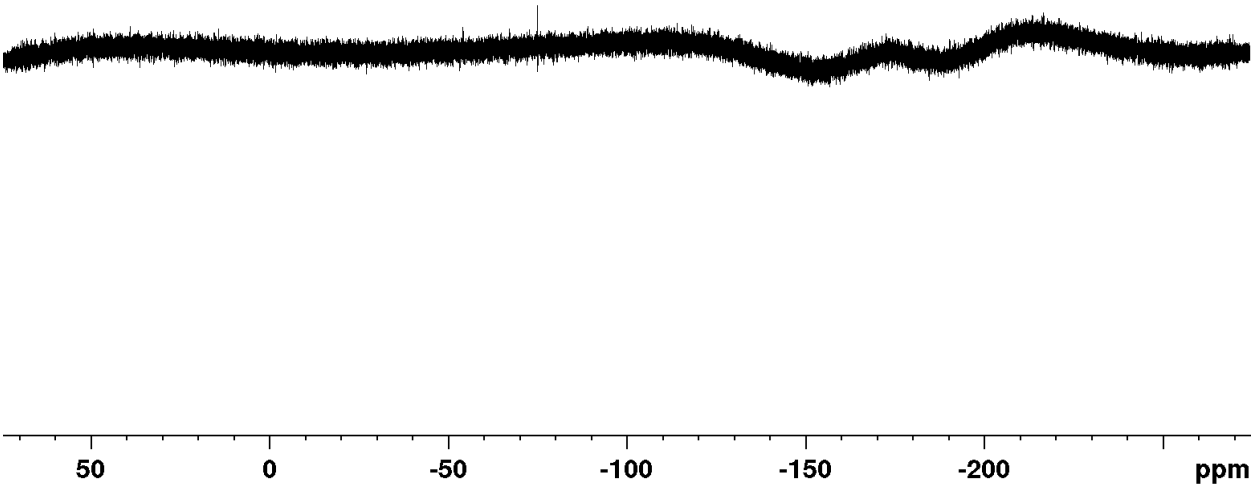

Appendix 18. **^{19}F NMR of the crude reaction mixture from the fluorination attempt of compound 21 with KF at 80 °C.**

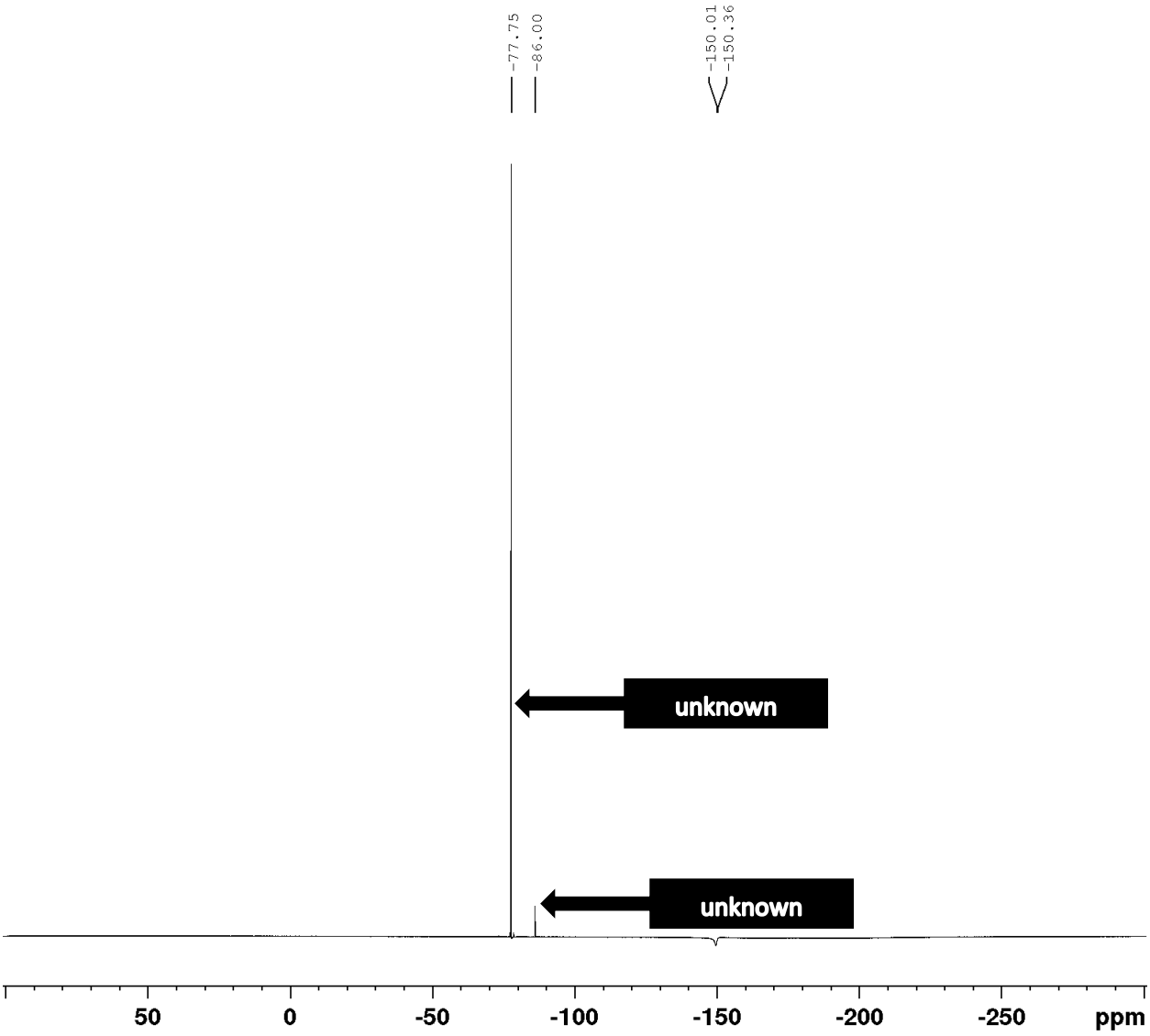

Appendix 19. ^{19}F NMR of the crude reaction mixture from the fluorination attempt of compound 21 with KF at 100 °C

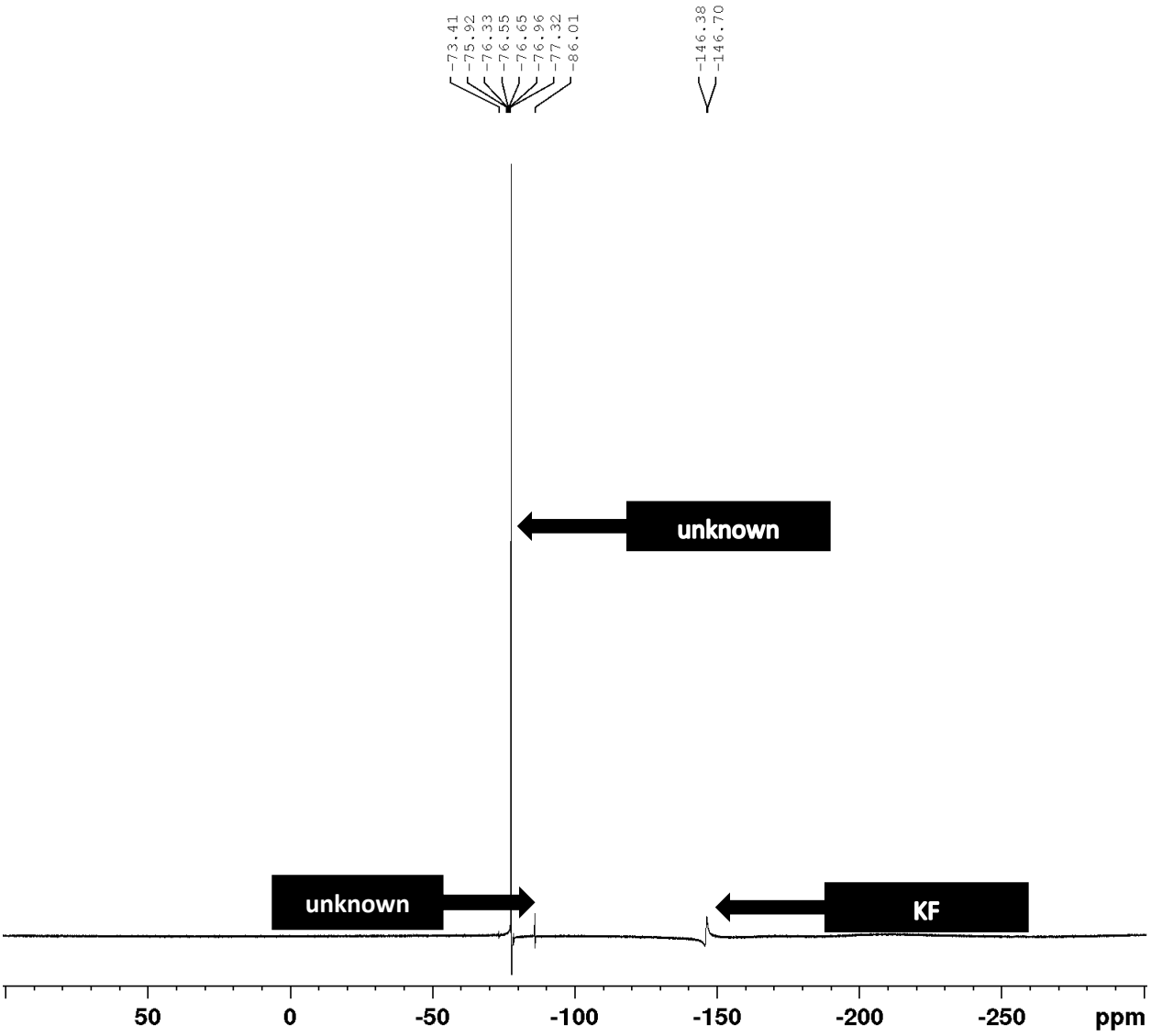

Appendix 20. ^{19}F NMR of the crude reaction mixture from the fluorination attempt of compound 21 with KF at 120 °C

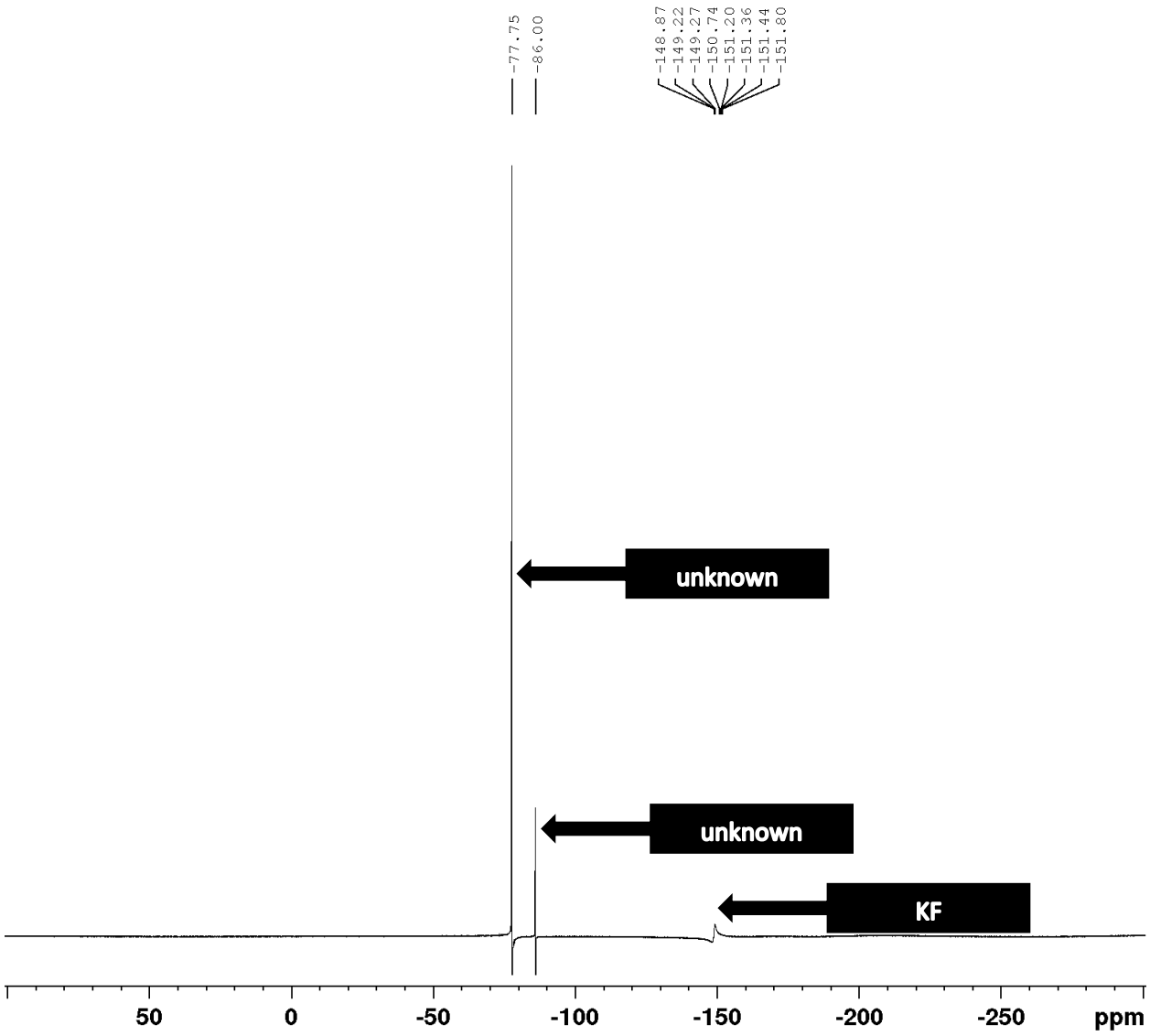

Appendix 21. HPLC-UV trace of compound 11

==== Shimadzu LabSolutions Analysis Report ====

Sample Name	: epm-3-13		
Sample ID	: October 30		
Data Filename	: epm-3-13-ms1.lcd		
Method Filename	: Emile standard.lcm		
Batch Filename	:		
Vial #	: 1-1	Sample Type	: Unknown
Injection Volume	: 1000 uL		
Date Acquired	: 30/10/2020 3:11:55 PM	Acquired by	: ShimadzuHPLC
Date Processed	: 10/12/2020 3:43:54 PM	Processed by	: ShimadzuHPLC

<PDA Chromatogram>

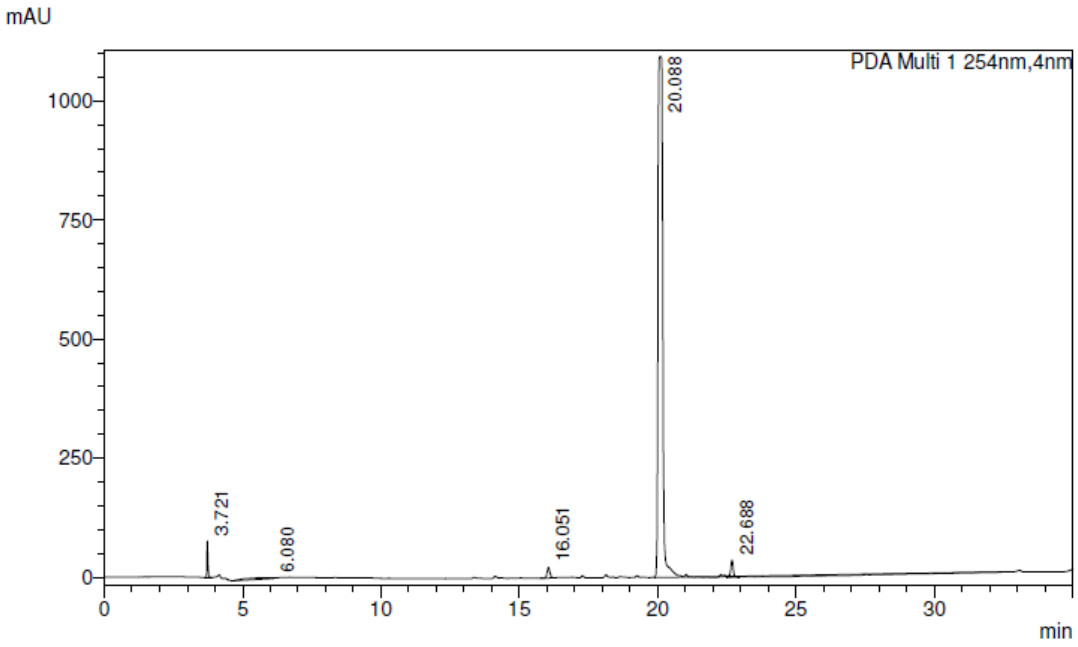

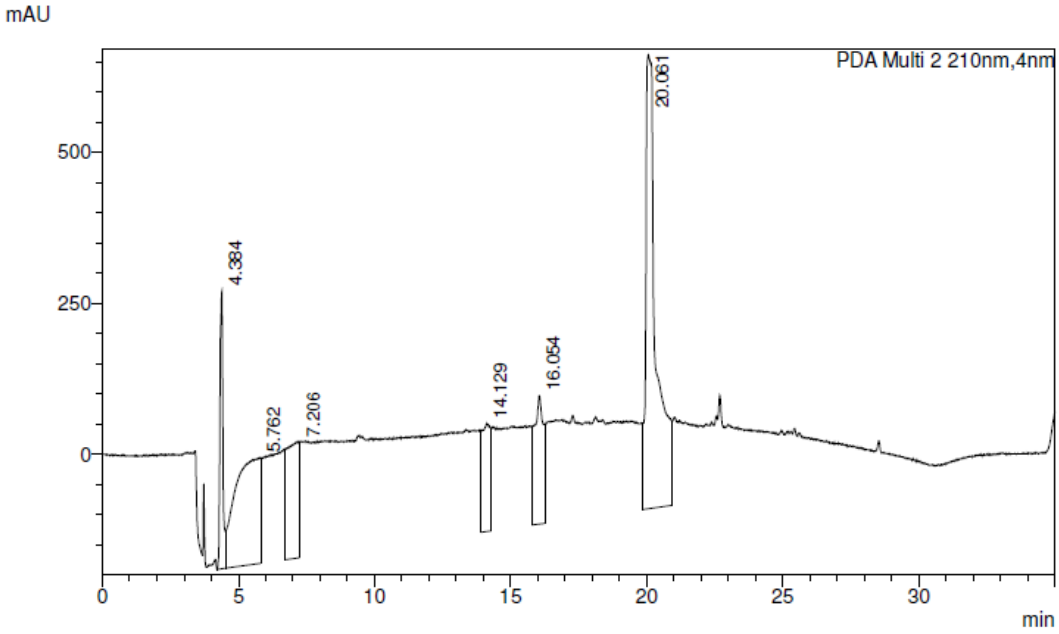

Peak Table

PDA Ch1 254nm

Peak#	Ret. Time	Area	Height	Area%
1	3.721	191973	74523	1.518
2	6.080	201775	1902	1.596
3	16.051	154693	22140	1.224
4	20.088	11862658	1094752	93.828
5	22.688	231936	35962	1.834
Total		12643034	1229279	100.000

PDA Ch2 210nm

Peak#	Ret. Time	Area	Height	Area%
1	4.384	3480685	458295	6.943
2	5.762	11173079	174722	22.286
3	7.206	6144161	192493	12.255
4	14.129	3969290	178415	7.917
5	16.054	5084434	212553	10.142
6	20.061	20282545	751962	40.457
Total		50134193	1968441	100.000

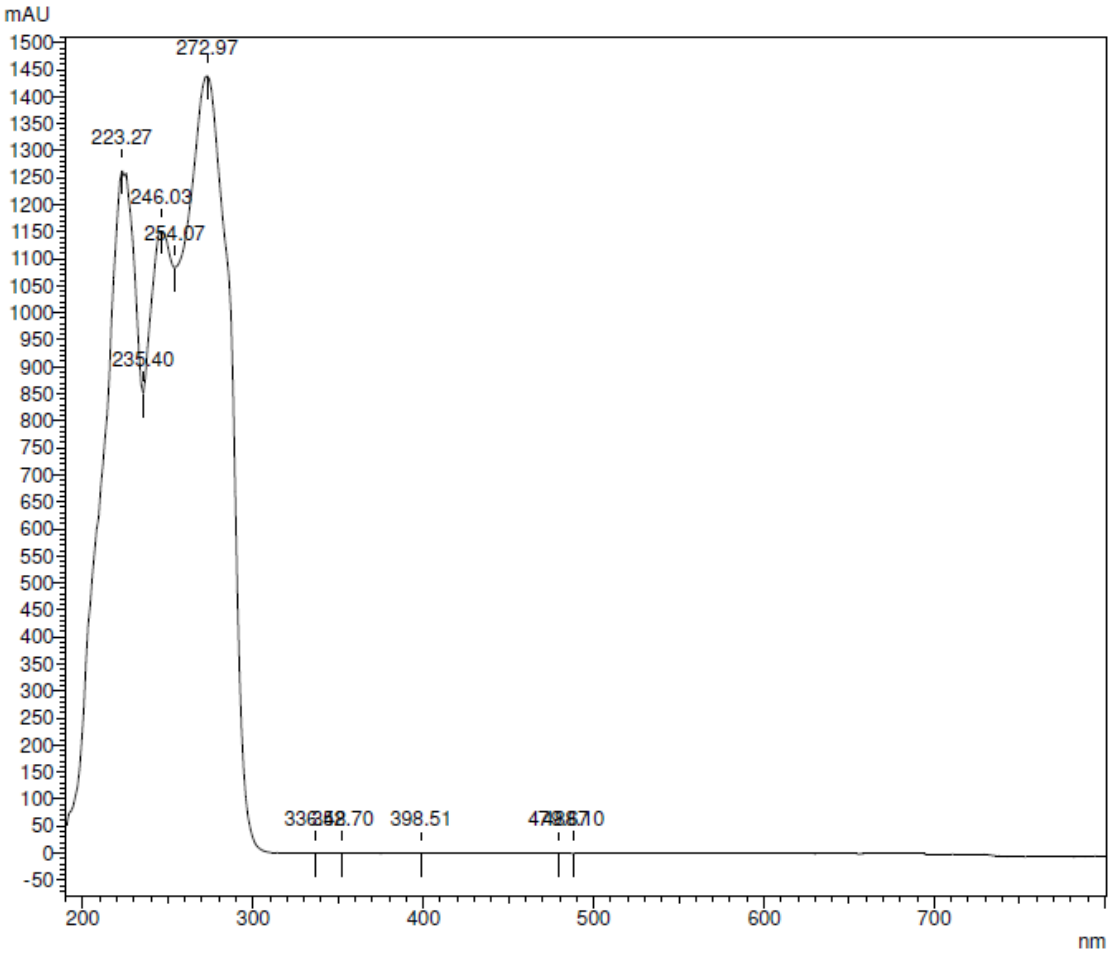
mAU
272.97
223.27
246.03
254.07
235.40
398.51
nm

Appendix 22. HPLC-UV trace of the crude reaction mixture of the fluorination of compound 11 with TBAF(Pin)$_2$ at 50 °C.

==== Shimadzu LabSolutions Analysis Report ====

Sample Name	: epm-3-30-2_2		
Sample ID	: August 18		
Data Filename	: epm-3-30-2_2.lcd		
Method Filename	: Emile standard.lcm		
Batch Filename	:		
Vial #	: 1-1	Sample Type	: Unknown
Injection Volume	: 5000 uL		
Date Acquired	: 19/08/2020 12:19:17 PM	Acquired by	: ShimadzuHPLC
Date Processed	: 19/08/2020 12:54:19 PM	Processed by	: ShimadzuHPLC

<PDA Chromatogram>

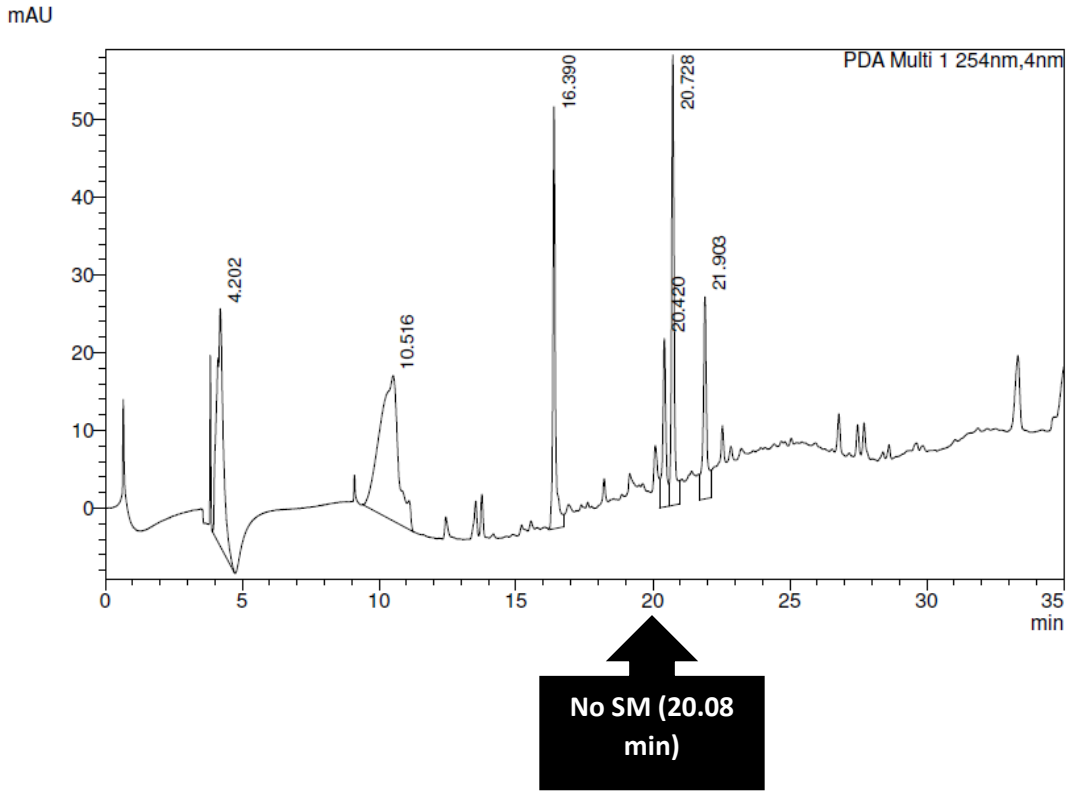

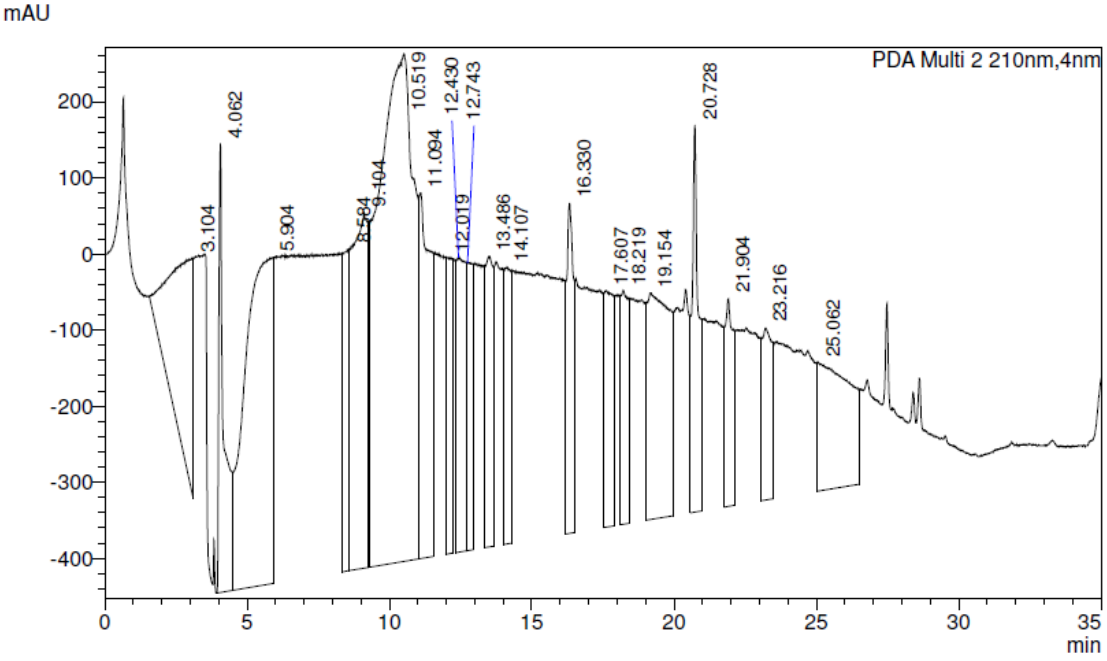

Peak Table

PDA Ch1 254nm

Peak#	Ret. Time	Area	Height	Area%
1	4.202	508986	30511	20.289
2	10.516	871538	18729	34.741
3	16.390	337653	54304	13.460
4	20.420	181323	21674	7.228
5	20.728	381162	57800	15.194
6	21.903	227996	25962	9.088
Total		2508658	208980	100.000

PDA Ch2 210nm

Peak#	Ret. Time	Area	Height	Area%
1	3.104	14853640	314188	5.954
2	4.062	7704426	590337	3.088
3	5.904	29587022	428235	11.859
4	8.584	6452216	423083	2.586
5	9.104	18023386	467082	7.224
6	10.519	57027610	667193	22.858
7	11.094	13663231	480751	5.477
8	12.019	5776551	390087	2.315
9	12.430	9370650	387150	3.756
10	12.743	5427825	378424	2.176
11	13.486	7014135	381353	2.811
12	14.107	6409501	363535	2.569
13	16.330	7339604	433443	2.942
14	17.607	6629018	311214	2.657
15	18.219	5479345	307248	2.196
16	19.154	16423155	297697	6.583
17	20.728	7976055	507759	3.197
18	21.904	5616961	272759	2.251
19	23.216	5475283	226281	2.195
20	25.062	13231485	169343	5.304

Appendix 23. HPLC-UV trace of the crude reaction mixture of the fluorination of compound 11 with TBAF(Pin)$_2$ at 80 °C.

SHIMADZU LabSolutions **Analysis Report**

<Sample Information>

Sample Name	: epm-5-11		
Sample ID	: July 07		
Data Filename	: epm-5-11.lcd		
Method Filename	: Emile standard.lcm		
Batch Filename	:		
Vial #	: 1-1	Sample Type	: Unknown
Injection Volume	: 1000 uL		
Date Acquired	: 06/07/2021 9:47:43 AM	Acquired by	: ShimadzuHPLC
Date Processed	: 06/07/2021 10:22:46 AM	Processed by	: ShimadzuHPLC

<Chromatogram>

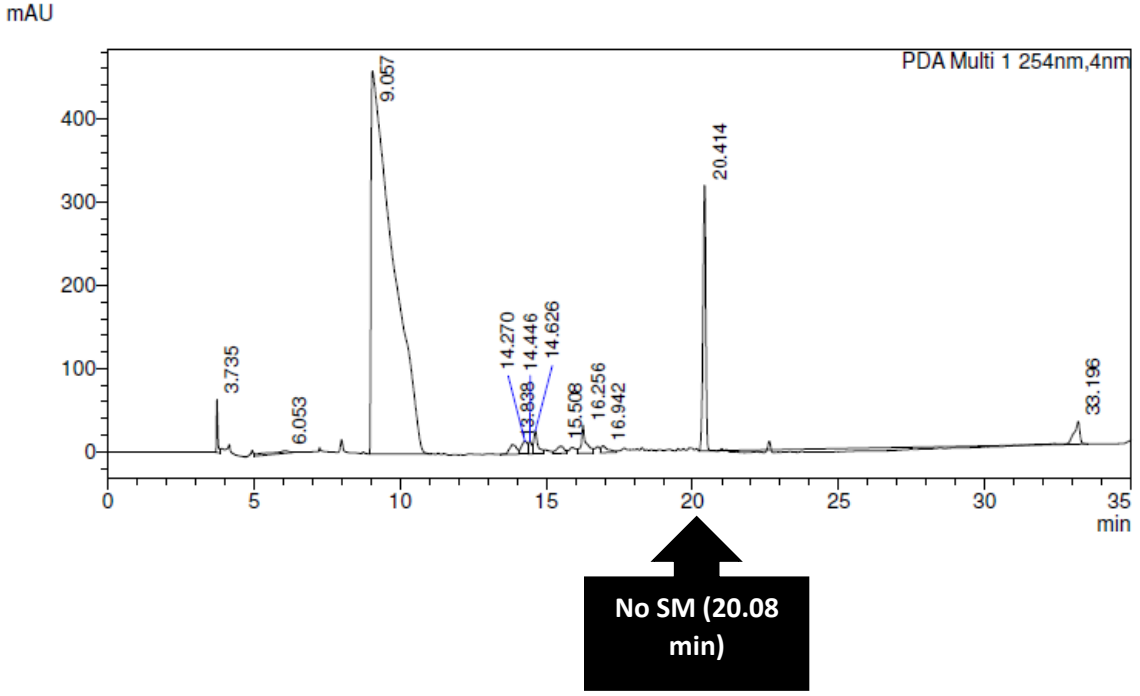

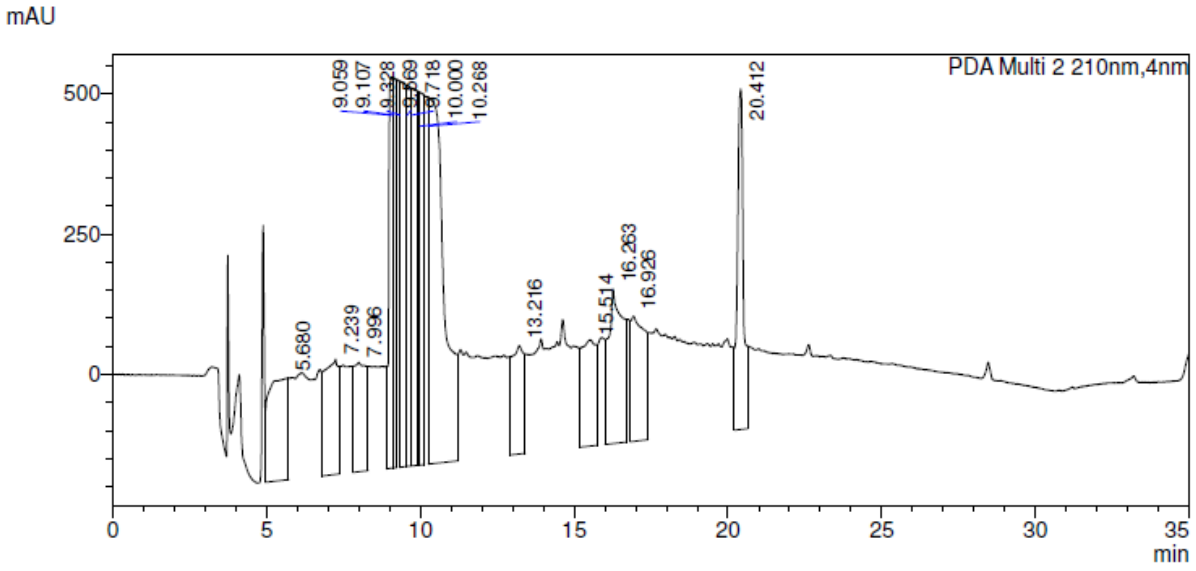
mAU
PDA Multi 2 210nm,4nm
500
250
0
9.059
9.107
9.328
9.669
9.718
10.000
10.268
20.412
5.680
7.239
7.996
13.216
15.514
16.263
16.926
0
5
10
15
20
25
30
35
min

<Peak Table>

PDA Ch1 254nm

Peak#	Ret. Time	Area	Height	Area%	Height%
1	3.735	186255	63846	0.717	6.427
2	6.053	163006	2854	0.627	0.287
3	9.057	23494161	459746	90.389	46.281
4	13.838	202800	11770	0.780	1.185
5	14.270	216121	15675	0.831	1.578
6	14.446	120039	15739	0.462	1.584
7	14.626	272949	27714	1.050	2.790
8	15.508	163464	8674	0.629	0.873
9	16.256	372330	33380	1.432	3.360
10	16.942	144258	8329	0.555	0.838
11	20.414	287954	318622	1.108	32.075
12	33.196	368887	27029	1.419	2.721
Total		25992224	993379	100.000	100.000

PDA Ch2 210nm

Peak#	Ret. Time	Area	Height	Area%	Height%
1	5.680	7891918	180875	6.571	2.652
2	7.239	6583806	205177	5.482	3.008
3	7.996	5733066	194928	4.774	2.858
4	9.059	5985289	697082	4.984	10.219
5	9.107	5323976	695065	4.433	10.190
6	9.328	9197722	688288	7.658	10.091
7	9.569	6821746	680538	5.680	9.977
8	9.718	8362717	674440	6.963	9.888
9	10.000	5081091	663639	4.231	9.729
10	10.268	23140242	654189	19.267	9.591
11	13.216	5147576	192922	4.286	2.828
12	15.514	6037677	189264	5.027	2.775
13	16.263	9331029	275266	7.769	4.036
14	16.926	7229440	223078	6.019	3.270
15	20.412	8233364	606350	6.855	8.889
Total		120100659	6821103	100.000	100.000

Appendix 24. HPLC-UV trace of the crude reaction mixture of the fluorination of compound 11 with TBAF at 50 °C.

SHIMADZU LabSolutIons **Analysis Report**

<Sample Information>

Sample Name	: epm-4-7		
Sample ID	: January 27		
Data Filename	: epm-4-7.lcd		
Method Filename	: Emile standard.lcm		
Batch Filename	:		
Vial #	: 1-1	Sample Type	: Unknown
Injection Volume	: 1000 uL		
Date Acquired	: 27/01/2021 2:08:23 PM	Acquired by	: ShimadzuHPLC
Date Processed	: 03/02/2021 1:03:32 PM	Processed by	: ShimadzuHPLC

<Chromatogram>

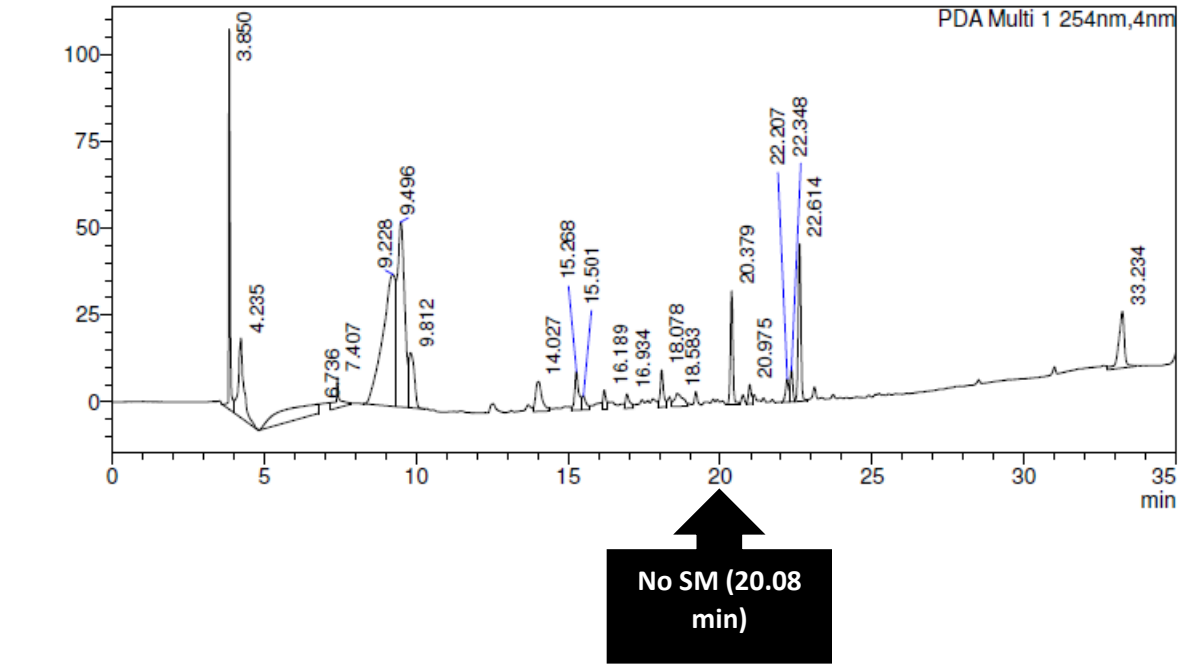

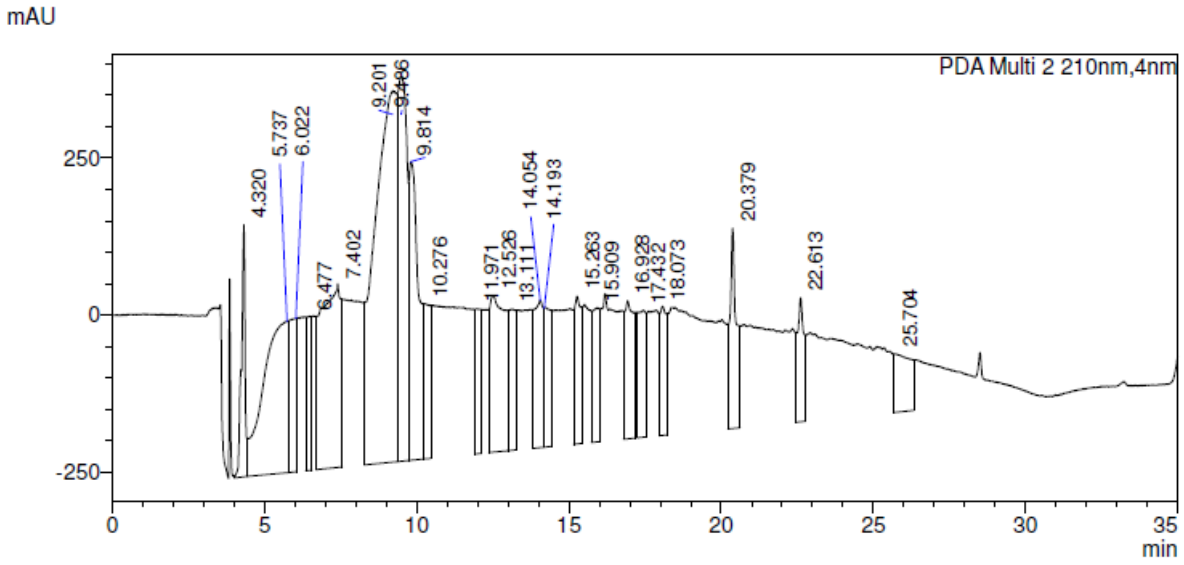

<Peak Table>

PDA Ch1 254nm

Peak#	Ret. Time	Area	Height	Area%	Height%
1	3.850	325768	106611	7.193	25.948
2	4.235	282284	22837	6.232	5.558
3	6.736	348785	2699	7.701	0.657
4	7.407	74643	8736	1.648	2.126
5	9.228	1114103	37984	24.598	9.245
6	9.496	881288	53215	19.458	12.952
7	9.812	203724	15857	4.498	3.859
8	14.027	123871	8523	2.735	2.074
9	15.268	102645	11077	2.266	2.696
10	15.501	37774	4081	0.834	0.993
11	16.189	39093	5423	0.863	1.320
12	16.934	38772	4069	0.856	0.990
13	18.078	80032	10624	1.767	2.586
14	18.583	71981	3780	1.589	0.920
15	20.379	186429	32455	4.116	7.899
16	20.975	35520	5493	0.784	1.337
17	22.207	44585	6617	0.984	1.610
18	22.348	54833	9117	1.211	2.219
19	22.614	270932	45346	5.982	11.037
20	33.234	212192	16313	4.685	3.970
Total		4529256	410857	100.000	100.000

PDA Ch2 210nm

Peak#	Ret. Time	Area	Height	Area%	Height%
1	4.320	3309720	399917	2.262	6.459
2	5.737	13437767	241365	9.182	3.898
3	6.022	3615366	244094	2.470	3.943
4	6.477	2936031	245447	2.006	3.964
5	7.402	13830273	291736	9.450	4.712
6	9.201	29653409	590464	20.262	9.537
7	9.486	12566819	611800	8.587	9.882
8	9.814	10708290	474907	7.317	7.671
9	10.276	3410524	247181	2.330	3.992
10	11.971	2869464	230590	1.961	3.724
11	12.526	8709040	248880	5.951	4.020
12	13.111	3644673	224846	2.490	3.632
13	14.054	5083329	234579	3.473	3.789
14	14.193	3472653	222241	2.373	3.590
15	15.263	3634891	234779	2.484	3.792
16	15.909	3446651	212844	2.355	3.438
17	16.928	4936598	219825	3.373	3.551
18	17.432	3263316	202136	2.230	3.265
19	18.073	2855754	205484	1.951	3.319
20	20.379	4694523	318045	3.208	5.137
21	22.613	2944819	197119	2.012	3.184
22	25.704	3325336	93044	2.272	1.503
Total		146349246	6191323	100.000	100.000

Appendix 25. HPLC-UV trace of the crude reaction mixture of the fluorination of compound 11 with TBAF at 80 °C.

SHIMADZU LabSolutions **Analysis Report**

<Sample Information>

Sample Name	: epm-4-8		
Sample ID	: January 27		
Data Filename	: epm-4-8.lcd		
Method Filename	: Emile standard.lcm		
Batch Filename	:		
Vial #	: 1-1	Sample Type	: Unknown
Injection Volume	: 1000 uL		
Date Acquired	: 27/01/2021 3:25:57 PM	Acquired by	: ShimadzuHPLC
Date Processed	: 04/02/2021 10:58:10 AM	Processed by	: ShimadzuHPLC

<Chromatogram>

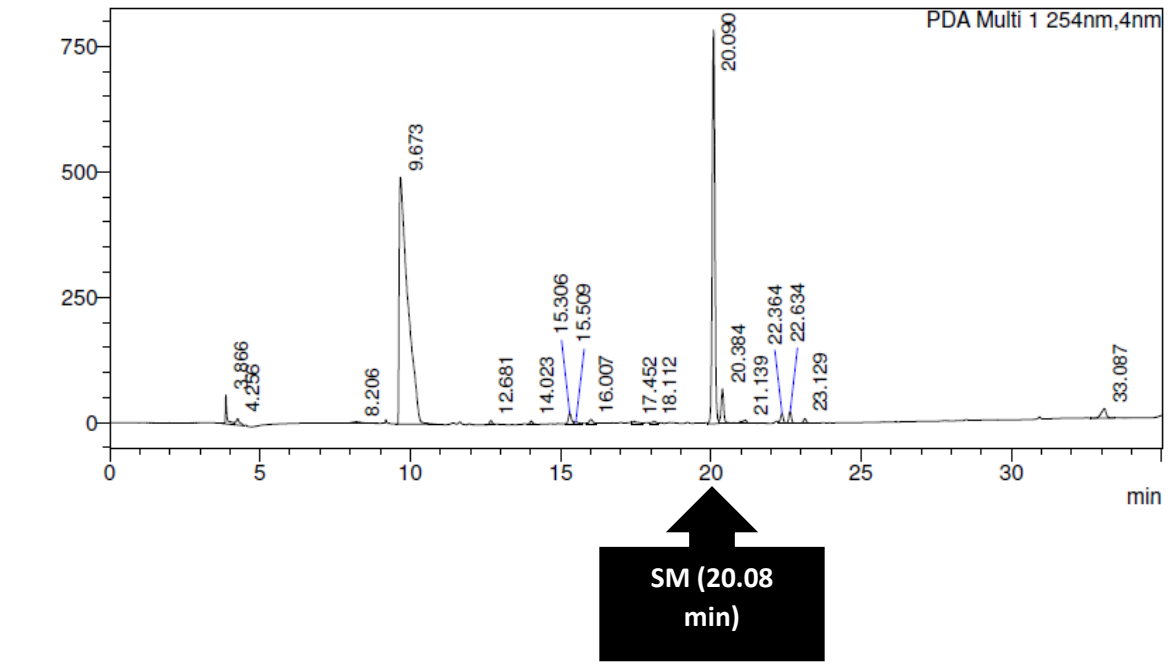

SM (20.08 min)

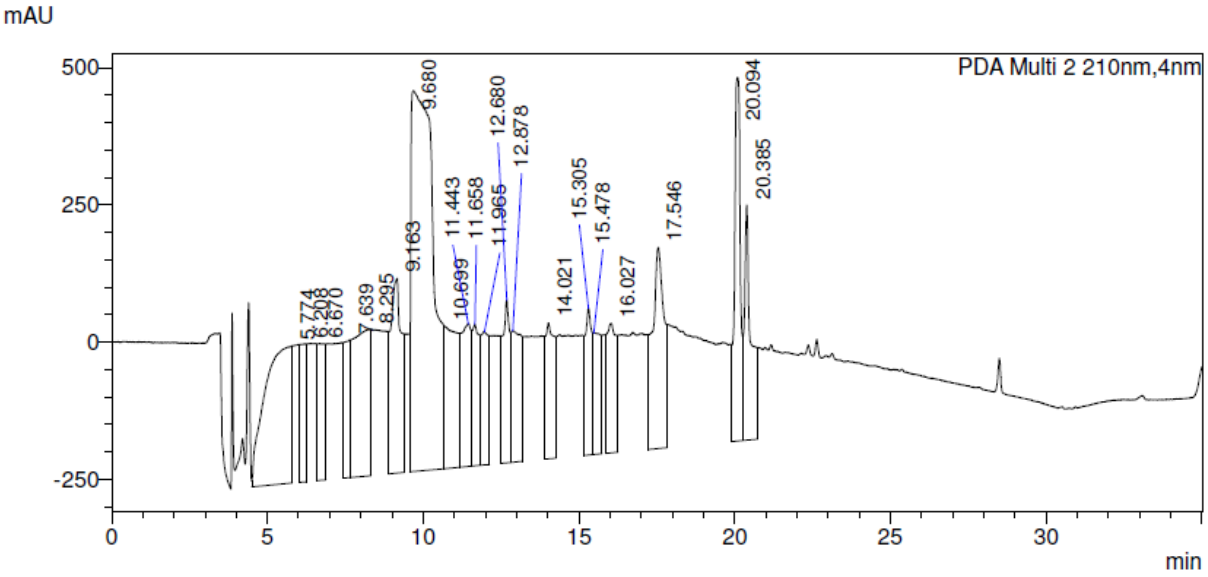

<Peak Table>

PDA Ch1 254nm

Peak#	Ret. Time	Area	Height	Area%	Height%	Area/Height
1	3.866	225195	56190	1.365	3.617	4.008
2	4.256	116497	12747	0.706	0.821	9.139
3	8.206	90493	3089	0.548	0.199	29.299
4	9.673	9710758	491318	58.846	31.628	19.765
5	12.681	54416	8421	0.330	0.542	6.462
6	14.023	51377	7138	0.311	0.459	7.198
7	15.306	165414	22208	1.002	1.430	7.448
8	15.509	51777	4382	0.314	0.282	11.817
9	16.007	93695	9759	0.568	0.628	9.601
10	17.452	75210	5836	0.456	0.376	12.888
11	18.112	59039	5553	0.358	0.357	10.631
12	20.090	4758163	781238	28.834	50.291	6.091
13	20.384	453124	68912	2.746	4.436	6.575
14	21.139	58781	6299	0.356	0.406	9.332
15	22.364	121520	19373	0.736	1.247	6.273
16	22.634	137178	23261	0.831	1.497	5.897
17	23.129	59149	8939	0.358	0.575	6.617
18	33.087	220229	18763	1.335	1.208	11.738
Total		16502015	1553425	100.000	100.000	

PDA Ch2 210nm

Peak#	Ret. Time	Area	Height	Area%	Height%	Area/Height
1	5.774	14687320	250248	9.540	3.969	58.691
2	6.208	3613829	250989	2.347	3.981	14.398
3	6.670	4174327	249493	2.711	3.957	16.731
4	7.639	3818464	250985	2.480	3.980	15.214
5	8.295	10225807	266996	6.642	4.234	38.299
6	9.163	8691064	355016	5.645	5.630	24.481
7	9.680	34595616	693957	22.470	11.006	49.853
8	10.699	7441719	259531	4.833	4.116	28.674
9	11.443	5902102	260372	3.833	4.129	22.668
10	11.658	4132013	257863	2.684	4.090	16.024
11	11.965	4120737	243186	2.676	3.857	16.945
12	12.680	4512964	296808	2.931	4.707	15.205
13	12.878	5283111	239695	3.431	3.801	22.041
14	14.021	5061086	247921	3.287	3.932	20.414
15	15.305	3886696	268024	2.524	4.251	14.501
16	15.478	3897517	222093	2.531	3.522	17.549
17	16.027	5118754	236363	3.325	3.749	21.656
18	17.546	9686182	365826	6.291	5.802	26.478
19	20.094	8644525	662461	5.615	10.506	13.049
20	20.385	6469184	427634	4.202	6.782	15.128
Total		153963019	6305461	100.000	100.000	

Appendix 26. HPLC-UV trace of the crude reaction mixture of the fluorination of compound 11 with TBAF at 110 °C.

SHIMADZU LabSolutions Analysis Report

<Sample Information>

Sample Name	: epm-4-8b		
Sample ID	: January 27		
Data Filename	: epm-4-8b1.lcd		
Method Filename	: Emile standard.lcm		
Batch Filename	:		
Vial #	: 1-1	Sample Type	: Unknown
Injection Volume	: 1000 uL		
Date Acquired	: 27/01/2021 4:39:15 PM	Acquired by	: ShimadzuHPLC
Date Processed	: 04/02/2021 11:01:04 AM	Processed by	: ShimadzuHPLC

<Chromatogram>

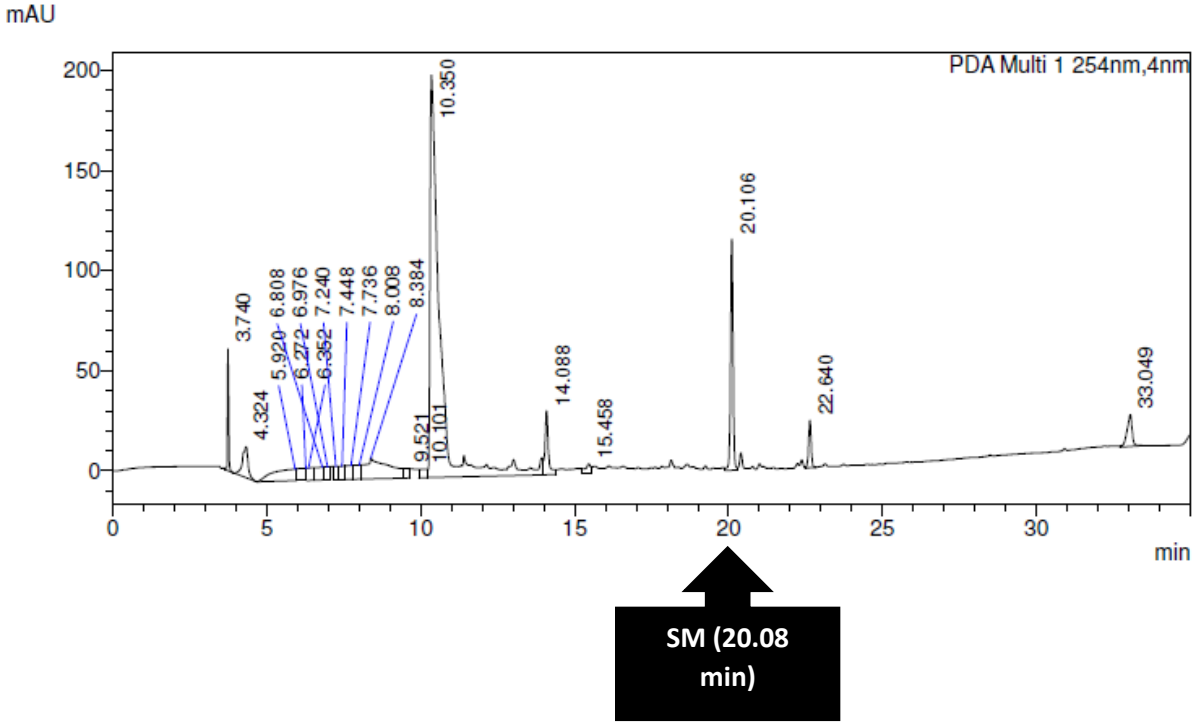

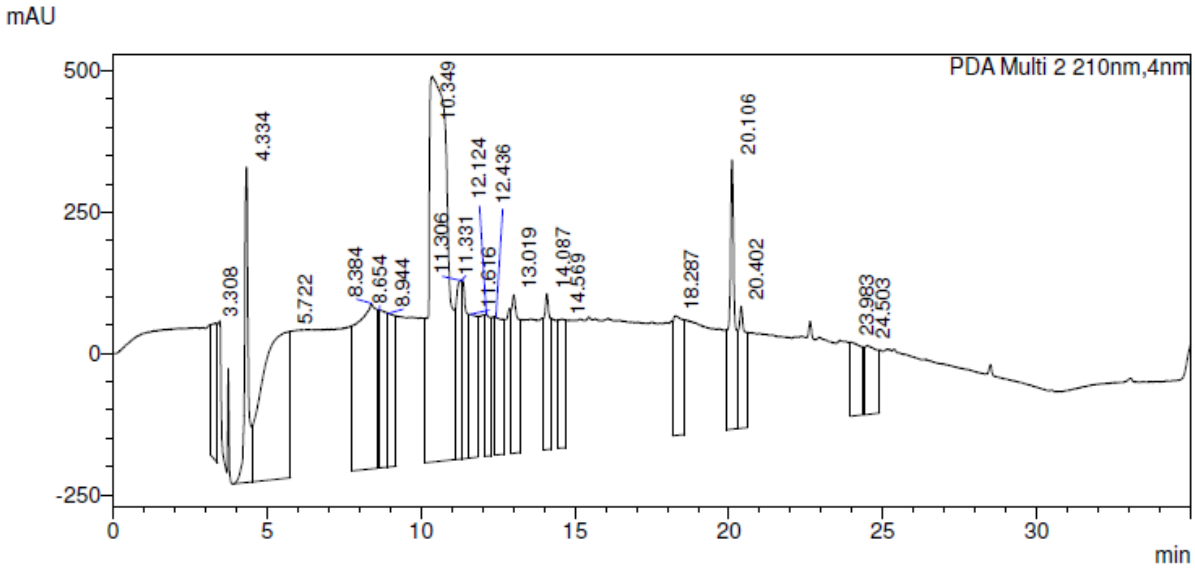

<Peak Table>

PDA Ch1 254nm

Peak#	Ret. Time	Area	Height	Area%	Height%	Area/Height
1	3.740	158963	59741	2.068	10.955	2.661
2	4.324	197507	15365	2.569	2.817	12.854
3	5.920	314138	5851	4.086	1.073	53.690
4	6.272	118642	6169	1.543	1.131	19.233
5	6.352	95836	6225	1.247	1.142	15.395
6	6.808	116537	6474	1.516	1.187	18.002
7	6.976	75098	6553	0.977	1.202	11.460
8	7.240	70218	6657	0.913	1.221	10.548
9	7.448	80958	6781	1.053	1.243	11.939
10	7.736	99206	6949	1.291	1.274	14.276
11	8.008	125282	7126	1.630	1.307	17.580
12	8.384	568297	10660	7.393	1.955	53.313
13	9.521	60578	4755	0.788	0.872	12.741
14	10.101	67817	4195	0.882	0.769	16.166
15	10.350	4246755	200900	55.243	36.839	21.139
16	14.088	245399	31793	3.192	5.830	7.719
17	15.458	67188	4847	0.874	0.889	13.862
18	20.106	655724	114856	8.530	21.061	5.709
19	22.640	139760	23618	1.818	4.331	5.918
20	33.049	183507	15834	2.387	2.904	11.589
Total		7687411	545349	100.000	100.000	

PDA Ch2 210nm

Peak#	Ret. Time	Area	Height	Area%	Height%	Area/Height
1	3.308	3321681	241447	2.621	4.093	13.757
2	4.334	4630192	557627	3.653	9.452	8.303
3	5.722	15950731	258943	12.585	4.389	61.599
4	8.384	13728627	292813	10.831	4.963	46.885
5	8.654	4764658	279255	3.759	4.734	17.062
6	8.944	4248831	271493	3.352	4.602	15.650
7	10.349	29147407	680955	22.996	11.543	42.804
8	11.306	4020298	315186	3.172	5.343	12.755
9	11.331	4137675	315987	3.264	5.356	13.094
10	11.616	3983602	253857	3.143	4.303	15.692
11	12.124	3325571	251346	2.624	4.261	13.231
12	12.436	3925019	243718	3.097	4.131	16.105
13	13.019	4629541	279691	3.653	4.741	16.552
14	14.087	3472043	275213	2.739	4.665	12.616
15	14.569	3263819	227652	2.575	3.859	14.337
16	18.287	4762441	211216	3.757	3.580	22.548
17	20.106	5587176	475246	4.408	8.056	11.756
18	20.402	3351075	215068	2.644	3.646	15.581
19	23.983	3078268	130858	2.429	2.218	23.524
20	24.503	3419417	121769	2.698	2.064	28.081
Total		126748072	5899340	100.000	100.000	

Appendix 27. HPLC-UV trace of the crude reaction mixture of the fluorination of compound 11 with KF/Kryptofix at 100 °C.

SHIMADZU LabSolutIons Analysis Report

<Sample Information>

Sample Name	: epm-4-15		
Sample ID	: February 2		
Data Filename	: epm-4-15.lcd		
Method Filename	: Emile standard.lcm		
Batch Filename	:		
Vial #	: 1-1	Sample Type	: Unknown
Injection Volume	: 1000 uL		
Date Acquired	: 02/02/2021 2:55:06 PM	Acquired by	: ShimadzuHPLC
Date Processed	: 04/02/2021 11:23:44 AM	Processed by	: ShimadzuHPLC

<Chromatogram>

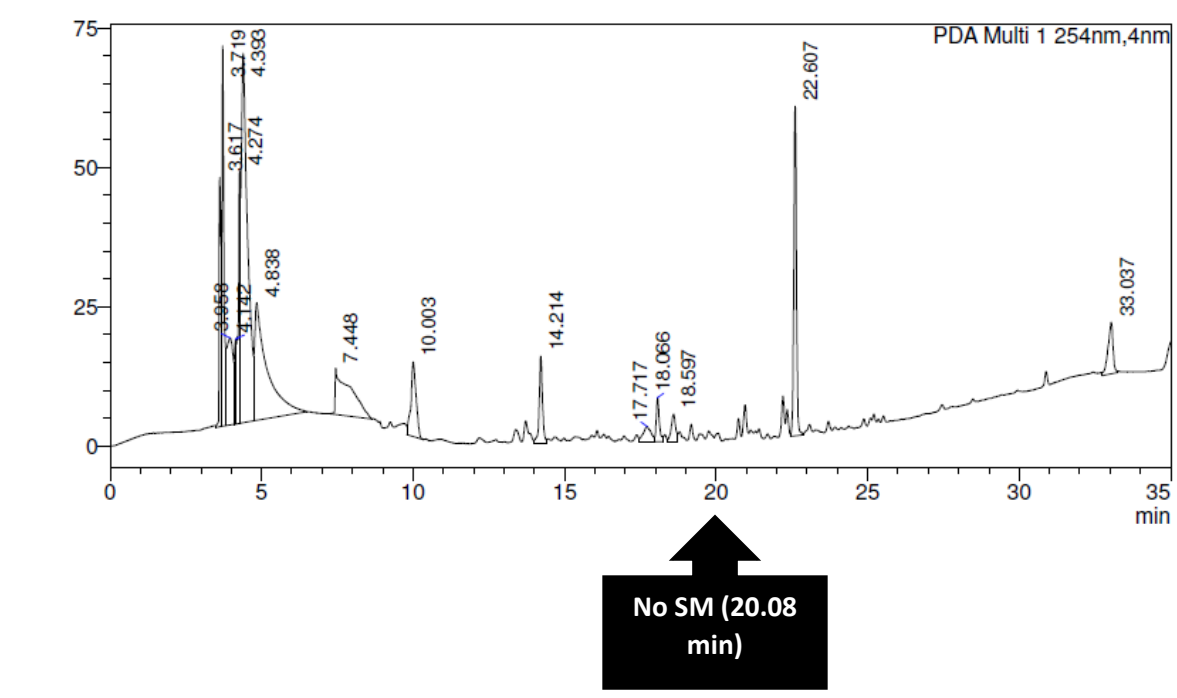

No SM (20.08 min)

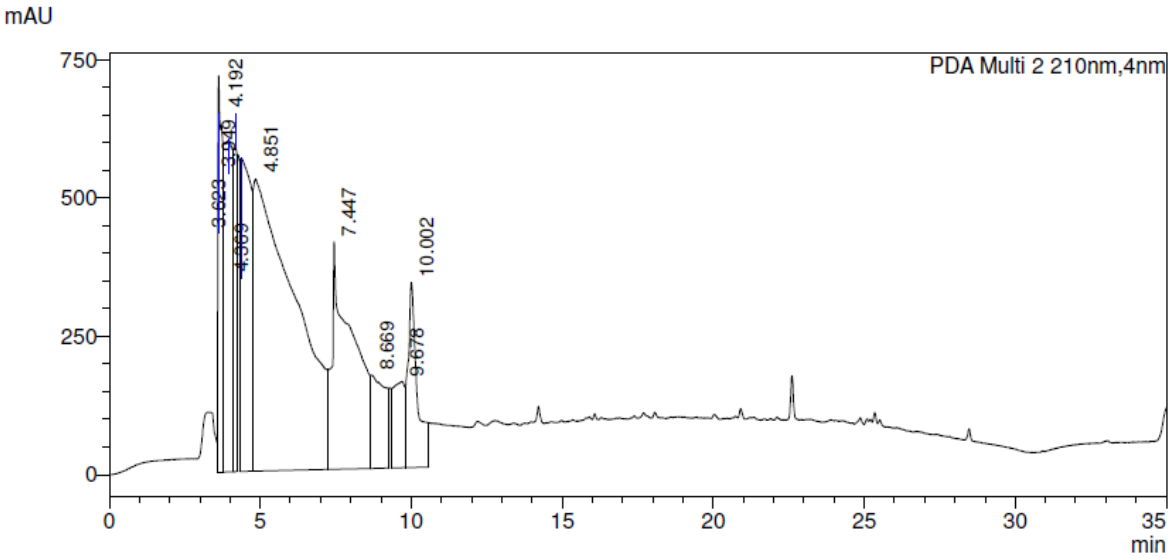
mAU
750
500
250
0
PDA Multi 2 210nm,4nm
4.192
4.851
7.447
10.002
8.669
9.678
0
5
10
15
20
25
30
35
min

<Peak Table>

PDA Ch1 254nm

Peak#	Ret. Time	Area	Height	Area%	Height%	Area/Height
1	3.617	184522	44363	4.883	11.174	4.159
2	3.719	328539	68173	8.695	17.170	4.819
3	3.958	212406	15644	5.621	3.940	13.578
4	4.142	66944	15283	1.772	3.849	4.380
5	4.274	222807	45071	5.897	11.352	4.943
6	4.393	960976	66291	25.432	16.696	14.496
7	4.838	617214	21121	16.335	5.320	29.222
8	7.448	288540	8317	7.636	2.095	34.692
9	10.003	160479	13323	4.247	3.356	12.045
10	14.214	117091	15586	3.099	3.926	7.513
11	17.717	50319	2765	1.332	0.696	18.200
12	18.066	55454	7869	1.468	1.982	7.047
13	18.597	50099	4908	1.326	1.236	10.209
14	22.607	356281	59080	9.429	14.880	6.031
15	33.037	106865	9244	2.828	2.328	11.561
Total		3778536	397037	100.000	100.000	

PDA Ch2 210nm

Peak#	Ret. Time	Area	Height	Area%	Height%	Area/Height
1	3.623	7150561	715136	5.698	17.605	9.999
2	3.949	12224610	599912	9.741	14.769	20.377
3	4.192	4178473	584483	3.329	14.389	7.149
4	4.369	14071227	565802	11.212	13.929	24.870
5	4.851	50677373	527710	40.380	12.991	96.033
6	7.447	20131759	411005	16.041	10.118	48.982
7	8.669	5554805	168594	4.426	4.150	32.948
8	9.678	4176323	155522	3.328	3.829	26.854
9	10.002	7337242	333888	5.846	8.220	21.975
Total		125502373	4062052	100.000	100.000	

Appendix 28. HPLC-UV trace of the crude reaction mixture of the fluorination of compound 11 with KF/Kryptofix at 120 °C.

SHIMADZU LabSolutions Analysis Report

<Sample Information>

Sample Name	: epm-4-16		
Sample ID	: February 2		
Data Filename	: epm-4-16.lcd		
Method Filename	: Emile standard.lcm		
Batch Filename	:		
Vial #	: 1-1	Sample Type	: Unknown
Injection Volume	: 1000 uL		
Date Acquired	: 02/02/2021 3:32:50 PM	Acquired by	: ShimadzuHPLC
Date Processed	: 04/02/2021 11:25:22 AM	Processed by	: ShimadzuHPLC

<Chromatogram>

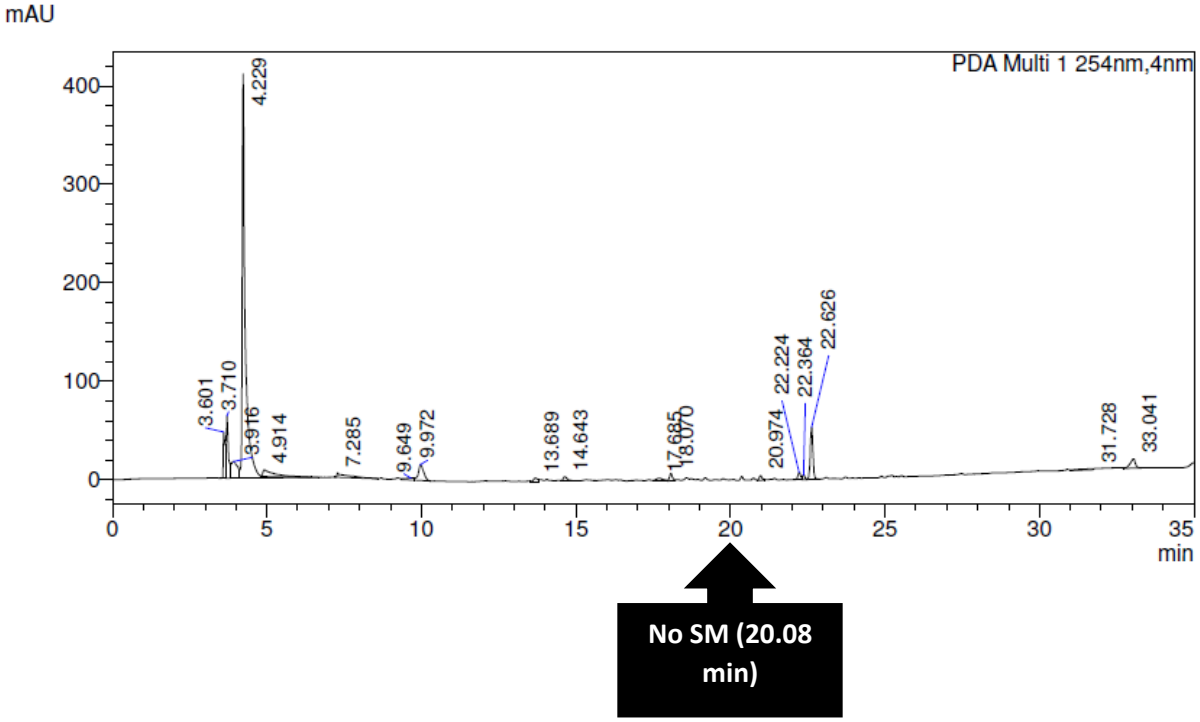

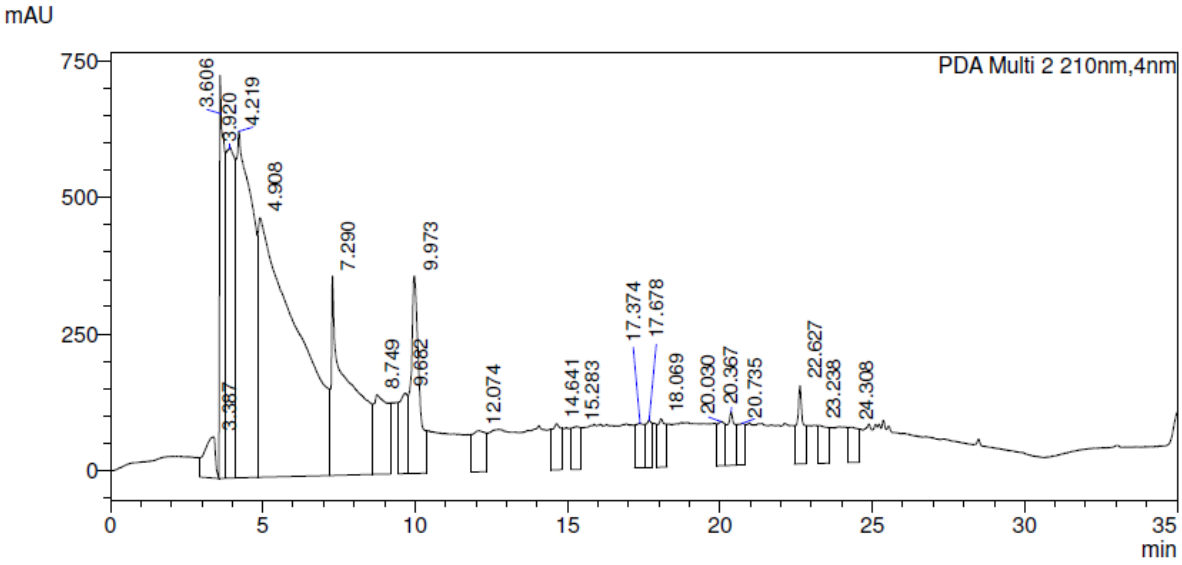

<Peak Table>

PDA Ch1 254nm

Peak#	Ret. Time	Area	Height	Area%	Height%	Area/Height
1	3.601	186017	46339	3.805	6.991	4.014
2	3.710	342134	63207	6.999	9.536	5.413
3	3.916	235425	16816	4.816	2.537	14.000
4	4.229	2851879	408076	58.339	61.568	6.989
5	4.914	176168	6603	3.604	0.996	26.680
6	7.285	111495	4585	2.281	0.692	24.316
7	9.649	38920	2151	0.796	0.325	18.093
8	9.972	193591	16029	3.960	2.418	12.078
9	13.689	33331	3449	0.682	0.520	9.665
10	14.643	50346	4743	1.030	0.716	10.615
11	17.685	44070	2569	0.902	0.388	17.156
12	18.070	51537	7541	1.054	1.138	6.834
13	20.974	30469	4733	0.623	0.714	6.437
14	22.224	46599	7541	0.953	1.138	6.179
15	22.364	28792	5028	0.589	0.759	5.727
16	22.626	318036	52833	6.506	7.971	6.020
17	31.728	38172	1075	0.781	0.162	35.510
18	33.041	111482	9485	2.281	1.431	11.753
Total		4888465	662803	100.000	100.000	

PDA Ch2 210nm

Peak#	Ret. Time	Area	Height	Area%	Height%	Area/Height
1	3.387	1883851	75424	1.398	1.651	24.977
2	3.606	8344495	735672	6.192	16.103	11.343
3	3.920	11442769	604498	8.491	13.232	18.929
4	4.219	23188341	633939	17.207	13.876	36.578
5	4.908	41959383	474406	31.136	10.384	88.446
6	7.290	14530931	363209	10.783	7.950	40.007
7	8.749	4725624	145664	3.507	3.188	32.442
8	9.682	2755554	147032	2.045	3.218	18.741
9	9.973	6688431	361283	4.963	7.908	18.513
10	12.074	2086920	75029	1.549	1.642	27.815
11	14.641	1727607	84272	1.282	1.845	20.500
12	15.283	1515270	78507	1.124	1.718	19.301
13	17.374	1568648	81696	1.164	1.788	19.201
14	17.678	1265190	86777	0.939	1.899	14.580
15	18.069	1679845	88654	1.247	1.941	18.948
16	20.030	1318241	81154	0.978	1.776	16.244
17	20.367	1782711	98165	1.323	2.149	18.160
18	20.735	1265726	76791	0.939	1.681	16.483
19	22.627	2079748	142571	1.543	3.121	14.587
20	23.238	1472953	69140	1.093	1.513	21.304
21	24.308	1479075	64711	1.098	1.416	22.857
Total		134761313	4568591	100.000	100.000	

Appendix 29. HPLC-UV trace of compound 21 using a long method.

==== Shimadzu LabSolutions Analysis Report ====

Sample Name	: epm-3-14		
Sample ID	: July 22		
Data Filename	: epm-3-14.lcd		
Method Filename	: Emile standard.lcm		
Batch Filename	:		
Vial #	: 1-1	Sample Type	: Unknown
Injection Volume	: 1000 uL		
Date Acquired	: 22/07/2020 11:26:04 AM	Acquired by	: ShimadzuHPLC
Date Processed	: 11/12/2020 10:01:37 AM	Processed by	: ShimadzuHPLC

<PDA Chromatogram>

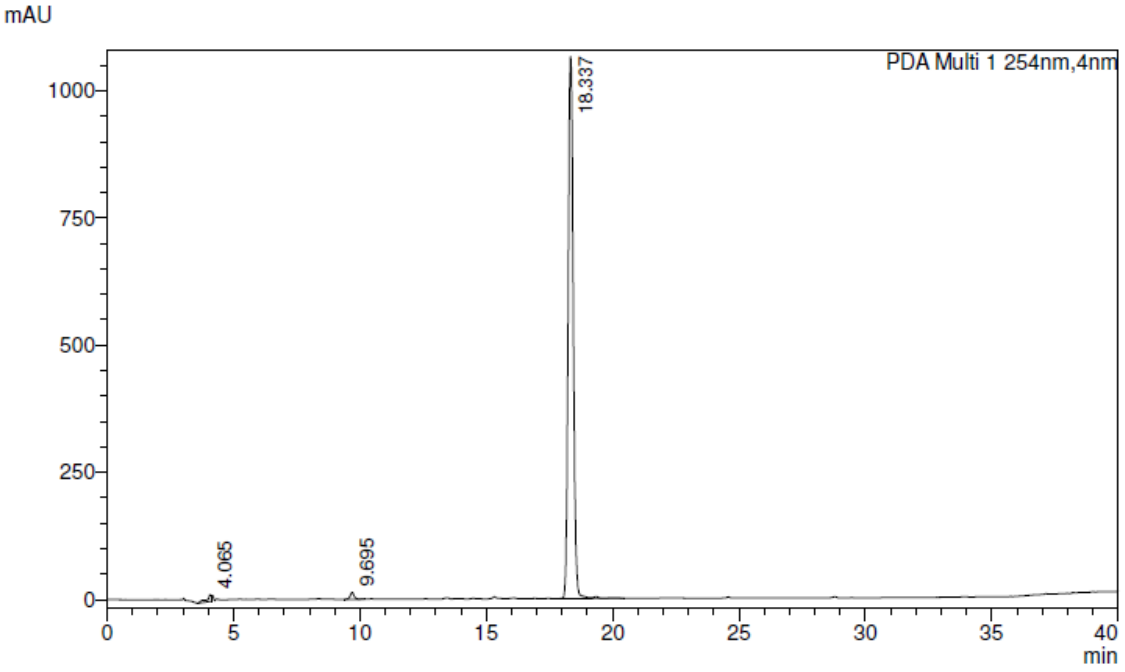

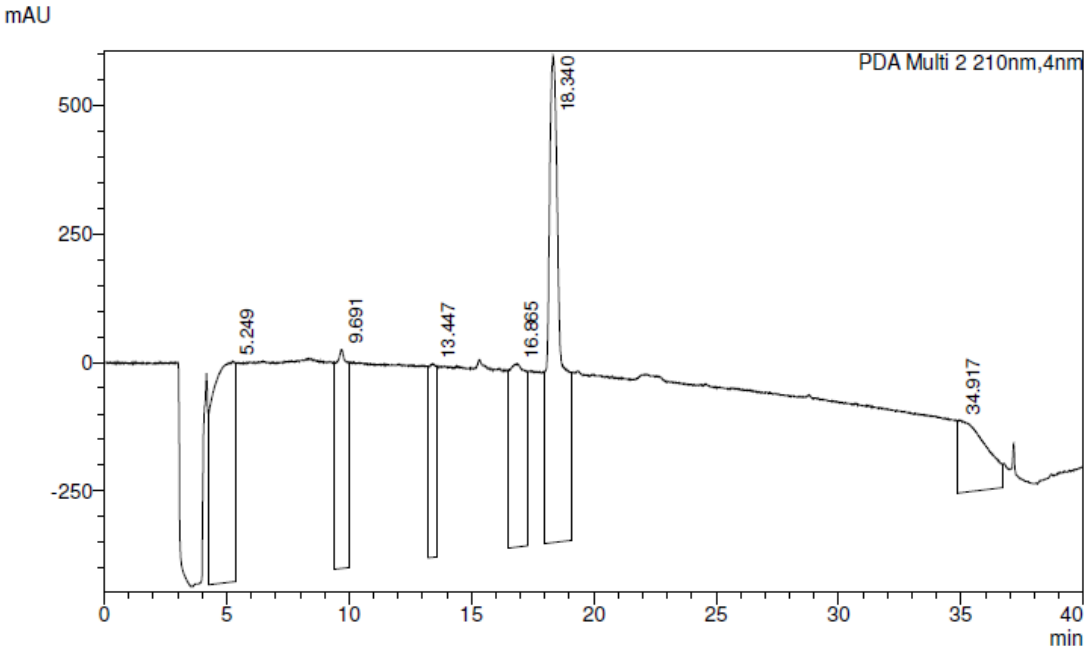

Peak Table

PDA Ch1 254nm

Peak#	Ret. Time	Area	Height	Area%
1	4.065	160342	13408	1.050
2	9.695	155978	13586	1.022
3	18.337	14952887	1064696	97.928
Total		15269207	1091690	100.000

PDA Ch2 210nm

Peak#	Ret. Time	Area	Height	Area%
1	5.249	27357245	429160	24.178
2	9.691	15065313	426067	13.315
3	13.447	8072360	375879	7.134
4	16.865	16542117	355846	14.620
5	18.340	35106989	944998	31.027
6	34.917	11004097	141182	9.725
Total		113148121	2673132	100.000

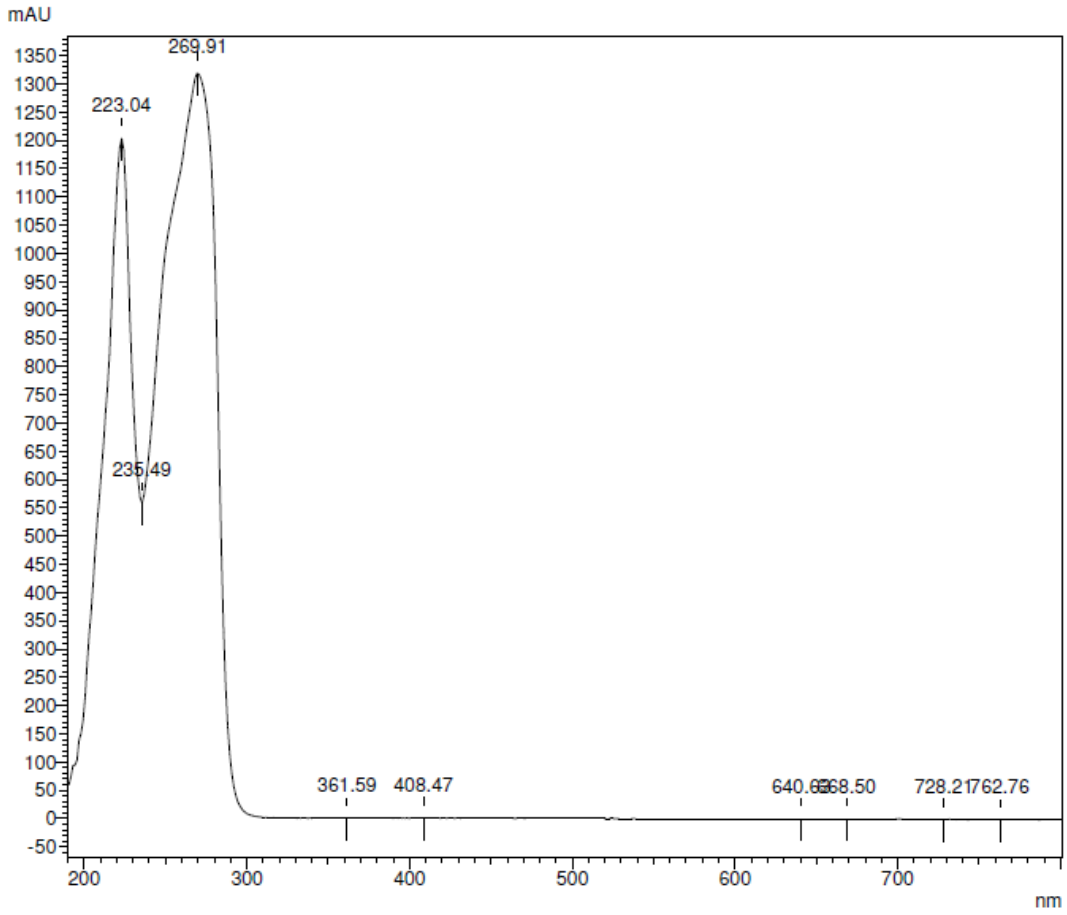
mAU
269.91
223.04
235.49
361.59
408.47
640.63
668.50
728.21
762.76
nm

Appendix 30. HPLC-UV trace of compound 21 using a short method

SHIMADZU LabSolutions **Analysis Report**

<Sample Information>

Sample Name	: epm-3-21-fast		
Sample ID	: July 29		
Data Filename	: epm-3-21-fast1.lcd		
Method Filename	: Emile standard.lcm		
Batch Filename	:		
Vial #	: 1-1	Sample Type	: Unknown
Injection Volume	: 1000 uL		
Date Acquired	: 29/07/2020 2:48:22 PM	Acquired by	: ShimadzuHPLC
Date Processed	: 29/07/2020 3:10:26 PM	Processed by	: ShimadzuHPLC

<Chromatogram>

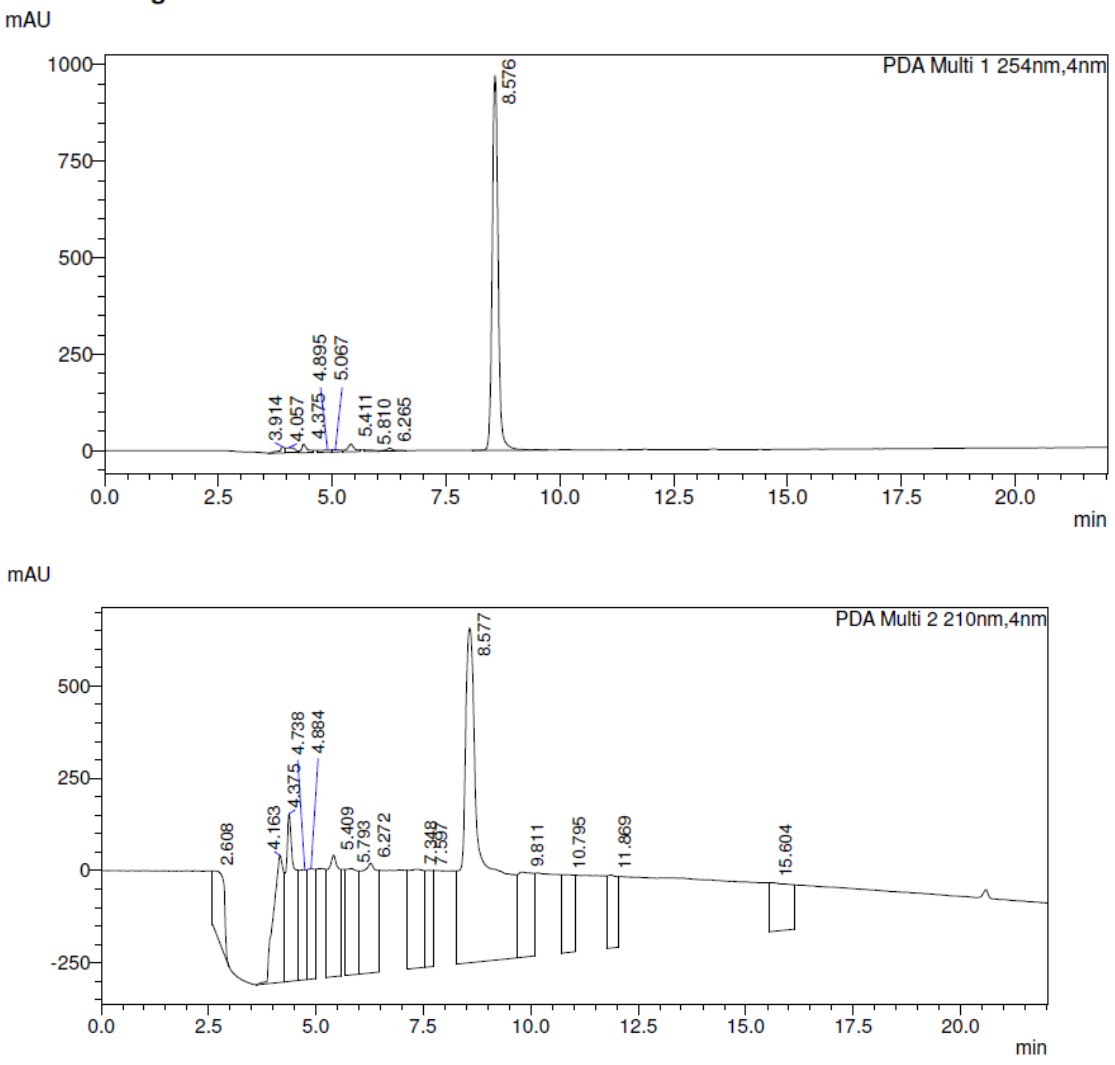

<Peak Table>

PDA Ch1 254nm

Peak#	Ret. Time	Area	Height	Area%	Height%
1	3.914	142520	16195	1.457	1.521
2	4.057	183944	13538	1.881	1.271
3	4.375	192949	21746	1.973	2.042
4	4.895	98117	5683	1.003	0.534
5	5.067	72547	5531	0.742	0.519
6	5.411	204769	20057	2.094	1.883
7	5.810	49069	3384	0.502	0.318
8	6.265	74979	6754	0.767	0.634
9	8.576	8760764	972080	89.582	91.278
Total		9779658	1064968	100.000	100.000

PDA Ch2 210nm

Peak#	Ret. Time	Area	Height	Area%	Height%
1	2.608	3125252	148760	3.165	3.187
2	4.163	5619796	343413	5.691	7.357
3	4.375	6591823	453959	6.675	9.726
4	4.738	3622140	298135	3.668	6.387
5	4.884	3433649	300060	3.477	6.428
6	5.409	6041570	329502	6.118	7.059
7	5.793	5467344	288256	5.536	6.176
8	6.272	8143578	297371	8.247	6.371
9	7.348	6301743	267521	6.381	5.731
10	7.597	3173646	261660	3.214	5.606
11	8.577	29581065	906387	29.955	19.419
12	9.811	5815431	230513	5.889	4.939
13	10.795	4030976	211854	4.082	4.539
14	11.869	3368536	197792	3.411	4.238
15	15.604	4435335	132462	4.491	2.838
Total		98751884	4667646	100.000	100.000

Appendix 31. HPLC-UV trace of the crude reaction mixture of the fluorination of compound 21 with CsF at 150 °C using the long method.

==== Shimadzu LabSolutions Analysis Report ====

Sample Name	: epm-3-14A		
Sample ID	: July 22		
Data Filename	: epm-13-4-A.lcd		
Method Filename	: Emile standard.lcm		
Batch Filename	:		
Vial #	: 1-1	Sample Type	: Unknown
Injection Volume	: 1000 uL		
Date Acquired	: 22/07/2020 4:51:33 PM	Acquired by	: ShimadzuHPLC
Date Processed	: 11/12/2020 11:32:18 AM	Processed by	: ShimadzuHPLC

<PDA Chromatogram>

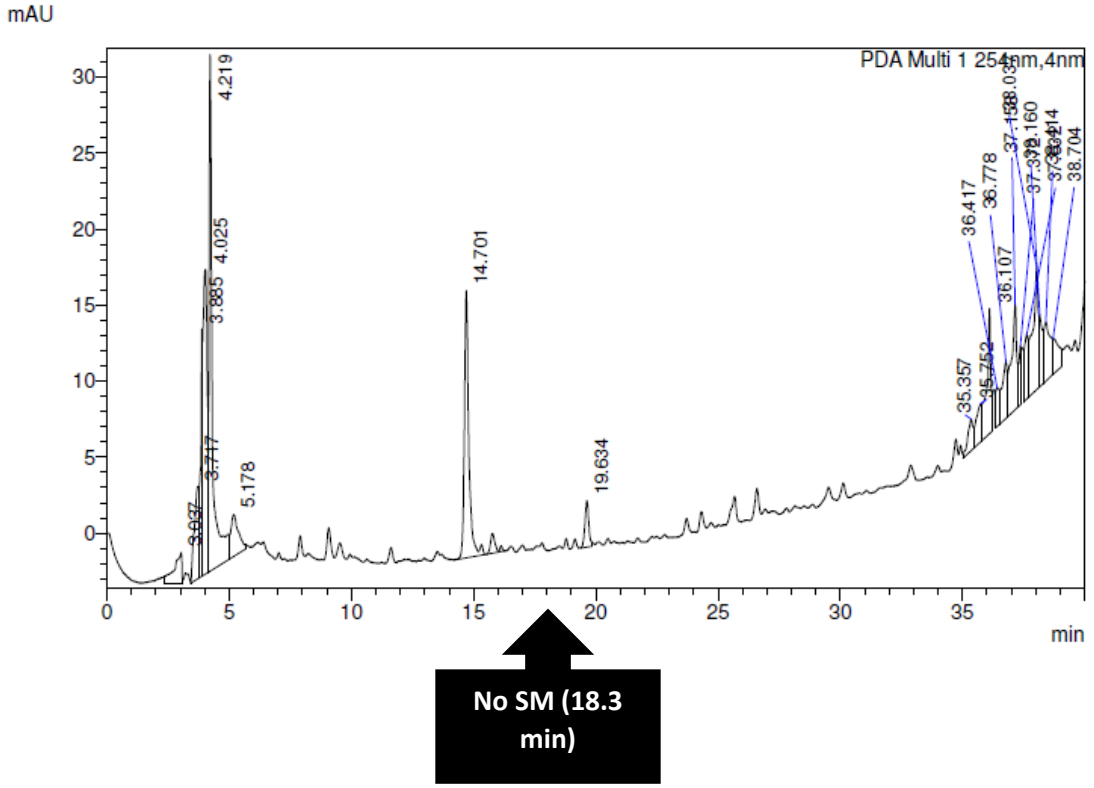

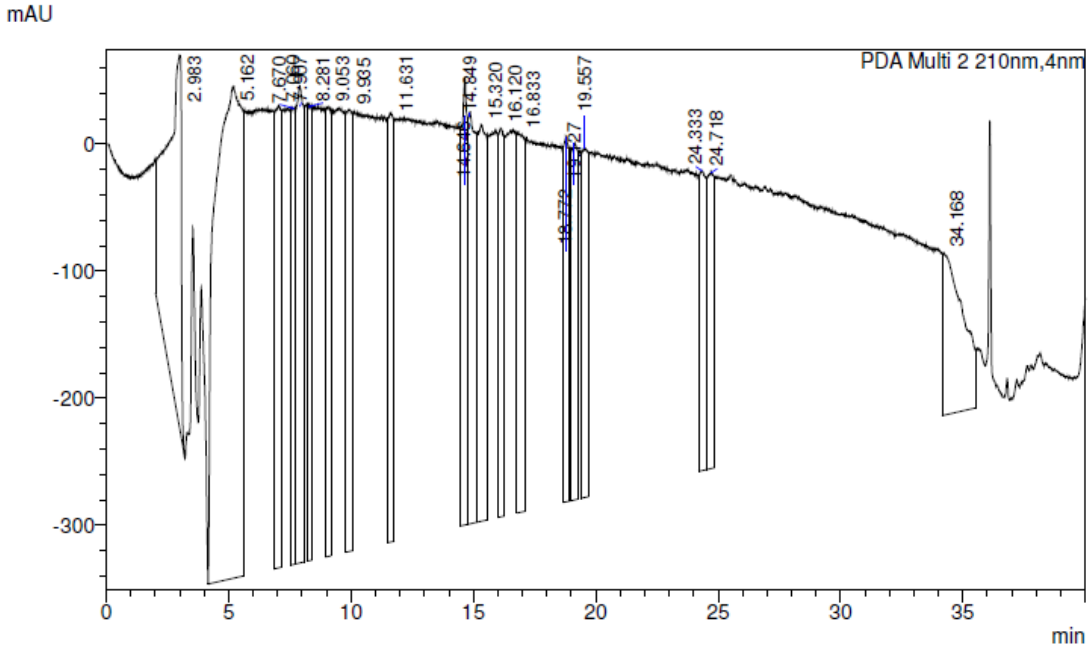
mAU
PDA Multi 2 210nm,4nm
2.983
5.162
7.670
8.281
9.053
9.985
11.631
14.849
15.320
16.120
16.833
19.557
24.333
24.718
34.168
0
-100
-200
-300
0
5
10
15
20
25
30
35
min

Peak Table

PDA Ch1 254nm

Peak#	Ret. Time	Area	Height	Area%
1	3.037	43653	2019	2.447
2	3.717	78290	6074	4.389
3	3.885	86968	16216	4.875
4	4.025	233130	20047	13.068
5	4.219	323778	33851	18.150
6	5.178	59200	2759	3.319
7	14.701	217179	17562	12.174
8	19.634	32955	3048	1.847
9	35.357	30913	2082	1.733
10	35.752	38863	2513	2.178
11	36.107	95878	8181	5.375
12	36.417	24518	2553	1.374
13	36.778	55943	3726	3.136
14	37.158	105822	6932	5.932
15	37.372	27663	3873	1.551
16	37.632	46603	4222	2.612
17	38.037	127351	8075	7.139
18	38.160	41417	4719	2.322
19	38.414	74036	3874	4.150
20	38.704	39777	2359	2.230
Total		1783938	154684	100.000

PDA Ch2 210nm

Peak#	Ret. Time	Area	Height	Area%
1	2.983	12062606	292280	8.318
2	5.162	28841681	386671	19.890
3	7.060	7278741	362967	5.019
4	7.670	4474876	358870	3.086
5	7.907	7888779	375356	5.440
6	8.281	4638881	358386	3.199
7	9.053	5409419	353337	3.730
8	9.935	6319035	347817	4.358
9	11.631	5467854	337473	3.771
10	14.646	6129935	351795	4.227
11	14.849	7367187	323813	5.080
12	15.320	7363394	312059	5.078
13	16.120	4933835	305585	3.402
14	16.833	5832962	298785	4.022
15	18.772	4732493	286448	3.264
16	19.127	4660086	279950	3.214
17	19.557	5239143	274534	3.613
18	24.333	4368642	235966	3.013
19	24.718	4656723	232657	3.211
20	34.168	7343212	127658	5.064
Total		145009483	6202406	100.000

Appendix 32. HPLC-UV trace of the crude reaction mixture of the fluorination of compound 21 with CsF at 90 °C using the long method.

==== Shimadzu LabSolutions Analysis Report ====

Sample Name	: epm-3-15conc		
Sample ID	: July 23		
Data Filename	: epm-3-15conc.lcd		
Method Filename	: Emile standard.lcm		
Batch Filename	:		
Vial #	: 1-1	Sample Type	: Unknown
Injection Volume	: 1000 uL		
Date Acquired	: 23/07/2020 3:45:11 PM	Acquired by	: ShimadzuHPLC
Date Processed	: 23/07/2020 4:25:13 PM	Processed by	: ShimadzuHPLC

<PDA Chromatogram>

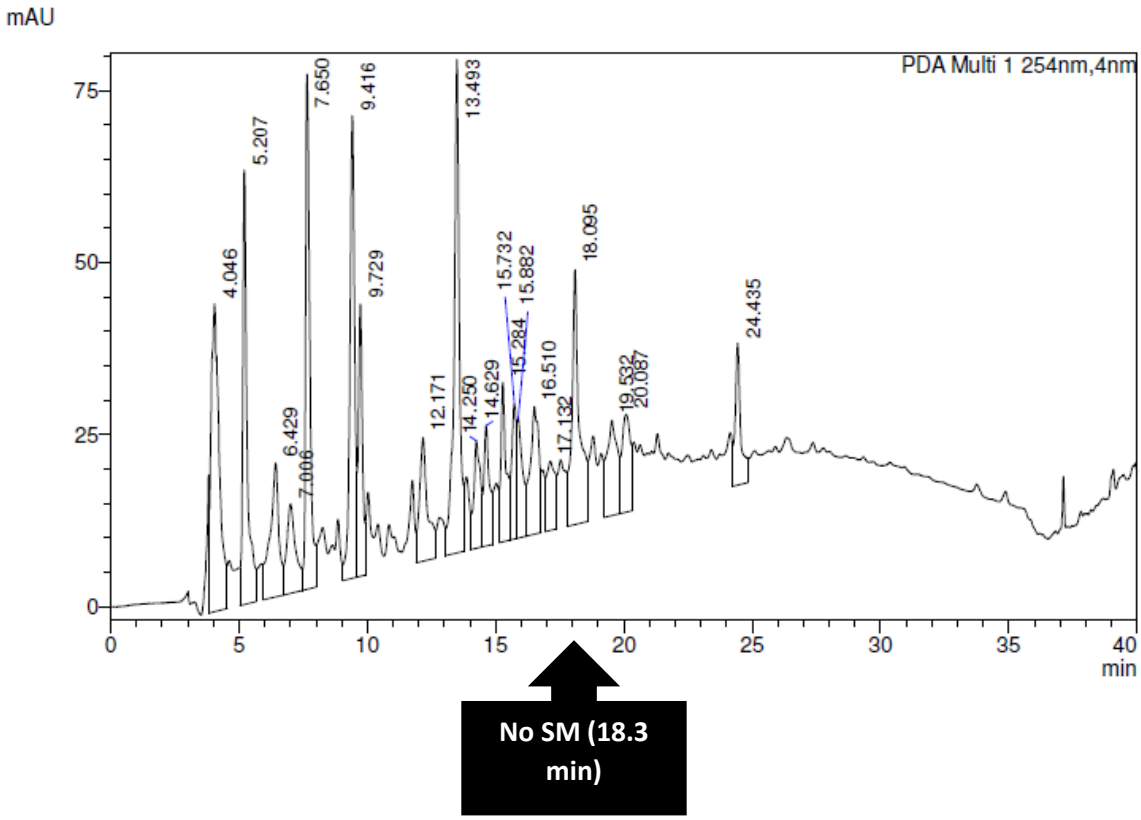

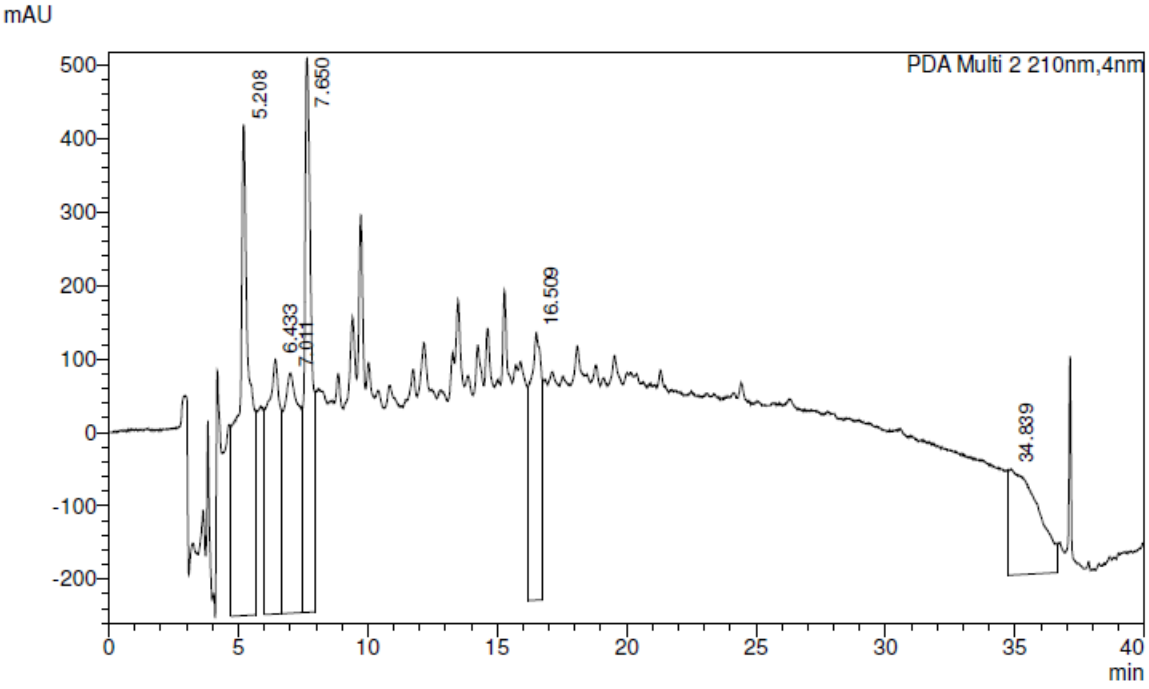
mAU
PDA Multi 2 210nm,4nm
5.208
6.433
7.011
7.650
16.509
34.839
500
400
300
200
100
0
-100
-200
0
5
10
15
20
25
30
35
40
min

Peak Table

PDA Ch1 254nm

Peak#	Ret. Time	Area	Height	Area%
1	4.046	975480	44702	9.789
2	5.207	756500	63082	7.591
3	6.429	465562	19430	4.672
4	7.006	317265	12949	3.184
5	7.650	859537	74657	8.625
6	9.416	877535	67131	8.806
7	9.729	421929	39502	4.234
8	12.171	397448	17923	3.988
9	13.493	1042673	71629	10.463
10	14.250	274016	15573	2.750
11	14.629	259914	17460	2.608
12	15.284	328967	23143	3.301
13	15.732	258767	19635	2.597
14	15.882	249411	17350	2.503
15	16.510	452865	18560	4.545
16	17.132	239905	10038	2.407
17	18.095	759327	36965	7.620
18	19.532	392304	13805	3.937
19	20.087	327194	14167	3.283
20	24.435	308494	20601	3.096
Total		9965092	618301	100.000

PDA Ch2 210nm

Peak#	Ret. Time	Area	Height	Area%
1	5.208	20139575	669713	23.990
2	6.433	12851065	346383	15.308
3	7.011	13390468	327180	15.950
4	7.650	14912337	754294	17.763
5	16.509	11453458	364207	13.643
6	34.839	11204608	144204	13.347
Total		83951510	2605981	100.000

Appendix 33. HPLC-UV trace of the crude reaction mixture of the fluorination of compound 21 with CsF at 120 °C using the long method.

==== Shimadzu LabSolutions Analysis Report ====

Sample Name	: epm-3-16		
Sample ID	: July 22		
Data Filename	: epm-3-16.lcd		
Method Filename	: Emile standard.lcm		
Batch Filename	:		
Vial #	: 1-1	Sample Type	: Unknown
Injection Volume	: 1000 uL		
Date Acquired	: 22/07/2020 3:41:23 PM	Acquired by	: ShimadzuHPLC
Date Processed	: 11/12/2020 12:15:26 PM	Processed by	: ShimadzuHPLC

<PDA Chromatogram>

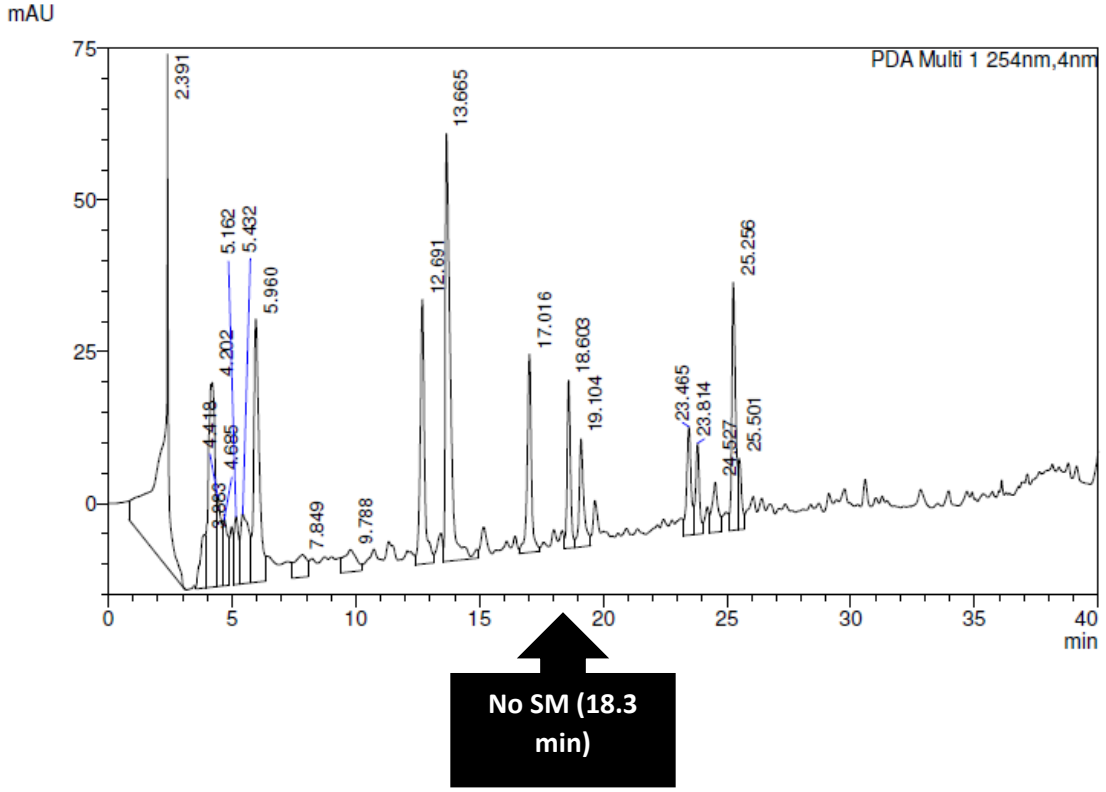

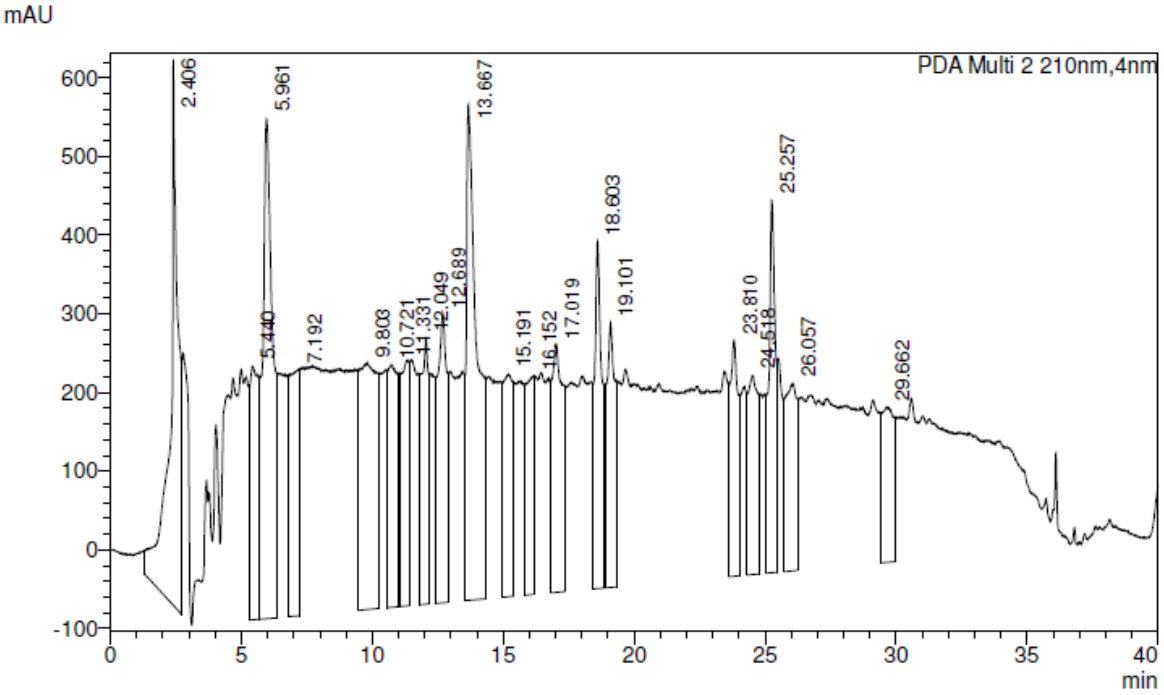
mAU
PDA Multi 2 210nm,4nm
2.406
5.961
13.667
25.257
18.603
19.101
12.689
12.049
11.331
10.721
9.808
5.440
7.192
15.191
16.152
17.019
23.810
24.518
26.057
29.662
600
500
400
300
200
100
0
-100
0
5
10
15
20
25
30
35
40
min

Peak Table

PDA Ch1 254nm

Peak#	Ret. Time	Area	Height	Area%
1	2.391	1290900	83688	18.056
2	3.883	128275	8762	1.794
3	4.202	624483	33667	8.735
4	4.418	180618	14925	2.526
5	4.685	154442	11005	2.160
6	5.162	135550	11199	1.896
7	5.432	272399	11534	3.810
8	5.960	661332	43434	9.250
9	7.849	125611	3694	1.757
10	9.788	127314	3683	1.781
11	12.691	529038	43556	7.400
12	13.665	981884	70421	13.734
13	17.016	381261	32644	5.333
14	18.603	257272	27604	3.599
15	19.104	232265	17733	3.249
16	23.465	216406	17861	3.027
17	23.814	165528	14991	2.315
18	24.527	135113	8193	1.890
19	25.256	436724	40815	6.109
20	25.501	113003	11663	1.581
Total		7149417	511073	100.000

PDA Ch2 210nm

Peak#	Ret. Time	Area	Height	Area%
1	2.406	15288403	693155	8.274
2	5.440	7475335	322488	4.046
3	5.961	17178091	635746	9.297
4	7.192	7873408	313695	4.261
5	9.803	14978237	313330	8.106
6	10.721	7552034	307711	4.087
7	11.331	6718259	312497	3.636
8	12.049	6436091	337319	3.483
9	12.689	8550814	366971	4.628
10	13.667	19004560	629503	10.286
11	15.191	7447884	282432	4.031
12	16.152	6014037	277775	3.255
13	17.019	9652173	316072	5.224
14	18.603	8342007	440601	4.515
15	19.101	6987189	335595	3.782
16	23.810	6440926	299951	3.486
17	24.518	6868485	253355	3.717
18	25.257	8487107	473423	4.593
19	26.057	7313559	238237	3.958
20	29.662	6160556	197142	3.334
Total		184769156	7346999	100.000

Appendix 34. HPLC-UV trace of the crude reaction mixture of the fluorination of compound 21 with KF/Kryptofix at 80 °C using the short method.

==== Shimadzu LabSolutions Analysis Report ====

Sample Name	: epm-3-22		
Sample ID	: July 30		
Data Filename	: epm-3-22.lcd		
Method Filename	: Emile standard.lcm		
Batch Filename	:		
Vial #	: 1-1	Sample Type	: Unknown
Injection Volume	: 1000 uL		
Date Acquired	: 30/07/2020 4:03:38 PM	Acquired by	: ShimadzuHPLC
Date Processed	: 11/12/2020 12:35:00 PM	Processed by	: ShimadzuHPLC

<PDA Chromatogram>

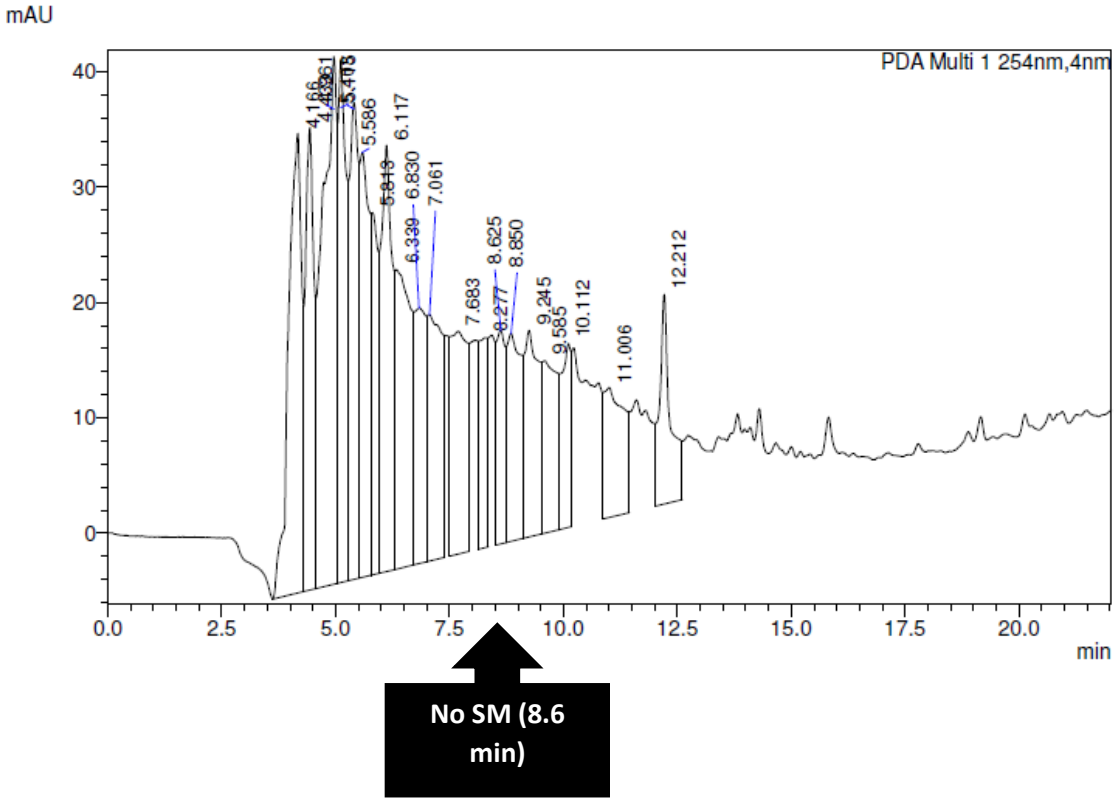

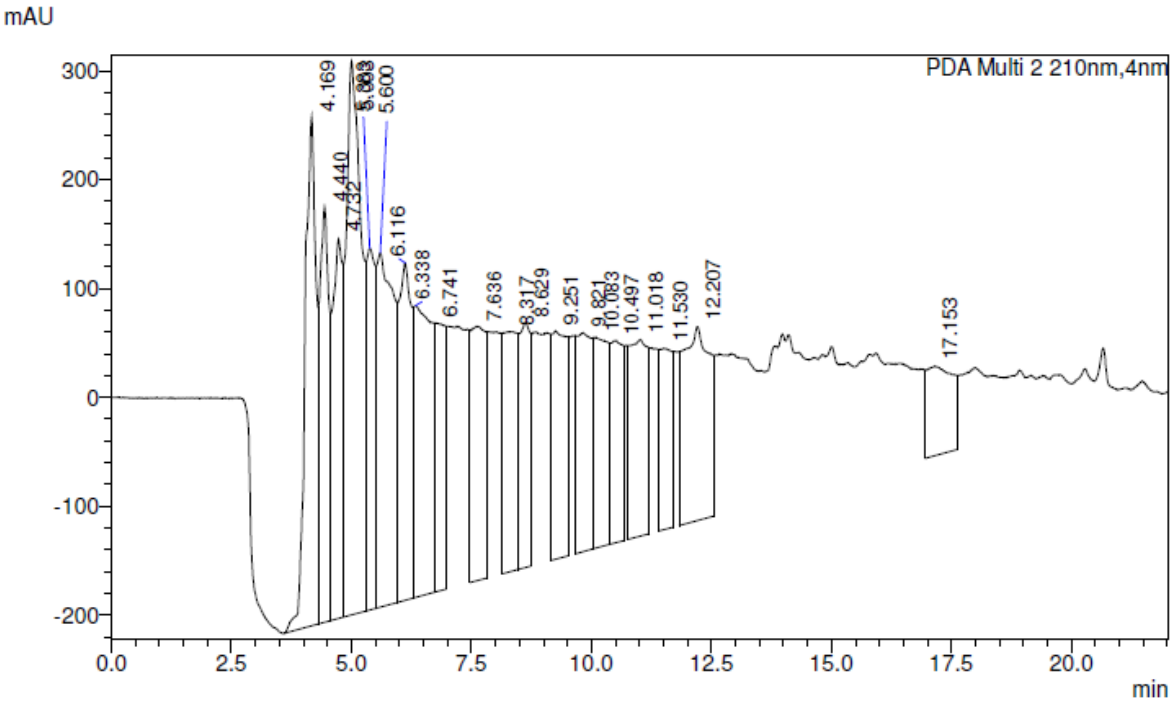
mAU
PDA Multi 2 210nm,4nm
300
200
100
0
-100
-200
4.169
4.440
4.732
5.600
6.116
6.338
6.741
7.636
8.317
8.629
9.251
9.821
10.083
10.497
11.018
11.530
12.207
17.153
0.0
2.5
5.0
7.5
10.0
12.5
15.0
17.5
20.0
min

Peak Table

PDA Ch1 254nm

Peak#	Ret. Time	Area	Height	Area%
1	4.166	802173	39849	8.580
2	4.433	518735	40109	5.548
3	4.961	1033468	45782	11.054
4	5.115	558954	45297	5.979
5	5.403	537830	41341	5.753
6	5.586	526198	36868	5.628
7	5.813	325086	31424	3.477
8	6.117	646260	36962	6.913
9	6.339	600411	25978	6.422
10	6.830	377415	22163	4.037
11	7.061	469029	21385	5.017
12	7.683	482037	19338	5.156
13	8.277	243550	18213	2.605
14	8.625	250766	18534	2.682
15	8.850	376560	18041	4.028
16	9.245	380397	17911	4.069
17	9.585	328531	14945	3.514
18	10.112	241955	15916	2.588
19	11.006	343933	11257	3.679
20	12.212	305839	18188	3.271
Total		9349126	539499	100.000

PDA Ch2 210nm

Peak#	Ret. Time	Area	Height	Area%
1	4.169	7438196	467559	7.191
2	4.440	5081806	381268	4.913
3	4.732	5096683	348605	4.928
4	5.003	11360193	508493	10.983
5	5.383	3945372	332017	3.814
6	5.600	7903806	325153	7.642
7	6.116	5844452	309972	5.651
8	6.338	6912367	267962	6.683
9	6.741	3598771	247158	3.479
10	7.636	4876137	233400	4.714
11	8.317	4220102	220263	4.080
12	8.629	3646918	224750	3.526
13	9.251	4335075	209609	4.191
14	9.821	4184104	201089	4.045
15	10.083	3892564	193658	3.763
16	10.497	3402927	185855	3.290
17	11.018	4746211	180446	4.589
18	11.530	2848723	165981	2.754
19	12.207	6966493	178100	6.735
20	17.153	3130449	82471	3.027
Total		103431350	5263808	100.000

Appendix 35. HPLC-UV trace of the crude reaction mixture of the fluorination of compound 21 with KF/Kryptofix at 100 °C using the short method.

==== Shimadzu LabSolutions Analysis Report ====

Sample Name	: epm-3-23		
Sample ID	: July 30		
Data Filename	: epm-3-23.lcd		
Method Filename	: Emile standard.lcm		
Batch Filename	:		
Vial #	: 1-1	Sample Type	: Unknown
Injection Volume	: 1000 uL		
Date Acquired	: 30/07/2020 4:33:45 PM	Acquired by	: ShimadzuHPLC
Date Processed	: 11/12/2020 12:39:05 PM	Processed by	: ShimadzuHPLC

<PDA Chromatogram>

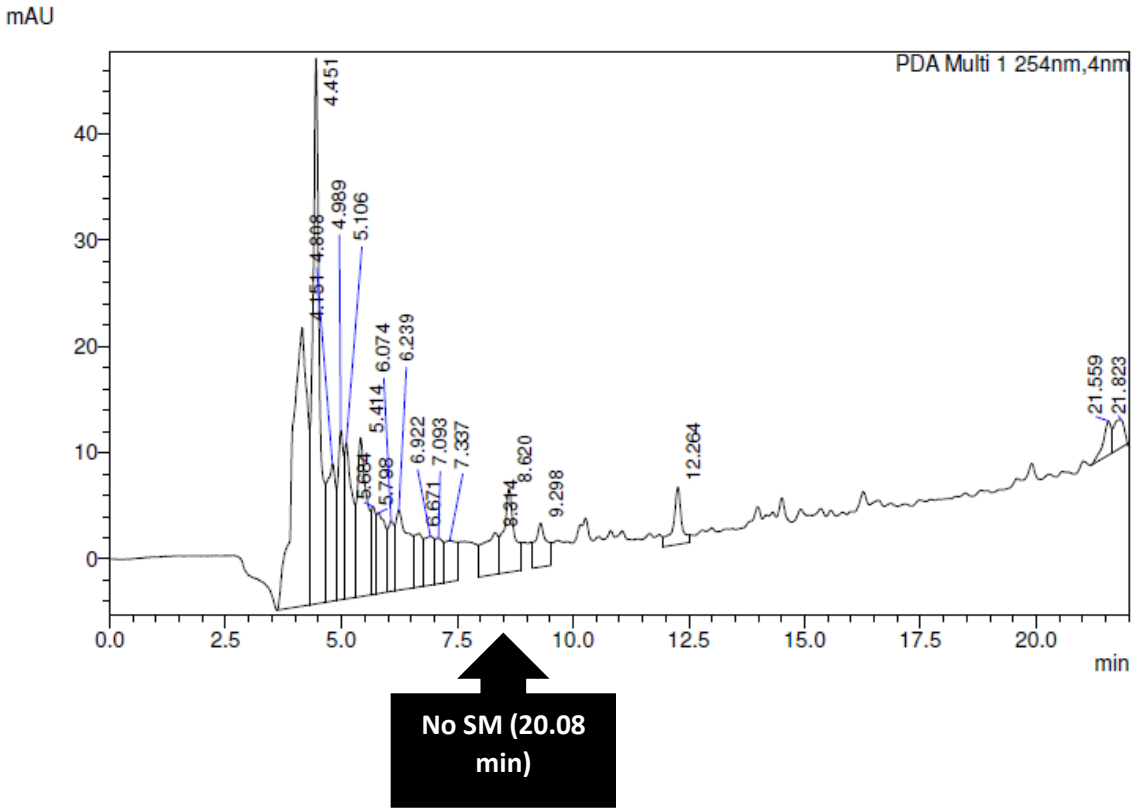

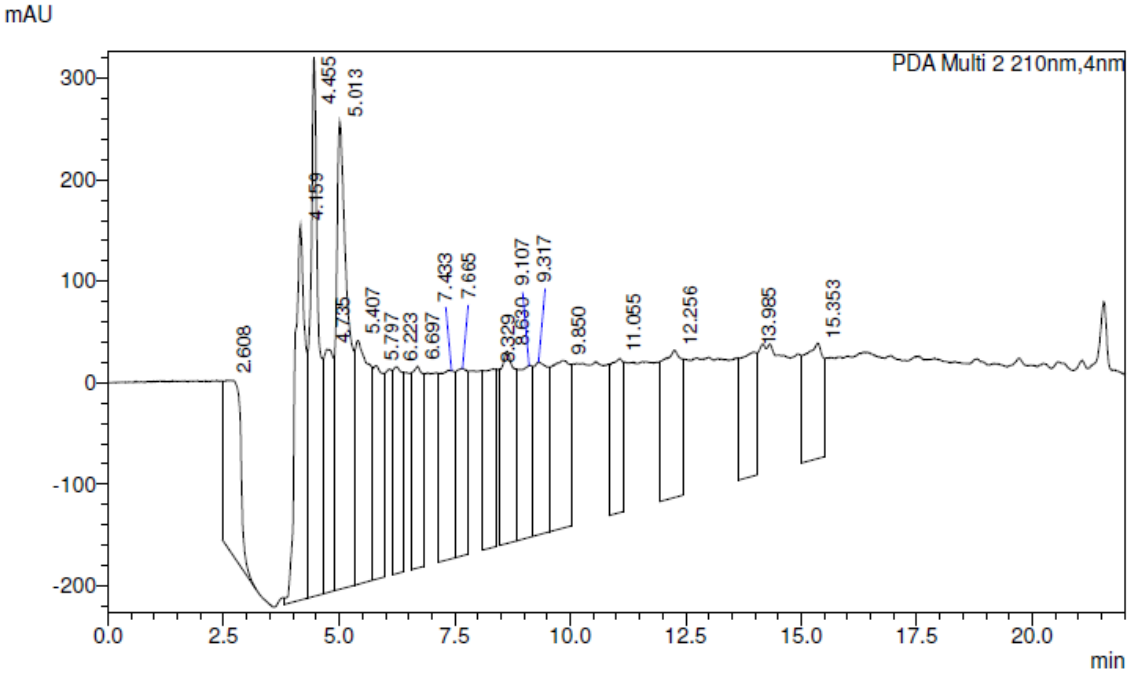
mAU
PDA Multi 2 210nm,4nm
300
200
100
0
-100
-200
2.608
4.159
4.455
5.013
4.735
5.407
5.797
6.223
6.697
7.433
7.665
9.107
9.317
9.850
11.055
12.256
13.985
15.353
0.0
2.5
5.0
7.5
10.0
12.5
15.0
17.5
20.0
min

Peak Table

PDA Ch1 254nm

Peak#	Ret. Time	Area	Height	Area%
1	4.151	578214	26208	20.399
2	4.451	526403	51360	18.572
3	4.808	172893	12935	6.100
4	4.989	133326	15936	4.704
5	5.106	169723	14689	5.988
6	5.414	215065	14950	7.587
7	5.684	60703	8265	2.142
8	5.798	96630	7575	3.409
9	6.074	56979	6635	2.010
10	6.239	144198	7534	5.087
11	6.671	65230	5040	2.301
12	6.922	65915	4603	2.326
13	7.093	45276	4282	1.597
14	7.337	72676	3883	2.564
15	8.314	90711	3930	3.200
16	8.620	124923	7892	4.407
17	9.298	67586	4137	2.384
18	12.264	66073	5418	2.331
19	21.559	40474	3195	1.428
20	21.823	41468	2633	1.463
Total		2834465	211101	100.000

PDA Ch2 210nm

Peak#	Ret. Time	Area	Height	Area%
1	2.608	4315485	166094	5.201
2	4.159	5545415	369041	6.684
3	4.455	6745013	530810	8.130
4	4.735	3319375	239668	4.001
5	5.013	8582739	460552	10.345
6	5.407	5293651	240008	6.380
7	5.797	3156545	210377	3.805
8	6.223	3203712	203958	3.861
9	6.697	3356114	198639	4.045
10	7.433	3911005	185286	4.714
11	7.665	3164895	184551	3.815
12	8.329	3034063	175684	3.657
13	8.630	4091881	189372	4.932
14	9.107	3549405	169366	4.278
15	9.317	3623485	170340	4.367
16	9.850	4688733	165029	5.651
17	11.055	2871382	151401	3.461
18	12.256	4370030	145398	5.267
19	13.985	2933448	121768	3.536
20	15.353	3211500	113128	3.871
Total		82967874	4390470	100.000

Appendix 36. HPLC-UV trace of the crude reaction mixture of the fluorination of compound 21 with KF/Kryptofix at 120 °C using the short method.

SHIMADZU LabSolutions **Analysis Report**

<Sample Information>

Sample Name	: epm-3-24		
Sample ID	: July 30		
Data Filename	: epm-3-24.lcd		
Method Filename	: Emile standard.lcm		
Batch Filename	:		
Vial #	: 1-1	Sample Type	: Unknown
Injection Volume	: 1000 uL		
Date Acquired	: 30/07/2020 5:03:18 PM	Acquired by	: ShimadzuHPLC
Date Processed	: 11/12/2020 12:48:11 PM	Processed by	: ShimadzuHPLC

<Chromatogram>

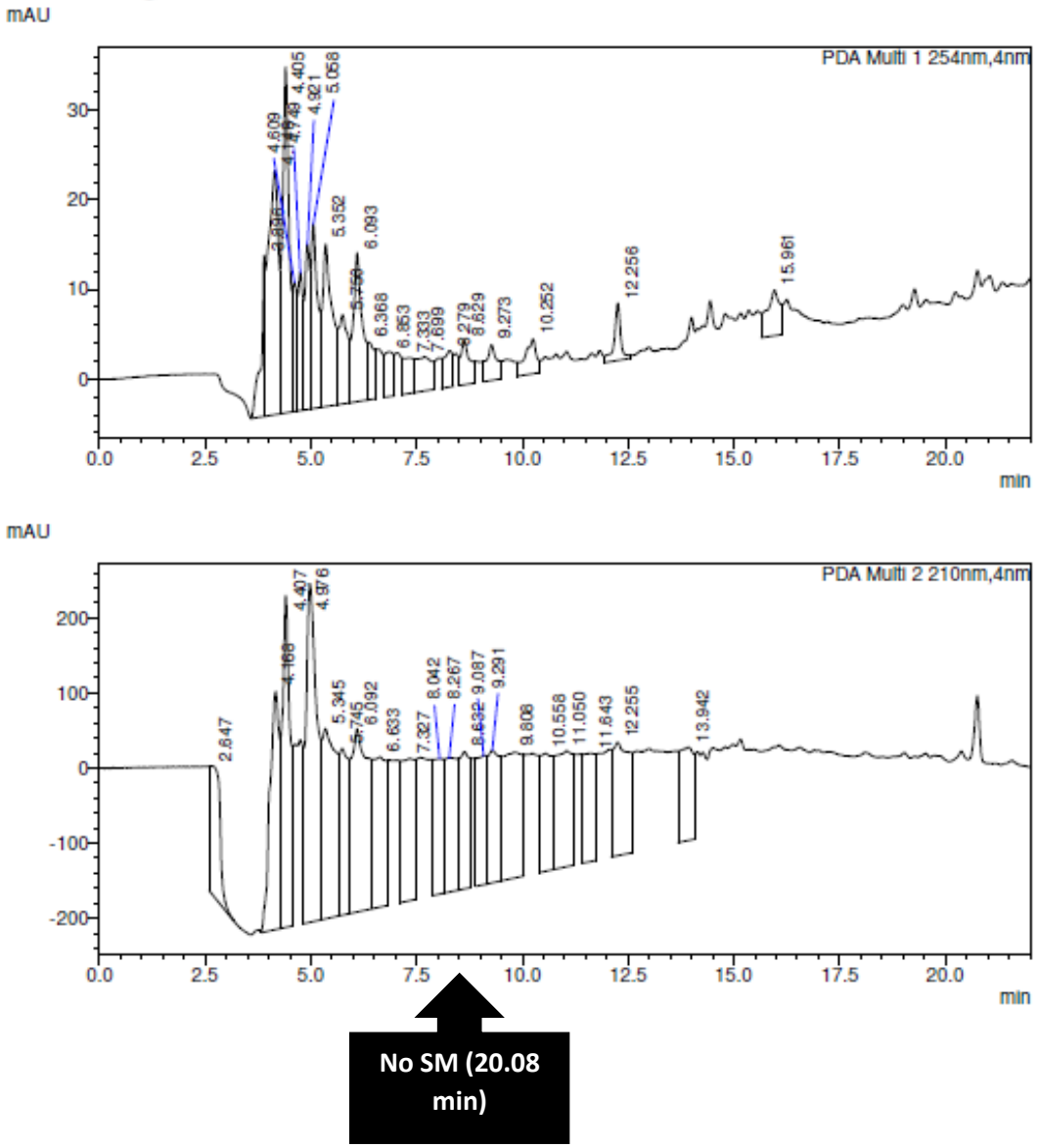

<Peak Table>

PDA Ch1 254nm

Peak#	Ret. Time	Area	Height	Area%
1	3.896	126700	17969	4.159
2	4.148	453075	27249	14.873
3	4.405	413198	38581	13.564
4	4.609	105832	14444	3.474
5	4.749	124593	15439	4.090
6	4.921	154068	18450	5.058
7	5.058	214243	20598	7.033
8	5.352	305987	18136	10.045
9	5.750	146870	9965	4.821
10	6.093	248205	16630	8.148
11	6.368	68600	6409	2.252
12	6.853	74615	4999	2.449
13	7.333	67795	3963	2.226
14	7.699	96040	3820	3.153
15	8.279	63069	4070	2.070
16	8.629	69777	4922	2.291
17	9.273	65399	3958	2.147
18	10.252	75824	3887	2.489
19	12.256	67760	6395	2.224
20	15.961	104628	5083	3.435
Total		3046278	244966	100.000

PDA Ch2 210nm

Peak#	Ret. Time	Area	Height	Area%
1	2.647	2896468	169478	3.454
2	4.168	4875869	316864	5.814
3	4.407	5506529	442304	6.566
4	4.976	8162752	451123	9.733
5	5.345	5682263	253771	6.776
6	5.745	3422242	222102	4.081
7	6.092	6829904	244324	8.144
8	6.633	4163893	200082	4.965
9	7.327	4096077	189244	4.884
10	8.042	2767607	180355	3.300
11	8.267	3637788	179340	4.338
12	8.632	3174591	182583	3.785
13	9.087	2735753	172275	3.262
14	9.291	3396233	176923	4.050
15	9.808	5400960	167597	6.440
16	10.558	2870092	157137	3.422
17	11.050	4363365	154412	5.203
18	11.643	2858926	143930	3.409
19	12.255	4229176	150943	5.043
20	13.942	2792570	123829	3.330
Total		83863057	4278614	100.000

Appendix 37. Compound 21 after 20 minutes in tBuOH at 120 degrees (top), Compound 21 standard (bottom)

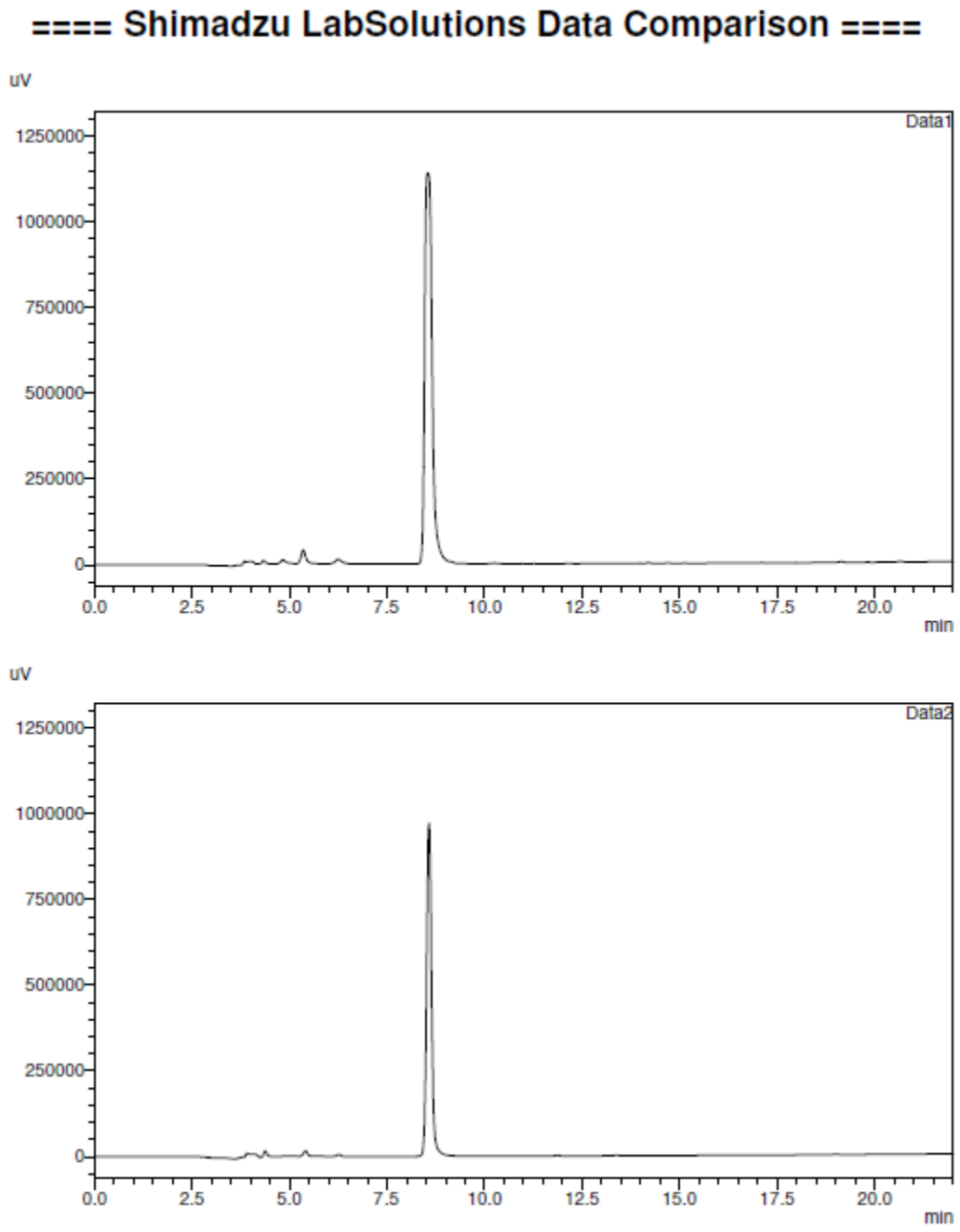

Appendix 38. Compound 21 after 60 minutes in DMSO at 120 degrees (top), Compound 21 standard (bottom)

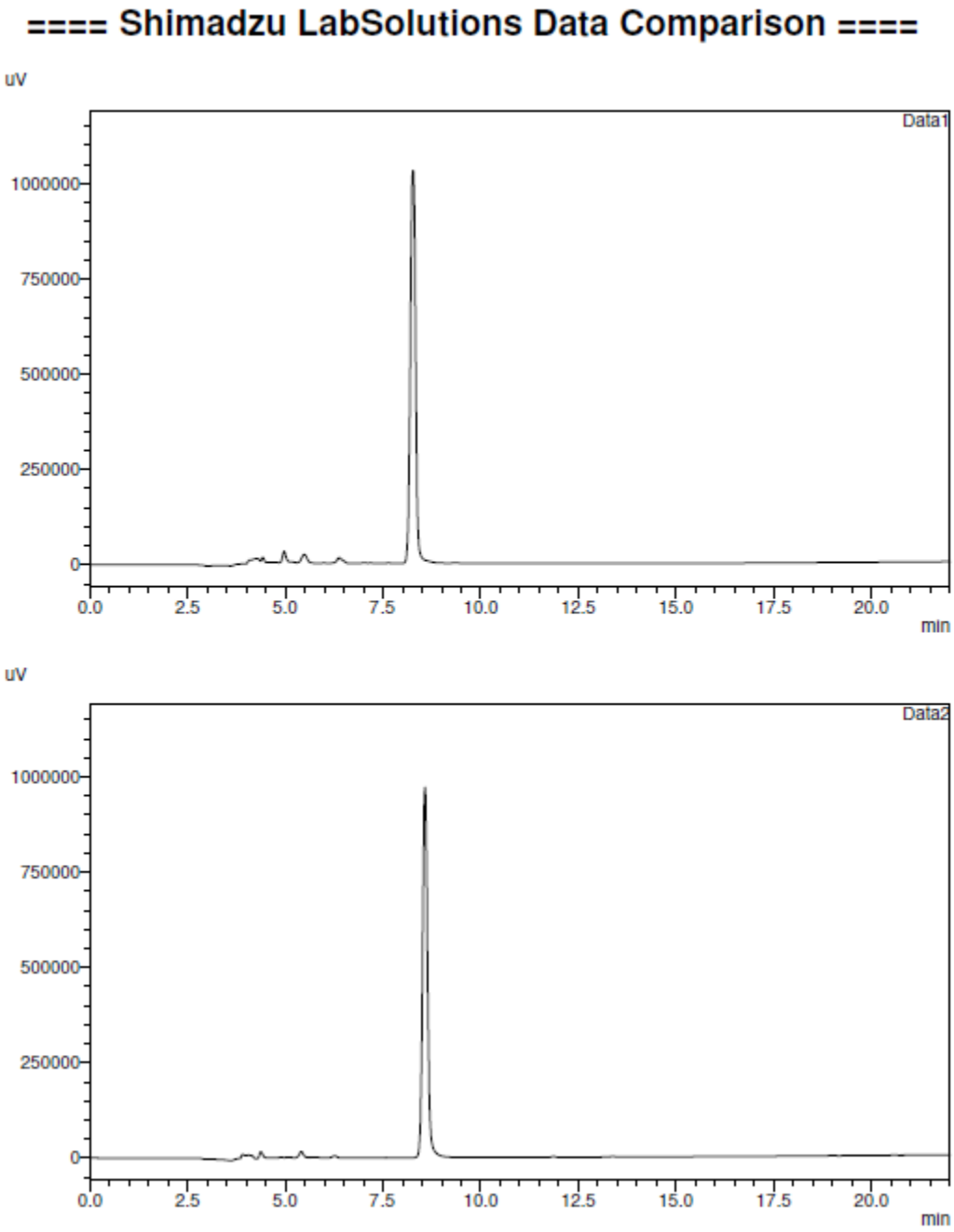

Appendix 39. Fluorine NMR of experiment with TsCl and TBAF attempted fluorination of alcohol 25.

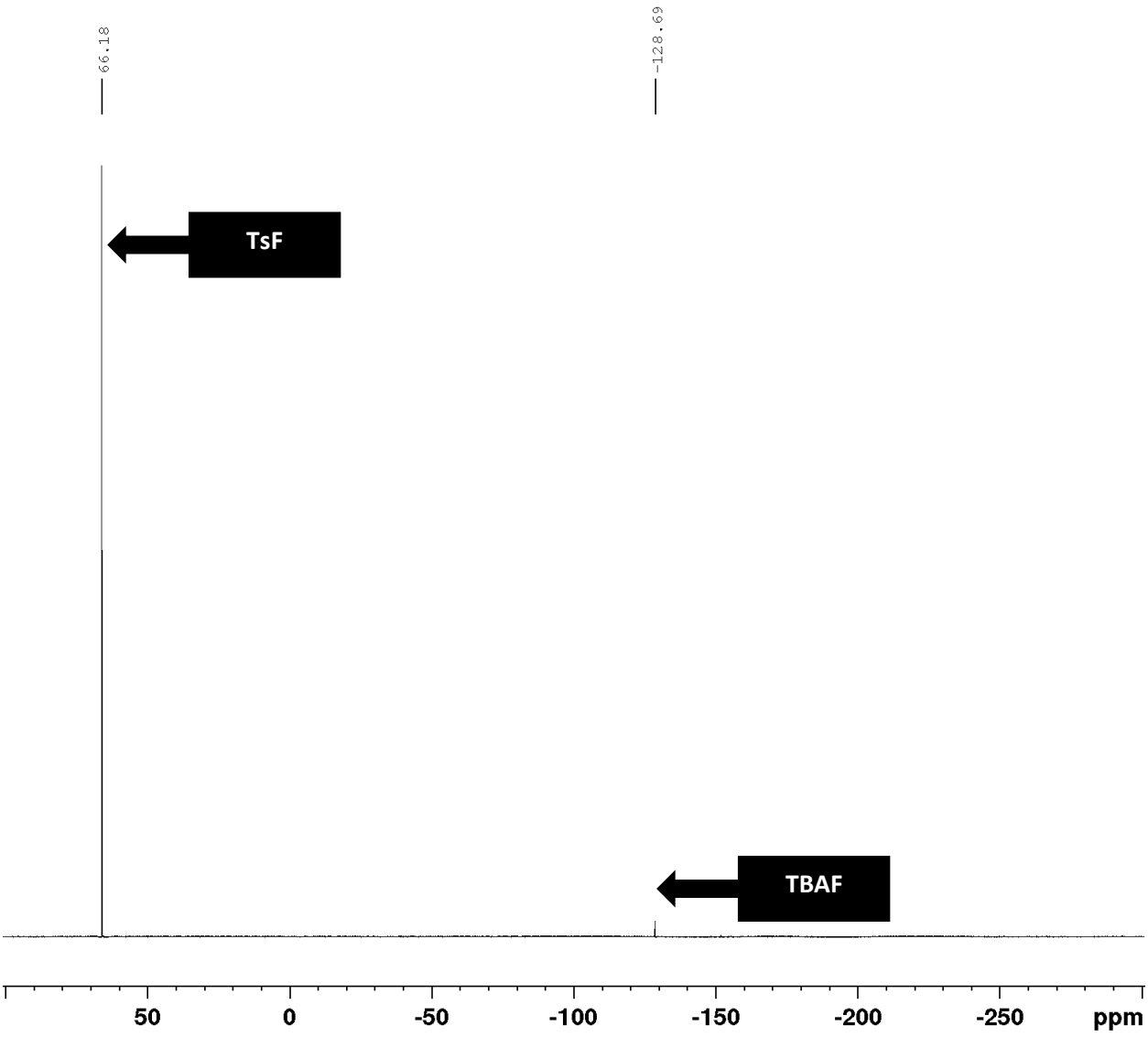

Appendix 40. HPLC-UV trace of the crude reaction mixture for the difluorination of aldehyde 27 with 1 equivalent of TMAF.

SHIMADZU LabSolutions Analysis Report

<Sample Information>

Sample Name	: epm-4-42		
Sample ID	: April 21		
Data Filename	: epm-4-42-short1.lcd		
Method Filename	: Emile standard.lcm		
Batch Filename	:		
Vial #	: 1-1	Sample Type	: Unknown
Injection Volume	: 1000 uL		
Date Acquired	: 21/04/2021 3:34:40 PM	Acquired by	: ShimadzuHPLC
Date Processed	: 21/04/2021 3:56:42 PM	Processed by	: ShimadzuHPLC

<Chromatogram>

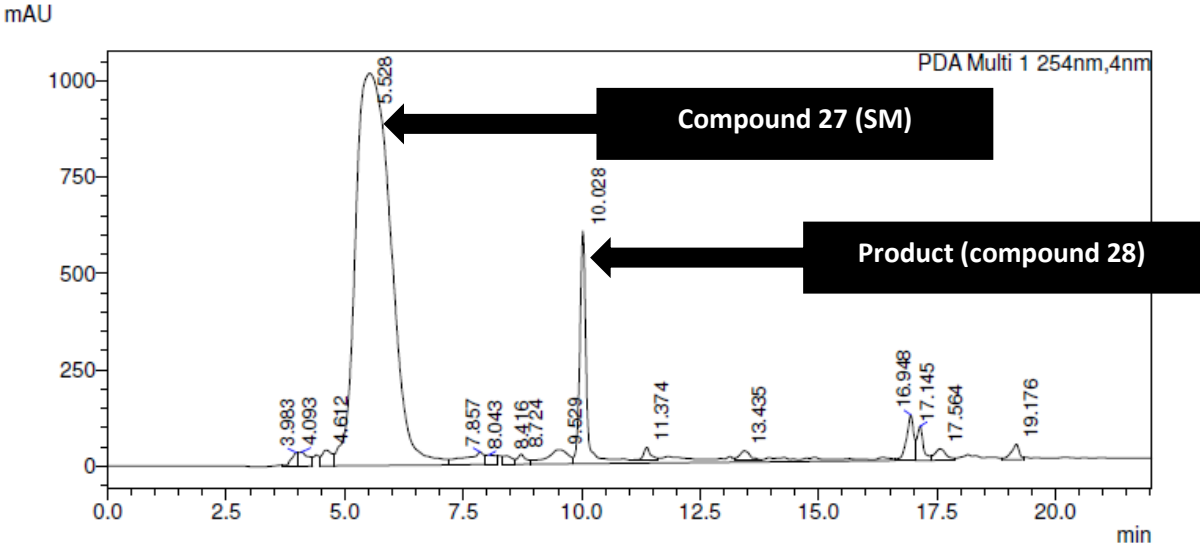

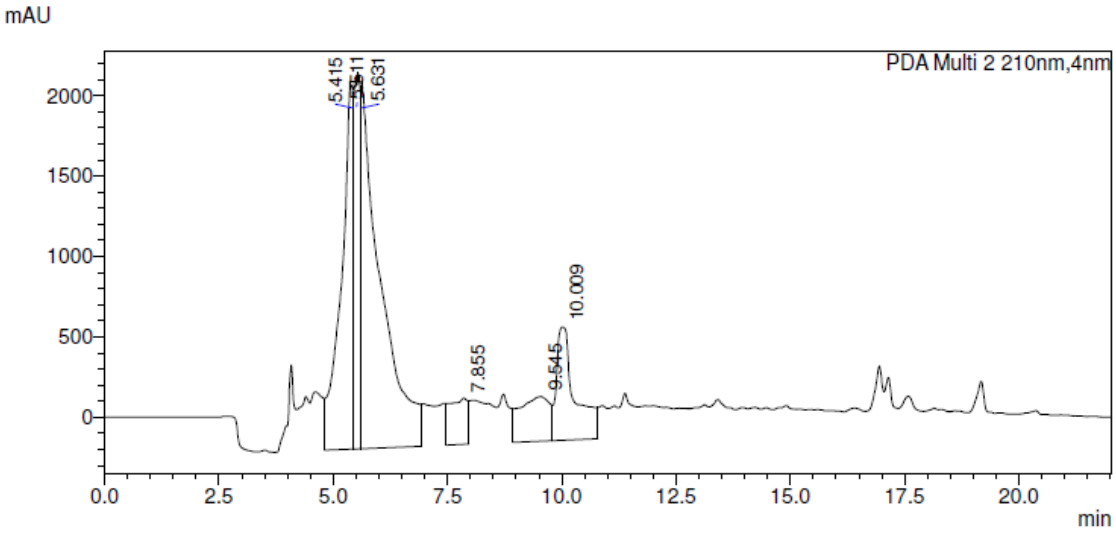
mAU
PDA Multi 2 210nm,4nm
2000
1500
1000
500
0
5.415
5.631
7.855
9.545
10.009
0.0
2.5
5.0
7.5
10.0
12.5
15.0
17.5
20.0
min

Appendix 41. HPLC-UV trace of the crude reaction mixture for the difluorination of aldehyde 27 with 0.5 equivalent of TMAF.

SHIMADZU LabSolutions **Analysis Report**

<Sample Information>

Sample Name	: epm-4-43		
Sample ID	: April 21		
Data Filename	: epm-4-43-short.lcd		
Method Filename	: Emile standard.lcm		
Batch Filename	:		
Vial #	: 1-1	Sample Type	: Unknown
Injection Volume	: 1000 uL		
Date Acquired	: 21/04/2021 3:04:31 PM	Acquired by	: ShimadzuHPLC
Date Processed	: 21/04/2021 3:26:33 PM	Processed by	: ShimadzuHPLC

<Chromatogram>

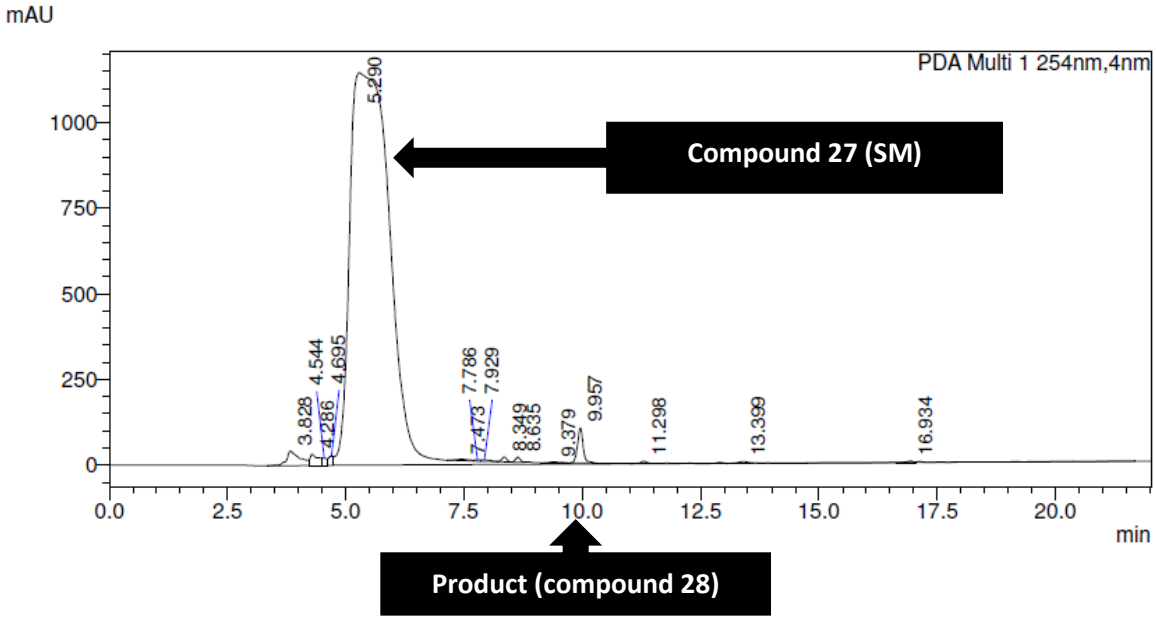

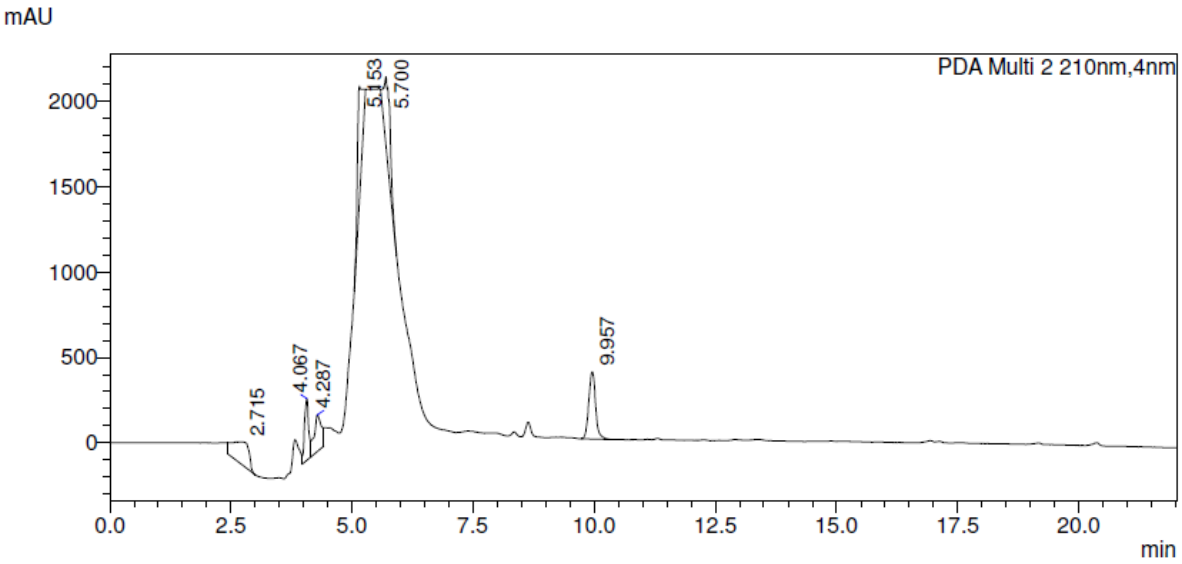
mAU
PDA Multi 2 210nm,4nm
2000
1500
1000
500
0
2.715
4.067
4.287
5.153
5.700
9.957
0.0
2.5
5.0
7.5
10.0
12.5
15.0
17.5
20.0
min

Appendix 42. HPLC-UV trace of the crude reaction mixture for the difluorination of aldehyde 27 after one hour at room temperature in ether.

SHIMADZU LabSolutIons Analysis Report

<Sample Information>

Sample Name	: epm-4-44		
Sample ID	: April 20		
Data Filename	: epm-4-44-60min.lcd		
Method Filename	: Emile standard.lcm		
Batch Filename	:		
Vial #	: 1-1	Sample Type	: Unknown
Injection Volume	: 1000 uL		
Date Acquired	: 20/04/2021 12:22:33 PM	Acquired by	: ShimadzuHPLC
Date Processed	: 20/04/2021 12:44:36 PM	Processed by	: ShimadzuHPLC

<Chromatogram>

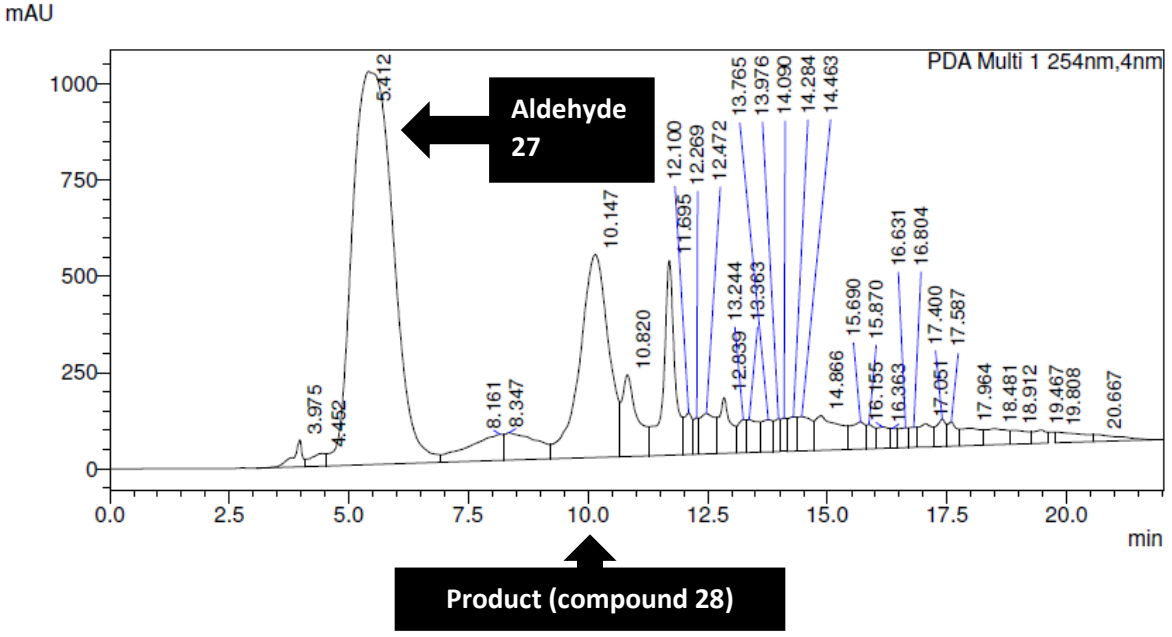

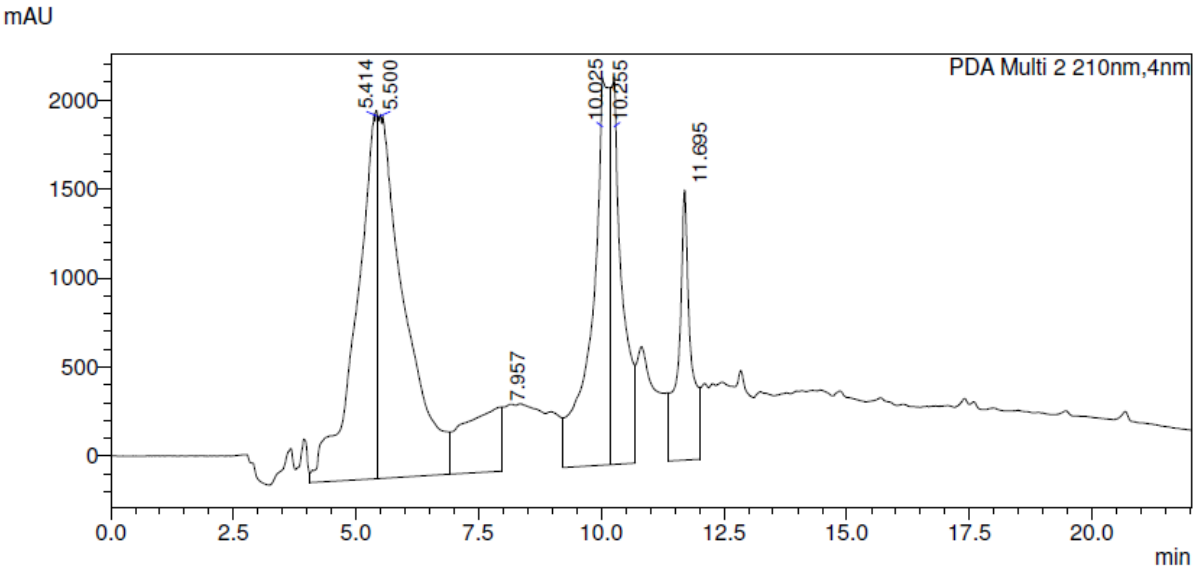
mAU
PDA Multi 2 210nm,4nm
5.414
5.500
7.957
10.025
10.255
11.695
2000
1500
1000
500
0
0.0
2.5
5.0
7.5
10.0
12.5
15.0
17.5
20.0
min

Appendix 43. HPLC-UV trace from mixture of pure aldehyde precursor 27 and difluorinated product.

SHIMADZU LabSolutions Analysis Report

<Sample Information>

Sample Name	: epm-difluorination		
Sample ID	: April 13		
Data Filename	: epm-difluor-test1.lcd		
Method Filename	: Mojmir method for nonpolar compounds.lcm		
Batch Filename	:		
Vial #	: 1-1	Sample Type	: Unknown
Injection Volume	: 1000 uL		
Date Acquired	: 13/04/2021 12:12:34 PM	Acquired by	: ShimadzuHPLC
Date Processed	: 13/04/2021 12:34:37 PM	Processed by	: ShimadzuHPLC

<Chromatogram>

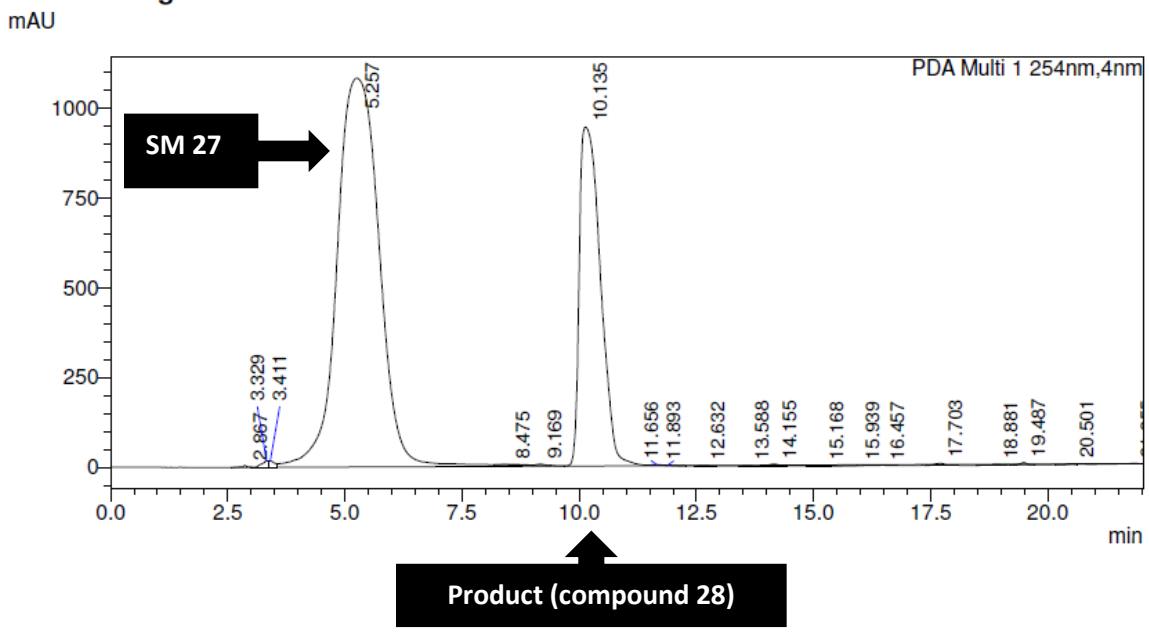

Compound characterization (NMR)

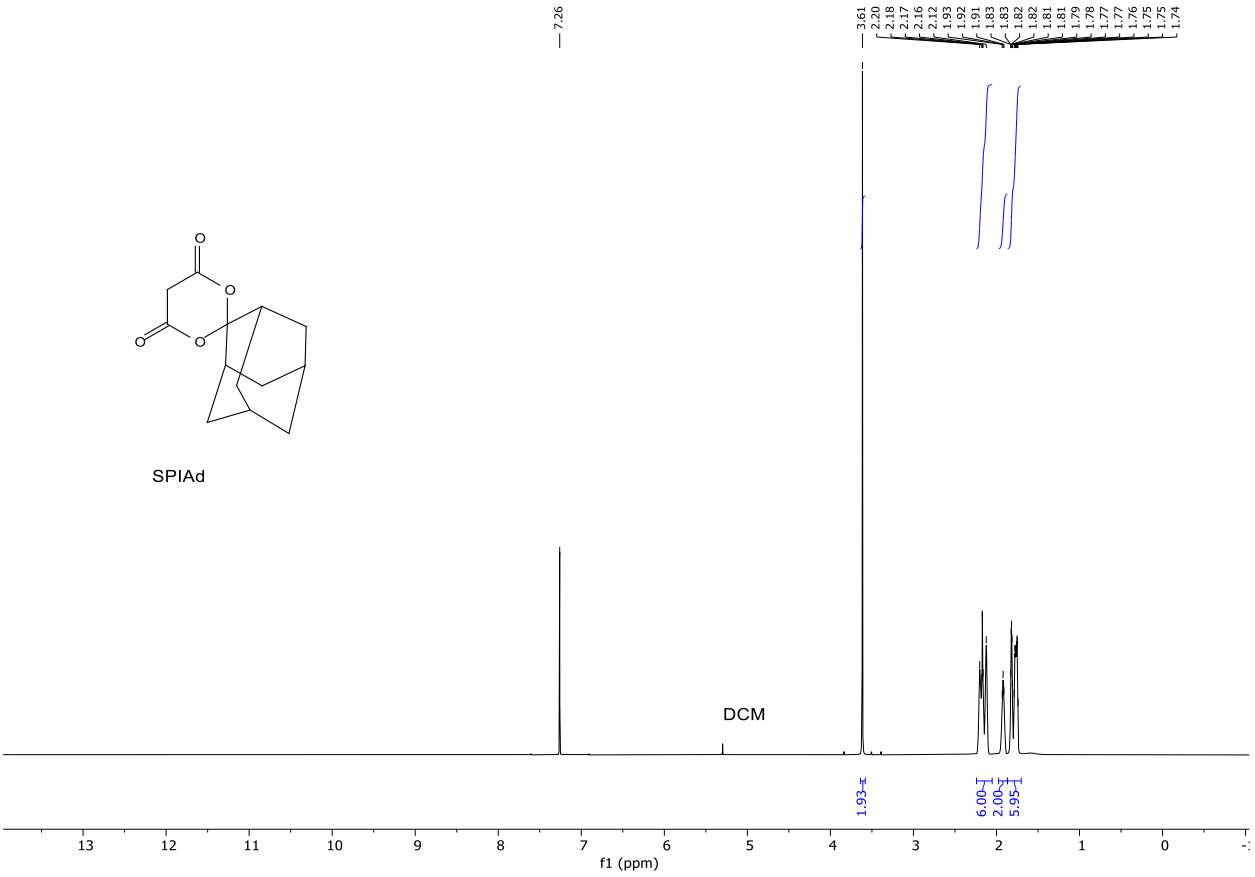

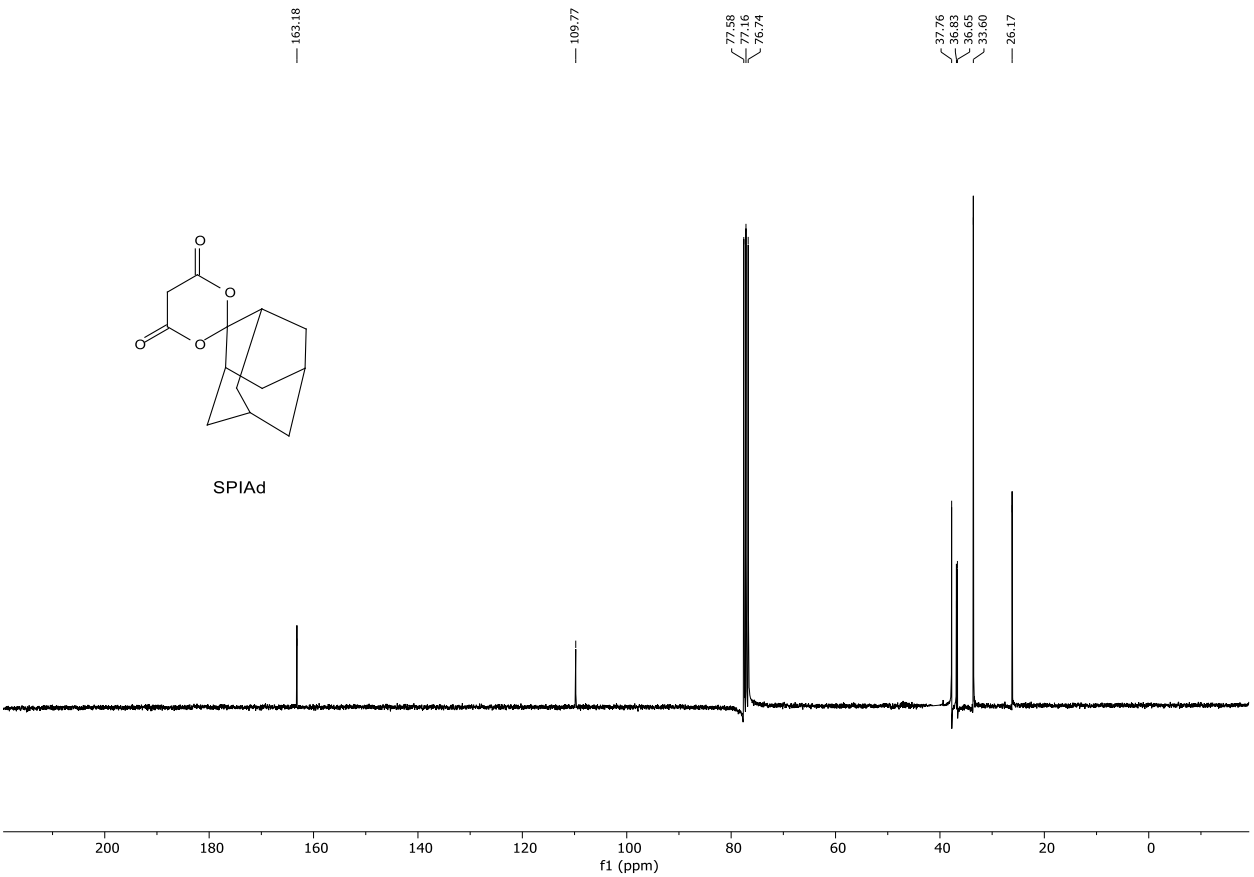
163.18
109.77
77.58
77.16
76.74
37.76
36.83
36.65
33.60
26.17
O
O
O
O
SPIAd
200
180
160
140
120
100
80
60
40
20
0
f1 (ppm)

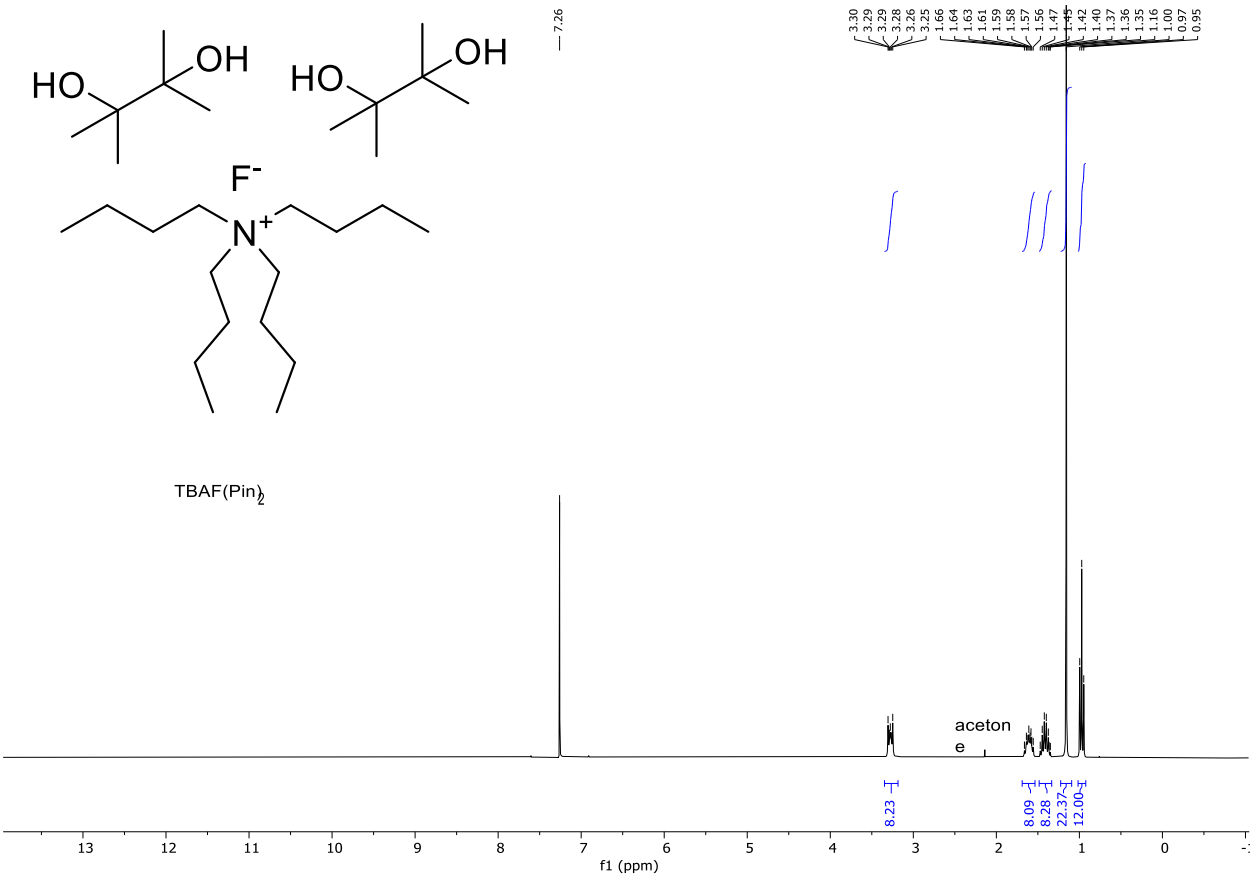
HO
OH
HO
OH
F-
N+
TBAF(Pin)2
7.26
3.30
3.29
3.29
3.28
3.26
3.25
1.66
1.64
1.63
1.61
1.59
1.58
1.57
1.56
1.47
1.45
1.42
1.40
1.37
1.36
1.35
1.16
1.00
0.97
0.95
aceton
e
8.23
8.09
8.28
22.37
12.00
13
12
11
10
9
8
7
6
5
4
3
2
1
0
f1 (ppm)

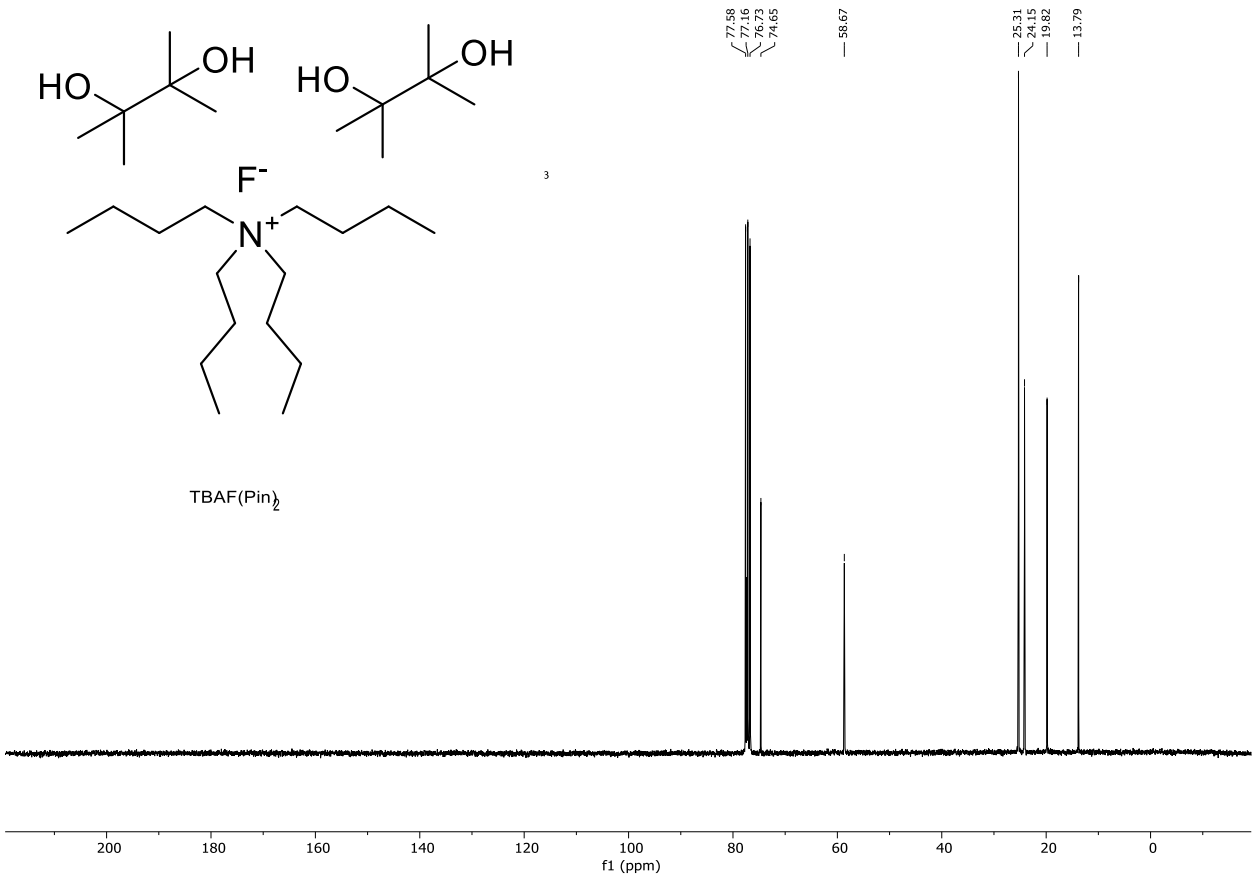
HO
OH
HO
OH
F-
N+
3
TBAF(Pin)2
77.58
77.16
76.73
74.65
58.67
25.31
24.15
19.82
13.79
200
180
160
140
120
100
80
60
40
20
0
f1 (ppm)

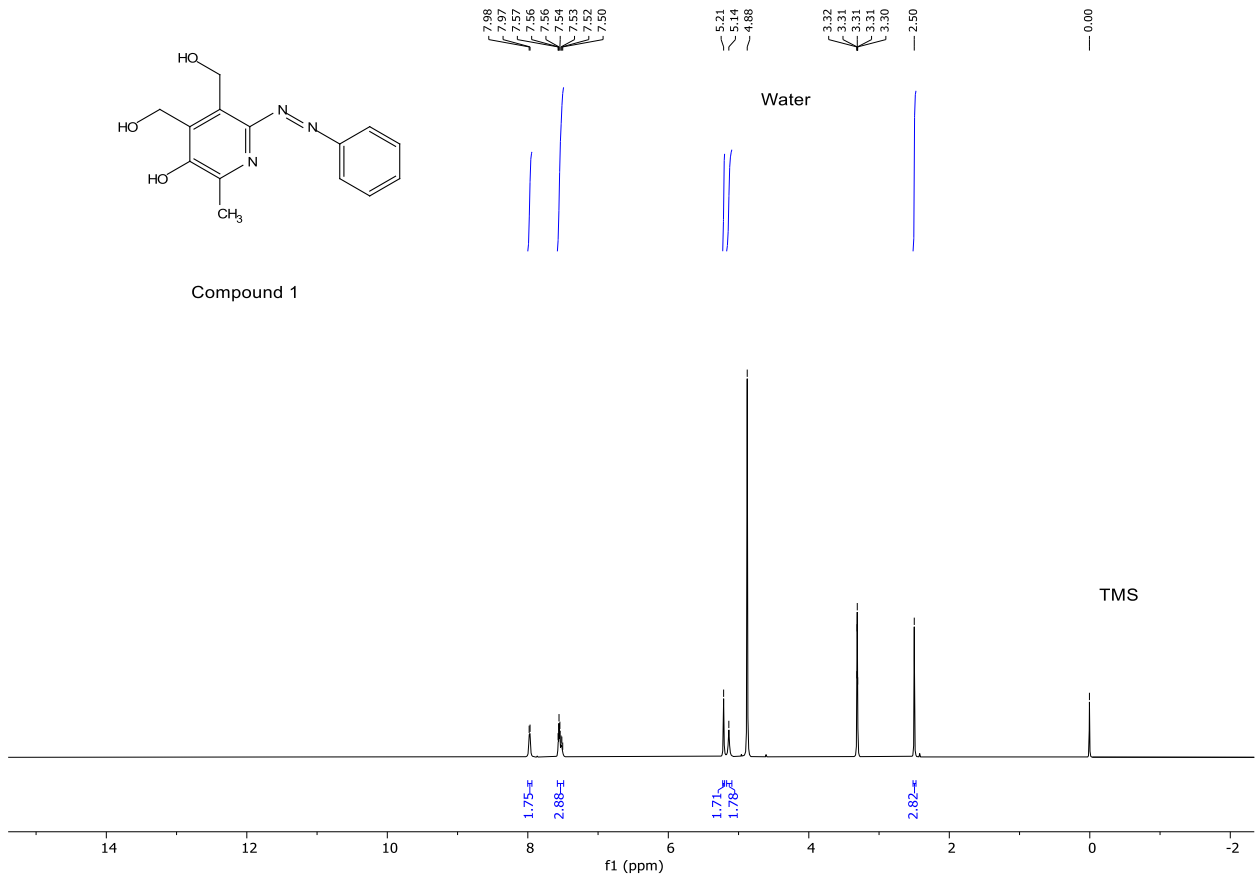
HO
HO
HO
N
N
N
CH3
Compound 1
7.98
7.97
7.57
7.56
7.56
7.54
7.53
7.52
7.50
5.21
5.14
4.88
3.32
3.31
3.31
3.31
3.30
2.50
0.00
Water
TMS
1.75
2.88
1.71
1.78
2.82
14
12
10
8
6
4
2
0
-2
f1 (ppm)

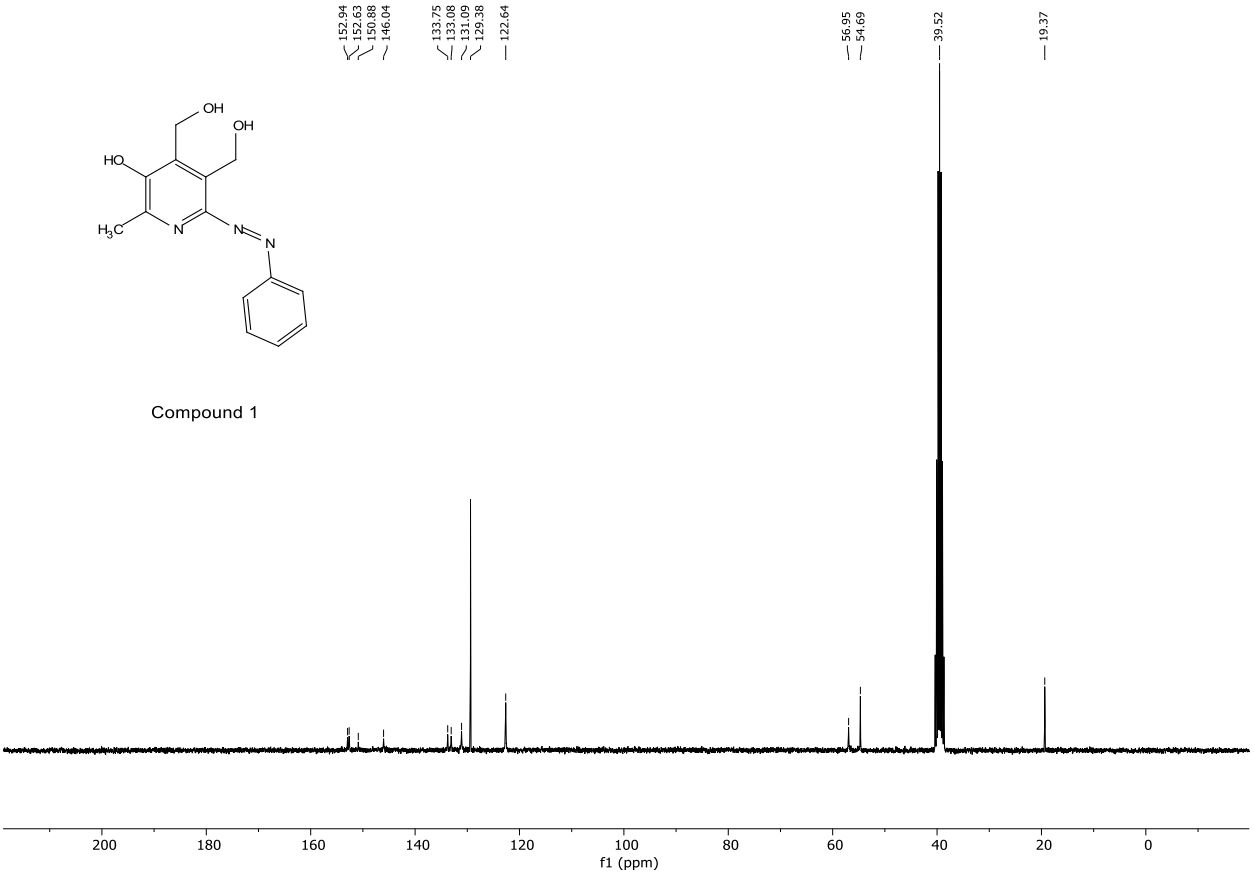
152.94
152.63
150.88
146.04
133.75
133.08
131.09
129.38
122.64
56.95
54.69
39.52
19.37
OH
OH
HO
H3C
N
N
N
200
180
160
140
120
100
80
60
40
20
0
f1 (ppm)

Compound 1

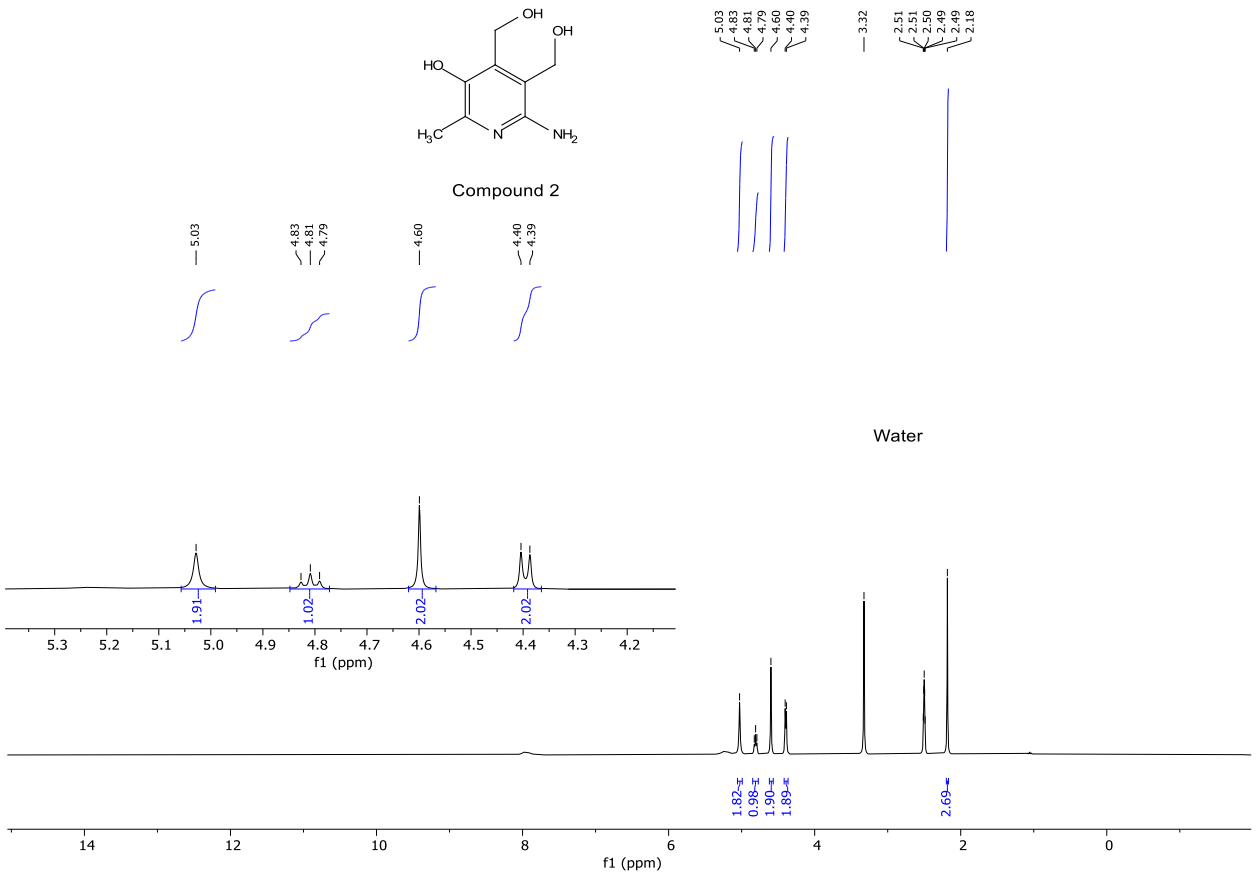
OH
OH
HO
H_3C
N
NH_2
Compound 2
5.03
4.83
4.81
4.79
4.60
4.40
4.39
3.32
2.51
2.51
2.50
2.49
2.49
2.18
Water
1.91
1.02
2.02
2.02
1.82
0.98
1.90
1.89
2.69
f1 (ppm)
f1 (ppm)

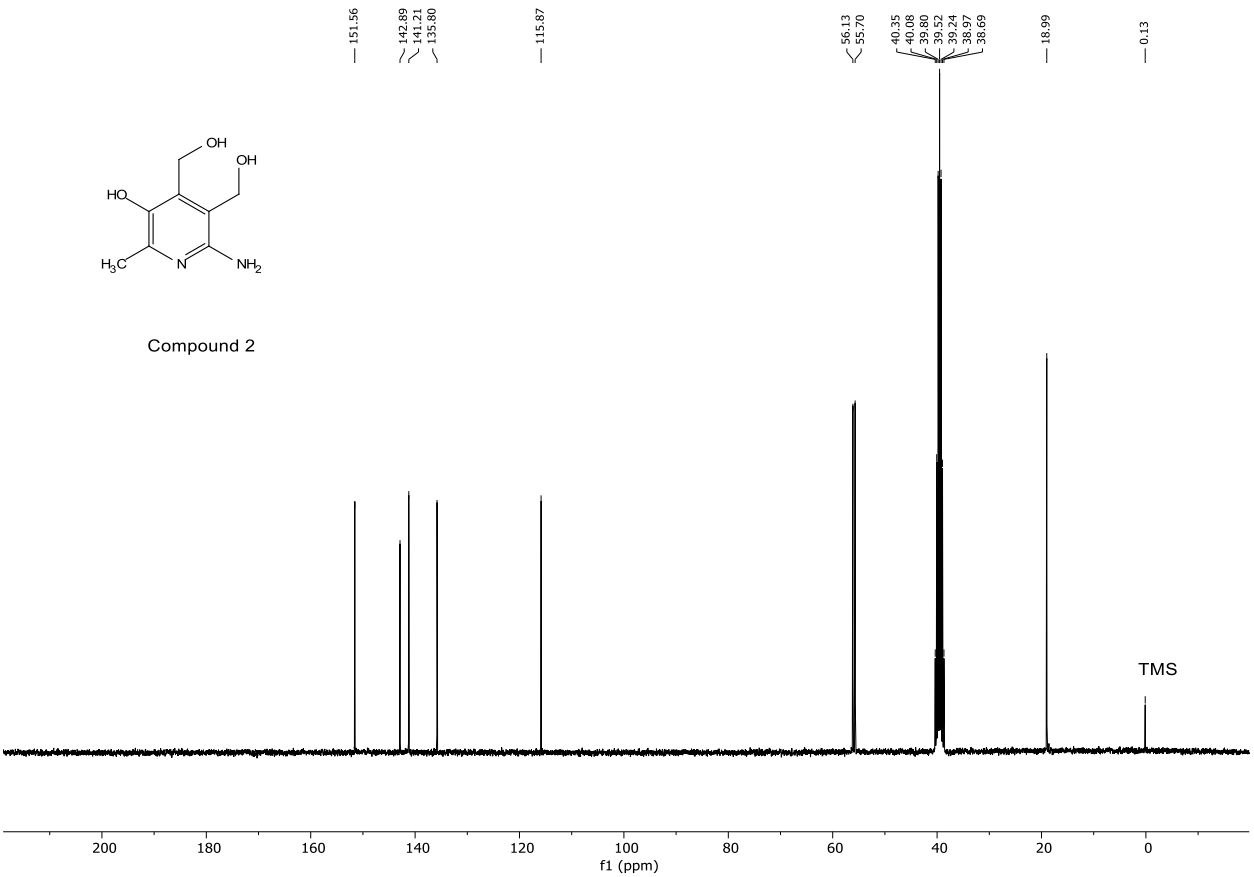
151.56
142.89
141.21
135.80
115.87
56.13
55.70
40.35
40.08
39.80
39.52
39.24
38.97
38.69
18.99
0.13
OH
OH
HO
H3C
N
NH2
Compound 2
TMS
200
180
160
140
120
100
80
60
40
20
0
f1 (ppm)

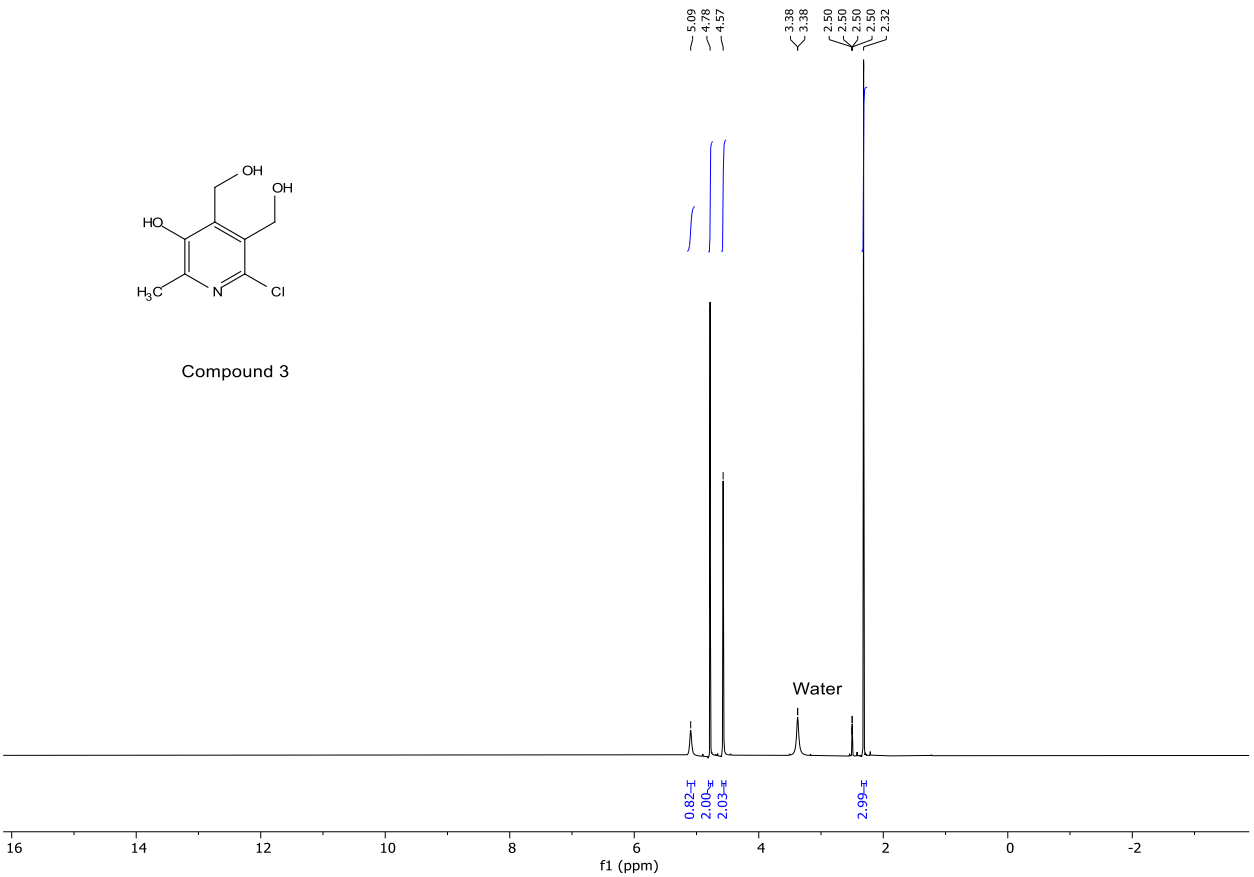
OH
OH
HO
H_3C
N
Cl
Compound 3
5.09
4.78
4.57
3.38
3.38
2.50
2.50
2.50
2.50
2.32
Water
0.82
2.00
2.03
2.99
16
14
12
10
8
6
4
2
0
-2
f1 (ppm)

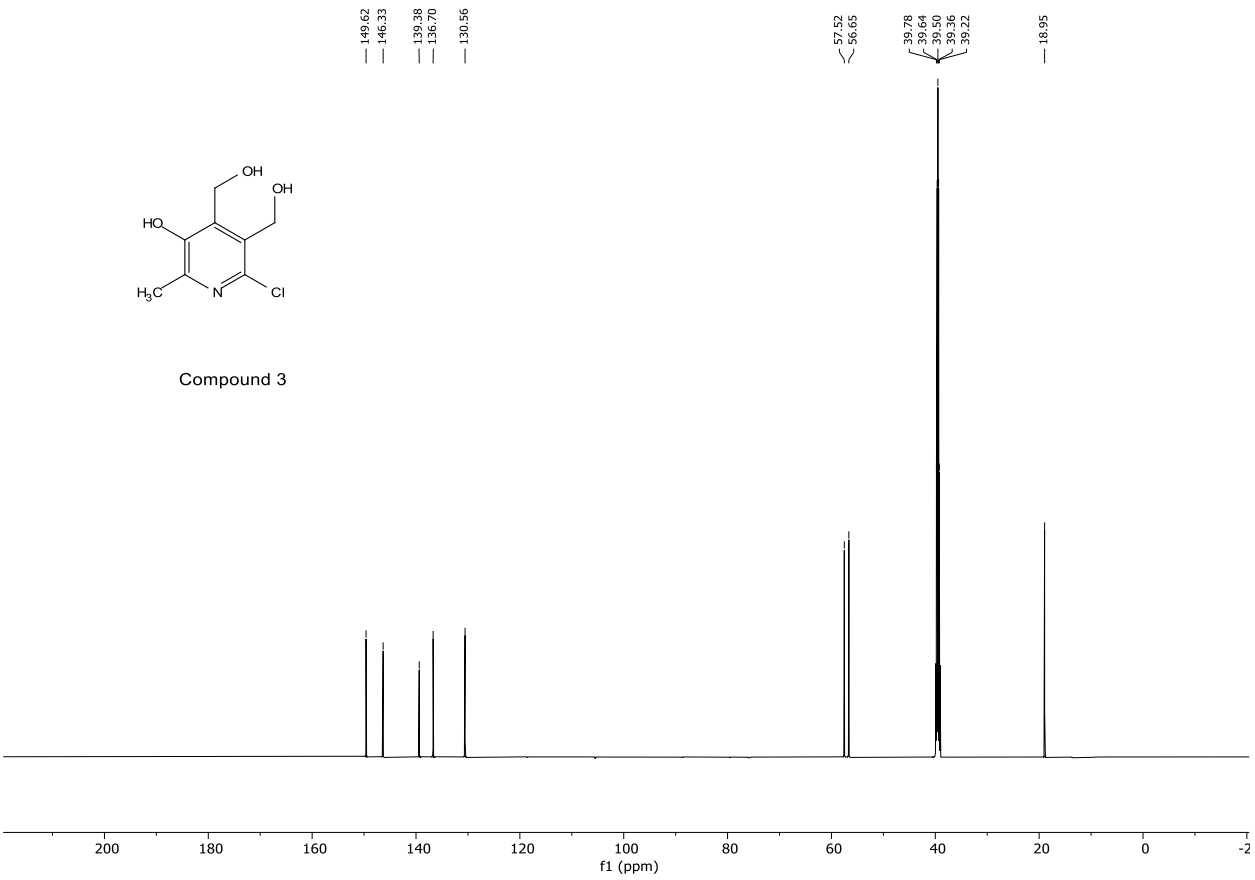
149.62
146.33
139.38
136.70
130.56
57.52
56.65
39.78
39.64
39.50
39.36
39.22
18.95
OH
OH
HO
H3C
N
Cl
Compound 3
200
180
160
140
120
100
80
60
40
20
0
-2
f1 (ppm)

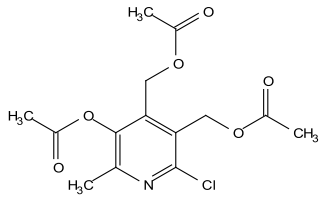
H3C
O
O
H3C
O
O
O
CH3
H3C
N
Cl

compound 4

7.26
5.36
5.17
2.39
2.38
2.08
2.02
1.79
1.78
2.57
2.97
2.63
2.67
14
12
10
8
6
4
2
0
f1 (ppm)

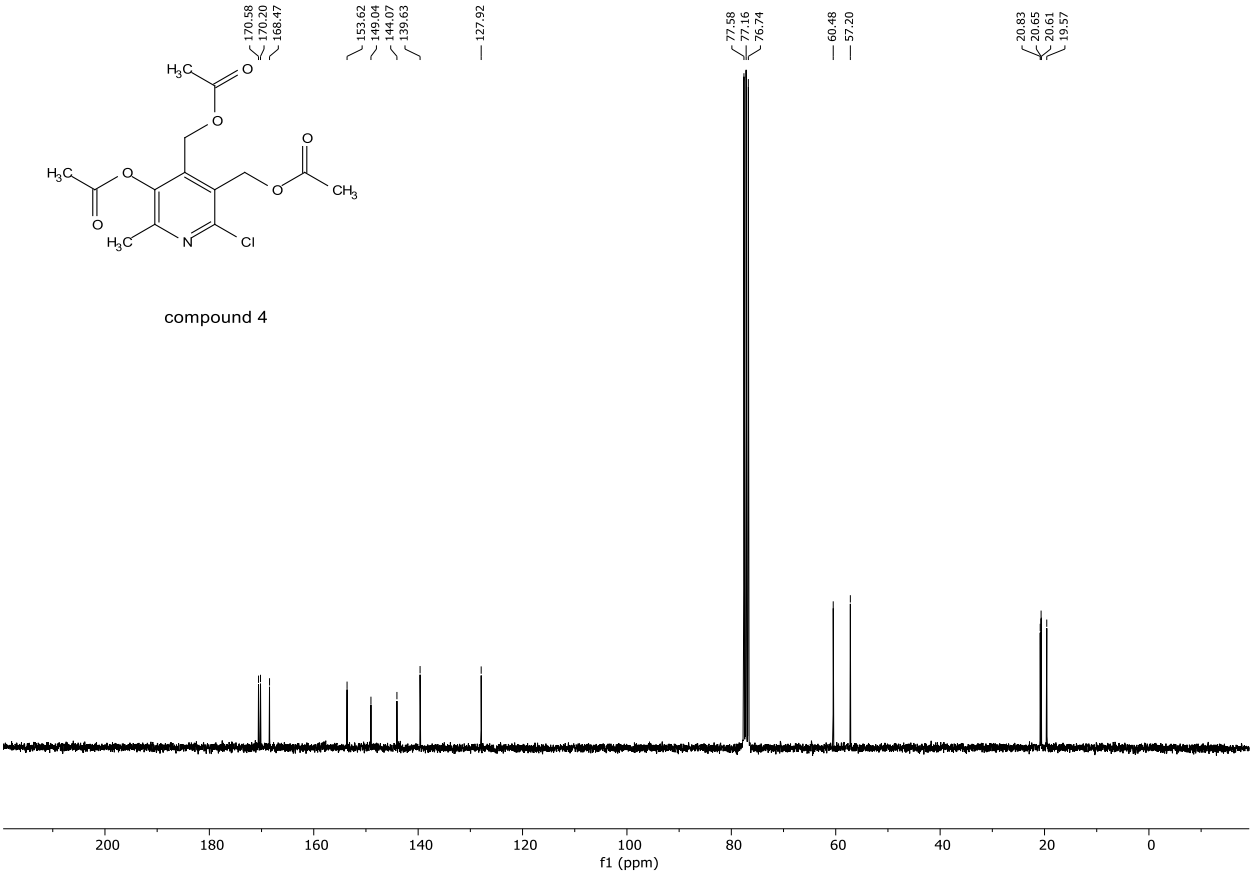
170.58
170.20
168.47
153.62
149.04
144.07
139.63
127.92
77.58
77.16
76.74
60.48
57.20
20.83
20.65
20.61
19.57
compound 4
200
180
160
140
120
100
80
60
40
20
0
f1 (ppm)

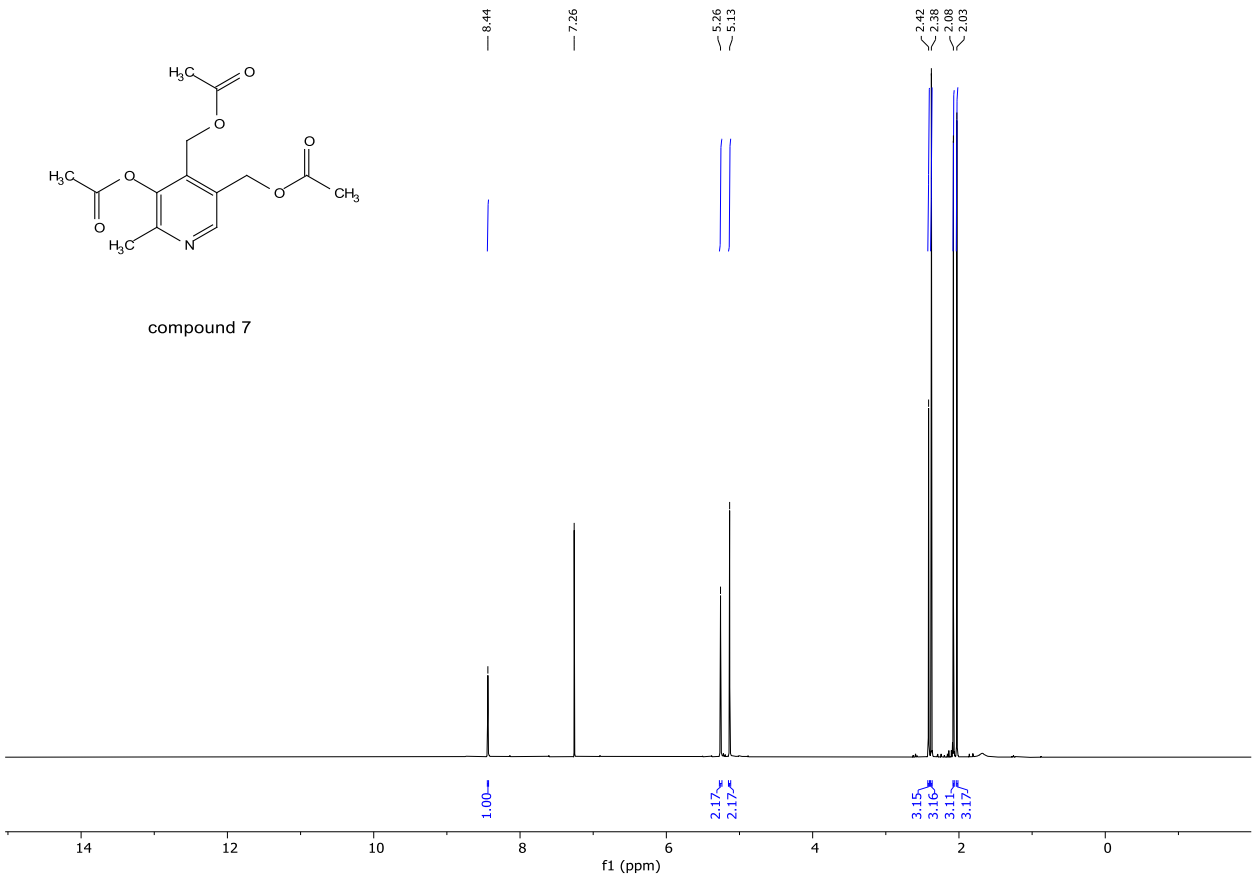
compound 7
8.44
7.26
5.26
5.13
2.42
2.38
2.08
2.03
1.00
2.17
2.17
3.15
3.16
3.11
3.17
14
12
10
8
6
4
2
0
f1 (ppm)

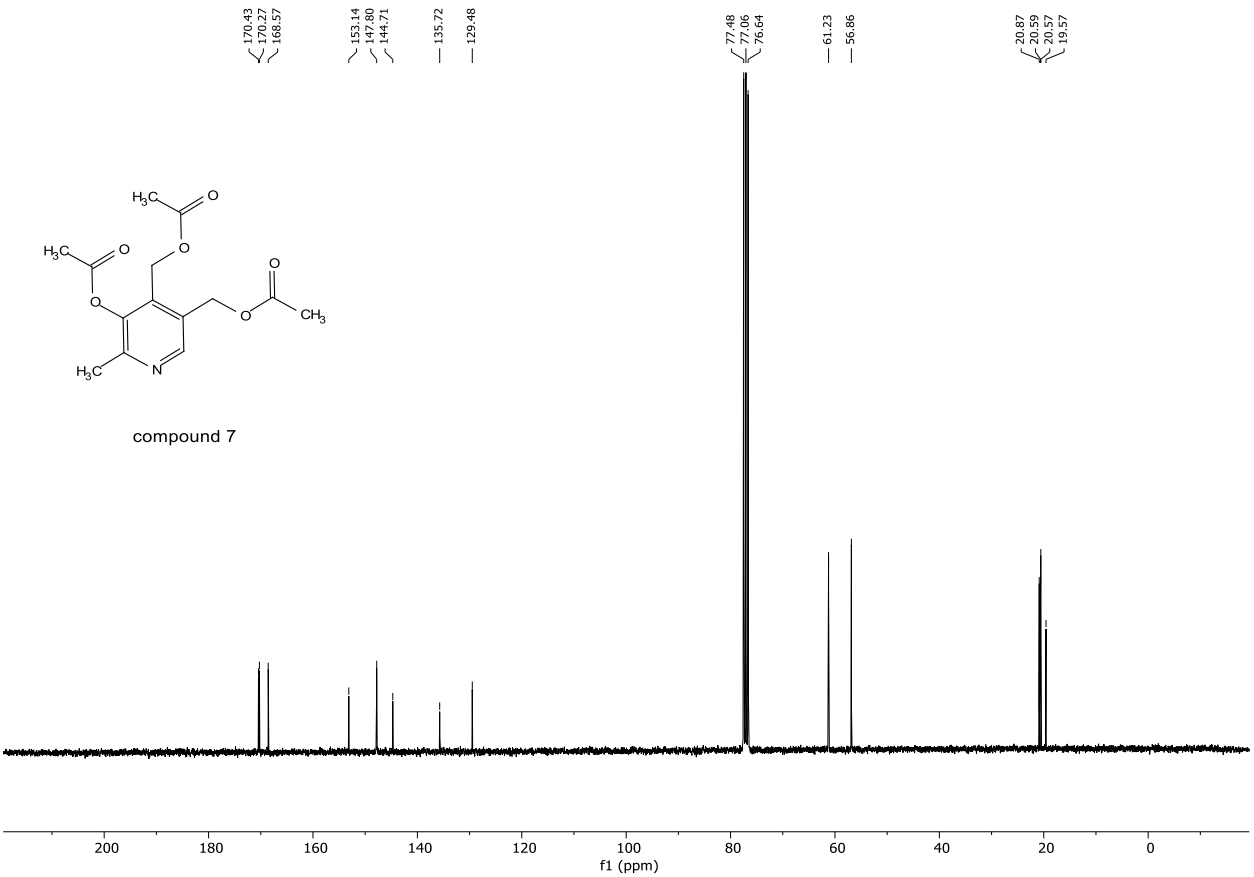
170.43
170.27
168.57
153.14
147.80
144.71
135.72
129.48
77.48
77.06
76.64
61.23
56.86
20.87
20.59
20.57
19.57
compound 7
200
180
160
140
120
100
80
60
40
20
0
f1 (ppm)

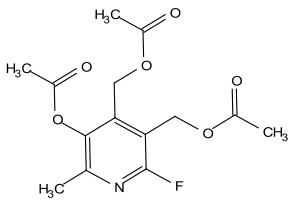
H3C
O
O
H3C
O
O
O
CH3
H3C
N
F

Compound 12

7.26
5.26
5.16
2.37
2.34
2.34
2.06
2.02
1.47
1.52
2.69
2.73
2.36
2.73
14
12
10
8
6
4
2
0
f1 (ppm)

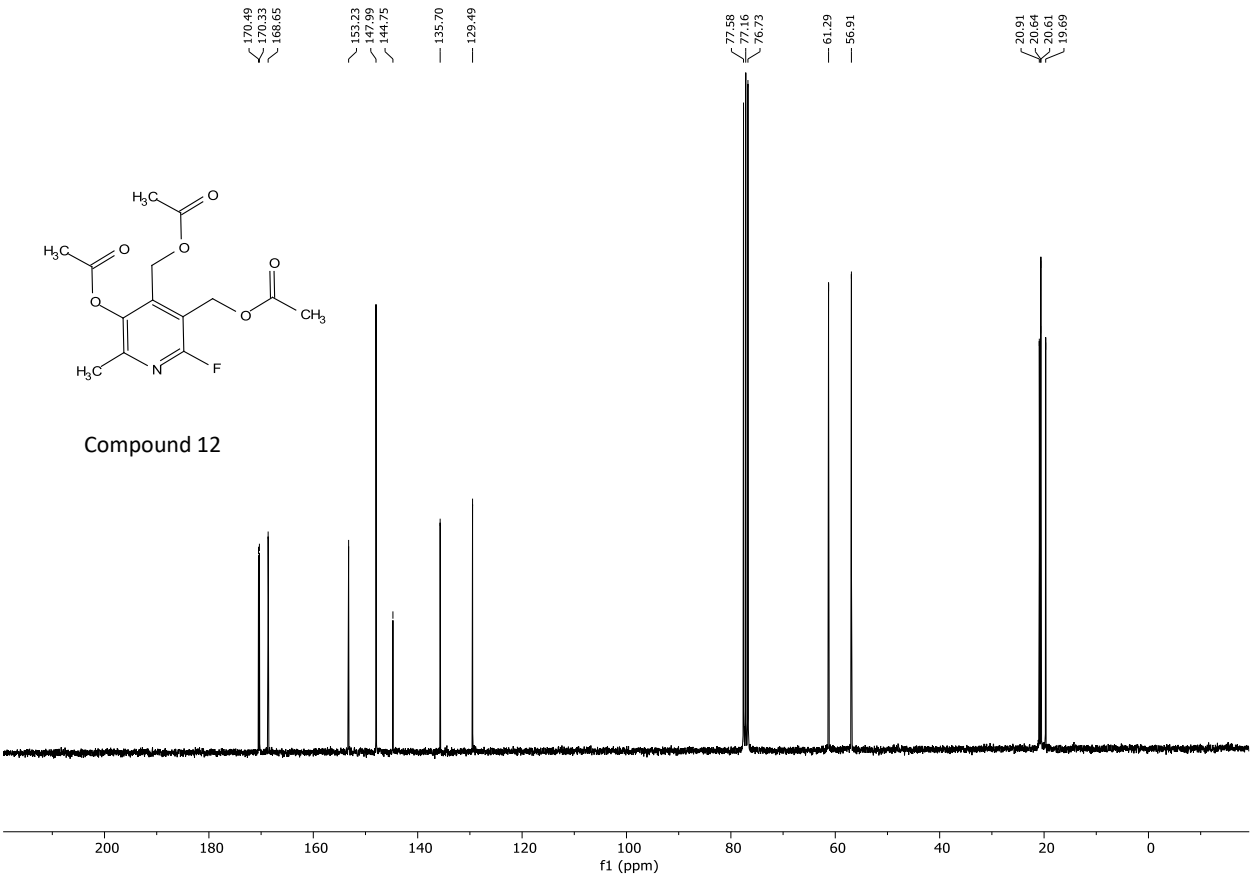
170.49
170.33
168.65
153.23
147.99
144.75
135.70
129.49
77.58
77.16
76.73
61.29
56.91
20.91
20.64
20.61
19.69
Compound 12
200
180
160
140
120
100
80
60
40
20
0
f1 (ppm)

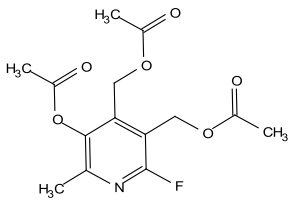

Compound 12

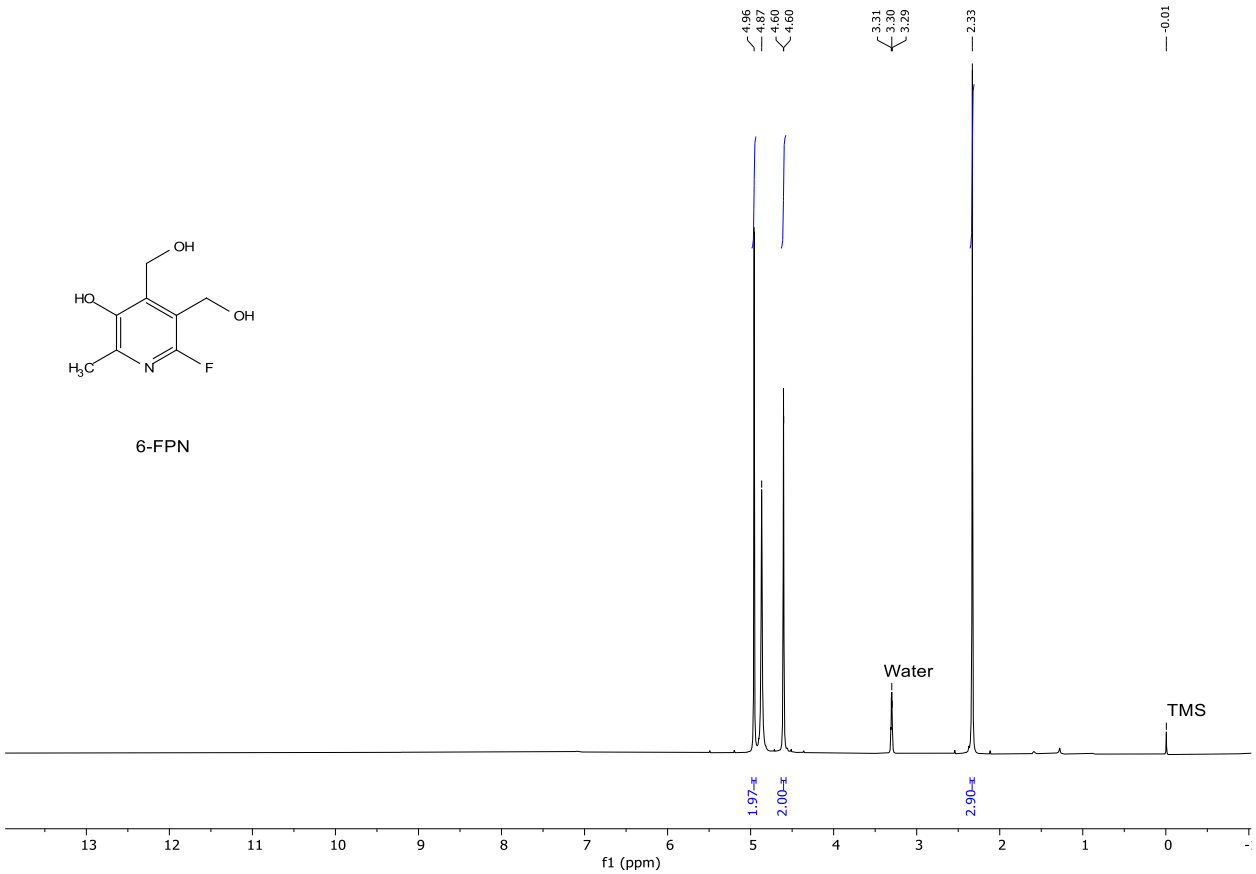
4.96
4.87
4.60
4.60
3.31
3.30
3.29
2.33
-0.01
OH
HO
OH
H3C
N
F
6-FPN
Water
TMS
1.97
2.00
2.90
13
12
11
10
9
8
7
6
5
4
3
2
1
0
f1 (ppm)

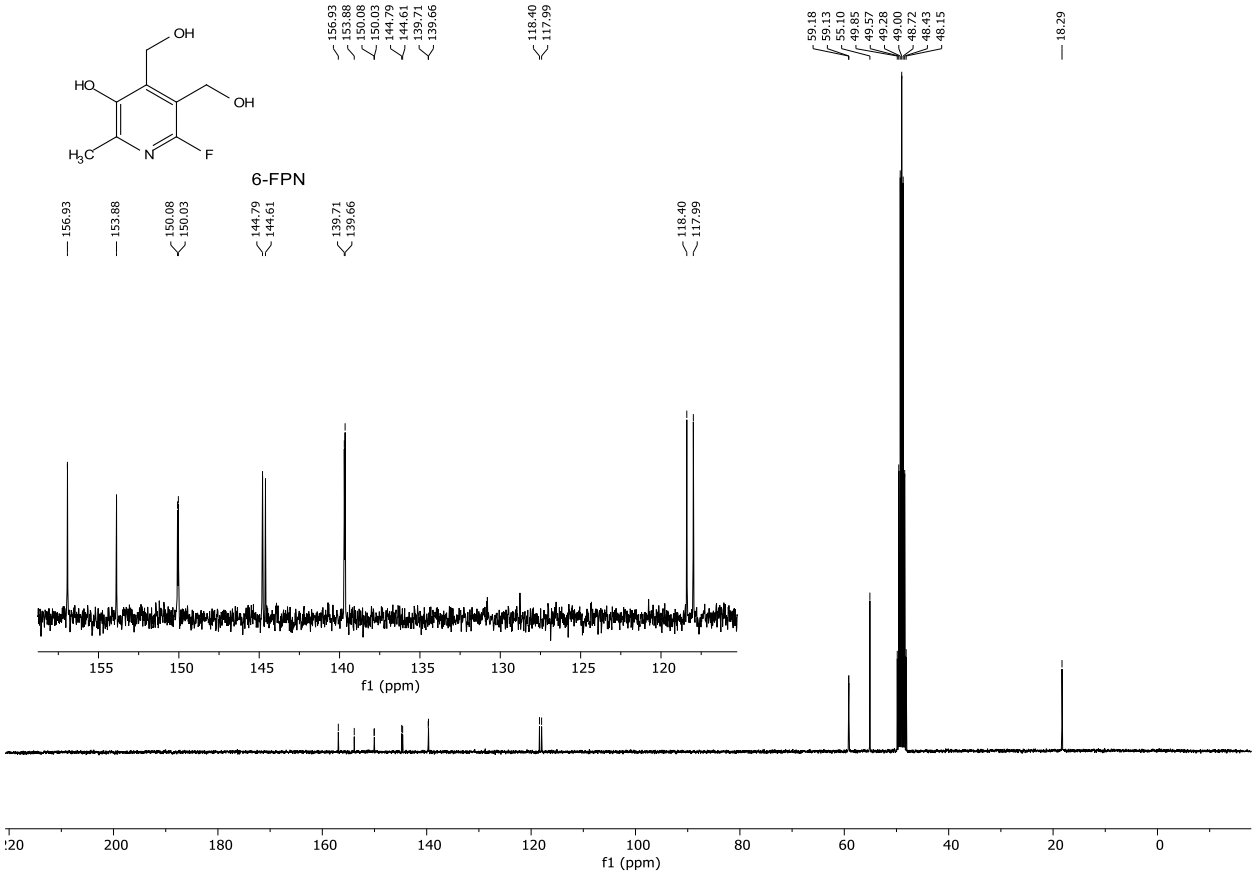
OH
HO
OH
H_3C
N
F
6-FPN
156.93
153.88
150.08
150.03
144.79
144.61
139.71
139.66
118.40
117.99
59.18
59.13
55.10
49.85
49.57
49.28
49.00
48.72
48.43
48.15
18.29
f1 (ppm)

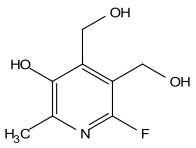

6-FPN

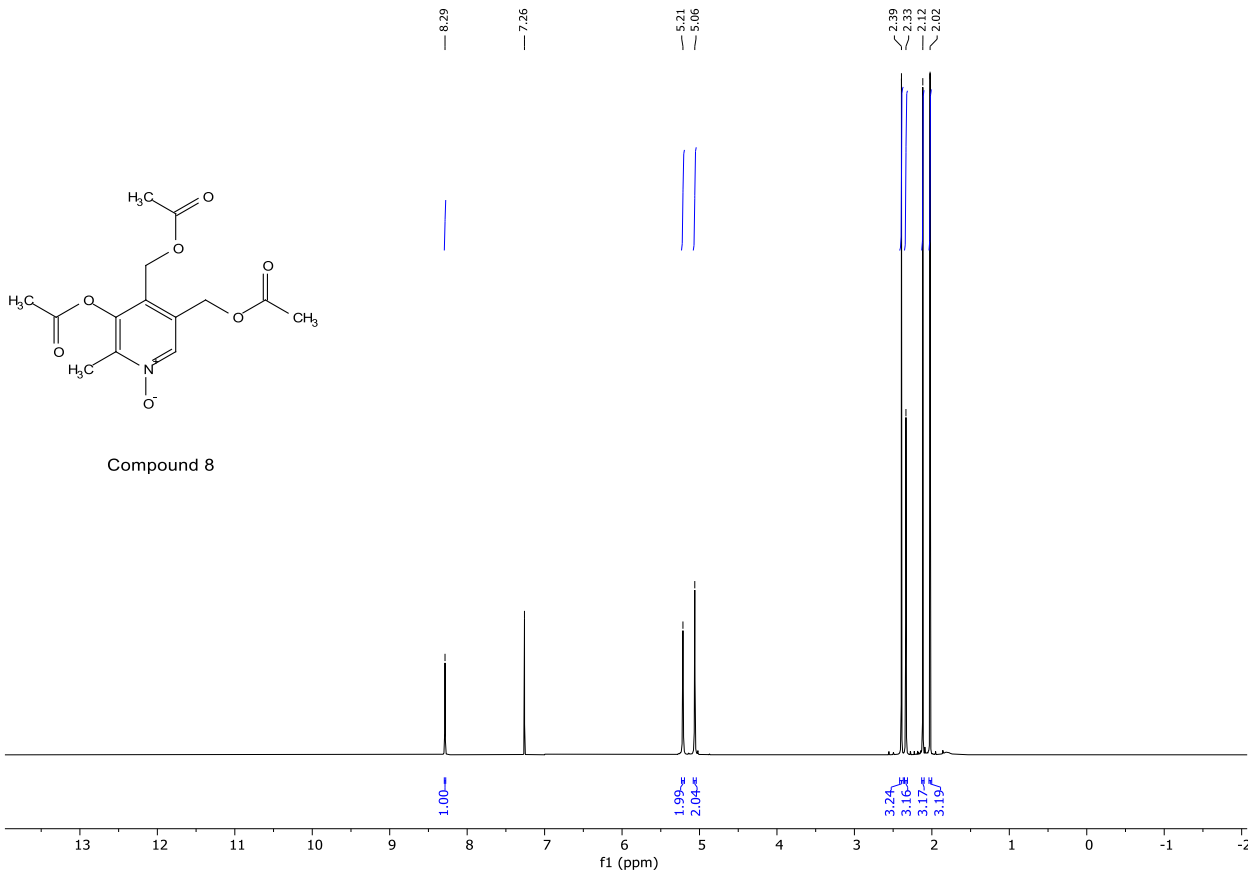
8.29
7.26
5.21
5.06
2.39
2.33
2.12
2.02
1.00
1.99
2.04
3.24
3.16
3.17
3.19
13
12
11
10
9
8
7
6
5
4
3
2
1
0
-1
f1 (ppm)

Compound 8

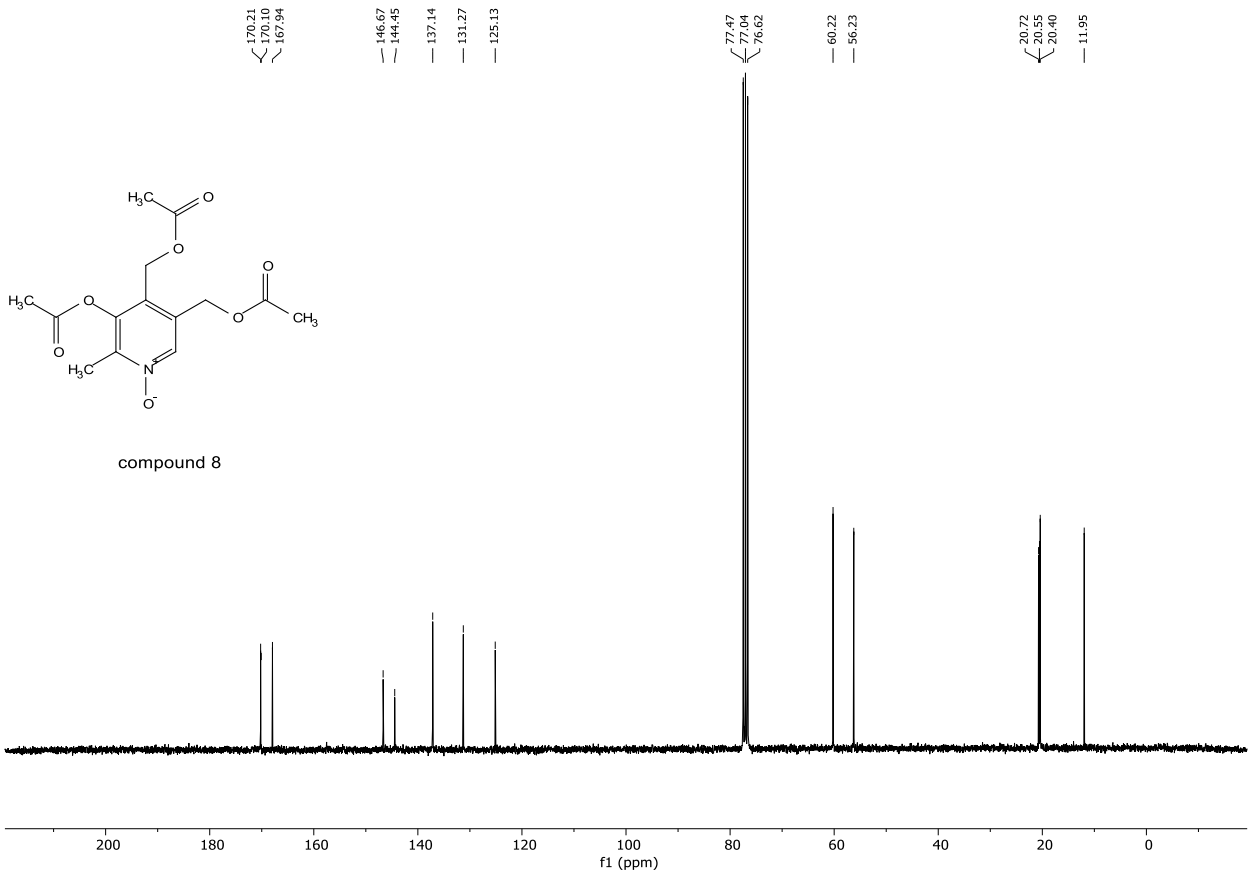
170.21
170.10
167.94
146.67
144.45
137.14
131.27
125.13
77.47
77.04
76.62
60.22
56.23
20.72
20.55
20.40
11.95
compound 8
200
180
160
140
120
100
80
60
40
20
0
f1 (ppm)

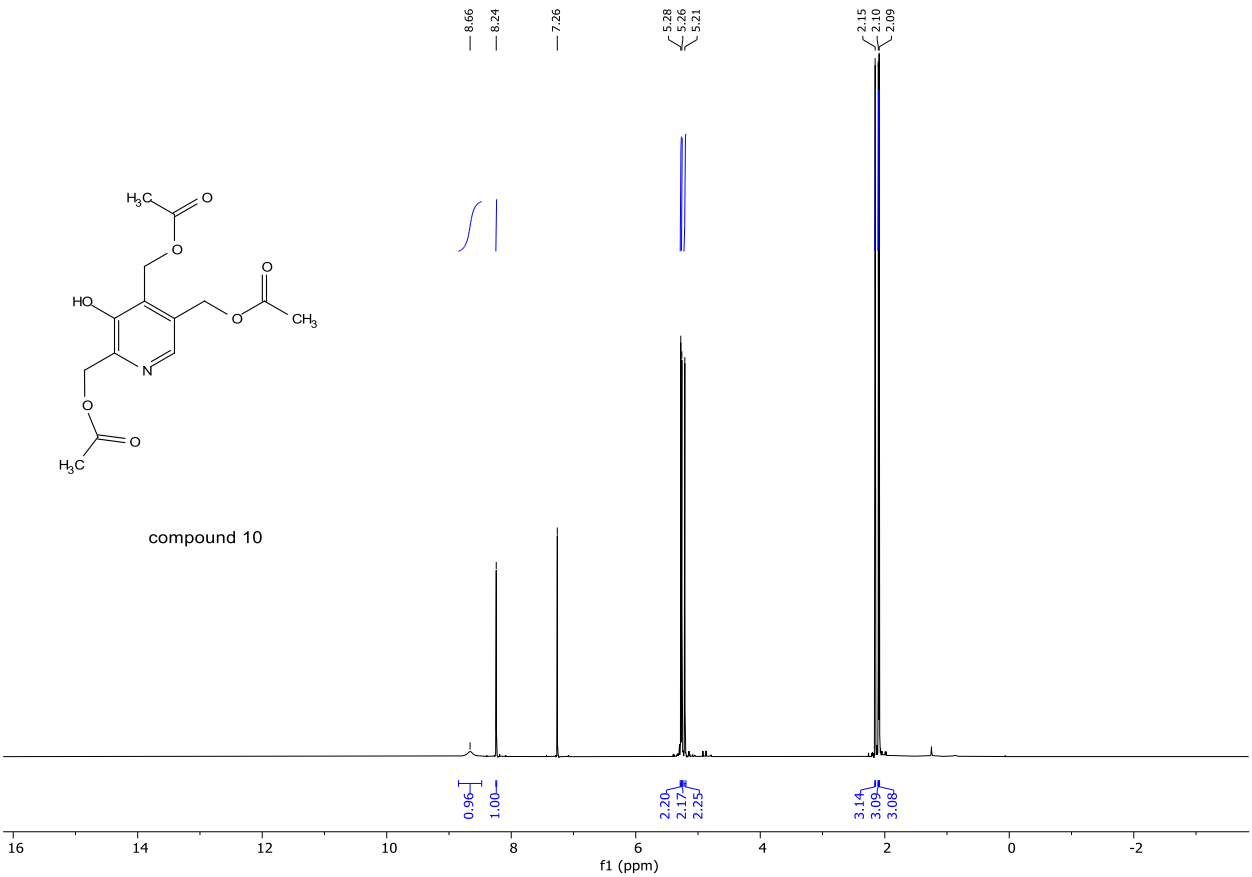
8.66
8.24
7.26
5.28
5.26
5.21
2.15
2.10
2.09
compound 10
0.96
1.00
2.20
2.17
2.25
3.14
3.09
3.08
16
14
12
10
8
6
4
2
0
-2
f1 (ppm)

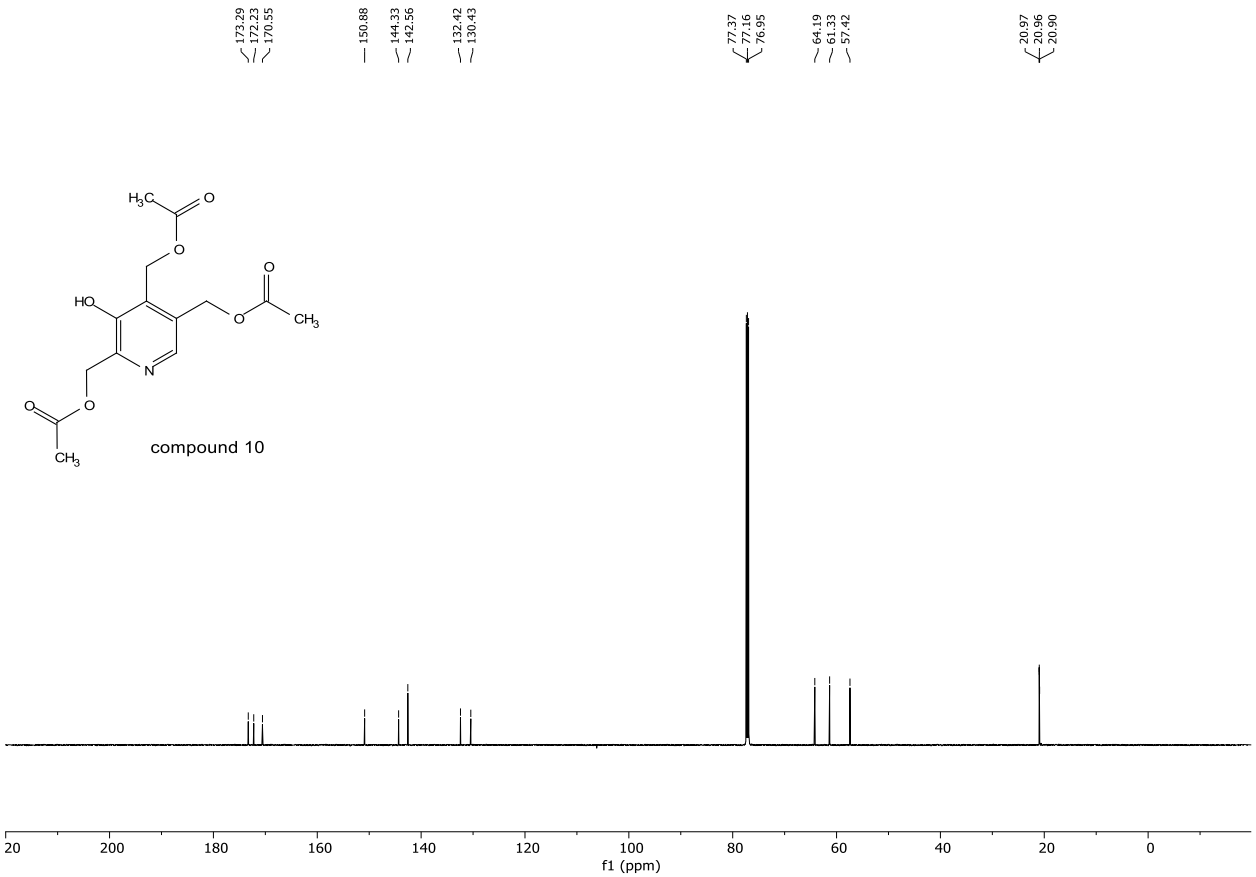
173.29
172.23
170.55
150.88
144.33
142.56
132.42
130.43
77.37
77.16
76.95
64.19
61.33
57.42
20.97
20.96
20.90
HO
N
O
CH3
compound 10
20
200
180
160
140
120
100
80
60
40
20
0
f1 (ppm)

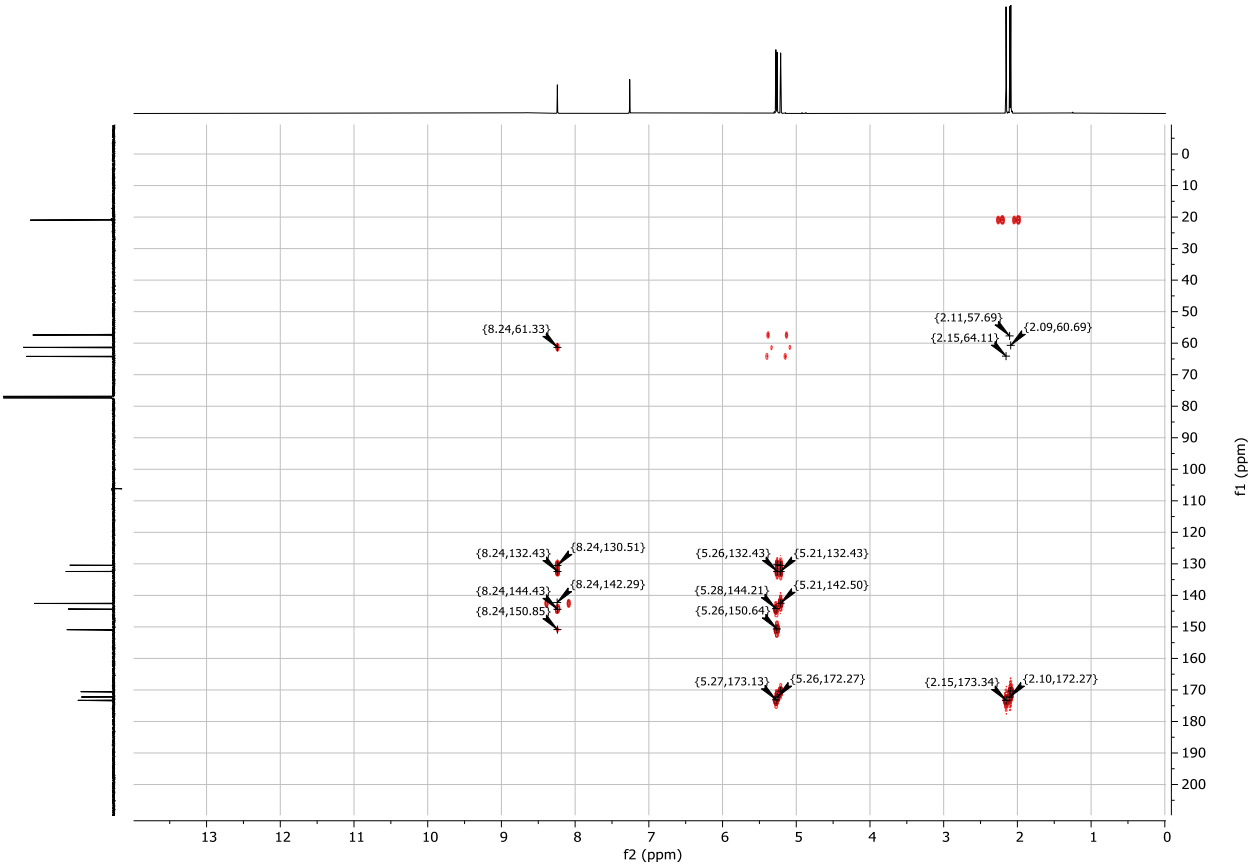
{8.24,61.33}
{2.11,57.69}
{2.15,64.11}
{2.09,60.69}
{8.24,132.43}
{8.24,130.51}
{8.24,144.43}
{8.24,142.29}
{8.24,150.85}
{5.26,132.43}
{5.21,132.43}
{5.28,144.21}
{5.21,142.50}
{5.26,150.64}
{5.27,173.13}
{5.26,172.27}
{2.15,173.34}
{2.10,172.27}
f2 (ppm)
f1 (ppm)

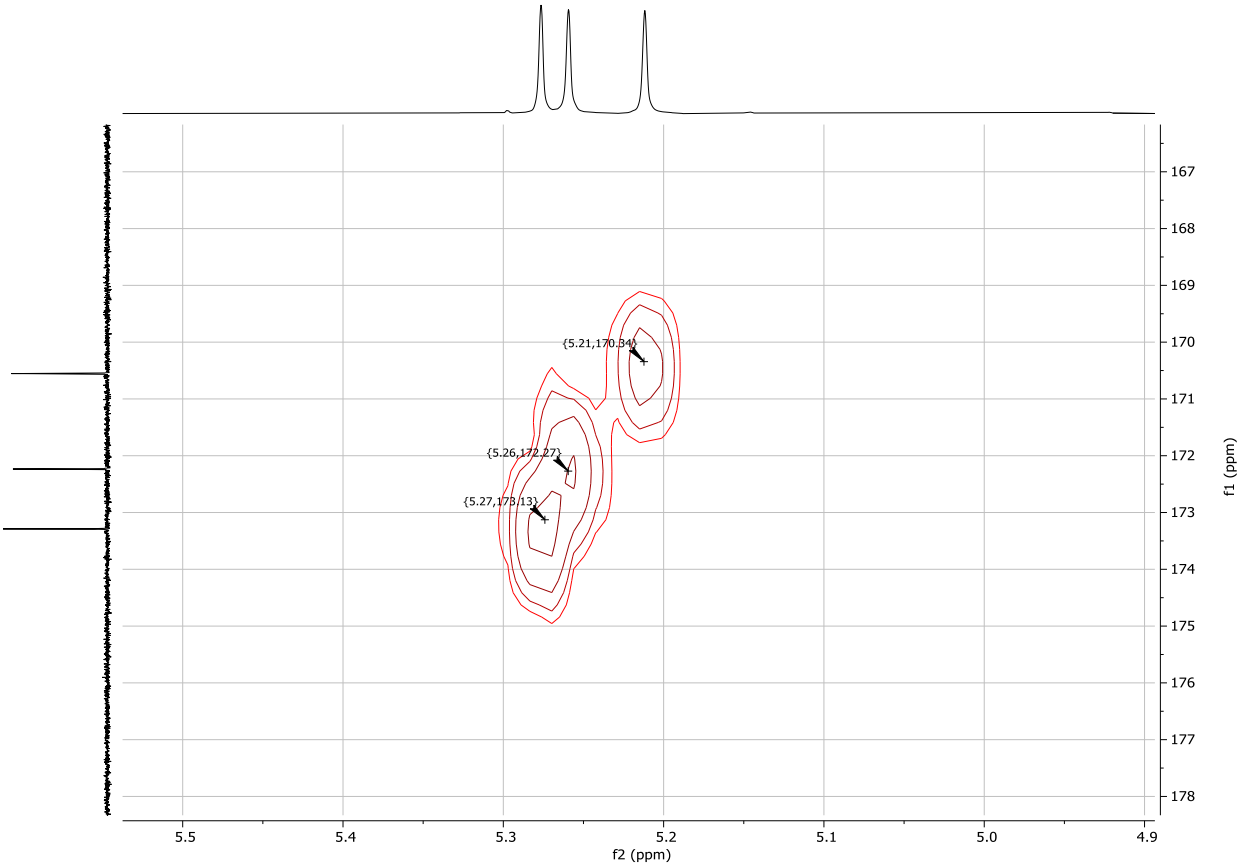
{5.21,170.34}
{5.26,172.27}
{5.27,173.13}
167
168
169
170
171
172
173
174
175
176
177
178
f1 (ppm)
5.5
5.4
5.3
5.2
5.1
5.0
4.9
f2 (ppm)

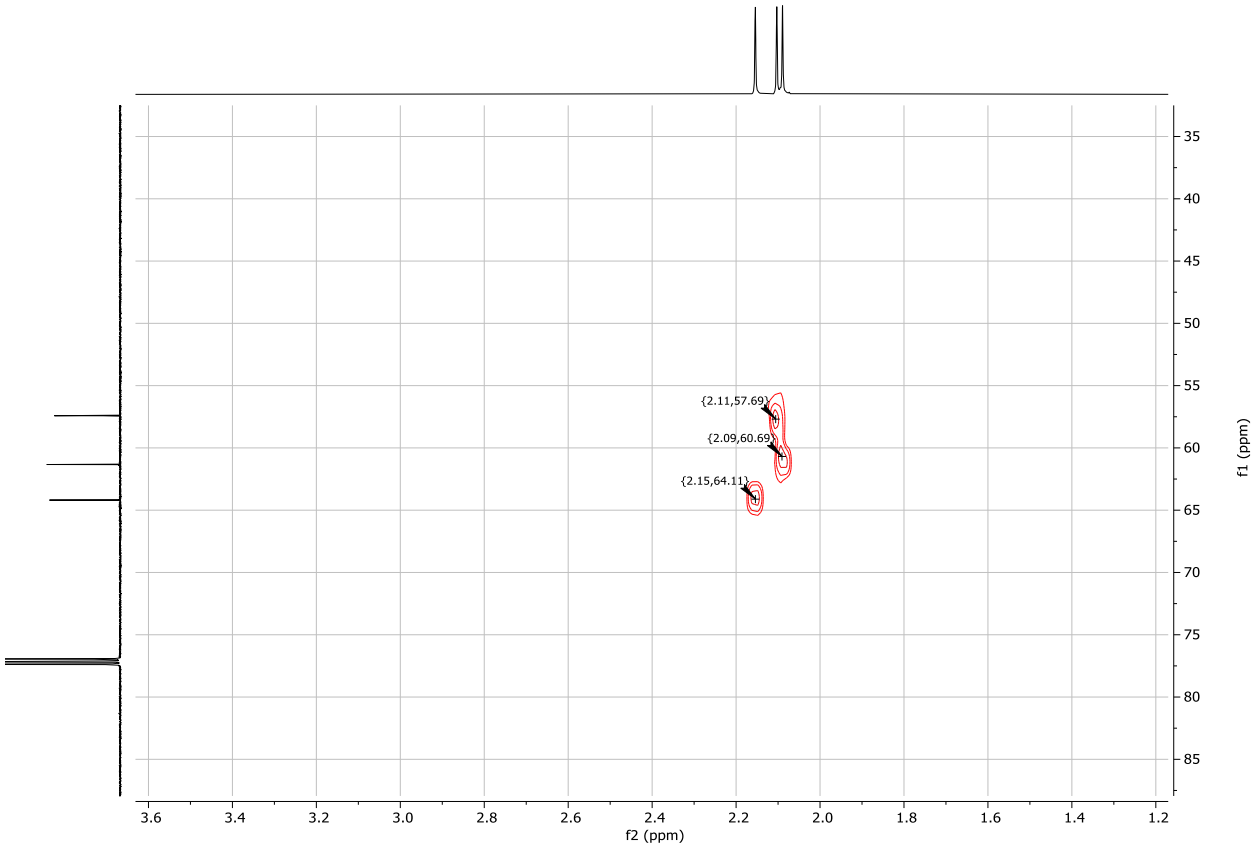
{2.11,57.69}
{2.09,60.69}
{2.15,64.11}
35
40
45
50
55
60
65
70
75
80
85
f1 (ppm)
3.6
3.4
3.2
3.0
2.8
2.6
2.4
2.2
2.0
1.8
1.6
1.4
1.2
f2 (ppm)

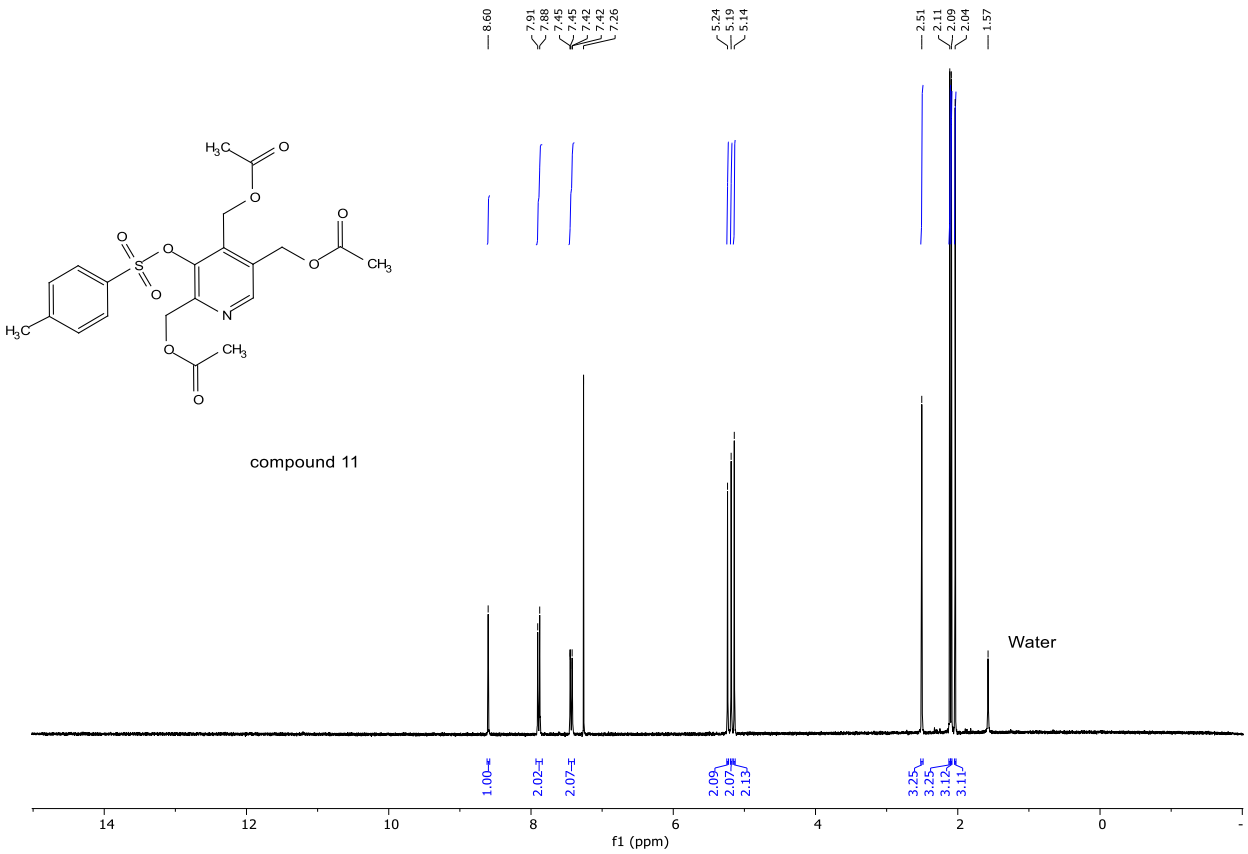
8.60
7.91
7.88
7.45
7.45
7.42
7.42
7.26
5.24
5.19
5.14
2.51
2.11
2.09
2.04
1.57
compound 11
Water
1.00
2.02
2.07
2.09
2.07
2.13
3.25
3.25
3.12
3.11
14
12
10
8
6
4
2
0
f1 (ppm)

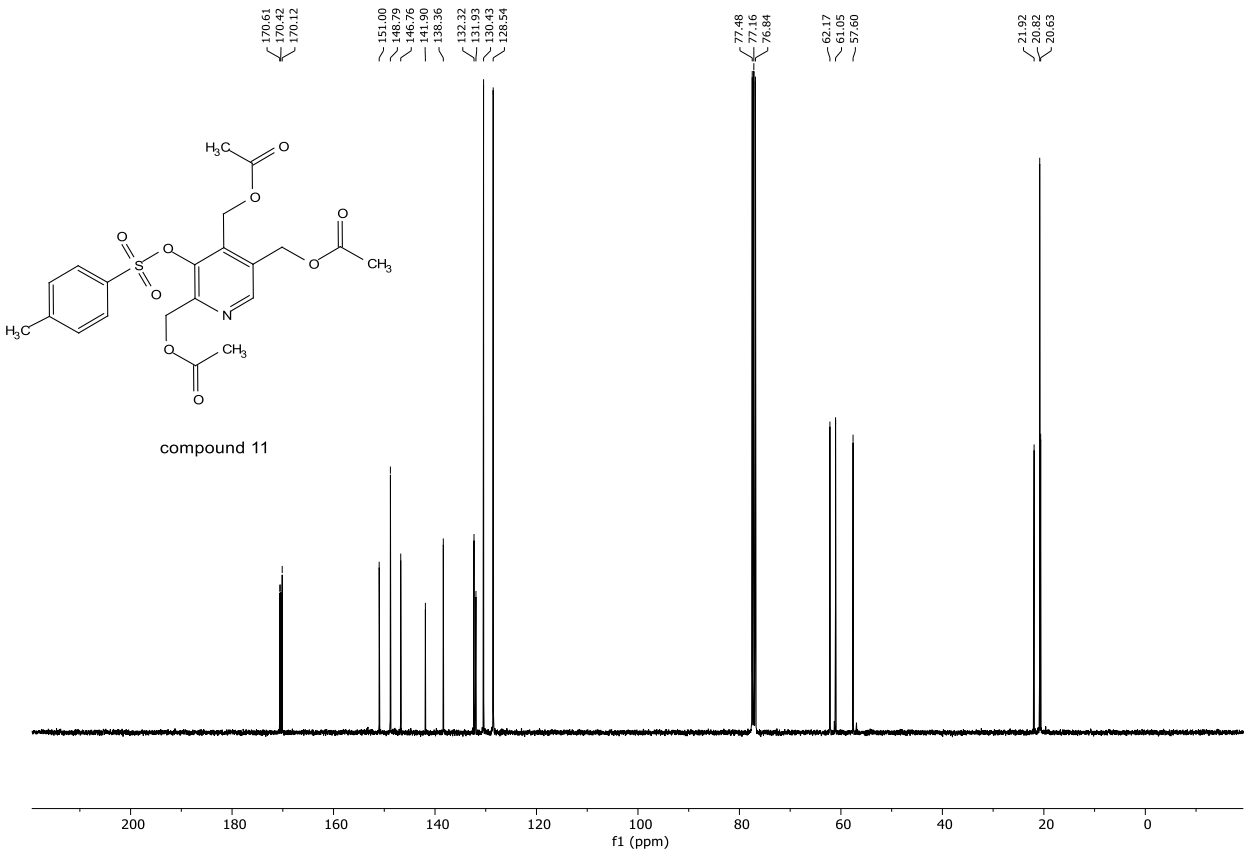
170.61
170.42
170.12
151.00
148.79
146.76
141.90
138.36
132.32
131.93
130.43
128.54
77.48
77.16
76.84
62.17
61.05
57.60
21.92
20.82
20.63
compound 11
200
180
160
140
120
100
80
60
40
20
0
f1 (ppm)

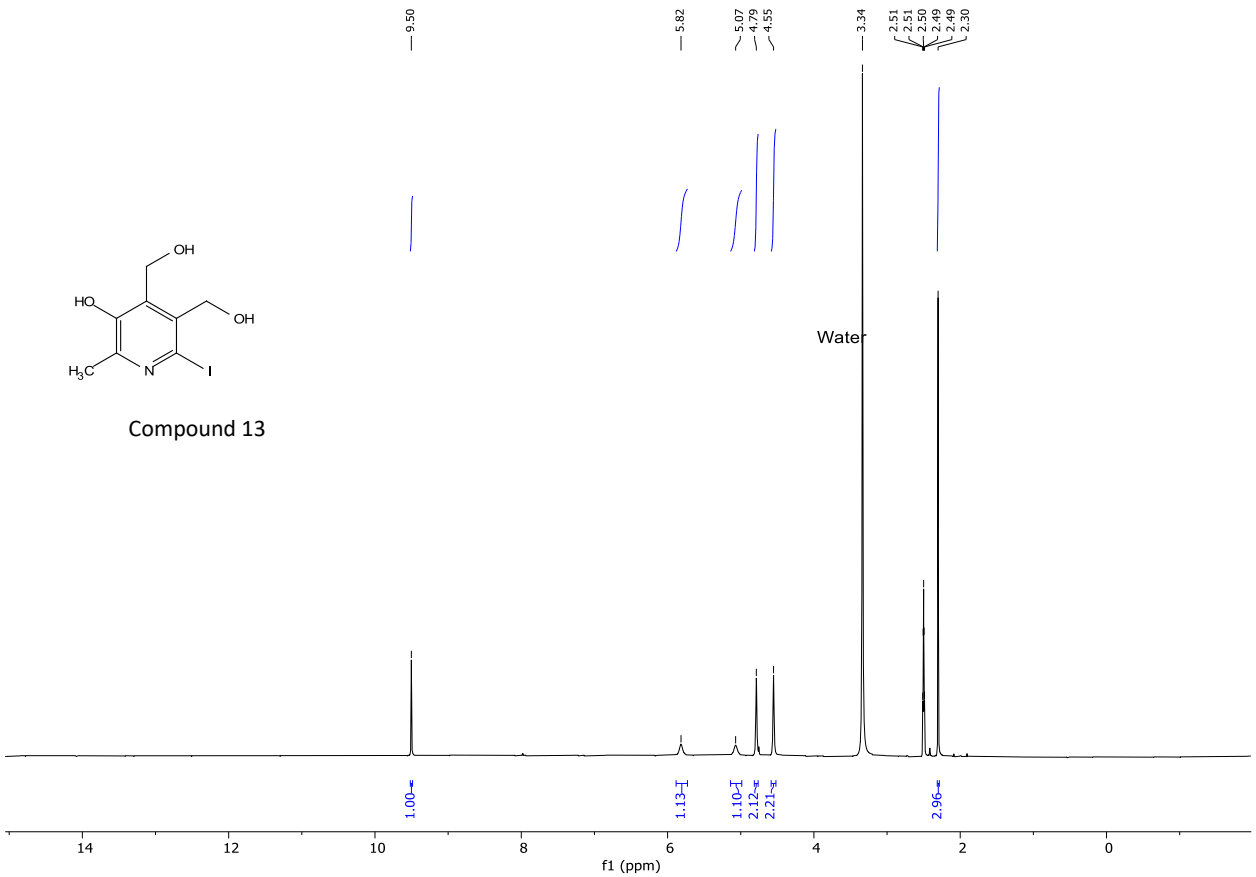
9.50
5.82
5.07
4.79
4.55
3.34
2.51
2.51
2.50
2.49
2.49
2.30
Water
OH
HO
OH
H3C
N
I
1.00
1.13
1.10
2.12
2.21
2.96
14
12
10
8
6
4
2
0
f1 (ppm)

Compound 13

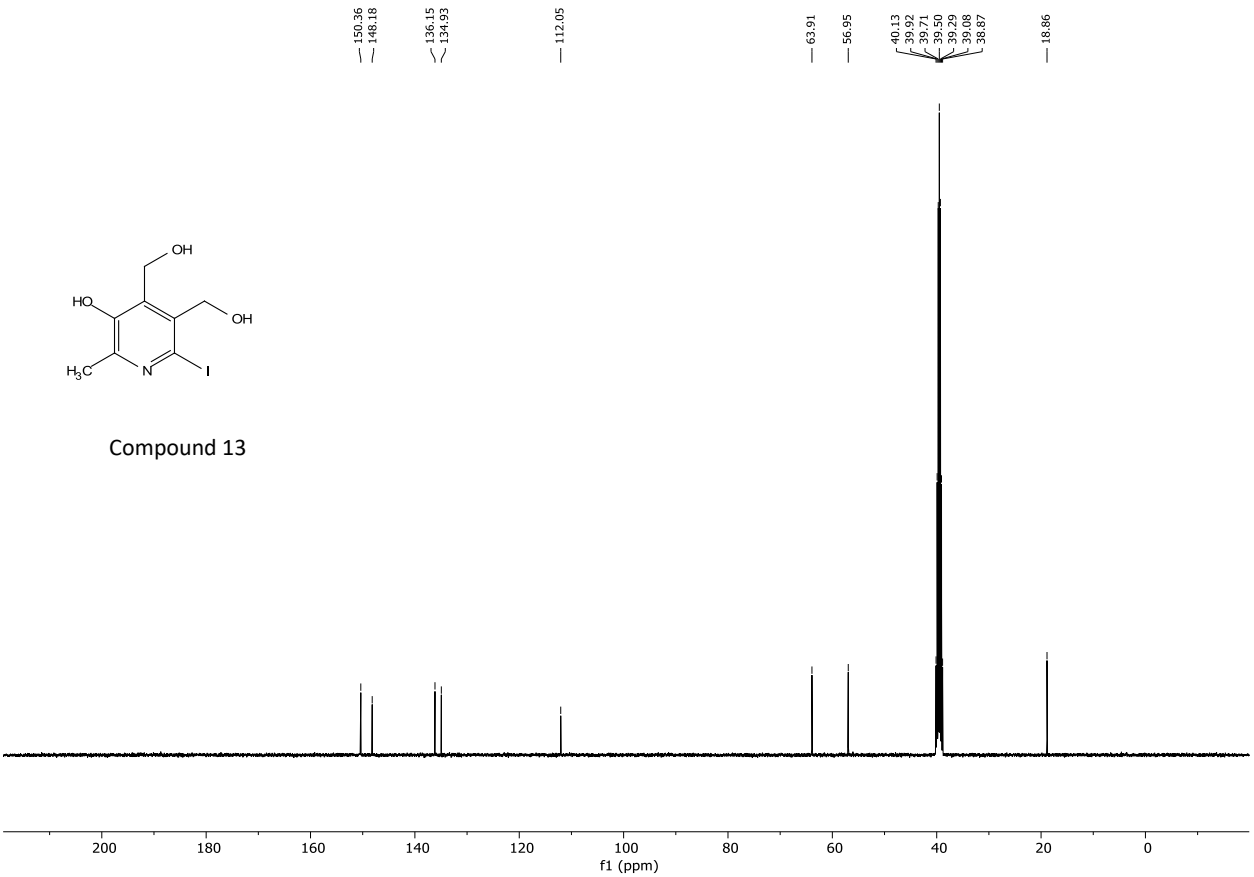
150.36
148.18
136.15
134.93
112.05
63.91
56.95
40.13
39.92
39.71
39.50
39.29
39.08
38.87
18.86
OH
HO
OH
H3C
N
I
200
180
160
140
120
100
80
60
40
20
0
f1 (ppm)

Compound 13

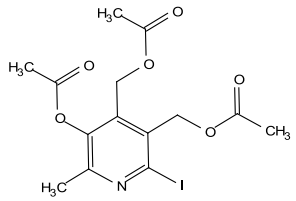

Compound 14

7.26
5.33
5.15
2.39
2.37
2.09
2.02
1.97
2.01
3.08
2.90
2.99
2.98
13
12
11
10
9
8
7
6
5
4
3
2
1
0
-1
f1 (ppm)

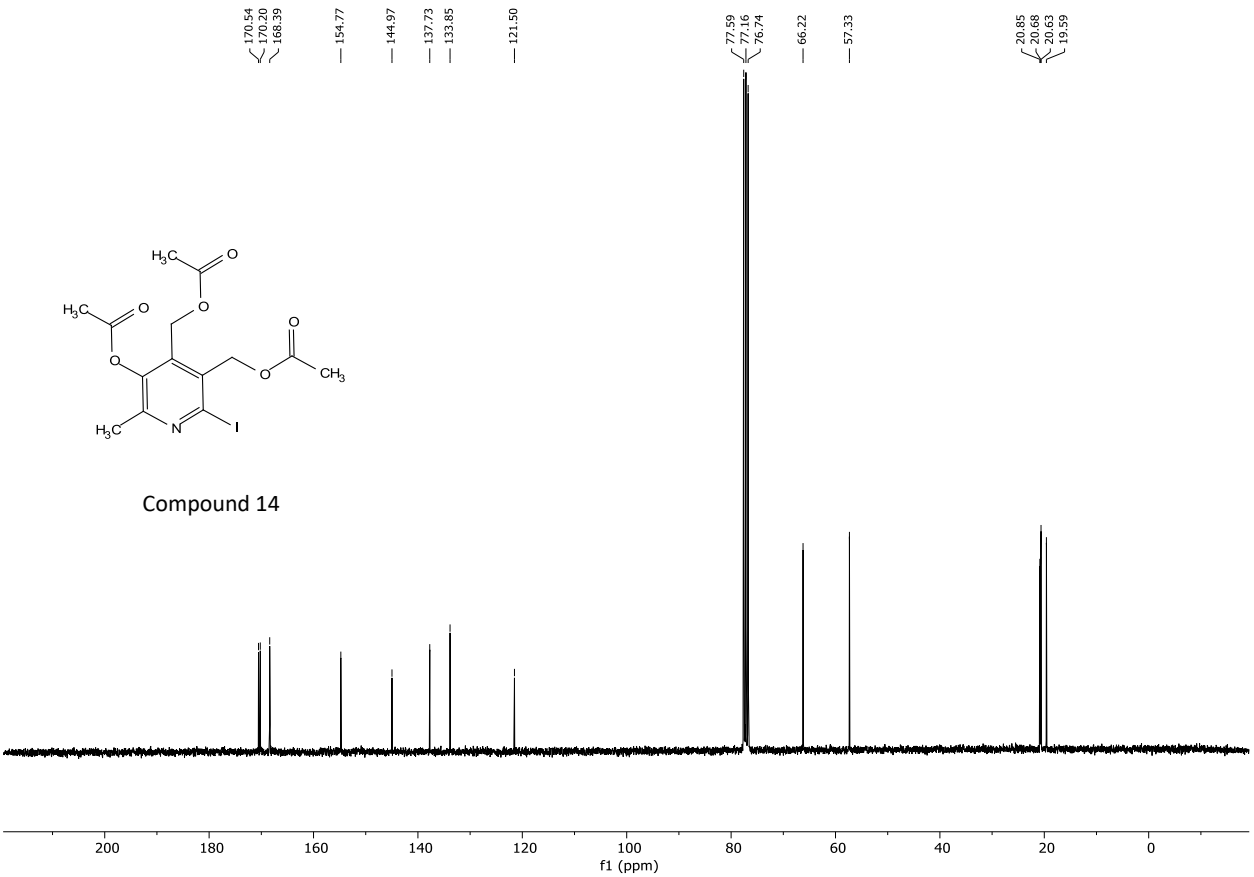
170.54
170.20
168.39
154.77
144.97
137.73
133.85
121.50
77.59
77.16
76.74
66.22
57.33
20.85
20.68
20.63
19.59
200
180
160
140
120
100
80
60
40
20
0
f1 (ppm)

Compound 14

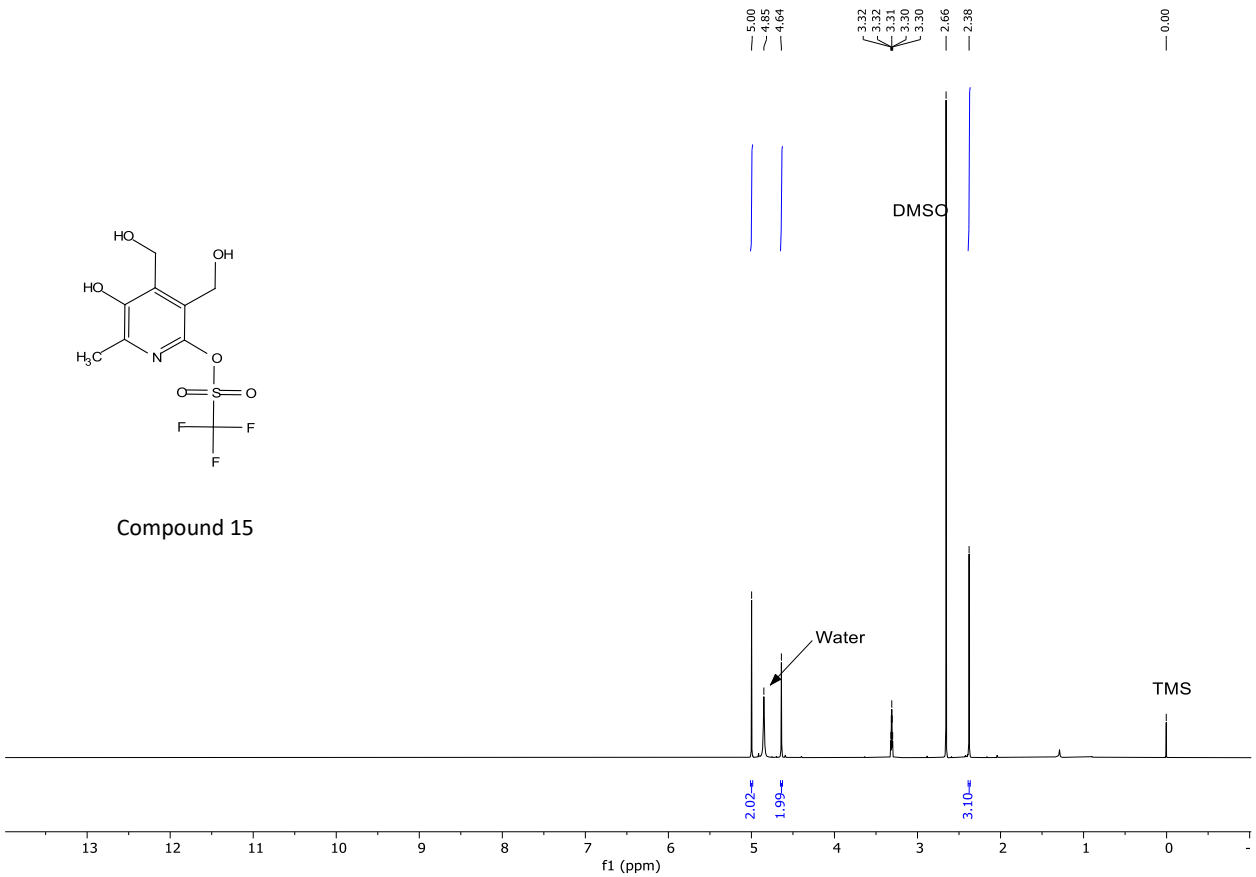
HO
OH
HO
H_3C
N
O
O=S=O
F
F
F
Compound 15
5.00
4.65
4.64
3.32
3.32
3.31
3.30
3.30
2.66
2.38
0.00
DMSO
Water
TMS
2.02
1.99
3.10
13
12
11
10
9
8
7
6
5
4
3
2
1
0
f1 (ppm)

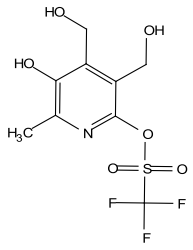
HO
OH
HO
H_3C
N
O
O
S
O
F
F
F

Compound 15

-74.92
0
-20
-40
-60
-80
-100
-120
-140
-160
-180
-200
f1 (ppm)

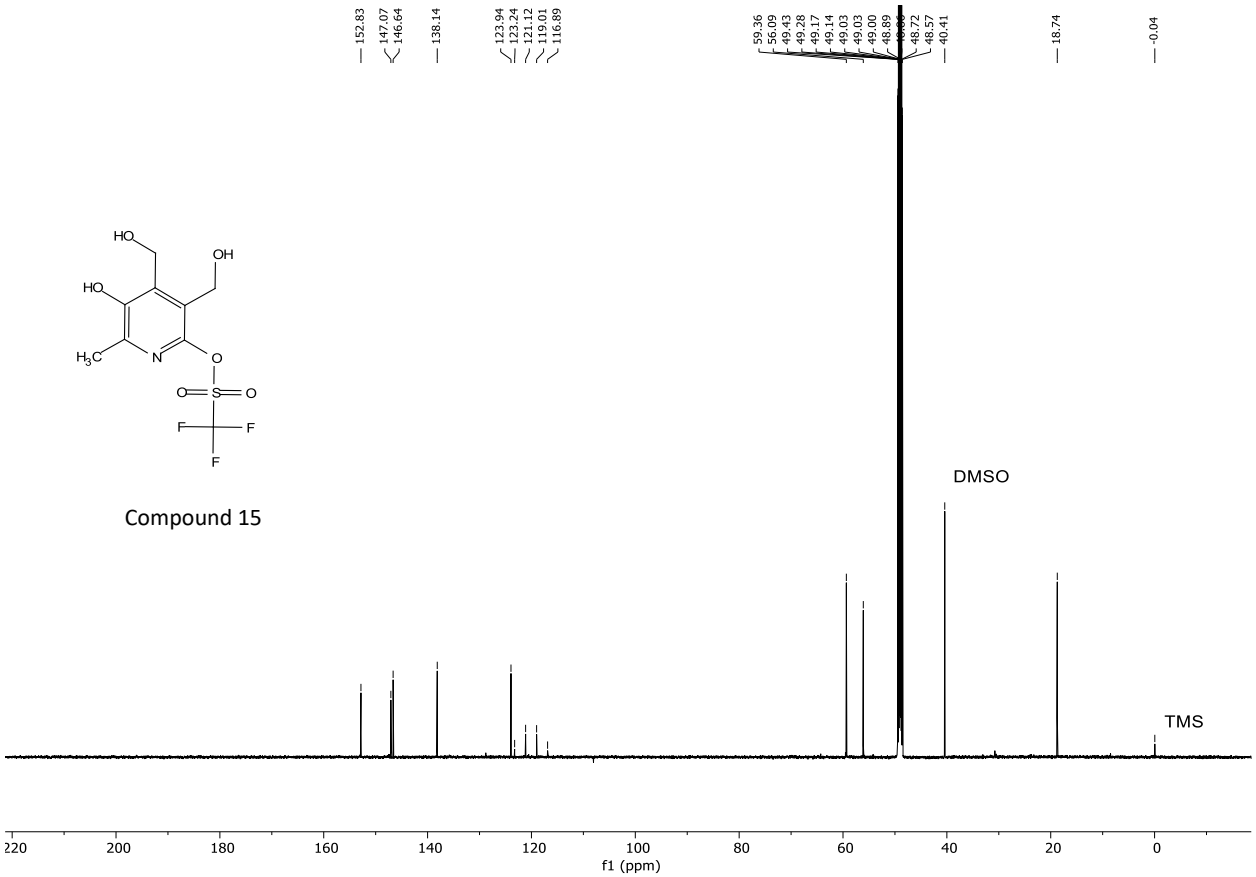
152.83
147.07
146.64
138.14
123.94
123.24
121.12
119.01
116.89
59.36
56.09
49.43
49.28
49.17
49.14
49.03
49.03
49.00
48.89
48.72
48.57
40.41
18.74
-0.04
HO
OH
HO
H_3C
N
O
O=S=O
F
F
F
DMSO
TMS
220
200
180
160
140
120
100
80
60
40
20
0
f1 (ppm)

Compound 15

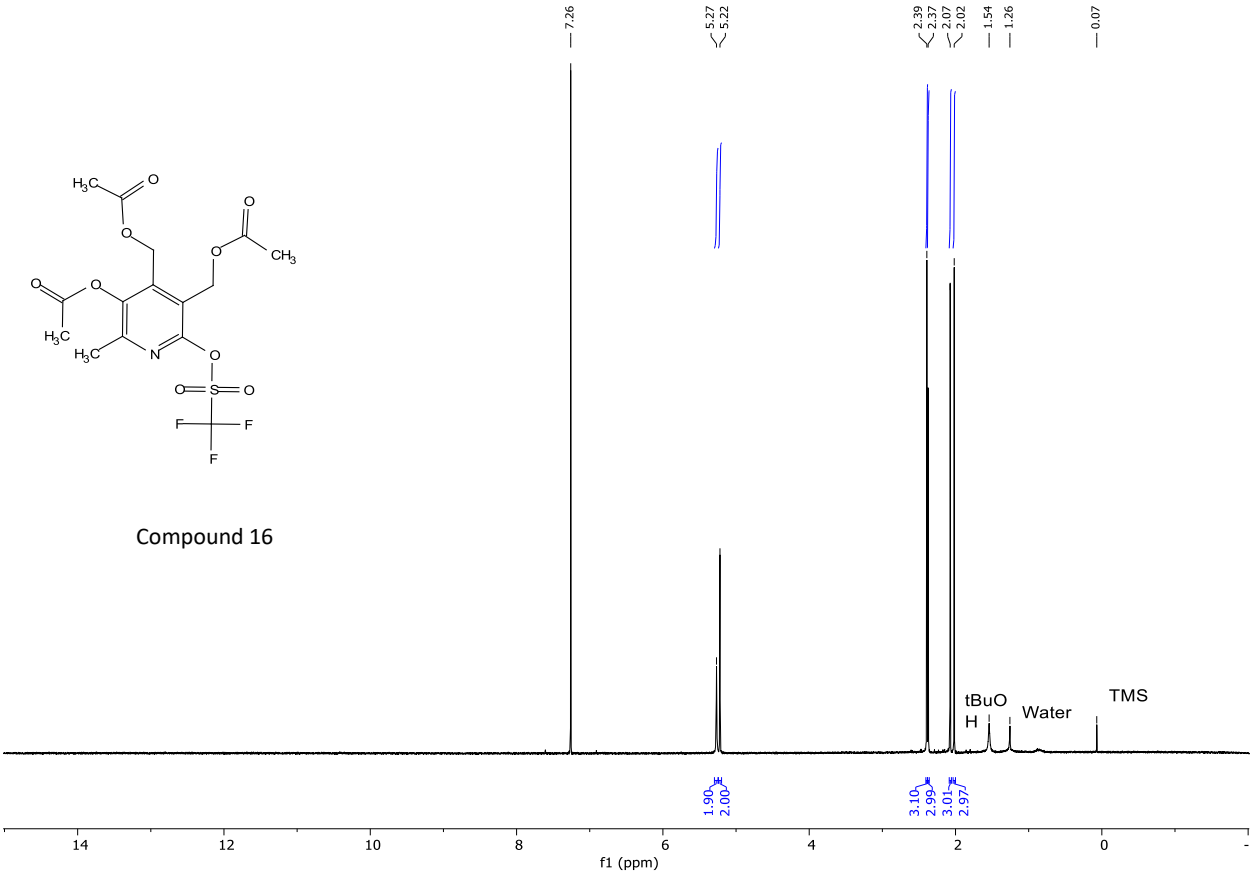
7.26
5.27
5.22
2.39
2.37
2.07
2.02
1.54
1.26
0.07
tBuO
H
Water
TMS
1.90
2.00
3.10
2.99
3.01
2.97
14
12
10
8
6
4
2
0
f1 (ppm)

Compound 16

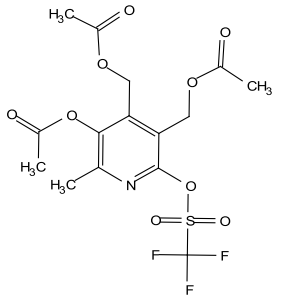

Compound 16

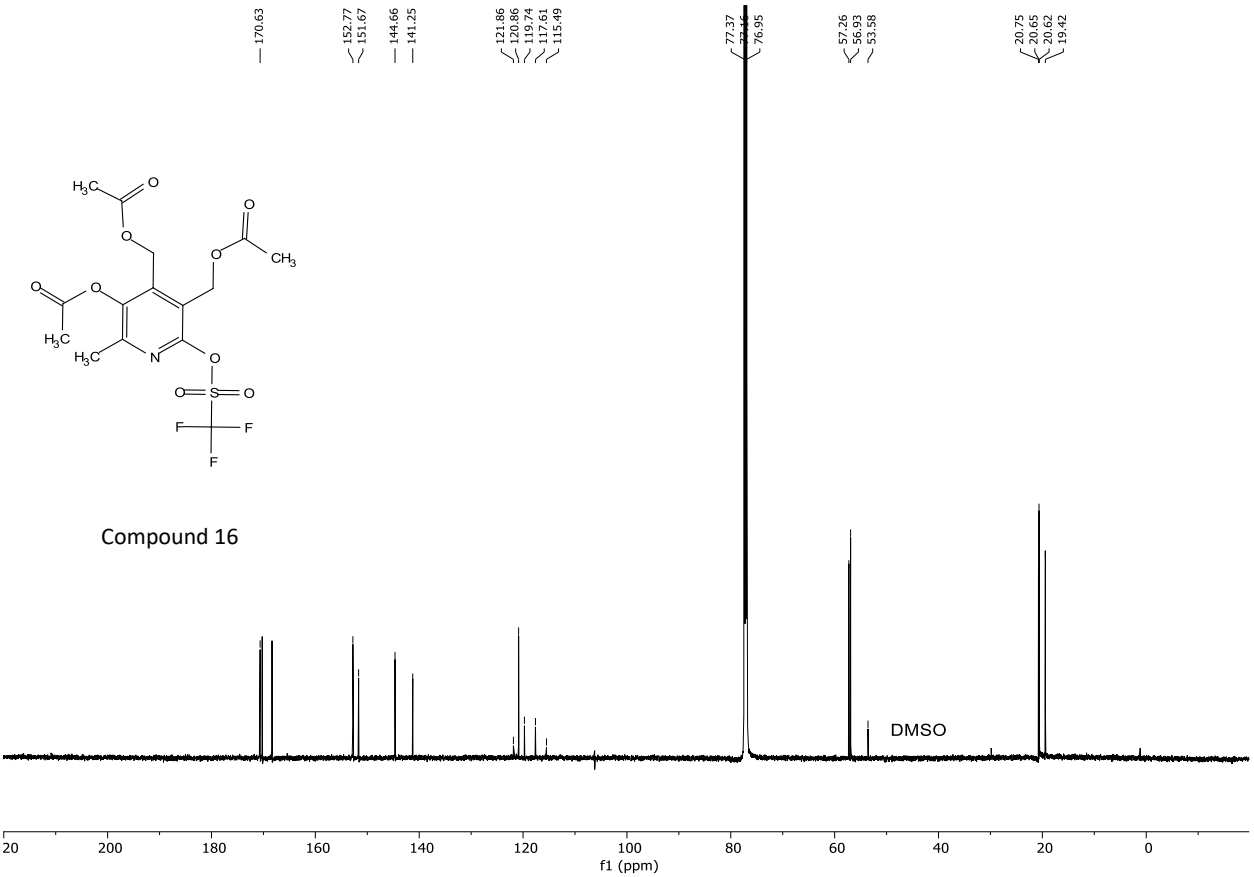
170.63
152.77
151.67
144.66
141.25
121.86
120.86
119.74
117.61
115.49
77.37
77.16
76.95
57.26
56.93
53.58
20.75
20.65
20.62
19.42
DMSO
20
200
180
160
140
120
100
80
60
40
20
0
f1 (ppm)

Compound 16

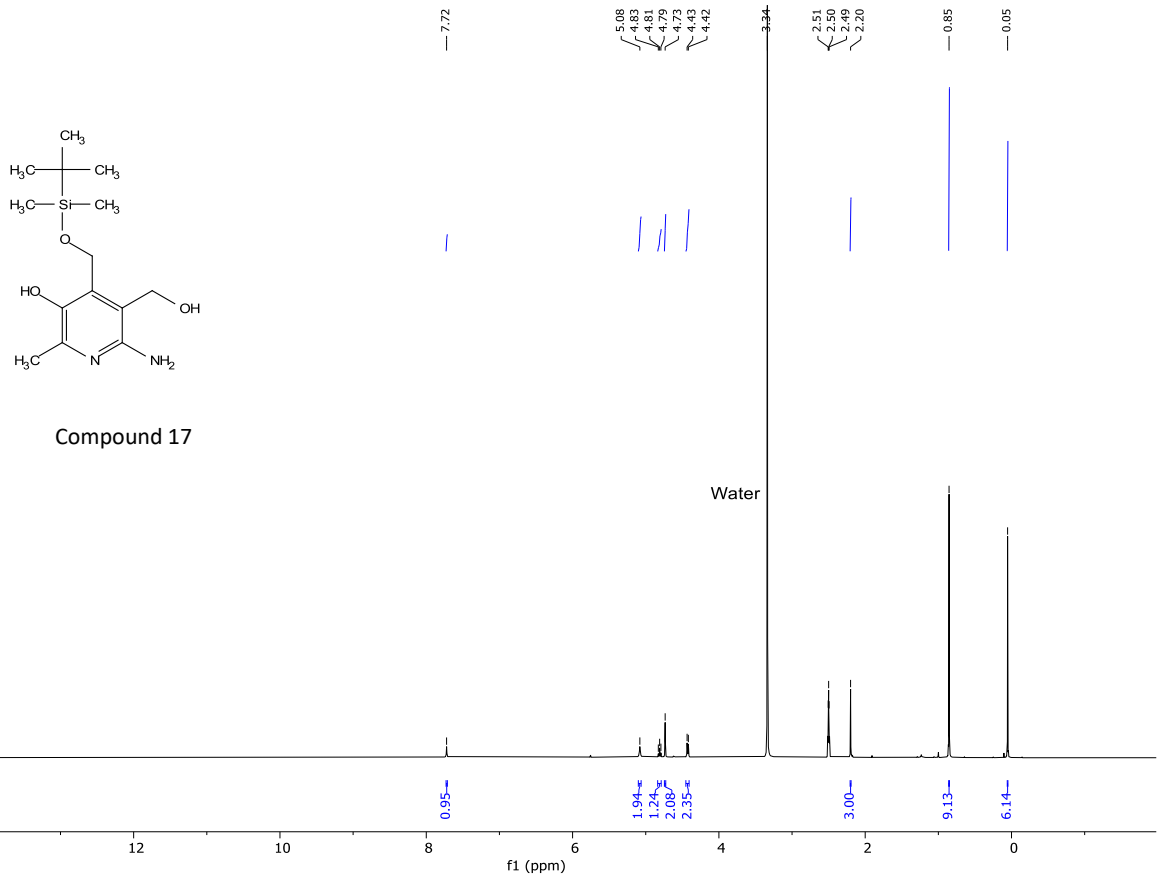
7.72
5.08
4.83
4.81
4.79
4.73
4.43
4.42
3.34
2.51
2.50
2.49
2.20
0.85
0.05
Water
0.95
1.94
1.24
2.08
2.35
3.00
9.13
6.14
14
12
10
8
6
4
2
0
f1 (ppm)

Compound 17

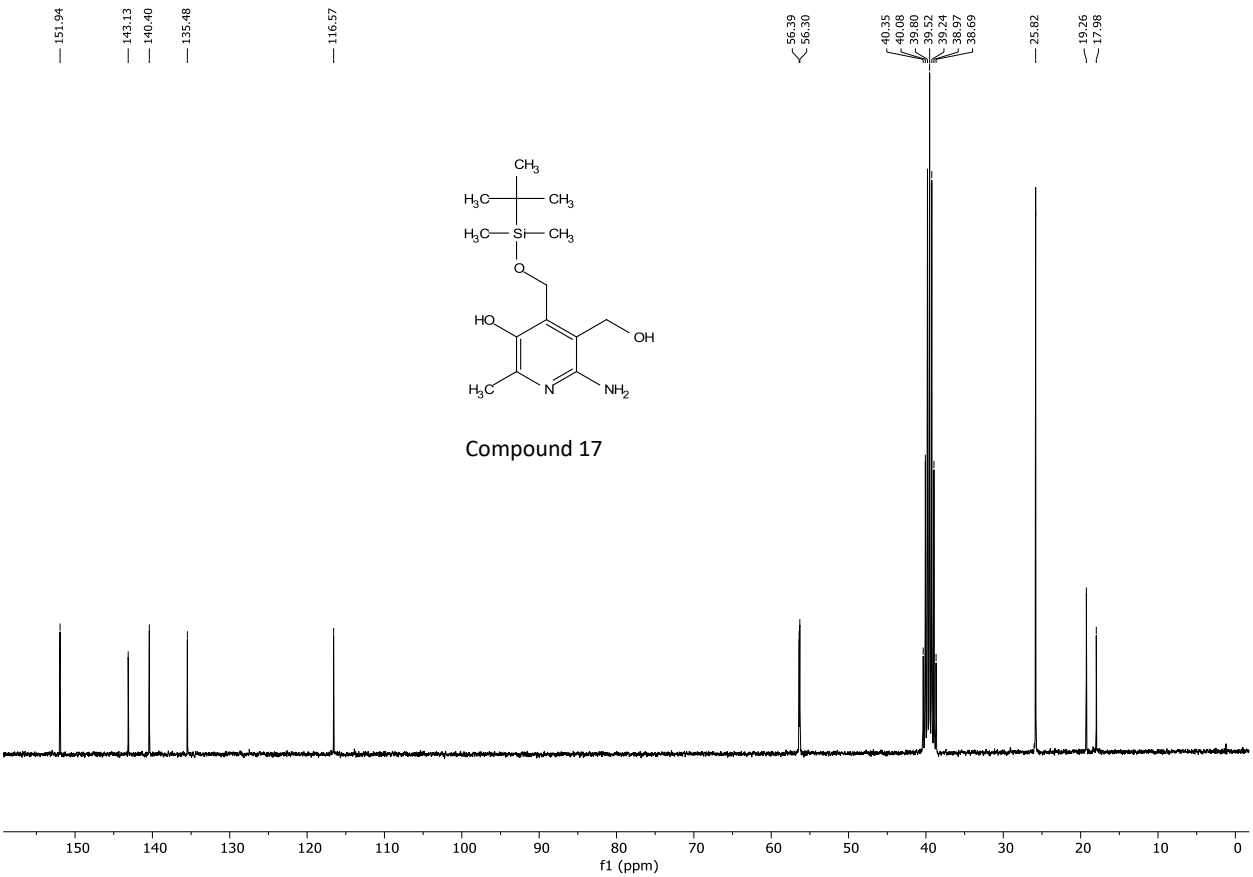
151.94
143.13
140.40
135.48
116.57
56.39
56.30
40.35
40.08
39.80
39.52
39.24
38.97
38.69
25.82
19.26
17.98
CH3
H3C
CH3
H3C
Si
CH3
O
HO
OH
H3C
N
NH2
150
140
130
120
110
100
90
80
70
60
50
40
30
20
10
0
f1 (ppm)

Compound 17

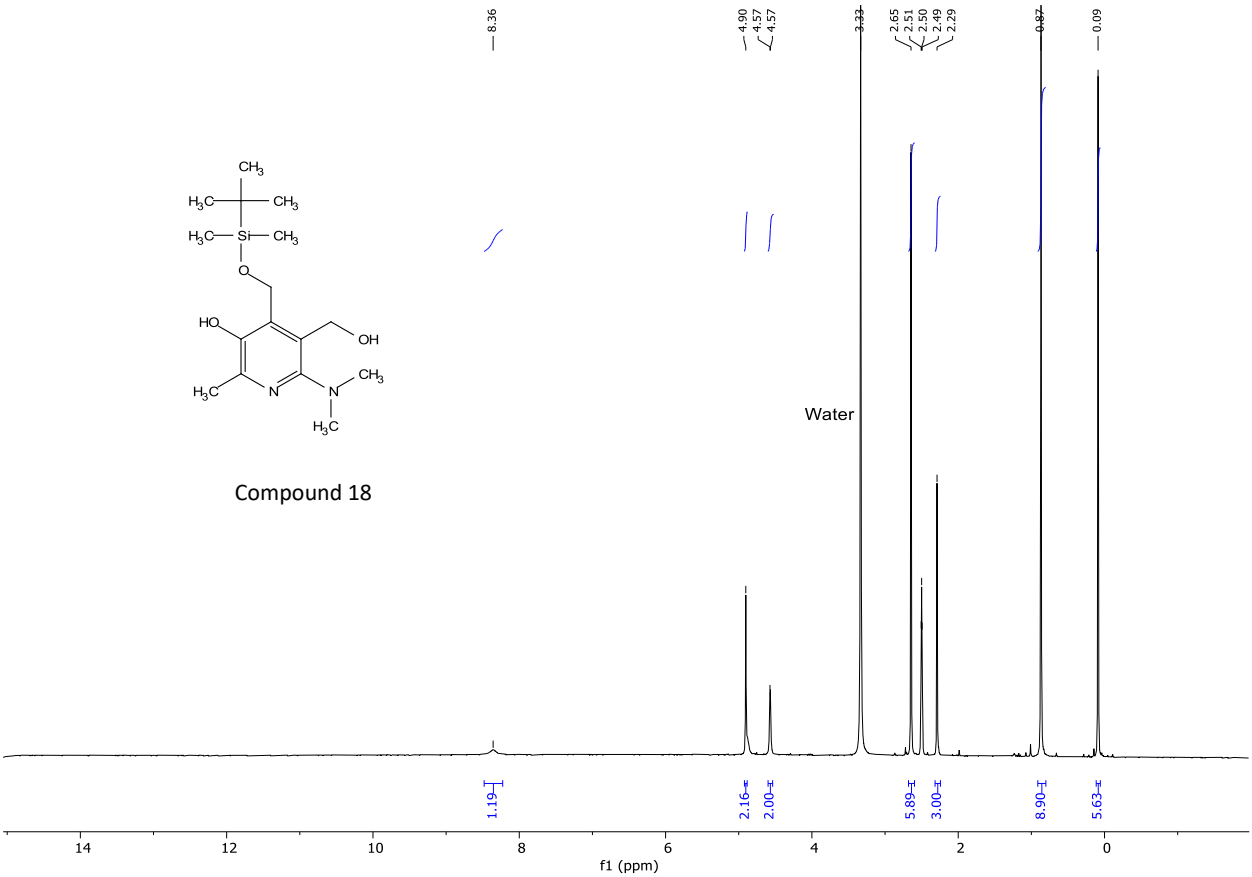
8.36
4.90
4.57
4.57
3.33
2.65
2.51
2.50
2.49
2.29
0.87
0.09
Water
1.19
2.16
2.00
5.89
3.00
8.90
5.63
14
12
10
8
6
4
2
0
f1 (ppm)

Compound 18

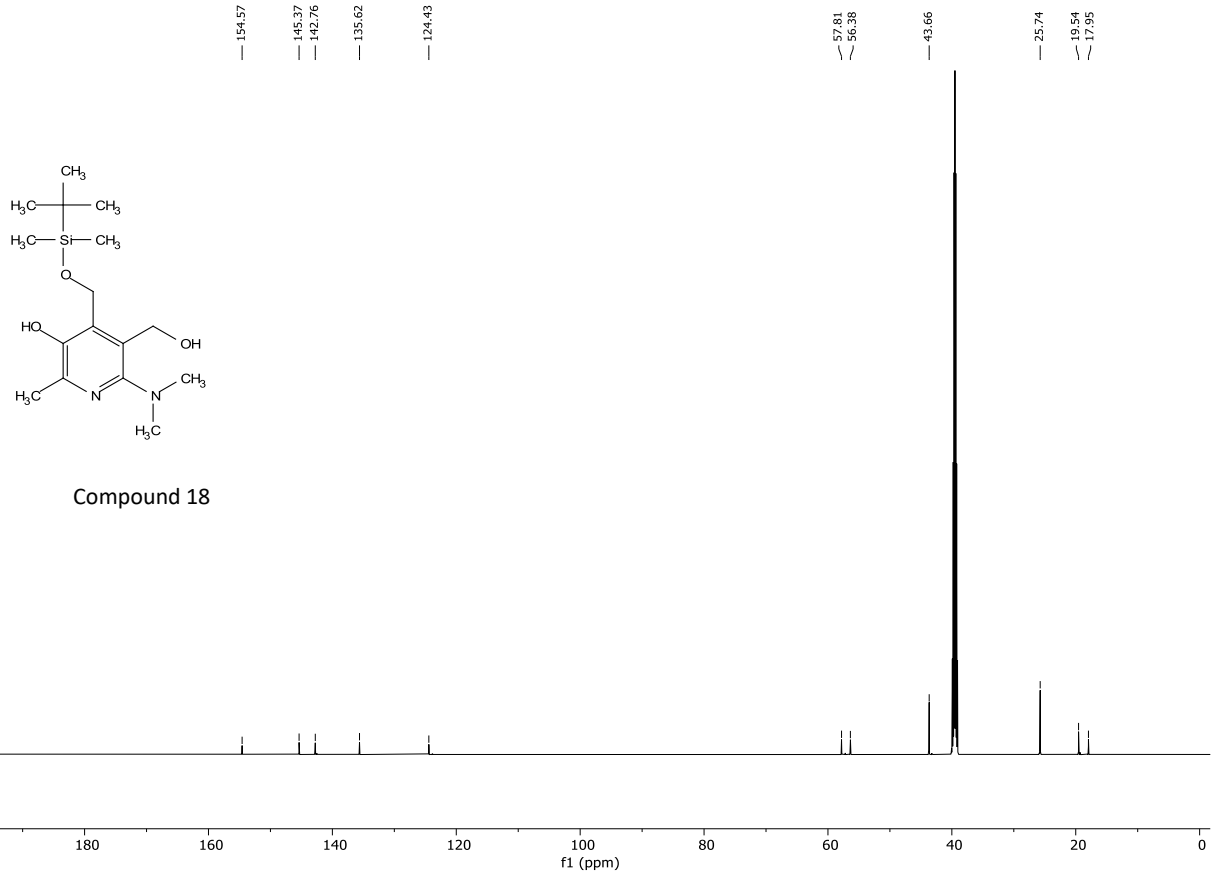
154.57
145.37
142.76
135.62
124.43
57.81
56.38
43.66
25.74
19.54
17.95
CH3
H3C
CH3
H3C
Si
CH3
O
HO
OH
H3C
N
N
CH3
H3C
180
160
140
120
100
80
60
40
20
0
f1 (ppm)

Compound 18

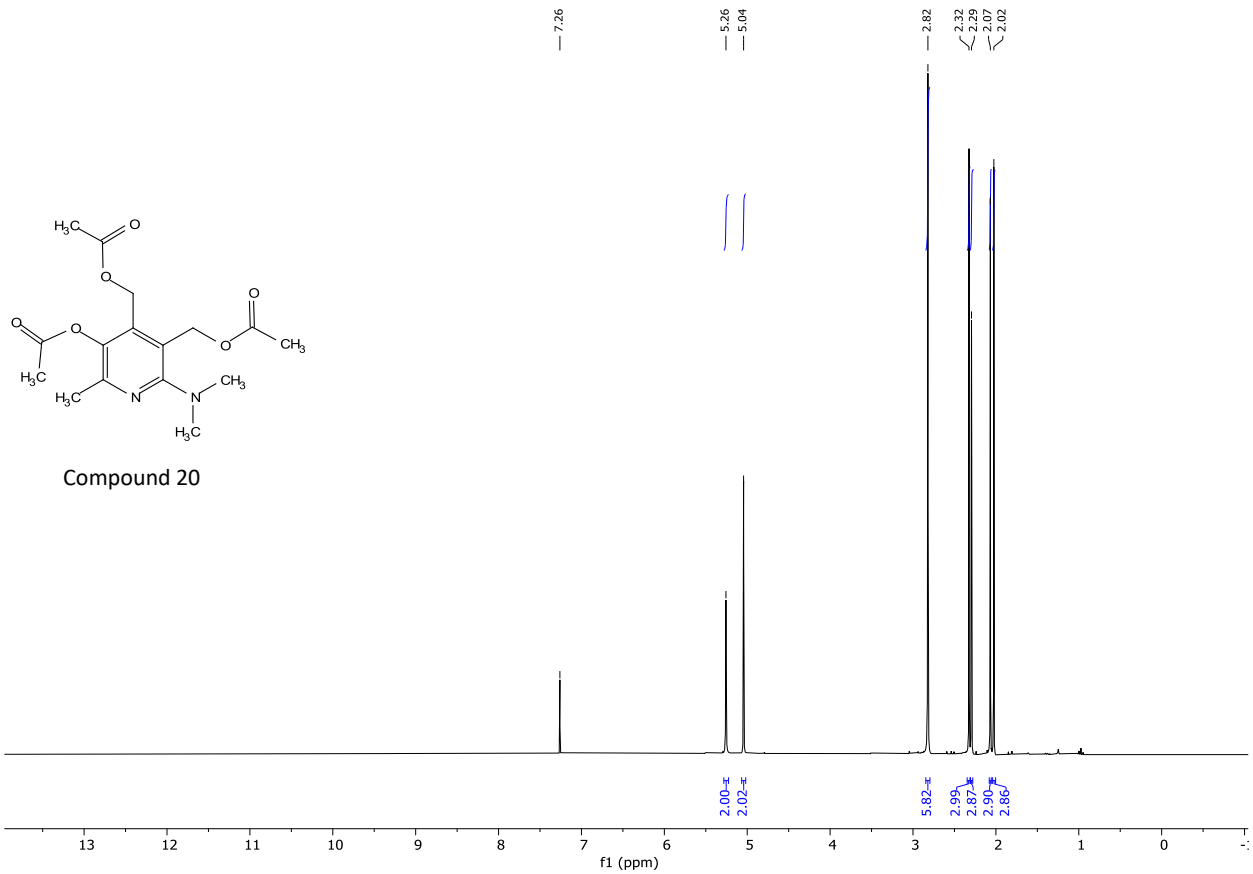
7.26
5.26
5.04
2.82
2.32
2.29
2.07
2.02
2.00
2.02
5.82
2.99
2.87
2.90
2.86
13
12
11
10
9
8
7
6
5
4
3
2
1
0
f1 (ppm)

Compound 20

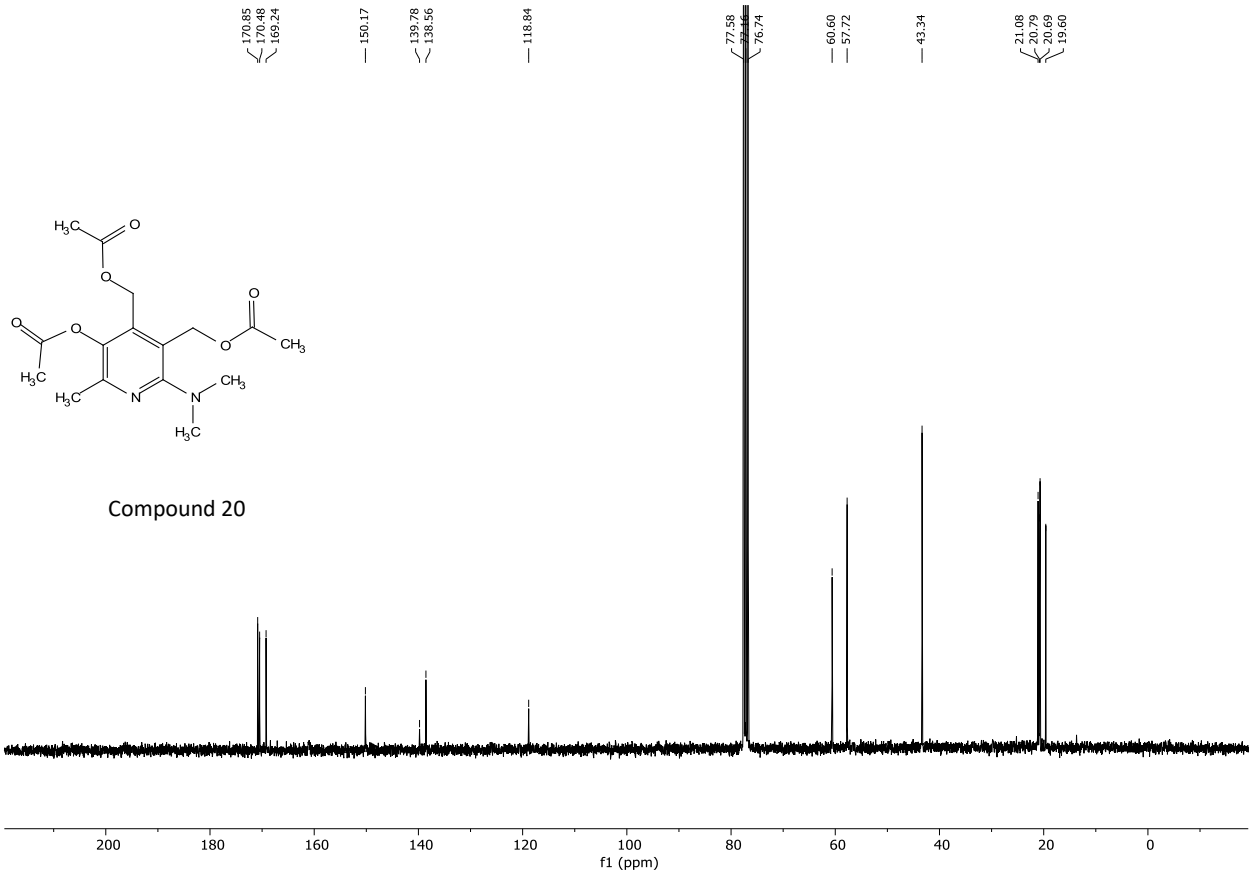
170.85
170.48
169.24
150.17
139.78
138.56
118.84
77.58
77.16
76.74
60.60
57.72
43.34
21.08
20.79
20.69
19.60
200
180
160
140
120
100
80
60
40
20
0
f1 (ppm)

Compound 20

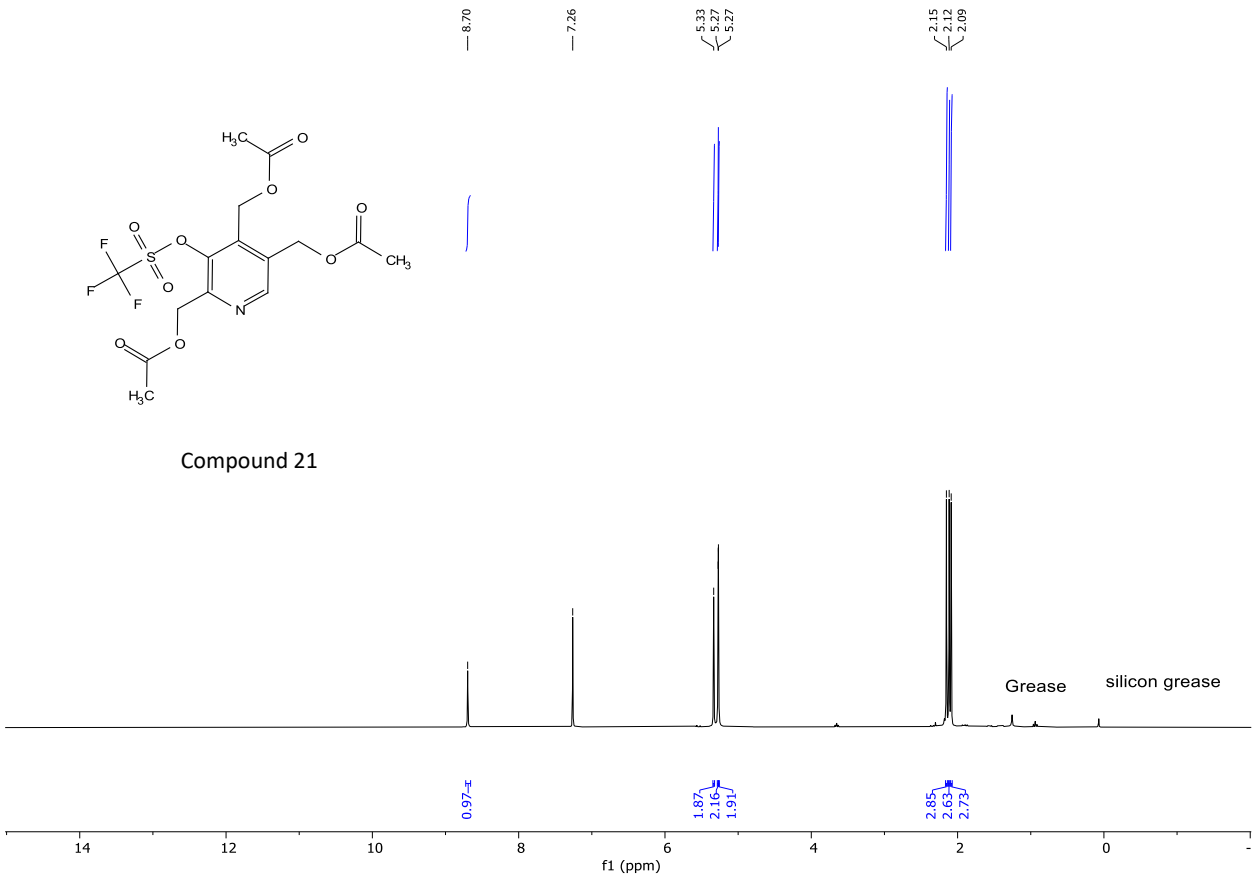
8.70
7.26
5.33
5.27
5.27
2.15
2.12
2.09
Grease
silicon grease
0.97
1.87
2.16
1.91
2.85
2.63
2.73
14
12
10
8
6
4
2
0
f1 (ppm)

Compound 21

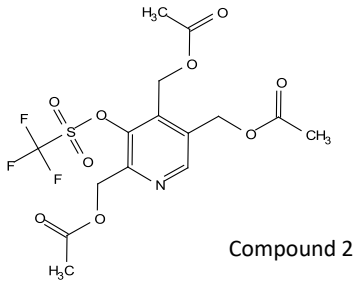

Compound 21

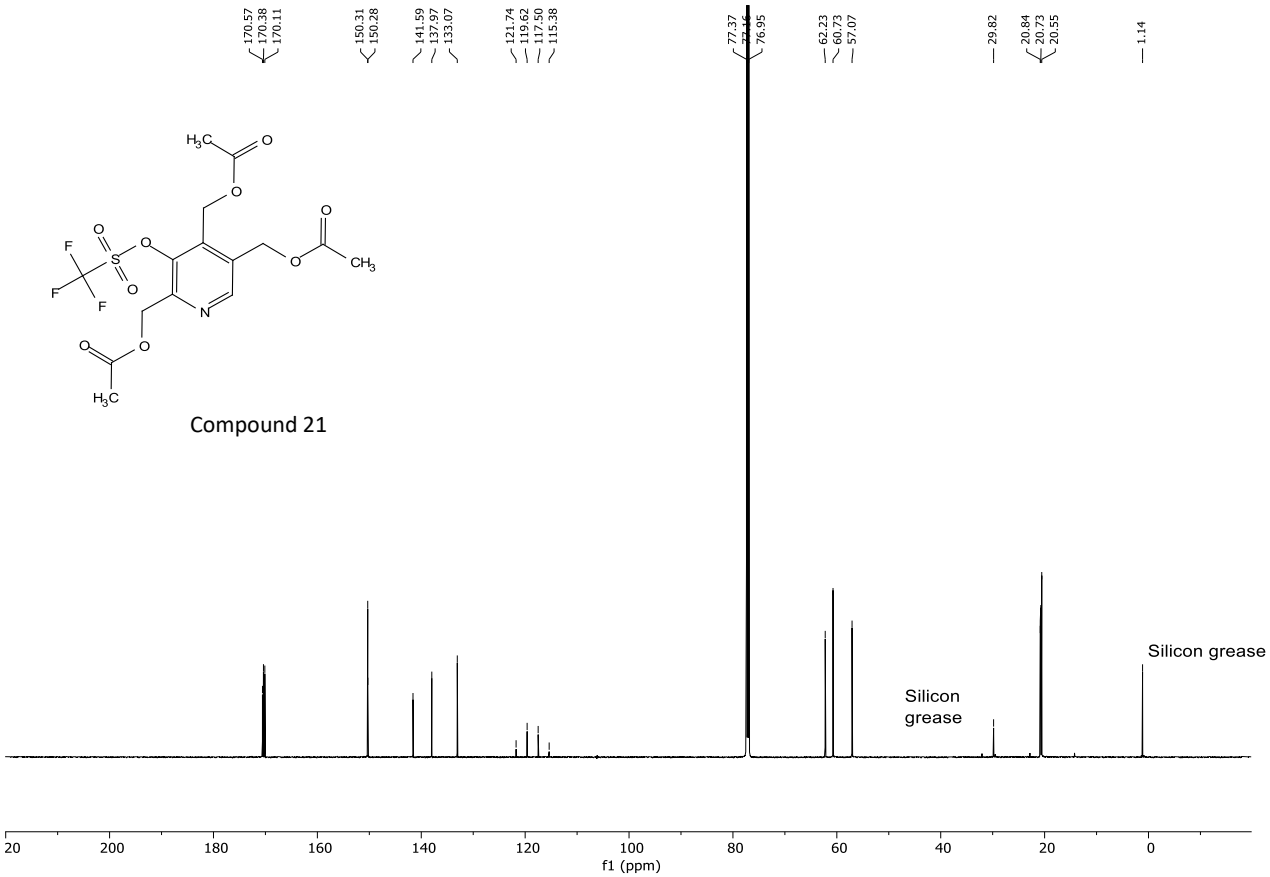
170.57
170.38
170.11
150.31
150.28
141.59
137.97
133.07
121.74
119.62
117.50
115.38
77.37
77.16
76.95
62.23
60.73
57.07
29.82
20.84
20.73
20.55
1.14
Silicon grease
Silicon grease
20
200
180
160
140
120
100
80
60
40
20
0
f1 (ppm)

Compound 21

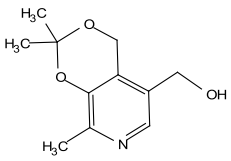
H3C
H3C
O
O
OH
H3C
N

Compound 22

7.79
7.26
4.93
4.54
2.36
1.54
acetone
1.00
2.03
2.02
3.02
6.19
14
12
10
8
6
4
2
0
f1 (ppm)

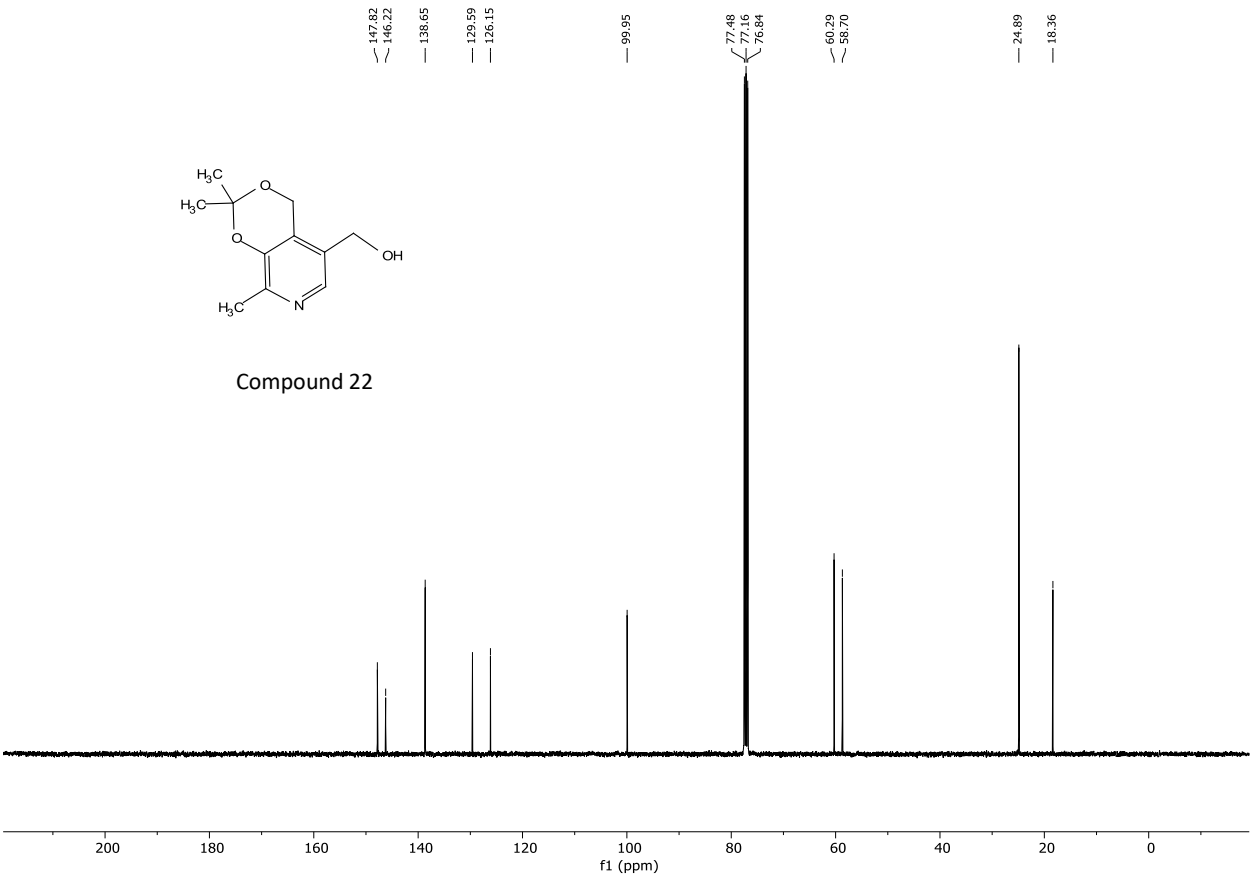
147.82
146.22
138.65
129.59
126.15
99.95
77.48
77.16
76.84
60.29
58.70
24.89
18.36
H3C
H3C
O
O
OH
H3C
N
200
180
160
140
120
100
80
60
40
20
0
f1 (ppm)

Compound 22

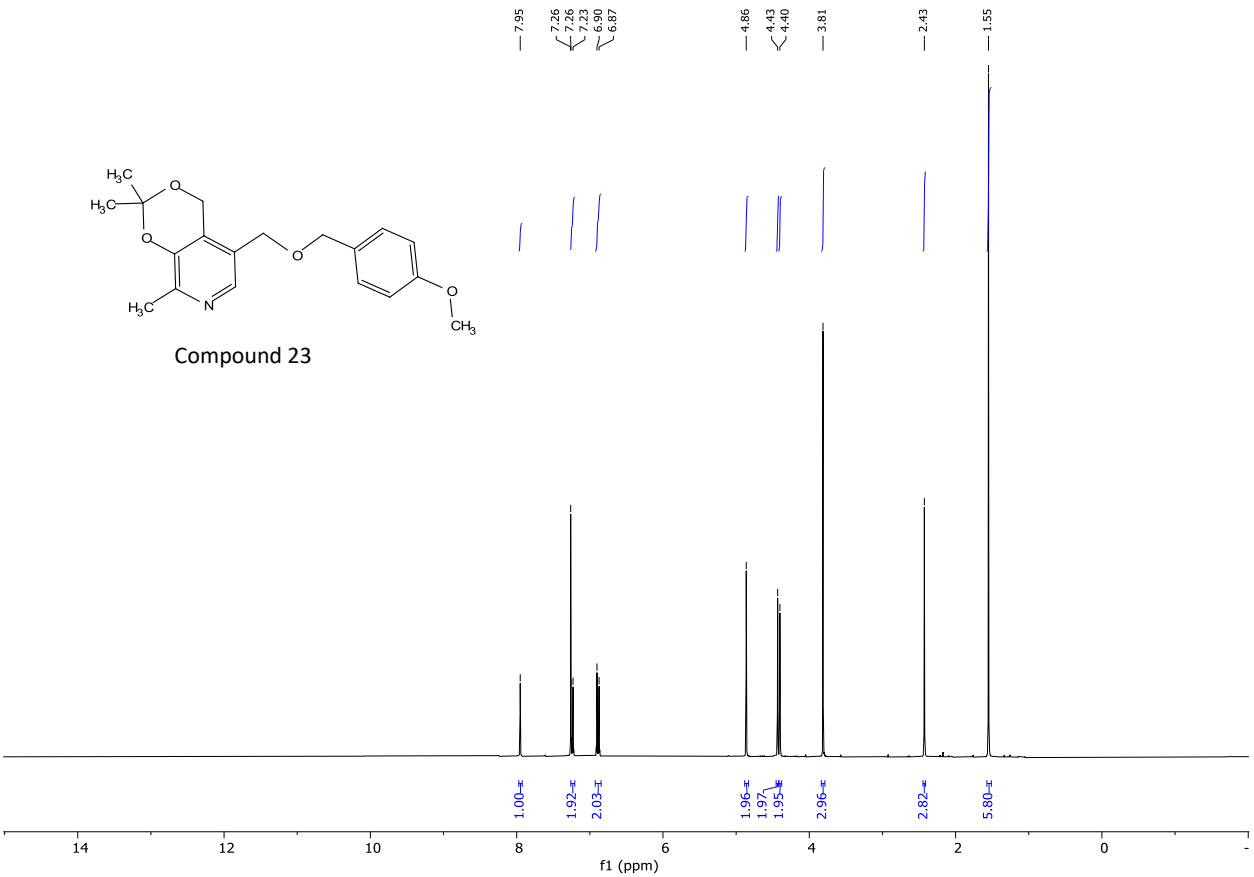
7.95
7.26
7.26
7.23
6.90
6.87
4.86
4.43
4.40
3.81
2.43
1.55
1.00
1.92
2.03
1.96
1.97
1.95
2.96
2.82
5.80
14
12
10
8
6
4
2
0
f1 (ppm)

Compound 23

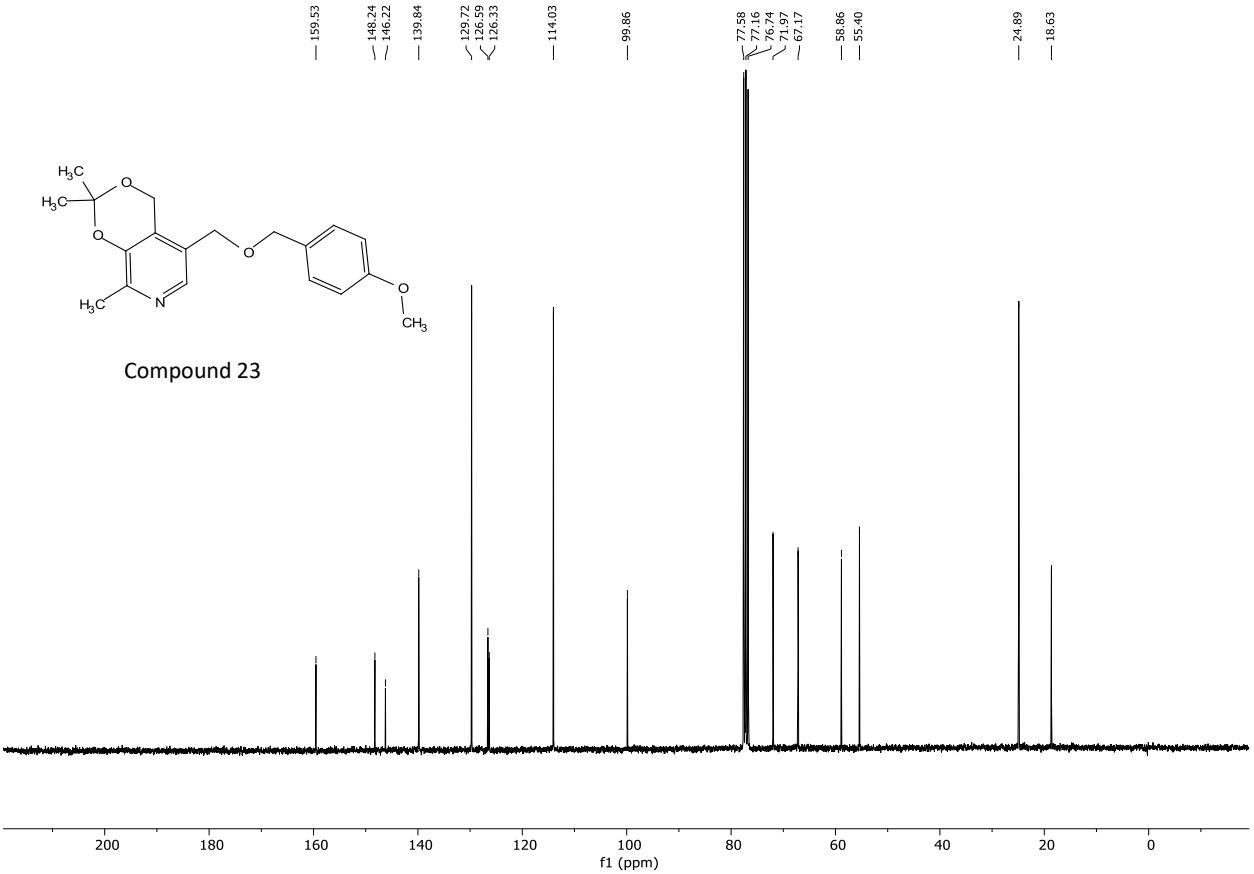
159.53
148.24
146.22
139.84
129.72
126.59
126.33
114.03
99.86
77.58
77.16
76.74
71.97
67.17
58.86
55.40
24.89
18.63
200
180
160
140
120
100
80
60
40
20
0
f1 (ppm)

Compound 23

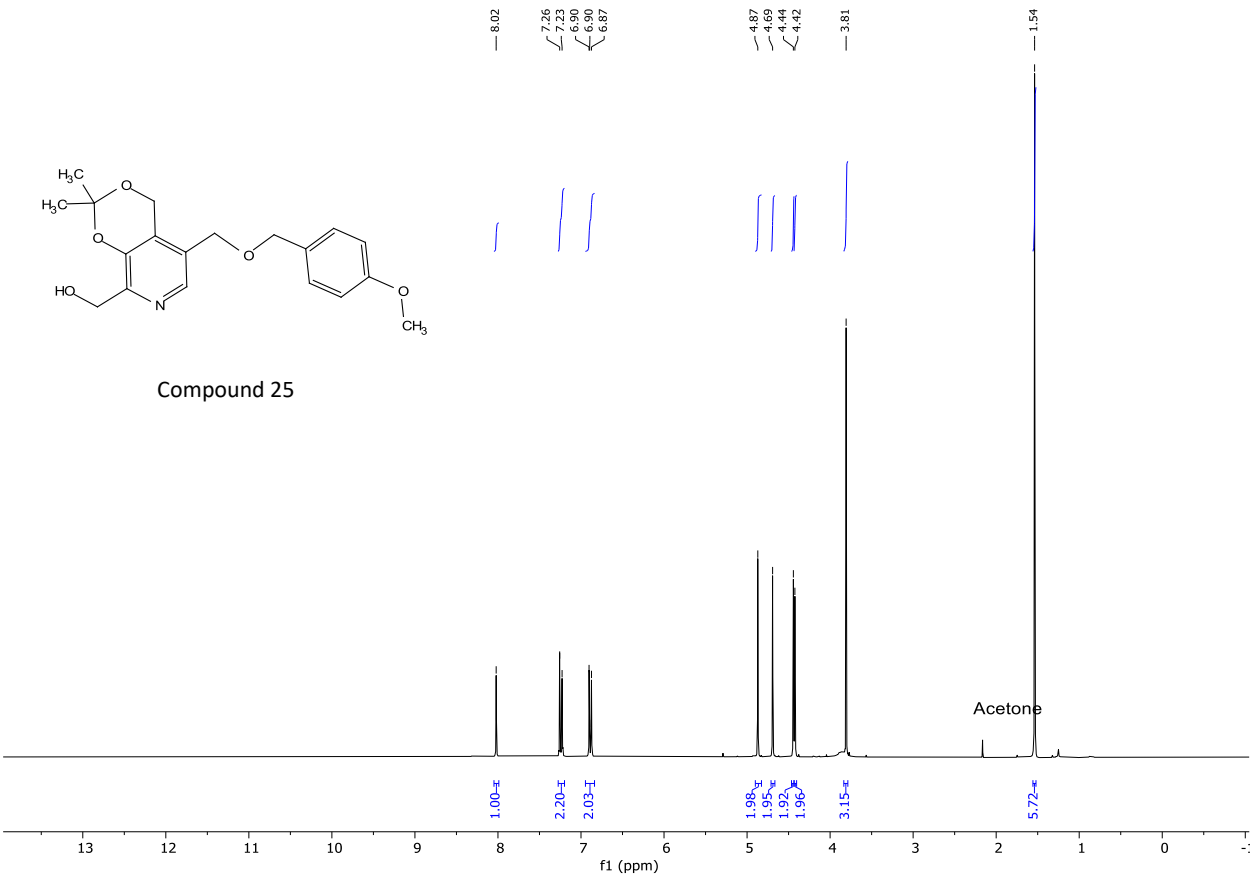
8.02
7.26
7.23
6.90
6.90
6.87
4.87
4.69
4.44
4.42
3.81
1.54
Acetone
1.00
2.20
2.03
1.98
1.95
1.92
1.96
3.15
5.72
f1 (ppm)

Compound 25

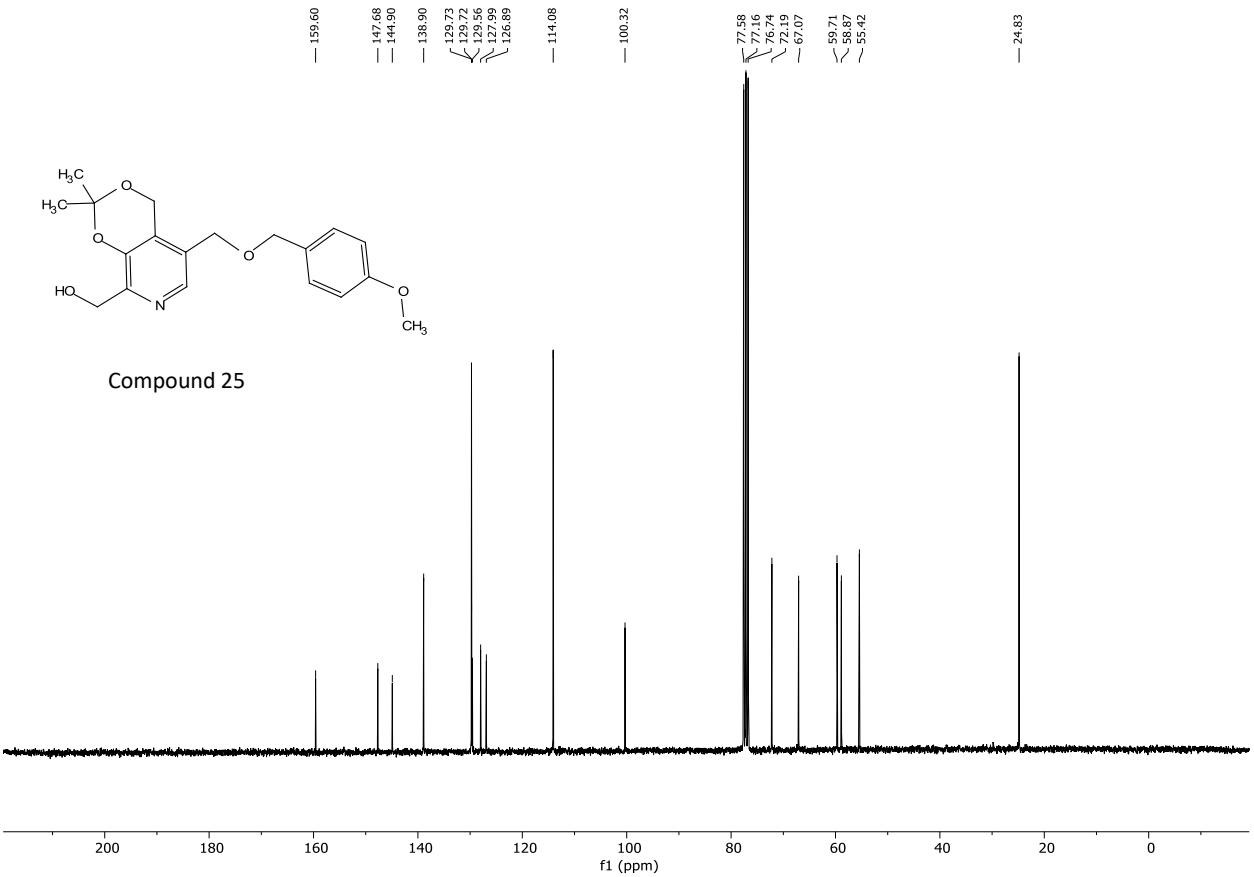
159.60
147.68
144.90
138.90
129.73
129.72
129.56
127.99
126.89
114.08
100.32
77.58
77.16
76.74
72.19
67.07
59.71
58.87
55.42
24.83
H3C
H3C
O
O
O
HO
N
O
CH3
200
180
160
140
120
100
80
60
40
20
0
f1 (ppm)

Compound 25

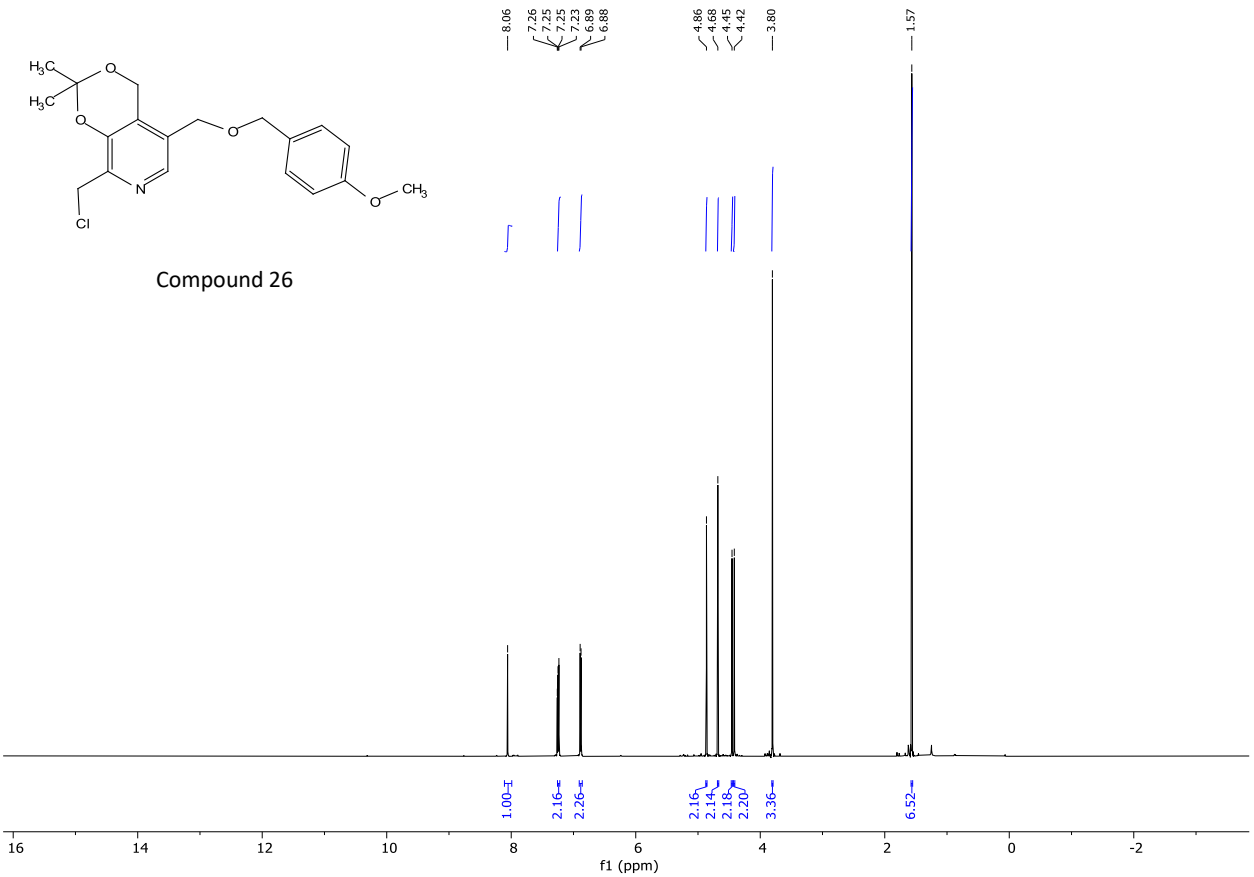
8.06
7.26
7.25
7.25
7.23
6.89
6.88
4.86
4.68
4.45
4.42
3.80
1.57
1.00
2.16
2.26
2.16
2.14
2.18
2.20
3.36
6.52
16
14
12
10
8
6
4
2
0
-2
f1 (ppm)

Compound 26

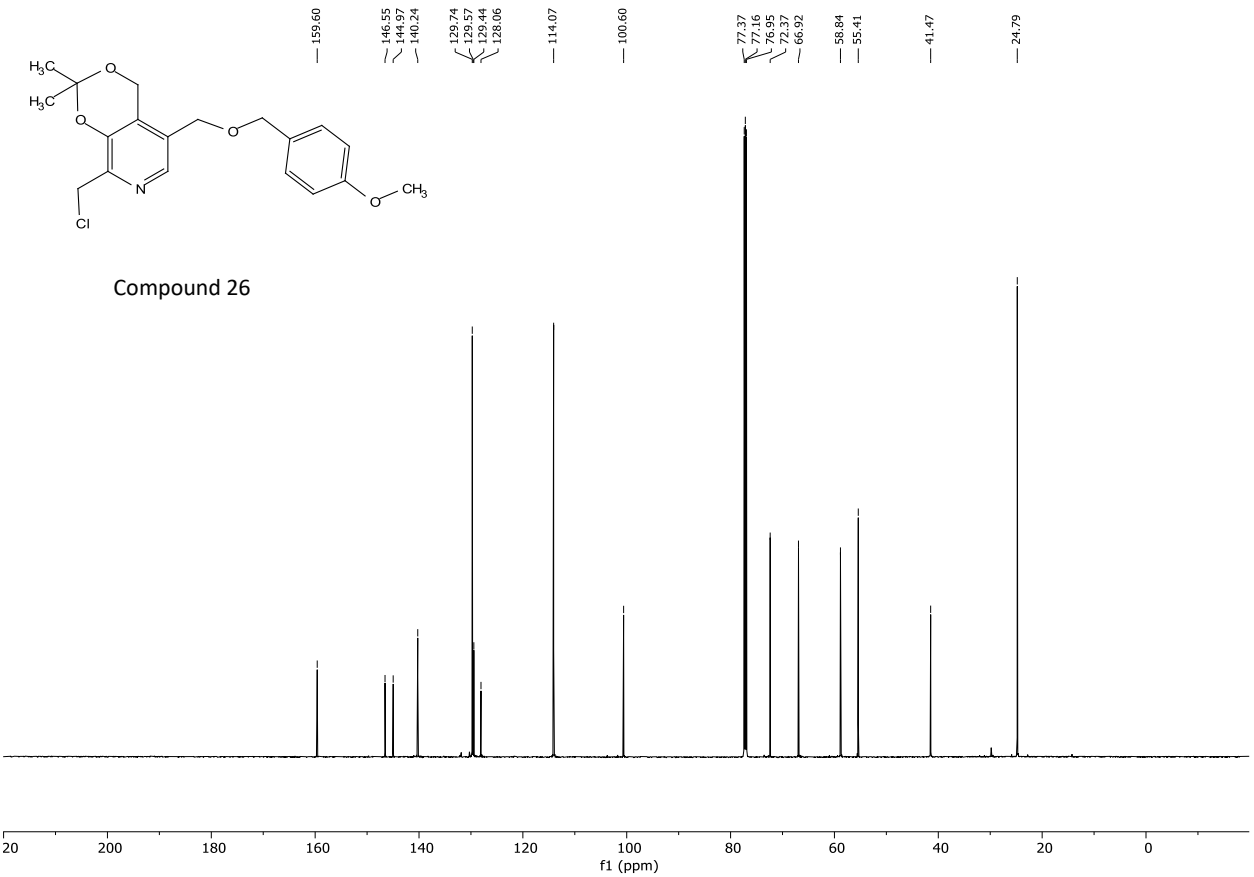
159.60
146.55
144.97
140.24
129.74
129.57
129.44
128.06
114.07
100.60
77.37
77.16
76.95
72.37
66.92
58.84
55.41
41.47
24.79
H3C
H3C
O
O
O
N
Cl
O
CH3
Compound 26
20
200
180
160
140
120
100
80
60
40
20
0
f1 (ppm)

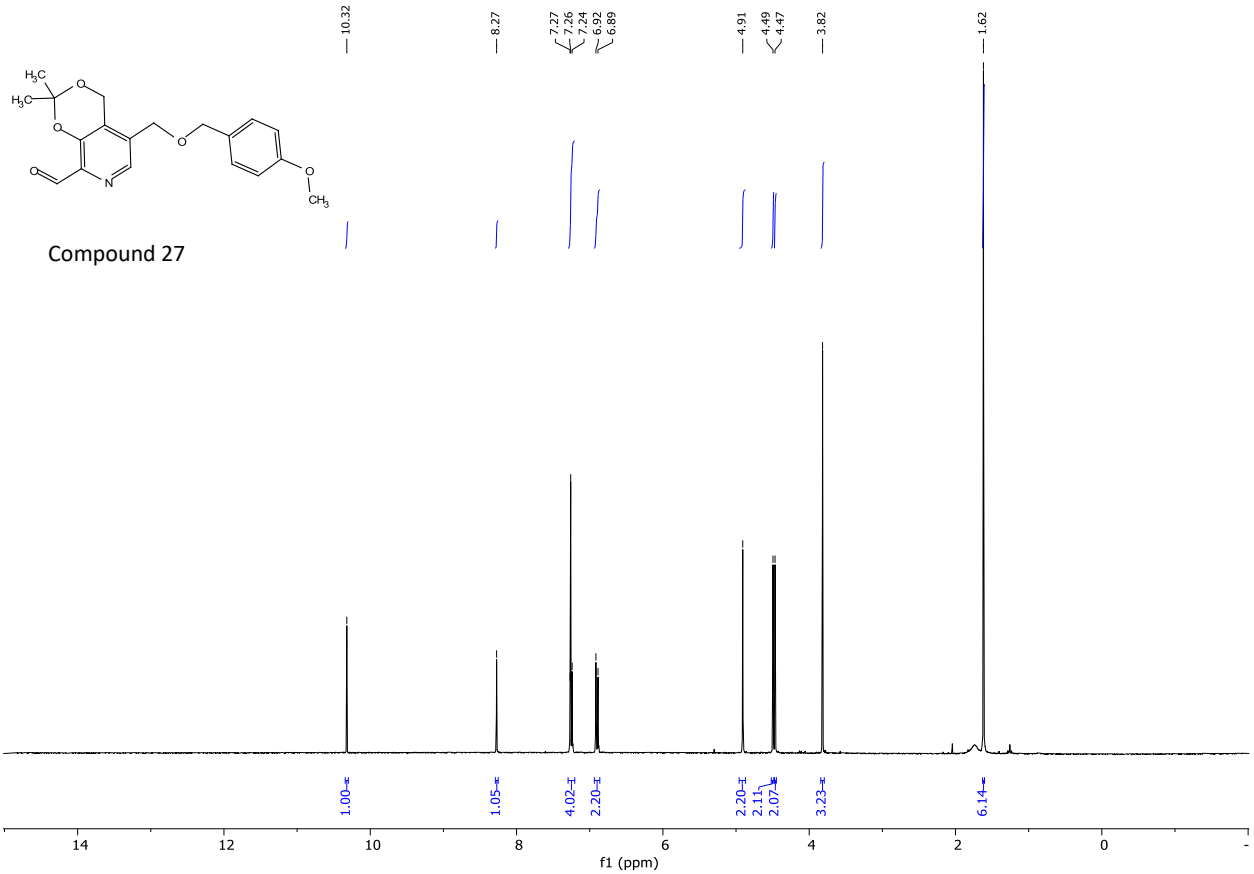
10.32
8.27
7.27
7.26
7.24
6.92
6.89
4.91
4.49
4.47
3.82
1.62
1.00
1.05
4.02
2.20
2.20
2.11
2.07
3.23
6.14
14
12
10
8
6
4
2
0
f1 (ppm)

Compound 27

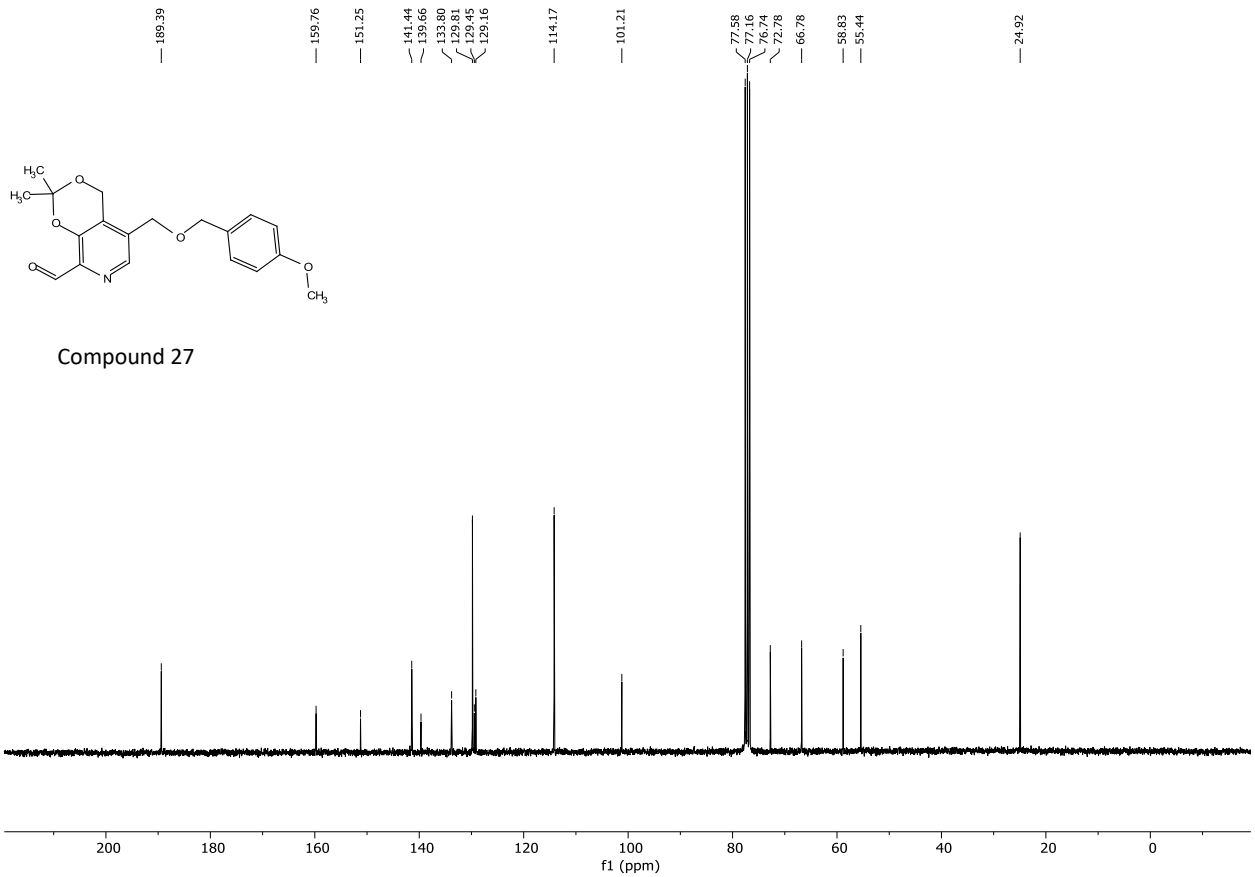
189.39
159.76
151.25
141.44
139.66
133.80
129.81
129.45
129.16
114.17
101.21
77.58
77.16
76.74
72.78
66.78
58.83
55.44
24.92
200
180
160
140
120
100
80
60
40
20
0
f1 (ppm)

Compound 27

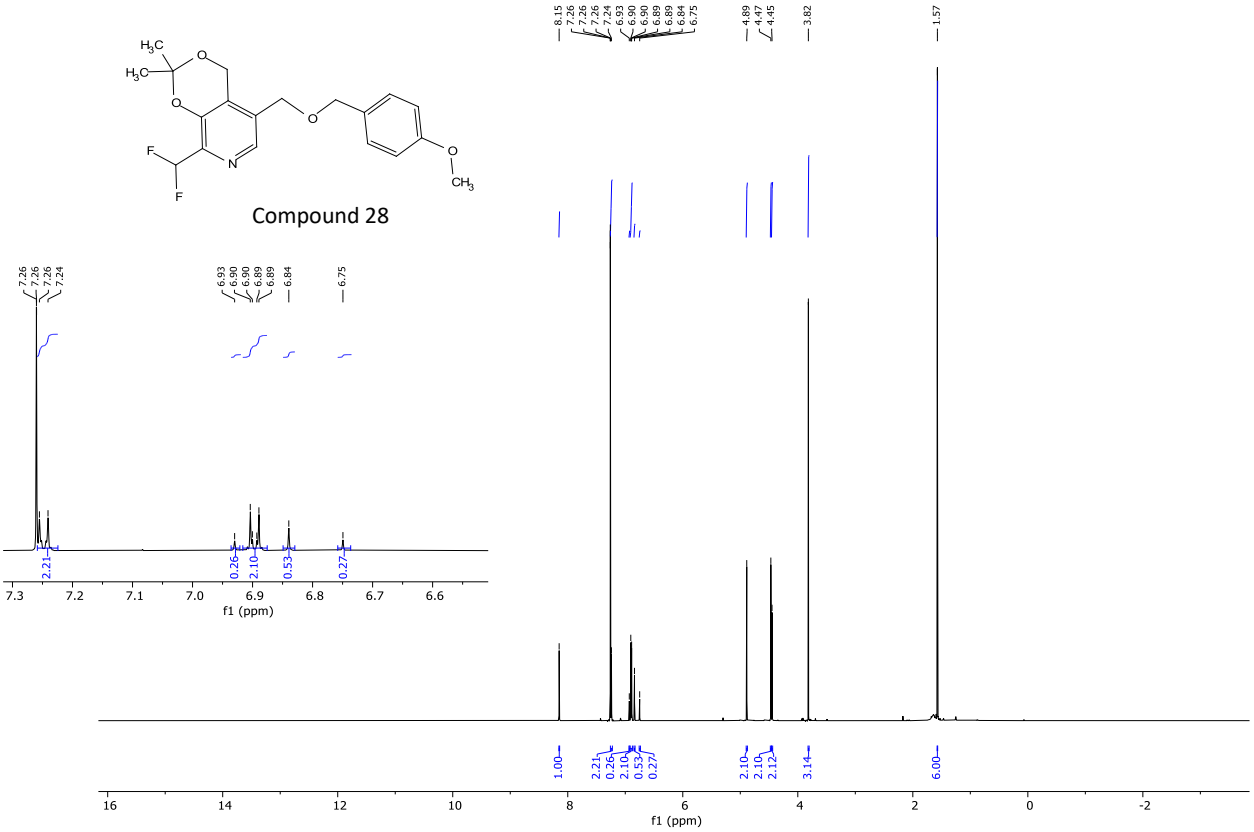
Compound 28
f1 (ppm)

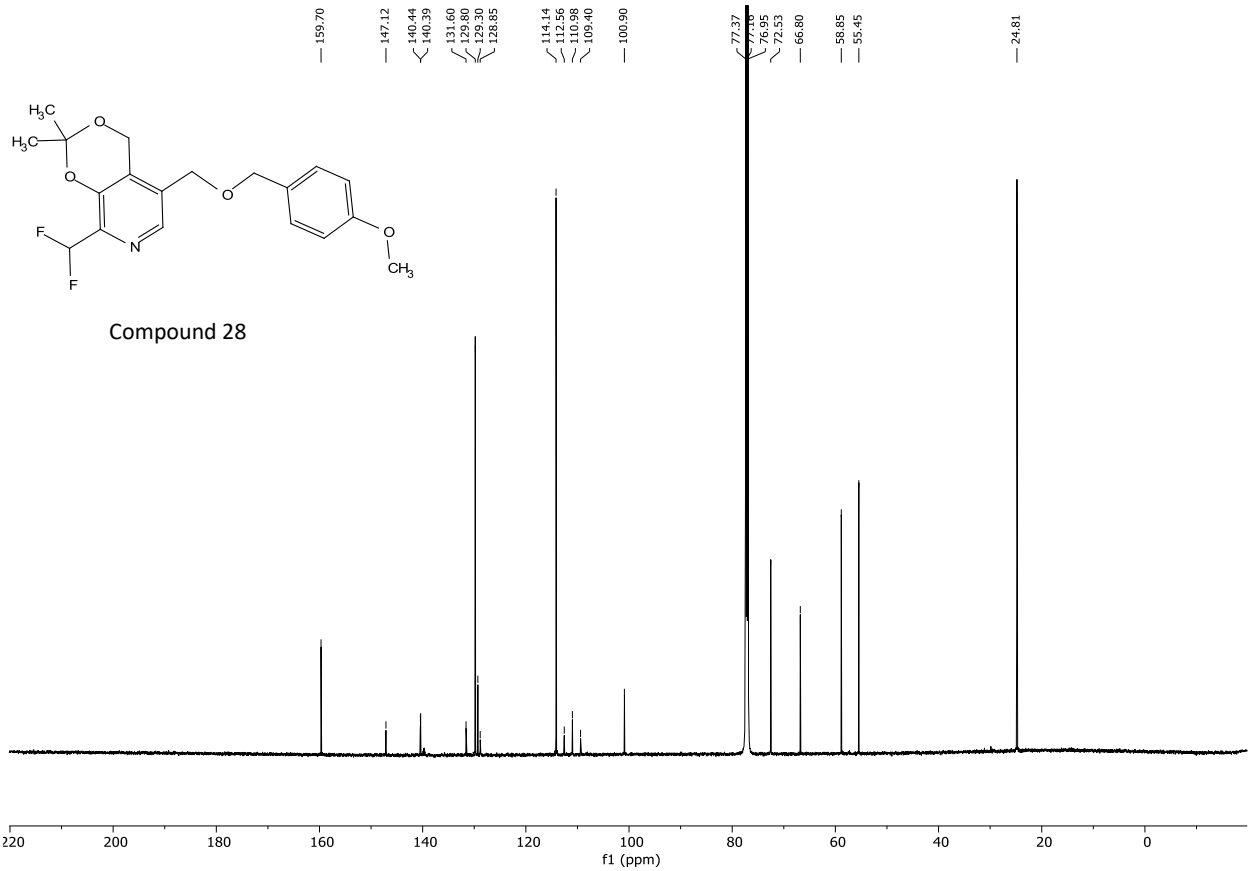
159.70
147.12
140.44
140.39
131.60
129.80
129.30
128.85
114.14
112.56
110.98
109.40
100.90
77.37
77.16
76.95
72.53
66.80
58.85
55.45
24.81
H3C
H3C
O
O
O
F
F
N
O
CH3
220
200
180
160
140
120
100
80
60
40
20
0
f1 (ppm)

Compound 28

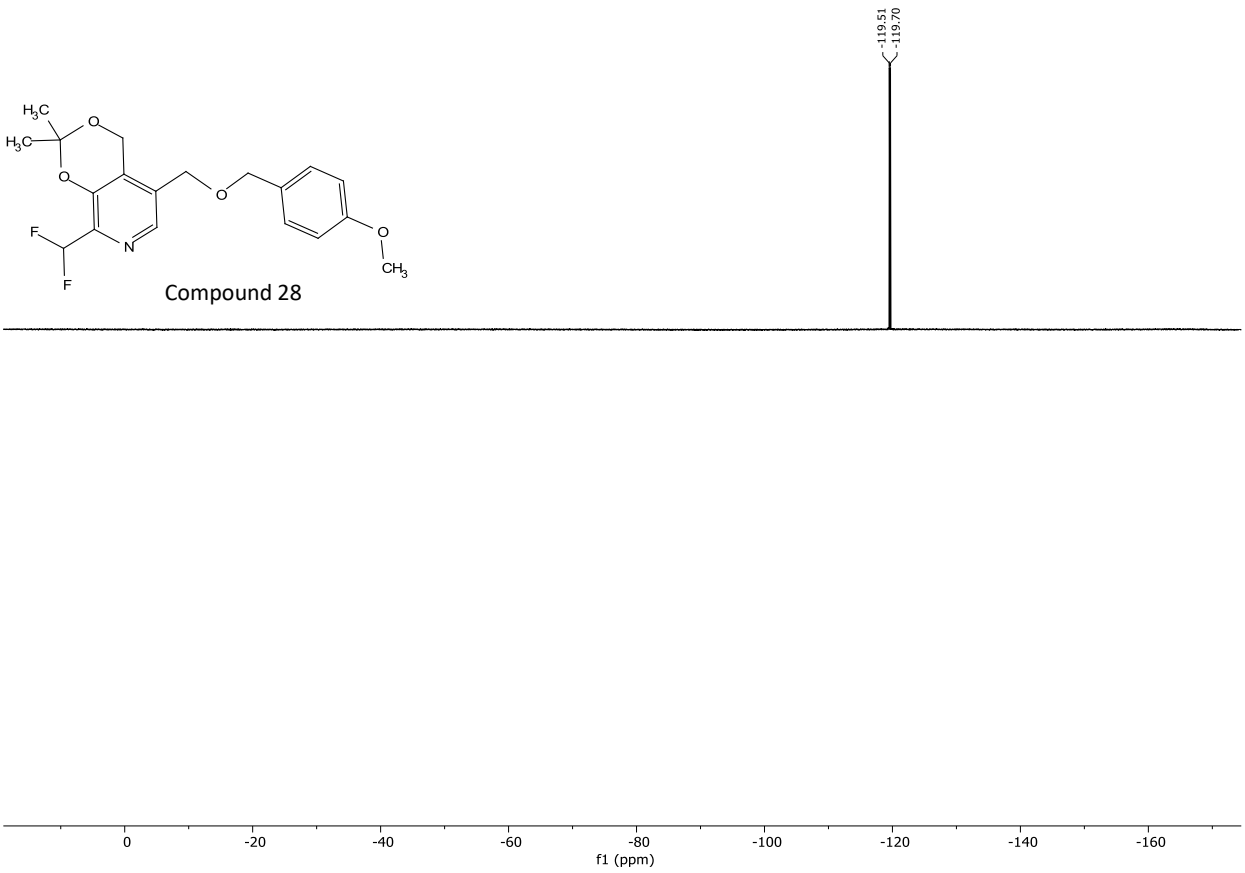
-119.51
-119.70
H3C
H3C
O
O
O
F
F
N
O
CH3
0
-20
-40
-60
-80
-100
-120
-140
-160
f1 (ppm)

Compound 28